



**Microenvironmental FGF2 regulates
glioblastoma stem cells through FGFR1-
ERK1/2-ZEB1 axis**

Ana Jiménez-Pascual

A thesis submitted for the Doctor of Philosophy at
Cardiff University
July 2019

Funded by
tenovus
cancer care
gofal canser



Declaration

This work has not been submitted in substance for any other degree or award at this or any other university or place of learning, nor is being submitted concurrently in candidature for any degree or other award.

Signed Ana Jiménez-Pascual Date: 2nd of July 2019

STATEMENT 1

This thesis is being submitted in partial fulfilment of the requirements for the degree of doctor of philosophy PhD

Signed Ana Jiménez-Pascual Date: 2nd of July 2019

STATEMENT 2

This thesis is the result of my own independent work/investigation, except where otherwise stated, and the thesis has not been edited by a third party beyond what is permitted by Cardiff University's Policy on the Use of Third Party Editors by Research Degree Students. Other sources are acknowledged by explicit references. The views expressed are my own.

Signed Ana Jiménez-Pascual Date: 2nd of July 2019

STATEMENT 3

I hereby give consent for my thesis, if accepted, to be available online in the University's Open Access repository and for inter-library loan, and for the title and summary to be made available to outside organisations.

Signed Ana Jiménez-Pascual Date: 2nd of July 2019

STATEMENT 4: PREVIOUSLY APPROVED BAR ON ACCESS

I hereby give consent for my thesis, if accepted, to be available online in the University's Open Access repository and for inter-library loans **after expiry of a bar on access previously approved by the Academic Standards & Quality Committee.**

Signed Ana Jiménez-Pascual Date: 2nd of July 2019

Acknowledgements

First and foremost, I would like to express my sincere gratitude to my supervisor, Dr. Florian Siebzehnrubl, for giving me the opportunity to undertake a PhD, and for his scientific knowledge, support, guidance, and care throughout these 4 years. Secondly, I would like to thank my second supervisor, Prof. Matt Smalley, for his helpful advice. I would also like to acknowledge Tenovus Cancer Care for supporting my research, and Cardiff University Michael Banfill Scholarship, William Morgan Thomas fund, and ECSCRI for supporting my attendance at national and international conferences.

I would like to thank everyone in ECSCRI, for the help, advice, and friendly environment, in particular to my colleague and friend Bhavana Gupta. I cannot be more grateful for your support and help during my thesis writing, for being such a nice, humble and friendly person and for working and sharing with you these 3 years in the lab. I also owe a big thanks to Leigh-anne Thomas for willingly taking on the task of reading my work. In addition, I would like to acknowledge all the students especially Anja, Jamie and Berit, for their enthusiasm, hard work and help and to Ben for always being so kind.

Particularly, I am grateful to my life-time friends that despite the distance, have always supported me in every adventure that I have undertaken. Of course to my amazing family of friends from Cardiff. I cannot be more lucky for your friendship, fun lunches at work, long days and weekends in the lab, nights out, or in playing board games, hiking, climbing etc. You have truly made these four years unforgettable.

I owe a big thanks to Pedro, for the endless support during the PhD, for the number of weekends he expended waiting for me in the lab, for the patience, for making me laugh constantly, for always having my back and for being there no matter what. I would like to thank my family and godfather Paulino, who has been such an important person in my life. Finalmente, a mis pilares en la vida, a mis padres, a los que dedico esta tesis. Desde muy pequeñita me enseñaron que todo se consigue con esfuerzo, tesón, trabajo, optimismo y humildad. Con el tiempo he aprendido que esas actitudes son imprescindibles en la vida pero también que sin vosotros y sin vuestro constante apoyo, esto y muchas otras cosas hubiesen sido imposibles de conseguir. No hay palabras para describir lo afortunada que soy por teneros como padres.

Abstract

Glioblastoma (GBM) is the most lethal and aggressive brain cancer in adults with a median survival of approximately 20 months after diagnosis. GBM represents a highly infiltrative and heterogenous tumour, formed by populations of cells harbouring diverse molecular signatures and responses to therapy. Tumour recurrence and poor prognosis have been thought to be a consequence of resident glioblastoma stem cells (GSCs), which are quiescent cells capable of self-renewal, migration and initiation of new tumours. These cells are subject to cell-autonomous factors and extrinsic cues, which are translated into cell responses that promote tumour progression. Particularly, trophic factors from the tumour microenvironment, such as fibroblast growth factor 2 (FGF2), are essential to GBM growth and GSC maintenance. FGF2 and its cognate receptors have been linked to malignancy and progression in GBM as they promote angiogenesis, proliferation and GSC self-renewal. However, the specific mechanisms of how this growth factor contributes to GSC functions remain incompletely understood.

Therefore, we analysed expression of FGF receptors (FGFRs) and the effects of FGF2 on patient-derived glioblastoma cells. We found that FGF2 induces expression of the stemness-associated transcription factors ZEB1, SOX2 and OLIG2. Analysis of FGFR1-3 function using knockdown approaches in patient-derived glioblastoma cell lines revealed that FGFR1 was the only FGFR relevant for GSC maintenance. FGFR1 knockdown reduced sphere/colony-formation, invasion and increased survival in xenograft mouse models. On the other hand, serial dilution orthotopic xenografts of FGFR1+ sorted cells revealed higher tumour formation capacity than FGFR1- cells, consistent with a stem cell population. We found that differentiated cancer cells showed a reduction in FGFR1, ZEB1, SOX2 and OLIG2 expression, and that FGFR1 regulated ZEB1 function through ERK1/2 signalling. Finally, analysis of large-scale gene-expression datasets revealed association of FGFR1 with the mesenchymal subclass of glioblastoma and increased expression levels of FGFR1 in 30-40% of cases. Therefore, in this thesis we demonstrate that FGF2-FGFR1 axis regulates key stemness transcription factors and identify FGFR1 as a potential GSC marker and therapeutic target.

Publications, conferences and scholarships

Publications

Hoang-Minh, L.B., Siebzehnrubl, F.A., Yang, C., Suzuki-Hatano, S., Dajac, K., Loche, T., Andrews, N., et al. (2018). Infiltrative and drug-resistant slow-cycling cells support metabolic heterogeneity in glioblastoma. *The EMBO Journal* **37**(23).

Jimenez-Pascual, A., Hale, J.S., Kordowski, A., Pugh, J., Silver, D.J., Bayik, D., Roversi, G., et al. (2019). ADAMDEC1 maintains a growth factor signaling loop in cancer stem cells. *Cancer Discovery*.

Jimenez-Pascual, A. and Siebzehnrubl, F.A. (2019). Fibroblast Growth Factor Receptor Functions in Glioblastoma. *Cells* **8**(7):715.

Conferences

Jimenez-Pascual, A., Hale J.S., Kordowski, A., Jamie, P., Rao, S., Silver, J.D., Chen, R., McIntyre, T.M., Colombo, G., et al (2018). A novel ADAMDEC1-FGF2-FGFR1 feedback loop maintains glioblastoma cancer stem cells through ZEB1. Poster session at: Society for Neuro-Oncology (SNO) Annual Meeting. 2018 Nov 15-18; New Orleans (Louisiana).

Jimenez-Pascual A, Kordowski A, Pugh J, Ashelford K, Holmberg-Olausson K, Silver D.J, Colombo G, Forsberg-Nilsson K and Siebzehnrubl FA. Microenvironmental FGF2 induces ZEB1 in stem cells through FGFR1-ZEB1. Poster session at: European Cancer Stem Cell Research Institute Symposium. 2018 Sep 13-14; Cardiff (UK). *Best PhD poster prize*.

Jimenez-Pascual, A., Holzmann, K., Smalley, M., and Siebzehnrubl, F.A. Microenvironmental FGF2 induces ZEB1 in glioblastoma. Poster session at: European Cancer Stem Cell Research Institute Symposium. 2017 Sep 12-13; Cardiff (UK).

Jimenez-Pascual, A., Holzmann K., Smalley, M., and Siebzehnrubl, F.A. Environmental FGF2 induces ZEB1 expression in glioblastoma. Poster session at: Brain Tumour Meeting. 2017 May 18-19; Berlin (Germany).

Scholarship funds

William Morgan Thomas Fund (Cardiff University). Awarded on the 28th of Aug 2018.

Michael Banfill Fund (Cardiff University). Awarded on the 28th of Aug 2018.

Table of contents

Declaration	ii
Acknowledgements	iii
Abstract	iv
Publications, conferences and scholarships	v
Table of contents	vii
List of tables	x
List of figures	xi
Abbreviations	xiii
Chapter 1 : Introduction	1
1.1 Glial cells and their function in the adult brain	2
1.2 Gliomas	3
1.2.1 WHO classification of gliomas	3
1.2.2 Updated WHO classification and introduction of molecular markers	4
1.2.3 Glioblastoma.....	6
1.2.3.1 Molecular subclassification.....	7
1.2.3.2 Standard of care therapy.....	9
1.3 Glioma stem cells	12
1.3.1 Cancer stem cell description and hypothesis	12
1.3.2 Evidences of CSCs and GSCs	13
1.3.3 NSCs in the adult mammalian brain	14
1.3.4 Similarities and differences between NSCs and GSCs	16
1.3.5 Cell of origin in gliomas.....	17
1.3.6 Models used to characterise GSC phenotypes and their caveats	18
1.3.6.1 Markers used for GSC enrichment.....	18
1.3.6.2 Tumour-sphere formation assay.....	19
1.3.6.3 <i>In vivo</i> models in GSCs	20
1.3.7 GSCs and their microenvironment regulation.....	21
1.3.8 Tumour recurrence and GSC therapies.....	23
1.4 ZEB1, SOX2, OLIG2– key stemness regulators of GSCs	26
1.4.1 ZEB1	26
1.4.2 SOX2	28
1.4.3 OLIG2	29
1.4.4 Cross-regulation interdependency of ZEB1, SOX2 and OLIG2.....	31
1.5 FGF-FGFR signalling pathway	33
1.5.1 FGF family members	33
1.5.2 FGF2 functions in the developing and adult brain	34
1.5.3 FGFR family and structure.....	35
1.5.4 FGFR signalling pathway.....	38
1.5.5 FGFR signalling pathway regulation.....	39
1.5.6 FGF-FGFR signalling in glioblastoma.....	41
1.5.6.1 FGF2 in glioblastoma	41
1.5.6.2 FGF2 function in GSC propagation <i>in vitro</i>	42
1.5.6.3 FGFR alterations in carcinogenesis and glioblastoma	43
1.5.6.4 Anti-FGFR therapies in glioblastoma.....	46
1.6 Thesis hypothesis and aims	48
Chapter 2: Materials and Methods	49
2.1 Tissue culture	50
2.1.1 Human cell lines	50
2.1.1.1 Primary human glioblastoma cells.....	50

2.1.1.2	Human Embryonic Kidney 293T cell line.....	51
2.1.1.3	Cell propagation	51
2.1.1.4	Differentiation of glioma stem cell progeny.....	52
2.1.2	Cell storage, cryopreservation and freeze-thaw recovery	53
2.1.3	Coating plates with Geltrex.....	53
2.1.4	Sphere-formation assay.....	53
2.1.5	Colony Forming Cell (CFC) assay	54
2.1.5.1	Limiting dilution CFC assay	54
2.1.6	Proliferation rate	54
2.1.7	FGF2 inhibitors	55
2.1.8	MTT assay	55
2.1.9	ERK1/2 inhibitor	56
2.2	Plasmids and DNA preparation	56
2.2.1	DNA vectors.....	56
2.2.2	DNA isolation and purification.....	58
2.3	DNA transformation and ligation.....	58
2.4	Gateway cloning system	58
2.4.1	LR recombinant reaction.....	58
2.4.2	Expression vector verification and amplification	60
2.5	Transfection.....	62
2.6	Production of lentiviral particles	62
2.6.1	Transfection and ultracentrifugation	62
2.6.2	Titration of lentiviral vectors	63
2.7	Lentiviral transduction of hGBM cells	64
2.8	Protein isolation and preparation of cell lysates	64
2.8.1	Protein isolation	64
2.8.2	Protein quantification	65
2.8.3	Protein separation and transfer to polyvinylidene difluoride (PVDF) membrane	65
2.8.4	Protein blotting and visualization	66
2.9	PathScan Intracellular Signalling Array Kit.....	67
2.9.1	Cell lysates	67
2.9.2	Assay procedure.....	68
2.9.3	Bound antibody detection by chemiluminescence.....	68
2.10	Orthotopic patient-derived glioblastoma xenografts	69
2.10.1	Mouse strain and husbandry	69
2.10.2	Preparation of cells for implantation	69
2.10.2.1	Genetically modified hGBM cells.....	69
2.10.2.2	Sorted cell populations	69
2.10.3	Intracranial implantation.....	69
2.10.4	Tumour growth monitoring.....	70
2.10.5	Perfusion fixation and tissue harvesting	72
2.10.6	Cryopreservation	74
2.11	Immunofluorescence of brain sections	74
2.11.1	Blocking and antibody incubation	74
2.11.2	Mounting of immunofluorescence sections.....	75
2.12	Flow cytometry and cell sorting	75
2.12.1	Extracellular single cell staining.....	75
2.12.2	Detection of apoptosis by annexin V	76
2.12.3	Cell Sorting	77
2.12.4	Purification of transduced cells	77
2.12.5	FGFR1 + and FGFR1- sorting	78
2.13	Image acquisition.....	78
2.14	Image data analysis	78
2.14.1	Quantification of KD percentage by immunofluorescence tissue staining	78
2.14.2	<i>In vivo</i> invasion index.....	79
2.14.3	Tumour-formation frequency analysis of hGBM LDA implants.....	79
2.15	Bioinformatics	80
2.16	Hierarchical cluster analysis.....	80
2.17	Statistical testing	81
2.18	Products supplier list	82

Chapter 3: Assessing the role of FGF2 in the regulation of stem-cell associated transcription factors ZEB1, SOX2 and OLIG2	83
3.1 Introduction	84
3.2 Aims and objectives	85
3.3 Results	86
3.3.1 FGF2 induces expression of stem cell-associated transcription factors	86
3.3.2 FGF2 induces sphere-formation capacity	87
3.3.3 Association of FGFRs with stem cell transcription factors using TCGA data analysis	90
3.3.4 Expression analysis of FGFRs in patient-derived GBM cells	92
3.3.5 FGFR1 expression decreases in differentiated hGBM cells	93
3.4 Discussion	95
Chapter 4: Investigating the role of FGFR1-3 in GSC regulation	99
4.1 Introduction	100
4.2 Aims and objectives	101
4.3 Results	102
4.3.1 <i>FGFR1</i> knockdown impairs hGBM cell proliferation and clonogenic capacity	102
4.3.2 Functional rescue of sh <i>FGFR1</i> by targeted expression of this receptor	105
4.3.3 Endogenous <i>FGFR1</i> promotes clonogenic capacity	106
4.3.4 <i>FGFR1</i> knockdown increases survival of tumour-bearing mice	107
4.3.5 Limiting dilution orthotopic xenografts indicate <i>FGFR1</i> is enriched in GSCs	110
4.3.6 <i>FGFR1</i> expression correlates with poor patient outcome in GBM	112
4.3.7 <i>FGFR1</i> knockdown reduces invasion in GBM xenografts	113
4.4 Discussion	115
Chapter 5: FGF2 signals through FGFR1 and ERK1/2 to regulate stemness-associated transcription factors	119
5.1 Introduction	120
5.2 Aims and objectives	121
5.3 Results	122
5.3.1 <i>FGFR1</i> regulates stem cell transcription factors in GBM	122
5.3.2 ERK1/2, STAT3 and p38 phosphorylation increases after FGF2 stimulation	124
5.3.3 <i>FGFR1</i> regulates ERK1/2 phosphorylation	126
5.3.4 ZEB1 is regulated by ERK1/2 signalling	128
5.4 Discussion	129
Chapter 6: Conclusions	133
6.1 FGF2 is associated with stemness-related transcription factors	134
6.2 FGFR2 and FGFR3 do not regulate GSCs	134
6.3 FGF2-FGFR1-ERK1/2 signalling as therapeutic target in GBM	135
6.4 FGFR1 controls the release of FGF2 through ADAMDEC1	137
6.5 Future directions	138
References	140

List of tables

Table 1.1. Common <i>FGFR</i> genomic aberrations in solid tumours.....	43
Table 2.1. Stock concentrations.....	52
Table 2.2. Cell culture medium and feeding solution components.....	52
Table 2.3. FGF2 inhibitor stock concentration.....	55
Table 2.4. FGFRs and ZEB1 Knockdown sequences.....	57
Table 2.5. LR recombinant reaction set up.....	59
Table 2.6. Restriction enzyme digestion.....	60
Table 2.7. Components required for lentiviral production.....	63
Table 2.8. Standard concentrations used for Bradford assay.....	65
Table 2.9. Western Blot antibody list.....	67
Table 2.10. Health monitoring score chart.....	71
Table 2.11. List of antibodies used for immunostaining.....	75
Table 2.12. List of antibodies used for flow cytometry and cell sorting.....	78
Table 2.13. Products supplier list.....	82

List of figures

Figure 1.1. Simplified overview of adult glioma development and classification.....	6
Figure 1.2. Schematic representation of the clonal evolution and CSC/hierarchical models.....	13
Figure 1.3. Summary of the similarities and differences between NSCs and GSCs.....	16
Figure 1.4. Schematic representation of <i>in vitro</i> and <i>in vivo</i> models used to characterised GBM cells..	21
Figure 1.5. Regulation of GSCs by intrinsic and extrinsic forces.....	23
Figure 1.6. Representation of ZEB1 transcription factor.....	26
Figure 1.7. Transformation of immortalized astrocytes.....	31
Figure 1.8. FGFR structure.....	35
Figure 1.9. Schematic representation of Ig-III splice isoforms (IIIb/IIIc).....	37
Figure 1.10. FGFR signalling pathway.....	39
Figure 1.11. FGFR signalling pathway regulation.....	40
Figure 1.12. FGFR1 splice isoforms in GBM.....	45
Figure 2.1. pGIPZ shRNA lentiviral vector map.....	57
Figure 2.2. Gateway cloning technology.....	59
Figure 2.3. Vector maps used for gateway cloning.....	61
Figure 2.4. Digestion analysis with Xho1 and Cla1 of a FGFR1 expression construct created by LR reaction of an entry clone.....	61
Figure 2.5. Intracranial injection representation.....	70
Figure 2.6. Mice ear code per cage.....	72
Figure 2.7. Representation of mouse transcardial perfusion fixation.....	73
Figure 2.8. Detection of apoptosis using annexin-V.....	76
Figure 2.9. Purification of transduced cell populations.....	77
Figure 2.10. Representative image of an invasive tumour.....	80
Figure 3.1. FGF2 is associated to stemness in GBM	86
Figure 3.2. FGF2 induces sphere-formation capacity of GSCs.....	87
Figure 3.3. Pharmacological inhibition of FGF2 reduces sphere/colony-formation capacity <i>in vitro</i>	88
Figure 3.4. FGF2 inhibitor is not toxic to patient-derived hGBM cells.....	89
Figure 3.5. Hierarchical clustering of TCGA data.....	91
Figure 3.6. FGFR expression and population in patient-derived hGBM cells.....	92
Figure 3.7. Differentiation of GSCs.....	94
Figure 3.8. Diagram depicting the role of FGF2 in GSCs.....	98
Figure 4.1. Knockdown validation of human short hairpin constructs against <i>FGFR1</i> , <i>FGFR2</i> and <i>FGFR3</i> (shFGFR1-3).....	102
Figure 4.2. <i>FGFR1</i> knockdown reduces sphere-forming capacity.....	103
Figure 4.3. <i>FGFR1</i> knockdown decreases clonogenic capacity and proliferation.....	104
Figure 4.4. <i>FGFR1</i> overexpression increases sphere formation in control and <i>FGFR1</i> knockdown cells.....	105

Figure 4.5. FGFR1+ cells induce colony-formation.....	106
Figure 4.6. <i>FGFR1</i> knockdown increases survival of tumour-bearing mice.....	108
Figure 4.7. <i>FGFR2</i> and <i>FGFR3</i> knockdown effects on survival of tumour-bearing mice.....	109
Figure 4.8. Limiting dilution orthotopic xenografts.....	111
Figure 4.9. Correlation of <i>FGFR</i> expression with patient survival.....	112
Figure 4.10. <i>FGFR1</i> knockdown reduces tumour invasion.....	114
Figure 4.11. Diagram depicting the role of FGFR1-3 in GSCs.....	118
Figure 5.1. FGFR1 knockdown decreases ZEB1, SOX2 and OLIG2 expression while the inverse effect is seen after FGFR1 overexpression.....	122
Figure 5.2. ZEB1, SOX2 and OLIG2 expression in FGFR1 knockdown cells is rescued after FGFR1 overexpression.....	123
Figure 5.3. FGFR1 is endogenously associated with a stem cell population.....	124
Figure 5.4. PathScan intracellular signalling-array map.....	125
Figure 5.5. Intracellular signalling array of hGBM L0 cells.....	126
Figure 5.6. FGFR1 knockdown decreases ERK1/2 phosphorylation.....	127
Figure 5.7. ERK1/2 inhibitor, SCH772984, reduces ZEB1 expression.....	128
Figure 5.8. FGF2-FGFR1 axis regulates ZEB1 through ERK1/2 signalling cascade.....	132
Figure 6.1. Diagram depicting the FGF2-FGFR1-ZEB1 signalling pathway described in this thesis.....	136
Figure 6.2. Diagram depicting the ADAMDEC1-FGFR1-ZEB1 feedback loop.....	138

Abbreviations

Symbols

α = Alpha

β = Beta

$^{\circ}\text{C}$ = Degrees Celsius

μg = Microgram

μL = Microlitre

μm = Micrometre

μM = Micromolar

- = Negative

+ = Positive

A

A = Amp

AB = Acidic box

ADAM = A desintegrin and metalloproteinase

ADAMDEC = A disintegrin and metalloproteinase domain-like protein decysin

AKT = AKT serine/threonine kinase

ALDH = Aldehyde dehydrogenase

AML = Acute myeloid leukaemia

Amp^R = Ampicillin resistance gene

ANOVA = Analysis Of Variance

ASCL1 = Achaete-scute complex-like 1

ASPA = Animals (Scientific Procedures) Act 1986

ATP = Adenosine triphosphate

ATRX = Alpha thalassemia/mental retardation syndrome X-linked

B

BAD = Bcl-2-associated death promoter protein

bHLH = Basic helix-loop-helix

BMP = Bone morphogenetic protein

BSA = Bovine serum albumin

C

Ca^{2+} = Calcium ions

ccdB = Control of cell death B (gene)

CD133 = Prominin1

CDKN2 = Cyclin dependent kinase Inhibitor 2

CFC = Colony forming Cell

Chk1/2 = Checkpoint Kinase 1/2

CID = Central interactive domain

CmR = Chloramphenicol resistance gene

CNS = Central nervous system

CO_2 = Carbon dioxide

cPPT = Central polypurine tract

CSC = Cancer stem cell

CtBP = C-terminal-binding protein

CTS = Central termination sequence

CZF = C terminal zinc finger

D

DAPI = 4',6-diamidino-2-phenylindole

DCX = Doublecortin

ddH₂O = Double-distilled water

DLX2 = Distal-less homeobox 2

DMEM/F-12 = Dulbecco's Modified Eagle Medium/Nutrient Mixture F-12

DMSO = Dimethyl sulfoxide

DNA = Deoxyribonucleic acid

DOCK1 = Deducator of cytokinesis protein 1

DTI = Diffusion tensor imaging

DTP = Developmental therapeutics program

E

ECL = Enhanced chemiluminescence

ECM = Extracellular matrix

ECSCRI = European Cancer Stem Cell Research Institute

EDTA = Ethylenediaminetetra-acetic acid

EF-1 α = Elongation factor-1 α

EGF = Epidermal growth factor

eGFP = Enhanced Green Fluorescent Protein

EGFR = Epidermal growth factor receptor

EGFRvIII = EGFR variant III
ELDA = Extreme limiting dilution analysis
ELISA = Enzyme-linked immunosorbent assay
EMT = Epithelial–mesenchymal transition
ERK = Extracellular signal-regulated kinase
ESRP1/2 = Epithelial splicing regulatory proteins1/2
EtOH = Ethanol

F

FACS = Fluorescence activated cell sorting
FBS = Foetal bovine serum
FDA = Food and Drug Administration
FGF = Fibroblast growth factor
FGF2 = Fibroblast growth factor-2
FGFR1/2/3/4 = Fibroblast growth factor receptor 1/2/3/4
FITC = Fluorescein-5-isothiocyanate
FRS2 = Fibroblast growth factor receptor Substrate 2
FUBP= Far upstream element-binding protein

G

GABRA1= Gamma-aminobutyric acid receptor subunit alpha-1
GAG = Glycosaminoglycan
GAPDH = Glyceraldehyde 3-phosphate dehydrogenase
GBM = Glioblastoma
G-CIMP = Glioma CpG island methylator phenotype
GF = Growth factor
GFAP = Glial fibrillary acidic protein
GFP = Green fluorescent protein
GKRS = Gamma knife radiosurgery
GLAST = Glutamate–aspartate transporters
GRB2 = Growth factor receptor bound 2
GSEA = Gene set enrichment analysis
GSC = Glioma stem cell

H

h= hour
HBS = Heparin binding site
HBSS = Hank's balanced salt solution
HCl = Hydrogen chloride
hCMV = Human cytomegalovirus
HD = Homeodomain
HEK = Human embryonic kidney
hGBM = Human glioblastoma
HGCC = Human glioma cell culture
HIF-1/2 α = Hypoxia-inducible factor 1/2 α
HIV = Human immunodeficiency virus
hnRNPs = Heterogeneous nuclear ribonucleoproteins
HPSE = Heparanase
HRP = Horseradish peroxidase
HS = Heparan sulfate
HSP27 = Heat shock protein 27
HSPG = Heparin/Heparan sulfate proteoglycan
HTA = Human Tissue Authority

I

IDH1/2 = Isocitrate dehydrogenase 1/2
Ig = Immunoglobulin
IL-2 = Interleukin-2
IP3 = Inositol-1,4,5-trisphosphate
IRES = Internal ribosomal entry site

J

JNK = C-Jun N-terminal kinase

K

KLF4 = Kruppel-like factor 4

L

LASA = Laboratory Animal Science Association
LB = Lysogeny broth
LDA = Limiting dilution cell transplantation assay

LTR = Long termination repeat

M

MAPK = Mitogen-activated protein kinase

MET= Mesenchymal–epithelial transition

MFI =Mean fluorescence intensity

mg = milligram

MGMT = O6-methylguanine DNA

methyltransferase

min = minute

MKP1/3 = Mitogen-activated protein kinase
phosphatase 1 /3

mL = millilitre

mm = millimetre

mM = millimolar

MOI = Multiplicity of infection

mRFP = Monomeric red fluorescence protein

MRI = Magnetic resonance imaging

mRNA = Messenger ribonucleic acid

mTOR = Mechanistic target of rapamycin
kinase

MTT = Thiazolyl blue tetrazolium bromide

N

n = Number of biological replicates

NACWO = Named Animal Care & Welfare
Officer

NADP+ = Nicotinamide adenine dinucleotide
phosphate

NADPH= Dihyronicotinamide-adenine
dinucleotide phosphate

NCI = National Cancer Institute

NEB = New England Biolabs

NEFL = Neurofilament, light polypeptide

NF1= Neurofibromin 1

NF-κB =Nuclear factor kappa-light-chain-
enhancer of activated B cells

ng = nanogram

NG2 = Neural-glia antigen 2

NIH = National Institutes of Health

nm = nanometre

nM = nanomolar

NSC = Neural stem cell

NVS = Named Veterinary Surgeon

NZF = N-terminal zinc finger

O

O₂ = Oxygen

OCT = Optimal Cutting temperature

OCT4 = Octamer-binding transcription factor 4

OD = Optical density

OLIG1/2 = oligodendroglial lineage-associated
transcription factors 1/2

P

p = Phospho

P53 = Protein 53

PAGE = Polyacrylamide gel electrophoresis

PARP = Poly(ADP-ribose) polymerase

PBS = Phosphate buffered saline

PBS-T = Phosphate buffered saline-tween 20

PCR = Polymerase chain reaction

PDGF = Platelet-derived growth factor subunit
PDGFR = Platelet-derived growth factor
receptor

pH = Potential hydrogen

PIC = Protease inhibitor cocktail

PIC2/3 = Phosphatase inhibitor cocktail 2/3

PI3K = Phosphatidylinositol-3-kinase

PIP2/3 = Phosphatidylinositol 4,5-
bisphosphate 2/3

PKC = Protein kinase C

PLC = Phospholipase C

PMSF = Phenyl methane sulfonyl fluoride

POU3F2 = POU Class 3 transcription factor 2

PS = Phosphatidylserine

PTEN = Phosphatase and tensin homolog

p-value = Probability value

PVDF = Polyvinylidene difluoride

R

RBP = RNA-binding protein
RFP = Red fluorescent protein
RIPA = Radio immunoprecipitation assay
RNA = Ribonucleic acid
RNA-seq = RNA-sequencing
rpm = Revolutions per minute
RRE = Rev response element
RT = Room temperature
RTK = Receptor tyrosine kinase

S

SALL2 = Spalt-like transcription Factor 2
SBD = Smad-binding domain
SCID = Severe combined immunodeficient
SDS = Sodium dodecyl sulfate
SDS-PAGE = Sodium dodecyl sulfate
polyacrylamide gel electrophoresis
SEM = Standard error of mean
SGZ = Subgranular zone
Sh = Short hairpin
SHH = Sonic hedgehog
shRNA = Short hairpin RNA
SOX2 = Sex determining region Y-box 2
SPRY = Sprouty
SR = Serine/Arginine-Rich
SSEA1= Stage-specific embryonic antigen-1
STAT = Signal transducer and activator of
transcription
STR = Short tandem repeat
SV40 = Simian virus 40
SVZ = Subventricular zone
SYT1= Synaptotagmin-1

T

TACC1/3 = Transforming acidic coiled-coil
containing Protein 1/3
TBS = Tris-buffered saline
TBS-T = Tris-buffered saline-0,1% Tween
TCGA = The Cancer Genome Atlas
TE = Tris-EDTA
TGF- β = Transforming growth factor- β

TGX = Tris-Glycine eXtended
TK1/2 = Tyrosine kinases 1/2
TKI = Tyrosine kinase inhibitor
TMZ = Temozolomide
TNF- α = Tumour necrosis factor- α
TPN = Transferrin-putrescine-sodium selenite
Tris-HCl = Tris hydrochloride
Trp53 = Transformation related protein 53
TTF = Tumour-treating fields
TUs = Transduced units

U

UCSC = University of California, Santa Cruz
UK = United Kingdom
USA = United States of America
UTR = Untranslated region

V

V = Volt
VEGF = Vascular endothelial growth factor
VEGFR = Vascular endothelial growth factor
receptor
v/v = Volume per volume

W

WGS = Whole genome sequencing
WHO = World Health Organization
WNT = Wingless
WPRE = Woodchuck hepatitis
posttranscriptional regulatory element
w/v = Weight per volume

X

xg = Centrifugal force

Y

YAP = Yes-associated protein

Z

ZEB1= zinc finger E-box binding homeobox 1

Chapter 1 : Introduction

1.1 Glial cells and their function in the adult brain

Glial cells were first distinguished from neurons by Rudolf Virchow in 1856 who described them as the “Nerven Kitt” or “nerve glue” of the brain (Kettenmann and Verkhratsky 2013; Jäkel and Dimou 2017). Although initially, glial cells were thought to only have passive roles, their importance in brain development and cooperation with neurons has been highlighted through research over the past few decades. They constitute 90% of the central nervous system (CNS) cells and are subdivided into astrocytes, oligodendrocytes and microglia (Baumann and Pham-Dinh 2001; Paw *et al.* 2015; Jäkel and Dimou 2017). Astrocytes and oligodendrocytes are derived from neural stem cells (NSCs), while microglia originate from hematopoietic cell precursors (Paw *et al.* 2015).

Astrocytes were first identified through the microscopic studies and drawings by Ramon y Cajal who described them as “star-like cells” (Ramón y Cajal 1913). Generally, astrocytes are characterised by their GFAP expression and interaction with capillaries (Kettenmann and Verkhratsky 2013). Astrocytes are the most abundant cells in the CNS and have the essential role of giving support and maintaining the structure of the brain parenchyma (Jäkel and Dimou 2017). In addition, they reinforce neurotransmission and synaptogenesis, and control local blood flow, providing neurons with the required metabolic support (Araque and Navarrete 2010; Vasile *et al.* 2017).

Oligodendrocytes and microglia were first described by Rio-Hortega (Rio-Hortega 1921; Rio-Hortega 1928). Functionally, oligodendrocytes are responsible for the generation of the myelin sheath that encases neuronal axons of the CNS, which is necessary for the conduction of nerve impulses. They also regulate axon growth, regeneration and maintenance (Baumann and Pham-Dinh 2001). Some oligodendrocytes, such as satellite oligodendrocytes, do not possess myelination capacity and control ionic homeostasis instead (Kettenmann and Verkhratsky 2013). On the other hand, microglia play an immunodefensive role and protect the brain from pathogens (Wake *et al.* 2012). Moreover, they are responsible for shaping neural circuits during development and neurogenesis as they control the appropriate function of synaptic connections (Allen and Barres 2009). Therefore, glial cells are crucial for

brain function and homeostasis and their default and/or deregulation can lead to brain injuries, lesions and tumours such as gliomas.

1.2 Gliomas

Gliomas are the most common primary brain tumours of the CNS (Goodenberger and Jenkins 2012). Despite a very small proportion of them derive from rare inherited syndromes, they usually occur sporadically (Schwartzbaum *et al.* 2006; Bondy *et al.* 2008). Gliomas are normally diagnosed by Magnetic Resonance Imaging (MRI) once the patient suffers neurologic symptoms such as headaches, seizures, aphasia and visual-field deficits among others (DeAngelis 2001; Noushmehr *et al.* 2010). The specific cell-of-origin of this heterogeneous disease is not yet completely understood. Nonetheless, previous studies have suggested that these tumours are derived from astroglial cells. Although gliomas were initially classified by their etiology, location and aggressiveness, their categorization has broadly changed in the past decades (Paw *et al.* 2015).

1.2.1 WHO classification of gliomas

The World Health Organization (WHO) Executive Board and World health assembly, initiated between 1956 and 1957, the process required to publish a classification of the existing human cancers (Louis *et al.* 2007). Clinicians and scientists used histopathological criteria, clinical outcome and patient survival data to organise tumours into grades with the objective to facilitate and improve the existent clinical trials and tumour diagnosis worldwide. The first classification of CNS tumours was not published until 1979 (Kleihues *et al.* 1993). Among the different CNS tumours, gliomas are classified, according to their presumed cell-of-origin and their histological and clinical features, into four broad groups: oligodendrogliomas, brain stem gliomas, ependymomas and astrocytomas, the latter being the most common form of glioma (Parpura *et al.* 2012; Otani *et al.* 2017). In addition, they are organised from low- to high-grade (I-IV) according to malignancy. Grade I pilocytic astrocytomas do not normally progress towards more malignant gliomas, have well-defined borders, do not invade the surrounding tissue, and have a good prognosis after surgical resection (Louis *et al.* 2007; Watanabe *et al.* 2009). Grade II-III (oligodendrogliomas and astrocytomas) and IV (glioblastomas; GBM) gliomas, are called diffuse or infiltrative

gliomas as they have a higher invasion capacity and therefore a poorer prognosis (Ceccarelli *et al.* 2016). Low-grade diffuse gliomas (II) occur in early adult life (40s) and are slow-proliferating, well-differentiated tumours with low mitosis activity and a lack of necrosis (Watanabe *et al.* 2009; Vigneswaran *et al.* 2015; Modrek *et al.* 2017). When treated, patients diagnosed with oligodendrogliomas have better prognosis than those with diffuse astrocytomas as they have a survival rate of 62% and 37% respectively at 10 years post-diagnosis (Weller *et al.* 2015). However, this rate decreases to 39% and 19% in anaplastic oligodendroglioma and anaplastic astrocytoma, which are both grade III gliomas (Ohgaki and Kleihues 2007; Vigneswaran *et al.* 2015; Weller *et al.* 2015). Grade III gliomas are described as high vascularized tumours with an invasive capacity and high mitotic activity. They normally progress to grade IV gliomas, termed GBMs, which constitute 55% of adult gliomas. GBMs have similar characteristics to grade III gliomas, although they acquire higher endothelial cell proliferation and necrosis which generates the least favourable prognosis among brain tumours (Goodenberger and Jenkins 2012). GBM will be further reviewed in section 1.2.3.

1.2.2 Updated WHO classification and introduction of molecular markers

After the first brain tumour WHO classification, updated editions have been published due to the development of new technologies such as whole genome sequencing (WGS), mRNA sequencing and whole genome methylation profiling. Deeper investigations, which have led to an improved characterisation and definition of each brain tumour entity, have made possible the evolution from a subjective histopathological criteria to a more molecular analysis as described in the last revised CNS classification system provided by WHO in 2016 (Louis *et al.* 2016; Otani *et al.* 2017). Despite, several studies have proposed other ways of organising these tumours in the last few years (Ceccarelli *et al.* 2016; Capper *et al.* 2018) and it is possible that a new updated version of the WHO classification is in progress, in this section we will focus on the 2016 WHO edition as it is the currently use criteria for defining grading in gliomas (Louis *et al.* 2016). The 2016 classification combines histological parameters with genetic information, aiming to reach more accurate diagnosis and design precise treatments for brain tumours. The main highlight of this classification is the organization of diffuse gliomas by the presence of genomic lesions,

specifically point mutations in isocitrate dehydrogenase 1 (*IDH1*) and 2 (*IDH2*) (DeAngelis 2001; Cohen *et al.* 2013; Louis *et al.* 2016). IDHs are homomeric enzymes that catalyse the reversible conversion of isocitrate into alpha-ketoglutarate (reducing NADP⁺ to NADPH and producing CO₂) and are important in regulating oxidative stress (Balss *et al.* 2008; Losman and Kaelin 2013). *IDH1* and *IDH2* alterations occur in the arginine at positions 132 and 172 respectively, located in the binding site of the isocitrate (Balss *et al.* 2008; Frezza *et al.* 2010). These mutations were first characterised by Parsons *et al.* who found that 12% of the analysed GBMs contained *IDH1* mutations (Parsons *et al.* 2008). *IDH2* mutations are not as common as *IDH1* (90% of gliomas) and are found in 3% of glial tumours (Cohen *et al.* 2013; Otani *et al.* 2017). *IDH1* mutants acquire the ability to reduce alpha-ketoglutarate into a new product, 2-hydroxyglutarate, that accumulates in gliomas and behaves as an “onco-metabolite” (Dang *et al.* 2009; Cohen *et al.* 2013; Otani *et al.* 2017).

In total, 80%-90% of low-grade gliomas (II-III) and secondary adult GBMs (IV) were reported to have *IDH1* mutations (Dang *et al.* 2009; Toedt *et al.* 2011; Losman and Kaelin 2013); on the other hand, these mutations were expressed in only 10-12% of primary GBMs (Balss *et al.* 2008). This finding implies that IDH-negative low-grade gliomas and IDH-positive primary GBMs are potentially misdiagnosed. *IDH1* mutations are present in 65% of astrocytomas, before they show loss of *TP53* and *ATRX*. In the case of oligodendrogliomas, this mutation appears before the loss of *CIC/FUBP1* and chromosome 1p/19q (70%), which is the defining molecular characteristic for oligodendrogliomas (Goodenberger and Jenkins 2012; Vigneswaran *et al.* 2015; Van Den Bent *et al.* 2017). Both findings suggest that the *IDH1* mutation is an essential genomic alteration for lower-grade gliomas and occurs in the early stages of tumour development (Watanabe *et al.* 2009; Toedt *et al.* 2011; Cohen *et al.* 2013). Despite being one of first and most common mutations in gliomas, it is not independently capable of tumour formation (Losman and Kaelin 2013; Johannessen *et al.* 2016). Therefore, it has been described as an oncogenic driver which requires other mutations to maintain gliomagenesis. Importantly, the accumulation of 2-hydroxyglutarate makes the cells more sensitive to radiation and toxic to therapies targeting metabolic molecules, thus generating a better prognosis (Frezza *et al.* 2010; Cohen *et al.* 2013; Johannessen *et al.* 2016). Based on this, aside from being histologically classified in grades, diffuse gliomas are now divided into three

subclasses according to an *IDH* wild-type status, presence of *IDH* mutations and not otherwise specified when *IDH* tests are not available (**Figure 1.1**).

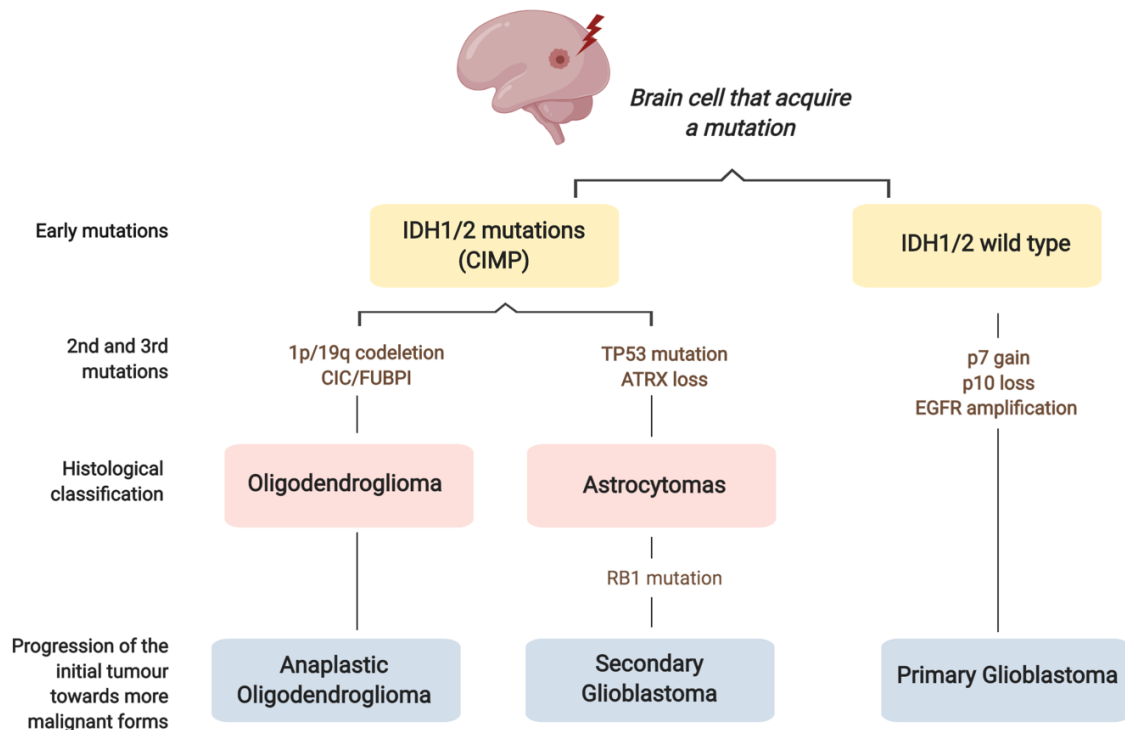


Figure 1.1. Simplified overview of adult glioma development and classification. Acquired somatic mutations occur progressively and their accumulation induces molecular changes in brain cells, leading to their malignant transformation into tumour cells. *IDH1/2* mutations are considered early mutations in glioma development and have been used to classify these tumours (WHO classification 2016). Secondary mutations, in addition to *IDH* mutations, lead the progression of gliomagenesis to specific tumour types; some mutations will promote the formation of oligodendrogliomas, while others will generate astrocytomas. These tumours will further progress towards more malignant forms like anaplastic oligodendrogliomas and secondary GBM. Cells lacking *IDH* mutations, but with alterations in chromosomes 7 and 10 and *EGFR* amplifications, form primary GBM. This histological and genetic classification can be complemented by the Verhaak *et al.* molecular classification of GBMs and unifying studies on molecular characterisation of low-grade and high-grade gliomas (Verhaak *et al.* 2010; Ceccarelli *et al.* 2016). Adapted image from Louis *et al.* 2016 and created with biorender.com

1.2.3 Glioblastoma

GBM is the most common and malignant brain cancer in adults (DeAngelis 2001; Sutter *et al.* 2007; Paw *et al.* 2015; Weller *et al.* 2015). It exhibits the poorest prognosis among gliomas with a median survival of 20 months following treatment (Stupp *et al.* 2009; Weller *et al.* 2017; Wick *et al.* 2017). GBM is more frequent in men than in women, and each year 3 out of 100,000 people are newly diagnosed worldwide. Although more than 50% of GBMs occur in older adults (50-60 year olds), there are

also diagnoses in young adults (approximately 45 years of age) and children (Weller *et al.* 2015). GBM is characterised by a rapid and uncontrolled infiltrative growth, high mitotic activity, pleomorphic cells, angiogenesis, cellular heterogeneity, and pseudopalisading necrosis (Olar and Aldape 2014; Pisapia 2017). GBM can be detected and diagnosed by Diffusion Tensor Imaging (DTI) and MRI, the latter showing a very invasive and infiltrative profile with irregular tumour shape, which reflects the capacity of this tumour to diffuse into the brain parenchyma, white matter and corpus callosum of both hemispheres (DeAngelis 2001; Paolillo *et al.* 2018). In young adults, this tumour most commonly arises either from a pre-existing lower-grade glioma (WHO II or III), called secondary GBM, or can rapidly develop *de novo* in 90% of diagnosed cases as a primary GBM (Peiffer and Kleihues 1999; DeAngelis 2001; Galli *et al.* 2004; Sutter *et al.* 2007). Although both primary and secondary GBM have similar histopathological characteristics and prognosis, they acquire different genomic alterations (Toedt *et al.* 2011). Secondary GBM is characterised, as previously mentioned, by *IDH1* mutations, followed by the acquisition of mutant *TP53* and less frequent loss of 10q, *PDGFR* overexpression, and promoter methylation of *MGMT* (Toedt *et al.* 2011; Ohgaki and Kleihues 2013). Meanwhile, primary GBM is featured by *EGFR* amplification (30%-40%) and *PTEN* deletions found in 80% of the cases (Goodenberger and Jenkins 2012; Vigneswaran *et al.* 2015).

1.2.3.1 Molecular subclassification

Since glioma clinicopathological and histological classification is not always representative of the tumour malignancy and combines different genetic subtypes within the same grade, a new GBM classification, based on large-scale gene expression, copy number, and methylation profiles, was suggested by Verhaak *et al.* (Verhaak *et al.* 2010). The data was collected by The Cancer Genome Atlas (TCGA) project 2008 that aimed to analyse a multitude of patient samples at the DNA, mRNA, and micro-RNA level, acquiring information about the molecular characteristics that drive tumour transformation (The Cancer Genome Atlas Network 2008; Meir *et al.* 2010). This classification divides GBM according to the expression of signature genes in four different subtypes: classical, mesenchymal, proneural and neural GBM (Verhaak *et al.* 2010; Paolillo *et al.* 2018). Classical tumours are characterised by chromosome 10 loss, chromosome 7 and *EGFR* amplification, *EGFRvIII* mutations

and aberrations in the RB pathway. Moreover, they have high expression of neural and stem cell markers and are associated with an astrocytic signature (Verhaak *et al.* 2010). On the other hand, the mesenchymal subgroup is formed by tumours with high angiogenesis, cell necrosis (through the NF-KB pathway) and expression of inflammatory genes. In addition, *NF1*, *TP53* and *PTEN* genes are inactivated (Phillips *et al.* 2006; Meir *et al.* 2010). The proneural subtype is associated with alterations in *PDGFRA*, *P53*, *PIK3* and *IDH* mutations and it is characterised by NOTCH signalling activation and expression of proneural development genes such as *SOX2* and *DCX* (Verhaak *et al.* 2010; Ohgaki and Kleihues 2011). This subtype was also associated with younger patients, secondary GBM and an oligodendrocytic signature (Phillips *et al.* 2006; Watanabe *et al.* 2009; Verhaak *et al.* 2010). Neural GBMs are not well known and characterized but are recognised by neuronal markers and genes that are found in healthy brain tissues (*NEFL*, *GABRA1* and *SYT1*) (Meir *et al.* 2010; Ozawa *et al.* 2014). Among these subtypes, Phillips *et al.* suggested that the highest percentage of GBMs (49%) corresponded to the mesenchymal subtype (Phillips *et al.* 2006). Despite the description of this molecular classification of GBM, Sottoriva *et al.* demonstrated that most patients presented different GBM subtypes within the same tumour (Sottoriva *et al.* 2013). This highlights the high heterogeneity and evolutionary dynamics present at the patient-level and suggests the classification of GBMs in subclasses may be affected by sample bias.

DNA methylation changes have been widely reported as a hallmark of gliomas. Promoter-associated CpG islands hypermethylation along the genome has been used to further stratify GBM molecular subtypes (Noushmehr *et al.* 2010; Cohen *et al.* 2013; Ceccarelli *et al.* 2016; Johannessen *et al.* 2016). The Glioma CpG island methylator phenotype (G-CIMP) is highly enriched in 87% of proneural GBM tumours which stratifies this group as G-CIMP positive and G-CIMP negative proneural tumours. Therefore, this aggregates one more level to the molecular classification of GBMs, which now divides into G-CIMP-positive and G-CIMP-negative proneural, mesenchymal, classical and neural GBMs. G-CIMP positive tumours are diagnosed in younger patients and have better prognosis (150 weeks) than G-CIMP negative tumours (42-54 weeks). Moreover they are highly associated with *IDH1* mutations (Sturm *et al.* 2012; Ceccarelli *et al.* 2016). G-CIMP positive tumours have downregulated genes related to invasion, migration and extracellular matrix and

demonstrate some upregulated processes such as cellular metabolism and transcriptional silencing (Noushmehr *et al.* 2010). Secondary GBM has higher hypermethylation frequency than primary GBM, which suggests that secondary GBM evolves from proneural-like low-grade gliomas grade II or III which may originate by *PDGFRA* gain, *PTEN* loss and *NF1* loss, successively (Ozawa *et al.* 2014). Finally, a recent study outlined the possibility of classifying gliomas based on their methylation profile independently of tumour grade and histopathological and molecular characteristics (Capper *et al.* 2018). Thus, new brain tumour classifications have been proposed during the last few years which demonstrates that this field is subject to constant evolution. New integrated classifications will be crucial to improve further research into these tumours and ensure that patients are correctly treated with the most beneficial targeted therapies for them.

1.2.3.2 Standard of care therapy

The current standard of care for patients with GBM is maximum safe and fluorescence-guided surgical resection, followed by radiotherapy and adjuvant chemotherapy and finalised with a maintenance treatment base on chemotherapy administration for 6-12 months (Stupp *et al.* 2009; Olar and Aldape 2014; Stupp *et al.* 2015). Although radiotherapy has been used for the last four decades, new techniques such as the Gamma Knife radiosurgery (GKRS) have improved its delivery by increasing the radiation dosage and reducing the tissue necrotic areas in recurrent GBMs (Larson *et al.* 2014).

The use of temozolomide (TMZ) for treating newly diagnosed GBM patients was approved by the FDA and the EU in 2005 (Omar and Mason 2009). Addition of TMZ as a chemotherapeutic agent to radiotherapy increased patient survival by 2.5 months. TMZ is an oral alkylating agent that rapidly converts into an active form and is able to cross the blood-brain barrier. TMZ delivers its cytotoxic effect by methylating guanine and adenine residues (ex: O⁶-methylguanine) and preventing cell proliferation (Hart *et al.* 2013). Thus, it is most effective in proliferative tumour cells as they tend to cycle more rapidly, but also has side effects in normal proliferating cells (Atif *et al.* 2015). Concomitant TMZ is applied during and after radiotherapy treatment and induces cell cycle arrest in G2/M phase and DNA double-strand breaks promoting the success of radiotherapy (Stupp *et al.* 2005; Chakravarti *et al.* 2006; Paolillo *et al.* 2018). Thus, the

combination of both therapies is important to, at least temporally, reduce GBM growth (Stupp *et al.* 2009). TMZ is particularly beneficial for patients with low MGMT, as MGMT confers resistance to chemotherapy (Silber *et al.* 1998). MGMT is a crucial enzyme for genome stability because it repairs DNA lesions (ex: methylation of O⁶-position of DNA guanines) and avoids DNA replication and transcription mismatch errors (Olar and Aldape 2014). For this reason, GBM cells with low expression of MGMT and/or promoter methylation MGMT have a better prognosis and response to chemotherapy as they are not able to repair the damage cause by this alkylating agent (Quinn *et al.* 2005; Ohka *et al.* 2012). MGMT promoter methylation is common in secondary GBMs. Nonetheless, almost half of the diagnosed GBMs have MGMT overexpression which makes the current therapy ineffective for the latter (Adair *et al.* 2014). O⁶-benzylguanine (O⁶BG) has been used to treat GBM with high MGMT content and restore TMZ sensitivity by binding and marking MGMT protein for degradation or inactivation (Silber *et al.* 1998; Quinn *et al.* 2005). However, although O⁶BG may restore TMZ sensitivity in other gliomas, its addition can induce myelosuppression and/or show limited beneficial effects in GBM (Quinn *et al.* 2009).

Aside from a maintenance treatment based on TMZ alone for up to 12 months, the combination of TMZ after radiation with tumour-treating fields (TTF) has been recently tested in phase III clinical trials and approved by the FDA. TTF is a non-invasive technique based on low-intensity alternating electrical fields which disrupt tumour cell division, cause cell cycle arrest and promote apoptosis, thus reducing GBM growth (Zhu and Zhu 2017). The cytotoxic effects of TTF have been reported to be low and the treatment regime of TTF combined with TMZ seems to increase the patient median survival from 15.6 (TMZ alone) to 20.5 months (Stupp *et al.* 2015).

Although, many attempts have been made to improve the poor prognosis of GBM patient, including changes in radiotherapy delivery methods, the dosage and timing of TMZ administration, the development of gene targeting therapies like EGFR and PDGFR inhibitors and antiangiogenic drugs, the results have shown little success (Stupp *et al.* 2009). Other strategies have focused on developing therapies based on delivery of drugs in nanoparticles, immunotherapy, antibody-drug conjugated therapy, oncolytic viruses and vaccines (Paolillo *et al.* 2018). However, despite advances in new technologies, detection techniques and the progress made in other cancer types,

GBM patients present low survival times of 2-5 years in the most favourable cases (10 to 27% of the cases). The challenges of the existing therapies are based on the lack of successful targets and the difficulty of drugs passing the blood-brain barrier. Moreover, the high tumour heterogeneity generates clones of cells with different responses and resistance levels to current therapies. In addition, due to the high infiltrative characteristics of GBMs, total or complete surgical resection is impossible and post-treatment, the recurrent glioma commonly transforms into more aggressive forms. Tumour recurrence and therapeutic resistance to TMZ treatment have been linked to the existence of a population of quiescent glioma cells which are able to migrate and colonise other parts of the brain (Paolillo *et al.* 2018). This population of cells that are capable of initiating new gliomas are termed glioma stem cells (GSCs) and have become a new target to treat GBM in the last decades (Lima *et al.* 2012).

1.3 Glioma stem cells

1.3.1 Cancer stem cell description and hypothesis

To understand the concept of cancer stem cells (CSCs), it is important to first define two terms: “stem cell” and “stemness”. A stem cell, based on functional criteria, is a cell capable of self-renewal, of re-entering cell proliferation after being in a quiescent state, and of differentiating into multiple cell lineages. Stemness is the degree to which a cell retains these characteristics (Lathia and Liu 2017). Although normal stem cells and CSCs share these features, CSCs have the unusual ability to form tumours that resemble the characteristics of the primary tumour upon serial transplantation *in vivo* (Hemmati *et al.* 2003).

Two different models have been described to explain how tumour cells develop and differentiate into their progeny (Piccirillo *et al.* 2006). The first model is the stochastic or clonal evolution model which claims that all cells within a tumour are tumorigenic (Rahman *et al.* 2011). Clonal evolution describes cancer as a very complex tissue ecosystem in which clones of cells accumulate single or multiple mutations and compete for their survival (Greaves and Maley 2012), representing the Darwinian selective pressure of the most fit clone (Nowell 1976). This model highlights the importance in developing treatments that prevent the adaptive resistance of a clone once intratumoral heterogeneity has been reduced by surgical debulking and chemo- and radiotherapies (**Figure 1.2**) (Osuka and Van Meir 2017). On the other hand, the CSC model or hierarchical model is based on the presumption that only a minority of mutated cells (CSCs) are responsible for tumour initiation, invasion and metastasis (Adams and Strasser 2008; Shackleton *et al.* 2009). This model proposes the existence of a cellular hierarchy within the tumour in which only cells that can self-renew and differentiate into other tumour cells are capable of extensive proliferation and of sustaining tumour growth. Importantly, this subset of cancer cells is described as the determinant of tumour recurrence after therapy (**Figure 1.2**).

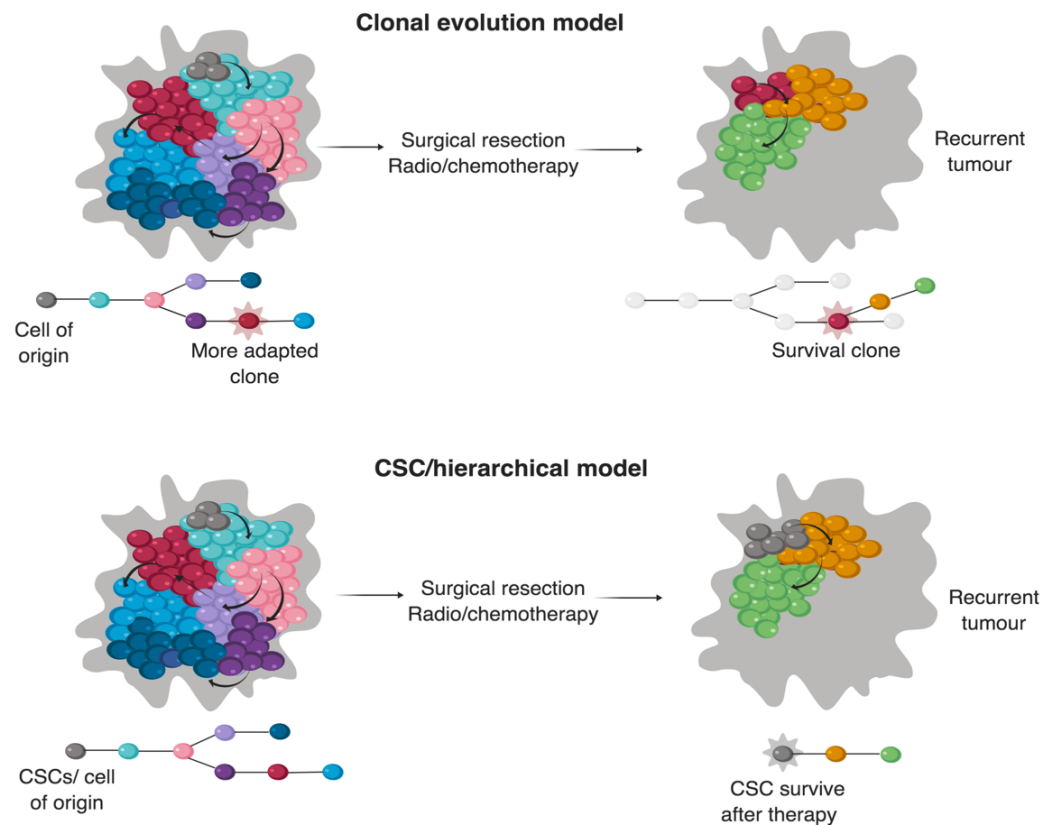


Figure 1.2. Schematic representation of the clonal evolution and CSC/hierarchical models. In the clonal evolution model, all tumour cells are capable of tumour initiation (in this image, the grey cells represent the clone of origin). However, only the most adapted clone of cells (represented by red cells) are responsible for tumour recurrence after therapy (upper panel). On the other hand, the CSC hypothesis claims the existence of a minority of cells (grey cells) capable of tumour initiation, propagation and maintenance (lower panel). These cells are the cancer stem cells (CSCs) and survive after surgical resection and radio- and chemotherapy. Image created with biorender.com.

1.3.2 Evidences of CSCs and GSCs

Although the notion of a stem cell as a possible source of cancer was first proposed more than 150 years ago by Rudolph Virchow and Julius Cohnheim (Virchow 1855; Cohnheim 1867), the term CSC primarily arises from the discovery of hematopoietic stem cells by Bonnet and Dick (Bonnet and Dick 1997). In this study, human acute myeloid leukaemia (AML) cells were separated by the expression of CD34 and CD38, which are pluripotent and lineage commitment markers, respectively. Although both CD34⁺CD38⁺ and CD34⁺CD38⁻ populations formed colonies *in vitro*, only the latter was capable of transferring AML to immune-deficient mice (Bonnet and Dick 1997), supporting the idea that a rare population of cells, expressing markers of stem cells, was capable of tumour initiation. Subsequently, different studies showed evidence of CSCs in a range of human solid tumours (Shackleton *et al.* 2009).

GSCs were first described by Ignatova *et al.* who showed that GSCs had similar stem cell features than cells from neurogenetic niches (Ignatova *et al.* 2002). This was confirmed by Singh *et al.* who demonstrated that 20% of medulloblastoma and GBM cells could form neuro-spheres and that the bulk of the tumour was heterogeneous and maintained by GSCs (Singh *et al.* 2003). Other relevant studies followed describing GSCs in GBM (Ignatova *et al.* 2002; Hemmati *et al.* 2003; Galli *et al.* 2004). GSCs have been also termed glioma/tumour initiating-cells and glioma propagating cells (Rahman *et al.* 2011; Lathia *et al.* 2015). To avoid confusion, here I will refer to GSCs as cells capable of tumour formation upon secondary transplantation, extensive self-renewal and aberrant differentiation into progeny with different tumorigenic capacity.

In order to understand GBM biology and the existent debate of the “cell-of-origin” of brain tumours, it is necessary to describe the functionality and location of adult NSCs within the adult brain.

1.3.3 NSCs in the adult mammalian brain

Traditionally, the adult mammalian brain was thought to be an organ formed by fully differentiated cells with no postnatal regenerative capacities (Sutter *et al.* 2007); this belief was termed the “no new neuron” dogma (Ramon y Cajal 1928). Some studies (Altman and Das 1965; Dacey and Wallace 1974; Kaplan and Hinds 1977) suggested in the 1950s-70s the existence of new neurons in the adult mammalian brain. However, they were ignored due to the general lack of evidence of somatic stem cells (Rahman *et al.* 2011). This concept was challenged by Reynolds and Weiss in 1992, who proposed that neurogenesis was retained during adult life and not only during development. They found a small stem cell population (<0.1%) in the mature mammalian CNS capable of forming new neurons: these cells were able to form neuro-spheres which could be dissociated and replated as single cells that would generate secondary spheres *in vitro*, maintaining their stem-like properties (Reynolds and Weiss 1992). In addition, initial reports in rodents from Luskin and Lois and Alvarez-Buylla, demonstrated that this process occurs in the adult brain within the subventricular zone (SVZ) (Luskin 1993; Lois and Alvarez-Buylla 1994; Weiss *et al.* 1996) and Cameron *et al.* showed that it also happens in the subgranular zone (SGZ)

of the hippocampus (Cameron *et al.* 1993). These concepts were crucial for the understanding of brain tumours and GSCs.

In order to understand the role of GSCs in glioma initiation and progression it is important to describe the hierarchy of cell lineages in the CNS and the markers utilised to identify these cell populations. Although cells with stem cell properties have been found in the subcortical white matter and the subcallosal zone (Sanai *et al.* 2005), neurogenesis mainly occurs in two neurogenic regions in the adult mammalian brain: the SVZ of the lateral ventricles and the SGZ of the dentate gyrus in the hippocampus, as aforementioned (Doetsch 2003; Myers *et al.* 2003; Llaguno and Parada 2016). NSCs found in those regions (also known as type B cells in the SVZ and type I cells in the hippocampus) are quiescent cells expressing GFAP and capable of persisting through asymmetric self-renewal divisions. NSCs differentiate into all brain cell types (except microglia) through the transient amplification of multipotent progenitors (termed type C and type II cells in the SVZ and SGZ, respectively) (Doetsch 2003; Sutter *et al.* 2007). Type C cells from the SVZ produce neuroblasts (Type A cells) which migrate through the rostral migratory stream and differentiate into granule cells and interneurons in the olfactory bulb (Lois and Alvarez-Buylla 1994; Doetsch 2003). On the other hand, type II cells in the SGZ differentiate into neurons that migrate into the granule cell layer (Llaguno and Parada 2016). In addition, NSCs give rise to astrocytes in the olfactory bulb and oligodendrocytes in the corpus callosum and cortex (Mich *et al.* 2014).

NSCs have been identified by the expression of markers such as GFAP, NESTIN, CD133, and SOX2, while transient amplifying progenitors express DLX2 and ASCL1 (Doetsch *et al.* 1999; Morshead *et al.* 2003; Pastrana *et al.* 2009). Glial progenitors are characterised by expression of NG2, PDGFR α , OLIG1, OLIG2, A2B5, and GLAST (Canoll and Goldman 2008; Ma *et al.* 2009; Llaguno and Parada 2016). Some of these NSCs/progenitors markers (GFAP, OLIG2, SOX2 and PDGFR α) are also expressed in GBM (Alcantara-Llaguno *et al.* 2019).

1.3.4 Similarities and differences between NSCs and GSCs

NSCs and GSCs share many properties such as self-renewal capacity, high telomerase activity (Sanai *et al.* 2005) and expression of markers characteristic of immature and undifferentiated cells like CD133, NESTIN, MSI1 and SOX2, OCT4, NANOG, CD44, ALDH, and BMI1 among others (Lathia and Liu 2017) (**Figure 1.3**). They both proliferate and form neuro/tumour-spheres in non-adherent conditions and under the effect of growth factors (EGF and FGF2). However, spheres derived from NSCs can be cultured *in vitro* for less time and have lower expression of BMI1 (Hemmati *et al.* 2003). GSCs, but not NSCs, have genetic and epigenetic mutations that lead to dysregulation of pathways controlling stem cell properties (**Figure 1.3**). In particular, pathways regulating NSC self-renewal capacity and multipotency (SHH-GLI) (Bai *et al.* 2002), motility (PTEN) (Li *et al.* 2003), proliferation (BMI1) (Hemmati *et al.* 2003) and growth of neural progenitors (EGFR and C-MYC) (Maher *et al.* 2001; Oliver *et al.* 2003) are linked to aberrant function in GSCs (Vescovi *et al.* 2006). NSCs and GSCs have high capacities for invasion and migration and can differentiate into multiple lineages. While a cell lineage hierarchy has been shown in NSCs, GSCs present aberrant differentiation (expressing both neural and glial markers), that leads to a heterogenous population of cells with a variety of differentiation states (Sutter *et al.* 2007). NSCs exist in a defined niche, interacting with endothelial cells and microvessels, which maintain a fine-tuned balance between their proliferative and self-renewal rates (Goldberg and Hirschi 2009; Luo *et al.* 2017). However, GSCs are able to exist outside this niche (Schiffer *et al.* 2018), as will be discussed in section 1.3.7.

NSC and GSC	GSC
Motility	Mutations
Diversity of progeny	Dysregulation of stemness-related pathways
Proliferation potential	Aberrant differentiation
Self-renewal	Tumour formation capacity
High telomerase activity	Exist outside a niche
CD133, NESTIN, MSI1, SOX2, BMI1, OCT4 etc expression	
Formation of neuro/tumour spheres <i>in vitro</i> (in EGF/FGF2 conditions)	

Figure 1.3. Summary of the similarities and differences between NSCs and GSCs. Left panel: NSC/GSC similarities. Right panel: GSC only features. Image created with biorender.com

1.3.5 Cell of origin in gliomas

Upon oncogenic transformation, both NSCs and progenitors can give rise to tumours (Lathia *et al.* 2015); however, there is still a lot of debate on the origin of gliomas. Evidence suggests that zones prone to malignant transformation in the mature brain are found within the neurogenic regions and in particular the SVZ (Globus and Kuhlenbeck 1944; Vescovi *et al.* 2006; Lee *et al.* 2018; Alcantara-Llaguno *et al.* 2019). Adult NSCs are likely to accumulate mutations due to their long life span and mitotically active status (Sutter *et al.* 2007). According to a classic study of the cancer hallmarks, between four and seven mutations in an adult somatic cell are sufficient for it to undergo neoplastic formation (Hanahan and Weinberg 2000). Transiently amplifying progenitors (such as type C cells in the SVZ) have limited but high cell proliferative and division rates, which makes them also prone to acquiring mutations and initiating glioma (Vescovi *et al.* 2006).

Transgenic animal models that utilise either NSC/progenitor cell-related promoters or the inactivation of tumour suppressor genes have been used to investigate the effect of sequential epigenetic and genetic mutations in NSCs and progenitors and their involvement in tumour initiation (Ahmed *et al.* 2013). Bachoo *et al.* showed that transgenic *Ink4a-Arf^{-/-}* mouse NSCs, transduced with constitutively active EGFR retrovirus, generated high-grade gliomas after transplantation, while transduced GFAP-expressing mature astrocytes induced malignancy only after acquiring an undifferentiated state (Bachoo *et al.* 2002). In addition, deletion of tumour suppressor genes (*TRP53*, *NF1*) (Zhu *et al.* 2005) or the activation of oncogenes (*RAS* and *AKT*) in undifferentiated NESTIN-positive cells (Holland *et al.* 2000), promoted gliomagenesis of a higher grade than in GFAP-positive astrocytes. Similarly, this occurred when *PDGF β* was overexpressed (Dai *et al.* 2001). *Ascl1-CreER* mice (targeting neural and oligodendrocyte progenitors) carrying *Nf1*, *Trp53* and/or *Pten* mutations induced GBM-like tumours (Alcantara-Llaguno *et al.* 2015). Recently, Lee *et al.* have demonstrated, using single-cell sequencing and mouse models, that NSCs from the SVZ with tumour-driver mutations can migrate to other regions of the brain and establish tumours. Therefore, they proposed NSCs as the cell-of-origin for gliomas (Lee *et al.* 2018).

By contrast activation of the *H-RasV12* oncogene with inactivation of *p53* has also been reported to promote astrocytes and mature neurons transformation (Friedmann-Morvinski *et al.* 2012) which suggests that immature cells can form gliomas (Ahmed *et al.* 2013). However, a recent study demonstrated that targeting of *Nf1*, *Trp53*, and *Pten* tumour suppressor mutations in NSCs and bipotential progenitors, induced glioma formation while targeting more differentiated neural progenitors did not (Alcantara-Llaguno *et al.* 2019). Therefore, although some studies have suggested that mature astrocytes can de-differentiate and gain stem cell properties driven by the acquisition of mutations (Doetsch *et al.* 2002), many studies are consistent with reporting NSCs and transiently dividing progenitors cells as the origin for GBM.

1.3.6 Models used to characterise GSC phenotypes and their caveats

1.3.6.1 Markers used for GSC enrichment

The difficulty of isolating GSCs is a result of the lack of universal markers and informative gene expression profiles (Shackleton *et al.* 2009). Moreover, the high degree of genomic diversity in GBM adds another layer of complexity (Sundar *et al.* 2014). Nonetheless, great efforts have been dedicated to identify these cells. Most of the markers used to isolate GSCs have been appropriate from NSCs, due to molecular, cytological and histological similarities. SOX2, NANOG, OLIG2, C-MYC, MSI1, NESTIN, BMI-1 and ID1, among others, are examples of markers that are used to detect both NSCs and GSCs (Molina *et al.* 2014; Sundar *et al.* 2014). However, isolation of GSCs with transcription factors is challenging due to the lack of reliable antibodies and methods to analyse these cells by cell sorting and flow cytometry. For these reasons, many cell surface markers have been suggested to isolate GSCs; one of these is the cell surface glycoprotein, CD133 which is also known as Prominin-1 (Hemmati *et al.* 2003). CD133+ GBM cells have been shown to differentiate into GSCs progeny that phenotypically resemble the primary tumour (Singh *et al.* 2004), to confer radioresistance in human glioma xenografts and human GBM specimens (Bao *et al.* 2006) and to lose tumorigenic capacity after differentiation with BMP4 (Piccirillo *et al.* 2006). Moreover, the symmetric division rate is higher in CD133+ than in CD133- cells which is indicative of increased self-renewal capacity (Lathia *et al.* 2011). Despite the aforementioned pieces of evidence and the fact that this marker has broadly been used in brain tumour research, other studies have shown that cells

expressing CD133 are not always representative of GSCs (Joo *et al.* 2008; Wang *et al.* 2008). Moreover, CD133 expression in GBM is regulated by hypoxia and oxidative stress, suggesting that this marker may not be linked to a stemness phenotype in an obligatory sense (Griguer *et al.* 2008). Aside from CD133, other cell surface markers, such as CD44, CD15, integrin $\alpha 6$ and integrin $\alpha 7$, have also been used to purify this population of cells (Lathia *et al.* 2010; Sundar *et al.* 2014; Haas *et al.* 2017). Therefore, the difficulty of GSC enrichment is not dependent on the lack of markers but on the lack of combinatorial approaches that take into account tumour heterogeneity and use multiple markers to more accurately identify stem cell-like populations within the tumour.

1.3.6.2 Tumour-sphere formation assay

Tumour-sphere formation imitates the neuro-sphere formation assay *in vitro* (**Figure 1.4**), in which GSCs are maintained in non-adherent conditions and in a defined medium supplemented with growth factors. Initially, this technique was used to functionally characterise and quantify the self-renewal capacity of GSCs. Ignatova *et al.* showed a GSCs frequency of 0.05%-1.26% in GBM cell populations plated in sphere-forming conditions (Ignatova *et al.* 2002), while Galli *et al.* reported a frequency of GSCs ranging from 0.1% to 31% (Galli *et al.* 2004). Following these two studies, the tumour-sphere formation assay has been broadly used in brain tumour research due to its low cost and simplicity (Deleyrolle *et al.* 2008). Nonetheless, it has been criticized as a predictor for GSC enrichment and stemness. This assay can overestimate the number of stem cells as a percentage of spheres can be derived from progenitors with limited proliferation capacity and not GSCs. Therefore, the read-out of stem cell frequency can be unreliable (Marshall *et al.* 2007). Importantly, Pastrana *et al.* suggest that this assay may not represent quiescent stem cells (Pastrana *et al.* 2011). To overcome the limitations of the tumour-sphere assay, Louis *et al.* adapted and optimised the previously and widely used colony-forming cell assay from haematopoiesis to NSC studies (Louis *et al.* 2008). In this assay, the cells are embedded in a semi-solid collagen matrix which ensures that a colony is derived from a single cell and not from cell aggregates. Most importantly, this assay may distinguish between NSCs and their progeny, as only colonies derived from a “true” NSC would have a diameter greater than 2mm (Louis *et al.* 2008). Both assays are the closest

techniques used to demonstrate GSCs stemness *in vitro* and while they may be used for preliminary data analysis, these results need to be interpreted with caution and validated, e.g. with the use of a limiting-dilution xenotransplantation assay, to formally test GSCs tumour-formation capacity.

1.3.6.3 *In vivo* models in GSCs

Although genetically engineered mouse and viral/chemical induced models have been involved in the study of primary brain tumours, xenografting has been broadly utilised to functionally test two crucial characteristics that define GSCs, tumour-formation capacity and self-renewal (**Figure 1.4**). Xenografting is the implantation of patient-derived cancer cells or biopsies into immune-compromised mice (Huszthy *et al.* 2012). Although this method is the most sensitive model to facilitate GSCs engraftment, it presents certain limitations. This model cannot recreate the effects that the patient's tumour microenvironment has on the transplanted cells. Indeed, many of the factors that coordinate the interaction between the cell and microenvironment are incompatible between mouse and human (Rahman *et al.* 2011). Moreover, the lack of immune system does not allow the testing of the patient's immune response against the tumour (Shackleton *et al.* 2009). These limitations constitute an important problem for experimental drugs and therapies in pre-clinical studies, as many treatments that have beneficial results in *in vivo* models subsequently fail in clinical trials (Huszthy *et al.* 2012; Aldape *et al.* 2019). Despite these problems, the use of xenotransplantation assays of human GSCs have been very informative for the understanding of GSCs and glioma/GBM development. Nonetheless, this model can be improved by using humanized mice (mimicking vasculature, organs and cytokines of human origin), locally injecting human microenvironmental cells and co-transplanting human immune cells (Valent *et al.* 2012).

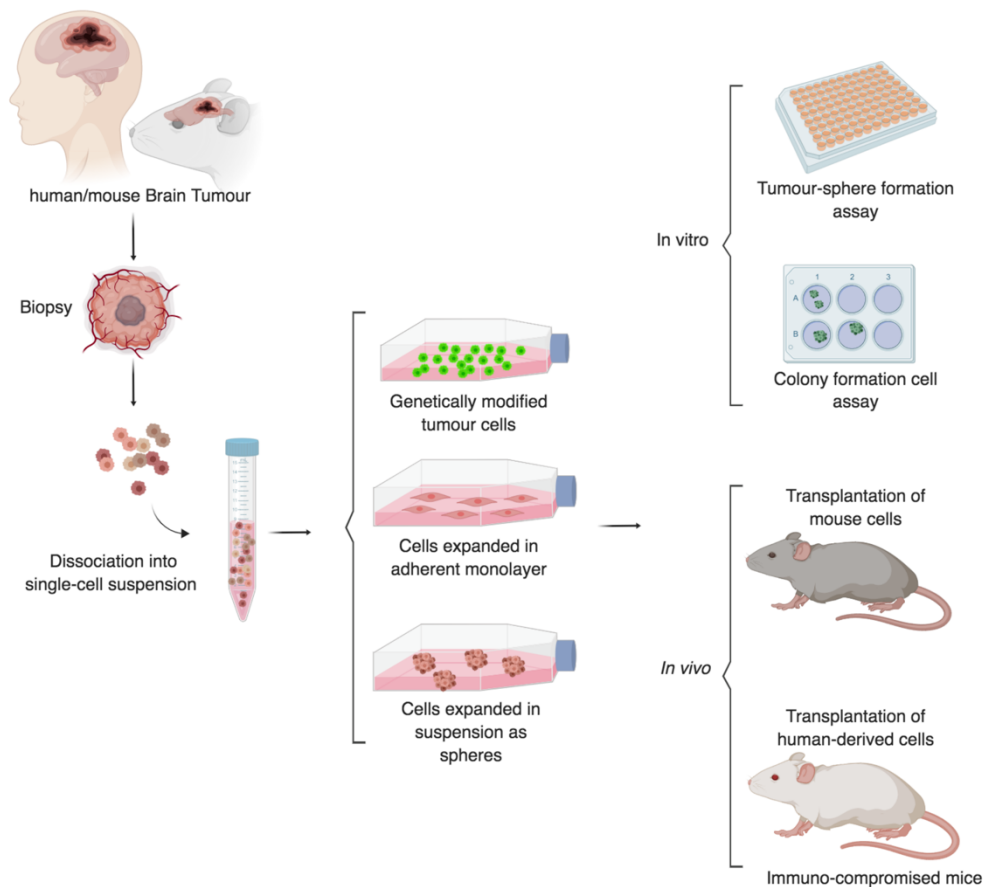


Figure 1.4. Schematic representation of *in vitro* and *in vivo* models used to characterised GBM cells. Tumour tissue can be isolated from patients or rodent models. Biopsies are dissociated into single cells that are propagated *in vitro* (in adherent or suspension cultures), in serum free media supplemented with EGF and FGF2. Tumour cells can be genetically modified and used in functional assay such as sphere/colony-forming assay. Despite not being mentioned in this image, many other genetic and chemical assays can be performed. Tumour cells are transplanted into mice to study tumour progression and tumour formation *in vivo*. Image created with biorender.com.

1.3.7 GSCs and their microenvironment regulation

GSCs interact with other cells within the tumour (endothelial cells, vascular pericytes, fibroblasts, macrophages and microglia, normal and reactive astrocytes etc.) and non-cellular elements such as growth factors and extracellular matrix molecules that surround the tumour. These interactions form a complex ecosystem termed the tumour microenvironment.

GBM niches are described as the regions where the combination of the aforementioned environmental elements allow GSCs to persist (Schiffer *et al.* 2018).

They play an important role in the regulation of GSC stemness, quiescence state and tumorigenicity and are mainly divided in three different zones: perivascular, necrotic or hypoxic and invasive or perineural zones (Silver and Lathia 2018). In the perivascular niche, GSCs are in direct contact with endothelial cells (capillaries and arterioles) (Calabrese *et al.* 2007). Beside GSCs, this growth zone contains many cell types such as normal and reactive astrocytes, pericytes, macrophages and myeloid cells (Schiffer *et al.* 2018). The interaction between endothelial cells and GSCs is bidirectional as GSCs produce VEGF (Bao *et al.* 2006), that together with angiopoietins and PDGF β , which is secreted by astrocytes, induces angiogenesis and tumour growth (Fidoamore *et al.* 2016). Moreover GSCs also contribute to vascular structure as they can trans-differentiate into endothelial phenotypes (Ricci-Vitiani *et al.* 2010; Wang *et al.* 2010; Cheng *et al.* 2013). The interactions between GSCs and endothelial cells permit the activation of NOTCH signalling, crucial for the maintenance of GSC self-renewal (Zhu *et al.* 2011) as its blockage reduces stemness antigens such as CD133, NESTIN and BMI-1 (Schiffer *et al.* 2018). Other soluble factors present within this niche such as SHH, FGF2 and CD44 among others, are also involved in the maintenance of stem cell-like properties of GSCs (Codruci *et al.* 2016; Silver and Lathia 2018)

The necrotic niche is localised within the main tumour mass and is characterised by a hypoxic environment and the presence of pseudopalisades (necrotic areas surrounded by GSCs) (Brat *et al.* 2004). Perinecrotic zones are the result of an imbalance between hyperproliferation of tumour cells and the reduced growth of vasculature (Schiffer *et al.* 2018). GSCs within this niche are mainly regulated by HIF family members, first reported by Li *et al.* (Li *et al.* 2009). While HIF-1 α is expressed in both GSCs and non-GSCs, HIF-2 α is specific to GSCs (Seidel *et al.* 2010). HIF-2 α maintains GSCs in an undifferentiated state as it regulates key stemness genes such as *SOX2*, *C-MYC*, and *OCT4* (Codruci *et al.* 2016). HIF factors also regulate the expression of VEGF and the induction of neovascularization in the perivascular niche (Molina *et al.* 2014).

As described in section 1.2.3, GBM is a highly invasive and infiltrative tumour. These invasive areas, distant to the tumour core, are normally described as the invasive niche of the tumour, or tumour edge. In this niche, single glioma cells infiltrate the

normal brain parenchyma due to their capacity for myelin proteolysis. Moreover, astrocytes from the surrounding area induce activation of matrix metalloproteinases, supporting the migration and invasion of GSCs via extracellular matrix (ECM) degradation (Le *et al.* 2003). ECM degradation causes the release of trophic factors crucial for GBM growth and GSC maintenance, such as FGF2. Among the matrix metalloproteinases, A Disintegrin and Metalloproteinase (ADAM) family of zinc-dependent proteinases has been shown to regulate GSCs and promote GBM chemoresistance (Dong *et al.* 2015; Sarkar *et al.* 2015). Apart from the tumour microenvironment, GSCs are also regulated by their metabolism, epigenetic signatures and the immune system (**Figure 1.5**). However, these regulatory systems are beyond the scope of this study.

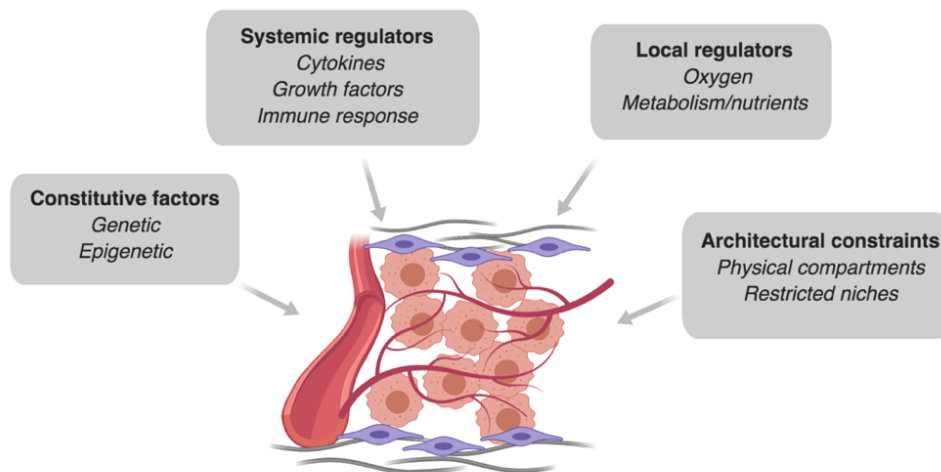


Figure 1.5. Regulation of GSCs by intrinsic and extrinsic forces. GSC survival is dependent on different regulatory systems such as constitutive factors (genetics and epigenetics), systemic regulators (cytokines, growth factors and immune system), local cues like oxygen, nutrients and metabolism and architectural constraints. Image created with biorender.com (Vescovi *et al.* 2006).

1.3.8 Tumour recurrence and GSC therapies

Currently there is no treatment that overcomes GBM tumour recurrence as both conventional and molecular targeted therapies have been unsuccessful (Osuka and Van Meir 2017). A major reason for treatment failure in GBM is tumour heterogeneity. Intertumoral heterogeneity is described as the differences in epigenetic/genetic aberrations and gene expression profiles among GBM patients (section 1.2.3). These differences can be the result of variations in the cell of origin of each tumour

(Alcantara-Llaguno *et al.* 2015). In addition, personalized therapies have not been successful either due to intratumoral heterogeneity, as subpopulations of cells within the same tumour also possess a variety of phenotypes and express different genes related to proliferation, hypoxia and immune response (Patel *et al.* 2014). This diversity, together with the limitations in the technology and assays used to study GBM tumours, complicates our understanding of GSCs and their origin.

Nonetheless, independent of the cell of origin, there is a group of cells or clones within the tumour that overcome current treatment strategies and are responsible for tumour recurrence (Bao *et al.* 2006; Chen *et al.* 2012). Bao *et al.* showed that CD133+ GSCs were more radioresistant than CD133- cells due to an efficient DNA damage repair process. Similarly, Chen *et al.* identified NESTIN-positive GSCs as the subpopulation of cells less responsive to TMZ treatment (Chen *et al.* 2012); these cells possess a number of molecular mechanisms such as DNA damage checkpoints, NOTCH and SHH signalling activation and antiapoptotic pathways (e.g. PARP) among many others, that mediate tumour therapeutic resistance (Lathia *et al.* 2015). Different studies have used therapies against these molecular mechanisms to increase TMZ efficiency in GBM treatment. Barazzuol *et al.* showed that a combination of PARP inhibitors (ABT-888), TMZ and radiotherapy increased apoptosis in GBM cells (Barazzuol *et al.* 2013). Inhibition of JNK and WNT/ β -catenin signalling increased TMZ efficiency through regulation of MGMT expression. In addition, blocking SOX2 and ZEB1 expression has also been linked to sensitization of GSCs to TMZ as these transcription factors are stemness regulators (Siebzehnrubl *et al.* 2013; Jiapaer *et al.* 2018).

The SHH inhibitor DC-0449 also known as Vismodegib (ClinicalTrials.gov Identifier: NCT00980343) was used in a clinical phase I trial in GBM patients; after trial completion, Vismodegib successfully blocked SHH pathway, but very little improvement was seen. Ulasov *et al.* demonstrated a higher efficacy of TMZ when treating GSCs with GSI-1, a small molecule γ -secretase inhibitor that inhibits NOTCH signalling (Ulasov *et al.* 2011). In addition, pharmacological inhibitors of CHK1 and CHK2 render CD133 + cells more sensitive to radiotherapy (Bao *et al.* 2006). GSCs therapeutic resistance is induced not only by cell intrinsic factors, but also by factors from the tumour microenvironment such as cytokines, HIFs and metabolic stress

(Heddleston *et al.* 2009; Xie *et al.* 2015). Small molecules targeting tyrosine kinase receptors involved in tumour angiogenesis such as VEGFR (bevacizumab) (Bao *et al.* 2006) have been developed, although without much success due to off-target effects in other signalling pathways.

On the other hand, immunotherapies based on cytokines, monoclonal antibodies, peptide vaccines and dendritic cells, have had promising results in clinical trials (Lathia *et al.* 2015; Sager *et al.* 2018). Phuphanich *et al.* used vaccines against tumour-specific antigens in a Phase I clinical trial, increasing the median and overall survival of the treated GBM patients (Phuphanich *et al.* 2013). Increased survival of mice bearing GL261 tumours was seen upon intratumoral injection of IL-2 secreting allogenic fibroblasts (Glick *et al.* 2006). Moreover, EGFRvIII peptide vaccines improved progression-free survival of newly diagnosed GBM patients in phase II clinical trials (Sampson *et al.* 2010).

Despite decades of research and efforts to develop new therapies, very little progress has been made in the treatment of patients with brain tumours. Therefore, the research community has to overcome this challenge and redesign the brain tumour research pipeline (Aldape *et al.* 2019). This involves the understanding of tumour biology and the role of the tumour microenvironment *in vitro* and *in vivo*, and the development of more elaborate and predictive pre-clinical models that allow testing of the efficiency of developed therapies. Thus, new therapies should have the capacity to target not only intrinsic forces regulating GSCs, but also extrinsic factors such as tumour-stroma interactions, the microenvironment and the immune system (Lathia *et al.* 2015).

1.4 ZEB1, SOX2, OLIG2– key stemness regulators of GSCs

Previous studies have identified three transcription factors, ZEB1, SOX2, and OLIG2, that are crucial for GSC maintenance and GBM development (Ligon *et al.* 2007; Gangemi *et al.* 2009; Siebzehnrubl *et al.* 2013) and act independently of putative GBM oncogenes (Singh *et al.* 2017). These transcription factors are co-expressed in GBM xenografts (Siebzehnrubl *et al.* 2013) and in 90% of human GBM samples analysed by tissue microarray (Singh *et al.* 2017). They are aberrantly upregulated in GSCs and their expression results in higher stemness and tumour formation capacity (Ligon *et al.* 2007; Gangemi *et al.* 2009; Rheinbay *et al.* 2013; Siebzehnrubl *et al.* 2013; Singh *et al.* 2017).

1.4.1 ZEB1

ZEB1, also known as δ EF1, is part of the ZEB family of transcription factors. Structurally, ZEB1 contains two zinc finger (ZF) clusters located at the N- terminal and C-terminal ends of the protein, a homeodomain, a SMAD binding domain and a CtBP interacting domain (**Figure 1.6**). This transcription factor binds to E-box-like elements on DNA through the ZF domain and acts as transcriptional repressor by recruiting CtBP (Liu *et al.* 2008; Vandewalle *et al.* 2009). However, it can also act as a transcriptional activator through interaction with p300, recruiting Smad proteins and inducing TGF- β /BMP signalling (Postigo 2003) or by directly binding the Hippo-pathway effector, YAP (Lehmann *et al.* 2016).

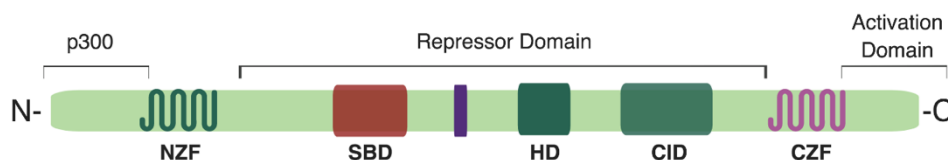


Figure 1.6. Representation of ZEB1 transcription factor. Two zinc finger clusters are present at the C-terminal (CZF) and N-terminal (NZF) of the protein and present a 88% and 93% homology with other transcription factors of the ZEB family. The homeodomain (HD) is centrally located between the Smad-binding domain (SBD) and the CtBP interaction domain (CID). Image created with biorender.com and adapted from Vandewalle *et al.* 2009.

The transcriptional silencing function of ZEB1 has been linked to the epithelial-to-mesenchymal transition (EMT), as it is a repressor of cell adhesion molecules (i.e. E-cadherin) and epithelial and polarity-related genes (Brabletz and Brabletz 2010; Edwards *et al.* 2011). EMT is an essential mechanism associated with embryonic development, wound healing, tissue regeneration and cancer metastasis (Kalluri and Weinberg 2009; Thiery *et al.* 2009). EMT occurs when epithelial cells, that are cross-linked by their cytoskeleton and have a high number of cell-cell adhesion contacts, undergo biochemical changes that promote a shift towards a mesenchymal state by inducing cellular motility, invasion and senescence (Burk *et al.* 2008; Kalluri and Weinberg 2009; Brabletz and Brabletz 2010; Tomlinson and Knowles 2010). Although this classic description implies a shift between two phenotypes, the concept of EMT has changed in the last decade because cells undergoing EMT do not always acquire full epithelial or mesenchymal features. This intermediate phenotype is termed partial EMT (Nieto *et al.* 2016) and is described as a plastic process in which cells oscillate between these two transitional states. Cells in this intermediate state are also called metastable cells as they have high flexibility to induce or reverse EMT.

EMT is an embryonic cell-fate and stemness program that is reused during carcinogenesis. EMT leads to tumour progression and invasion enhancing metastasis of CSC (Thomson *et al.* 2011). Moreover, disseminated cancer cells can undergo an EMT reverse process, termed the mesenchymal-to-epithelial transition (MET), which is essential for tumour outgrowth. EMT/MET programs induce tissue plasticity in cancer and contribute to therapy resistance and immune evasion. (Brabletz and Brabletz 2010; Goossens *et al.* 2017). EMT has mainly been studied in cancers outside the CNS because of the lack of epithelial and mesenchymal tissues in the brain; however EMT-transcription factors (ZEB1, SNAIL/SLUG, TWIST1/2 and ENGRAILED1) from epithelial tumours (Lamouille *et al.* 2014), have been shown to be active and also responsible for inducing invasion, chemoresistance and stemness in non-epithelial cancers such as GBM (Brabletz *et al.* 2018). Among the EMT-transcription factors, ZEB1 is a key regulator of stemness and its expression is predictive of poor prognosis and response to TMZ in GBM patients (Siebzehnrubl *et al.* 2013). In addition, cells with high levels of ZEB1 demonstrate key features of GSCs as they can survive in hypoxic conditions, self-renew, induce glioma recurrence and are located at the invasion front of the tumour in GBM (Siebzehnrubl *et al.* 2013;

Kahlert *et al.* 2015). Moreover, Hoang-Minh *et al.* have shown that ZEB1 is expressed in higher levels in slow-cycling cells compared to fast-cycling cells in GBM and that its knockdown reduces invasion of the former population (Hoang-Minh *et al.* 2018).

ZEB1 regulates GBM growth through a negative feedback-loop between ZEB1 and microRNAs and in particular the microRNA-200c (miR-200c) family (Wellner *et al.* 2009; Siebzehnruhl *et al.* 2013). MiR-200c activates epithelial differentiation genes and inhibits stemness, while ZEB1 promotes a non-polarised mesenchymal phenotype inducing an EMT-like process (Burk *et al.* 2008; Liu *et al.* 2008). ZEB1/miR-200 are involved in the regulation of two downstream targets, ROBO1 and C-MYB, that are responsible for GBM tumour progression. ZEB1 induces invasion and migration through ROBO1, a protein that promotes the cytoskeletal detachment of the cell adhesion molecule N-cadherin (Vandewalle *et al.* 2009; Brabletz and Brabletz 2010; Sánchez-Tilló *et al.* 2011; Siebzehnruhl *et al.* 2013). On the other hand, ZEB1 activates tumour recurrence by controlling stemness genes (*OLIG2* and *SOX2*) and therapy resistance by regulating C-MYB, which induces the expression of the chemoresistance enzyme, MGMT. Consequently, it has been shown that the median survival of *in vivo* models treated with TMZ increases when *ZEB1* is knocked down, and the overexpression of miR-200 renders GSCs less resistant to therapy (Brabletz and Brabletz 2010; Siebzehnruhl *et al.* 2013).

1.4.2 SOX2

SOX2 is a single exon gene member of the SRY-related high mobility group box (SOX) family of transcription factors. These proteins share two domains: a DNA-binding domain and an activation domain (Mansouri *et al.* 2016). *SOX2* expression is regulated by cell cycle regulators (E2F3a/b and p21), other transcription factors of the SOX family such as *SOX4* and a negative feedback loop with miR-200c (Ikushima *et al.* 2009; Peng *et al.* 2012; Marqués-Torrejón *et al.* 2013). *SOX2* is one of the core transcription factors, together with *OCT3/4*, *KLF4* and *NANOG*, required for the maintenance of pluripotency in embryonic stem cells (Niwa *et al.* 2000; Avilion *et al.* 2003; Chambers *et al.* 2003). Moreover, the breakthrough study of Yamanaka *et al.* demonstrated that among these three factors, Oct3/4 and Sox2 in conjunction with c-Myc and Klf4, are essential for the production of induced pluripotent stem cells

(Takahashi and Yamanaka 2006). The critical role of SOX2 in development, NSCs maintenance, proliferation and cell differentiation highlights the importance of this factor in glioma-initiation (Gangemi *et al.* 2009).

SOX2 has been reported to be dysregulated in GBM due to genetic amplifications and epigenetic mechanisms (Alonso *et al.* 2011; Brennan *et al.* 2013). Its expression correlates with glioma grade and is linked to poor clinical outcome (Ma *et al.* 2008; Vanner *et al.* 2014; Singh *et al.* 2017). The SOX2 gene is amplified in 14.4% of GBMs and is expressed in highly invasive areas of the tumour (Annovazzi *et al.* 2011). This transcription factor is enriched in human GSCs (McLendon *et al.* 2008; Gangemi *et al.* 2009) and contributes to invasive and malignant phenotypes seen in gliomas (DeCarvalho *et al.* 2010). This has been proven by Song *et al.* who demonstrated that SOX2 expression is higher in CD133+ cell populations (Song *et al.* 2016) and Gangemi *et al.* who reported that SOX2 knockdown in GSCs decreases clonogenicity and stops proliferation (Gangemi *et al.* 2009). Moreover, a recent study from Singh *et al.* showed that GBM cells that became independent of the *EGFRvIII* oncogene had increased expression levels of SOX2 (Singh *et al.* 2017).

Gene-set enrichment analyses identified SOX2 as a key regulator of sets of genes related to hypoxic and stress conditions, cell morphology, cell-cell adhesion and proliferation (Acanda De La Rocha *et al.* 2016). In addition, it has been demonstrated that Rapamycin (an inhibitor of the mTOR pathway) and cyclophosphamide (an inhibitor of SHH) sensitised GSCs to TMZ treatment and decrease levels of SOX2 (Jeon *et al.* 2011; Mamun *et al.* 2018). These findings highlight the importance of SOX2 in GBM chemoresistance (Garros-Regulez *et al.* 2016) and radioresistance (Mansouri *et al.* 2016).

1.4.3 OLIG2

OLIG2 is a member of the basic helix-loop-helix (bHLH) transcription factors and a marker for oligodendroglial lineage progenitors (transient-amplifying type C cells and NG2-positive glia) and mature oligodendrocytes in the adult brain (Bachoo *et al.* 2002; Singh *et al.* 2016; Tsigelny *et al.* 2016). OLIG2 is only expressed in the CNS and plays a crucial role in determining the fate of uncommitted neural progenitors during development (Meijer *et al.* 2012; Kosty *et al.* 2017). OLIG2 is expressed in diffuse

gliomas (Ligon *et al.* 2007) and together with SOX2, POU3F2, and SALL2, is one of the transcription factors involved in the de-differentiation of mature GBM cells into GSCs (Suvà *et al.* 2014). Moreover it is upregulated in both the core and invasion front of the tumour in GBM (Singh *et al.* 2016). According to Lu *et al.* Olig2 positive cells are essential for tumour propagation in the proneural subclass of GBM (Lu *et al.* 2016). This study showed that the elimination of mitotic Olig2-positive progenitor cells in murine proneural GBM *Pten/trp53* mutants and PDGFR β expression models, blocked tumour initiation and growth during the early phase of gliomagenesis. However, deletion of *Olig2* in *Olig2cKO* mice (*Pten^{fl/fl}; Trp53^{fl/fl}; Olig2^{fl/fl} : PDGFR β -Cre*), only decreased the tumour growth rate. In addition, this deletion promoted the downregulation PDGFR α and the upregulation of EGFR, resulting in a shift from oligodendrocyte precursor-related phenotypes to astroglia-associated genes characteristic of classical subtypes (Lu *et al.* 2016). Whether this shift occurs in patients is not yet known (Leelatian and Ihrie 2016). Furthermore, Ligon *et al.* reported that neural progenitors from *Ink4a/Arf*^{-/-} mice infected with constitutively active EGFRvIII retrovirus induced glioma-like tumours upon implantation in SCID mice, while *Ink4a/Arf*^{-/-} Olig2 null infected progenitors did not form tumours (Ligon *et al.* 2007). Both the Lu *et al.* and Ligon *et al.* studies suggest that Olig2 functions are context-dependent and crucial for gliomagenesis (Kosty *et al.* 2017).

Apart from context-dependent features, Singh *et al.* have demonstrated that the phosphorylation state of OLIG2 plays a role in its function in GBM. Unphosphorylated OLIG2 induces GSC invasion by activating mesenchymal genes (*ZEB1*) through the TGF β 2 pathway, while its phosphorylation promotes proliferation *in vivo* and *in vitro* (Singh *et al.* 2016). Moreover, this transcription factor sustains glioma growth and radio-resistance by direct repression of the cell cycle inhibitor p21 that in turn regulates p53 response to genotoxic damage (Ligon *et al.* 2007; Mehta *et al.* 2011). In addition, OLIG2 prevents apoptosis in GSCs by activation of BAD through a positive feedback mechanism between OLIG2, tyrosine kinase receptors and the AKT pathway (Tsigelny *et al.* 2016).

1.4.4 Cross-regulation interdependency of ZEB1, SOX2 and OLIG2

Due to ZEB1, SOX2 and OLIG2 being implicated in promoting gliomagenesis and maintaining GSC stemness, and being considered relevant targets for GBM treatment, many studies have suggested a possible cross-regulation among them. Siebzehnruhl *et al.* showed that SOX2 and OLIG2 were regulated by ZEB1 in GBM and identified miR-200c binding sites in the three transcription factors (Siebzehnruhl *et al.* 2013). Moreover, the negative regulation of miR-200c by ZEB1 contributes to the stabilization of the post-transcriptional program of SOX2 and OLIG2. In addition, Wellner *et al.* demonstrated that SOX2 is a target of the EMT-transcription factor ZEB1 (Wellner *et al.* 2009). Likewise, Singh *et al.* reported ZEB1 expression to be induced by unphosphorylated OLIG2, suggesting that ZEB1 was a direct target of the latter (Singh *et al.* 2016). The cross-regulation interdependency and a feedback loop among the three factors was finally reported by Singh *et al.* who showed that Zeb1-Sox2-Olig2 are co-ordinately expressed and constitute a driver of GBM (Singh *et al.* 2017). This study demonstrated that co-expression of Zeb1-Sox2-Olig2 is involved in the de-differentiation of astrocytes (**Figure 1.7**). Similarly, Suvà *et al.* showed that following serum treatment, differentiated GBM cells recovered stem-like functions upon overexpression of at least two of these transcription factors (Suvà *et al.* 2014).

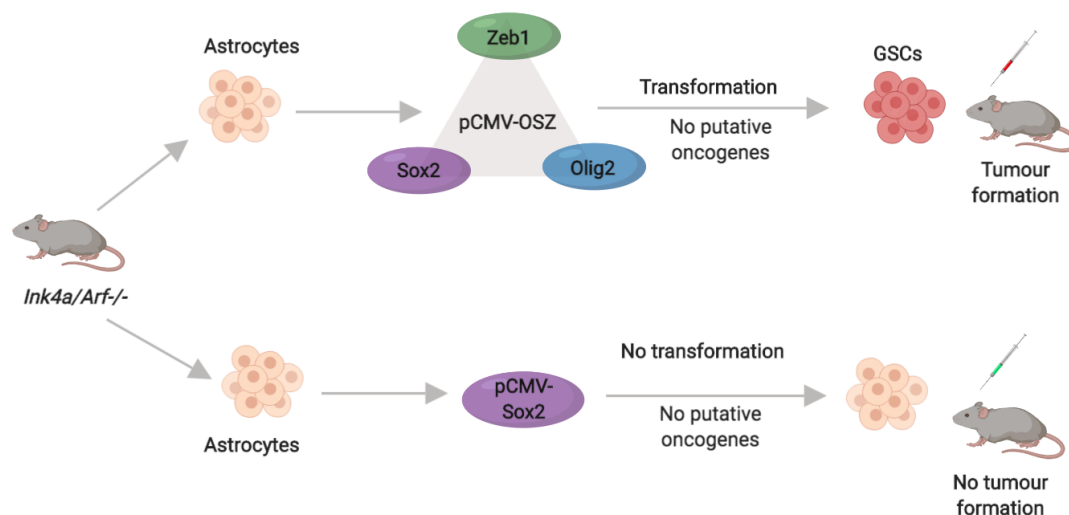


Figure 1.7. Transformation of immortalized astrocytes. Astrocytes and NSCs isolated from *Ink4a/Arf*^{-/-} transfected with an expression vector (pCMV-OSZ) that induces the coordinate expression of Olig2, Sox2 and Zeb1 transform those astrocytes in GSC like cells which generate tumours after implantation. Tumour-formation was not seen in wild type astrocytes or after implantation of astrocytes transfected with single expression vectors. Image created with biorender.com and adapted from (Singh *et al.* 2017).

Although the function of this set of transcription factors seems to be independent of putative GBM oncogenes such as *EGFR*, *PDGFRA* and *MET* (Singh *et al.* 2017), studies in other cancers have shown that ZEB1 is induced by FGF2, a cytokine highly prevalent in the brain and in the tumour microenvironment (Edwards *et al.* 2011; Lau *et al.* 2013). This suggests a possible role of the FGFR signalling pathway in their regulation.

1.5 FGF-FGFR signalling pathway

1.5.1 FGF family members

FGFs were first isolated from bovine brain extracts in 1939, and characterised by their ability to induce fibroblast proliferation *in vitro* (Trowell *et al.* 1939). Since then, 18 functional FGF ligands within the mammalian FGF family have been identified (Ahmad *et al.* 2012). FGFs are secreted growth factors that can be classified into two groups: hormone-like and canonical FGFs (Dieci *et al.* 2013). Hormonal-like FGFs (FGF 19, 21 and 23) are characterised by their capacity to diffuse into circulation and act as endocrine regulators (Guillemot and Zimmer 2011; Ahmad *et al.* 2012). FGF 19 and 23 interact with Klotho proteins to promote ligand-receptor binding, while FGF 21 can bind in a klotho-independent manner (Itoh and Ornitz 2011). On the other hand, canonical FGFs (FGF 1-10, 16-18 and 20) have autocrine and/or paracrine functions and can bind to their receptors in the presence of heparin/heparan sulphate proteoglycans (HSPGs). These proteoglycans increase ligand-binding affinity and activation of the signalling pathway by 2-3 fold (Roghani *et al.* 1994; Haugsten *et al.* 2010; Dieci *et al.* 2013; Touat *et al.* 2015).

The role of HSPGs in FGF signalling was first discovered by Rapraeger *et al.* and Yayon *et al.* (Rapraeger *et al.* 1991; Yayon *et al.* 1991). HSPGs are glycoproteins formed by a core protein decorated with heparin/heparan sulphate (HS) side chains covalently attached to its serine residues (Laremore *et al.* 2009). FGF family members share a homologous region where the HSGP binding site is located (Beenken and Mohammadi 2009). HS is one of the most abundant glycosaminoglycans (GAGs) in the extracellular matrix (ECM) of all tissues (Zhang *et al.* 2014). In addition, HSPGs are also present on the cell surface, where they cooperate with integrins and other ECM molecules that mediate cell-cell interactions (Sarrazin *et al.* 1965; Ori *et al.* 2008; Kundu *et al.* 2016). Apart from being involved in the stabilization of ligand-receptor binding and consequently in the activation of the cascade, these co-receptors also serve as FGF storage as they trap growth factors from the ECM preventing their degradation by proteases (Eswarakumar *et al.* 2005; Ahmad *et al.* 2012; Touat *et al.* 2015).

FGFs are involved in many cellular processes during embryonic development and adulthood, such as morphogenesis, cell survival, proliferation, differentiation, tissue repair and wound healing (Eswarakumar *et al.* 2005; Guillemot and Zimmer 2011; Irschick *et al.* 2013). Among them, FGF2, also known as basic FGF because of its isoelectronic point ($pI > 9.0$) and its basic canyon structure (Detillieux *et al.* 2003; Turner *et al.* 2012), is closely related to CNS development and adult neurogenesis.

1.5.2 FGF2 functions in the developing and adult brain

FGF2 is crucial for the formation of the hippocampus and the substantia nigra pars compacta and for the regulation of early neurogenesis (Woodbury and Ikezu 2014). In the adult brain, this growth factor is widely expressed in the parenchyma (3.33 ± 0.32 ng/mg in the cerebral cortex), as well as in the SVZ and the SGZ, the two neurogenic niches of the mammalian brain (Pettmann *et al.* 1985; Morrison *et al.* 1986; Mogi *et al.* 1996; Dehay *et al.* 2001; Frinchi *et al.* 2008; Shackleton *et al.* 2009; Werner *et al.* 2011; Woodbury and Ikezu 2014). FGF2 is mainly present in astrocytes and its expression increases in reactive astrocytes and decreases by cell contact inhibition (Joy *et al.* 1997).

FGF2 is required to preserve multipotency of NSCs both in embryonic and adult neurogenesis (Wagner *et al.* 1999; Raballo *et al.* 2000; Zheng *et al.* 2004). Although FGF2 maintains NSCs from further differentiation (Gritti *et al.* 1996), changes in its concentration regulate the production of the appropriate number of neurons and glial cells during gliogenesis (Qian *et al.* 1997; Guillemot and Zimmer 2011). FGF2 also controls the migration capacity and fate of NSCs as its deficiency impairs progenitor colonization in the cerebral cortex (Woodbury and Ikezu 2014). In addition, this growth factor is required for the proliferation of NSCs *in vitro* (section 1.3.7), however this role can be compensated *in vivo*. This was proven by Werner *et al.* who showed NSCs grow normally in *Fgf2* knockout mice (Werner *et al.* 2011). Apart from its role as a neurogenic factor, FGF2 is an important angiogenesis-promoting protein (Morrison *et al.* 1990; Joy *et al.* 1997).

1.5.3 FGFR family and structure

FGF2 and FGFs in general, are ligands of four FGFRs which were first discovered by Lee and colleagues (Lee *et al.* 1989). Human FGFR1-4 form part of the receptor tyrosine kinase family. A fifth member of the FGFR family, FGFR1, lacks a transmembrane domain and acts as a soluble antagonist to FGFR signalling (Steinberg *et al.* 2010). Structurally, FGFR1-4 consist of three different domains: an extracellular domain that binds FGF ligands, heparin/HS and ECM molecules, a transmembrane domain and an intracellular domain that interacts with cytoplasmic molecules and transduces FGFR signals (Harmer *et al.* 2004; Haugsten *et al.* 2010; Guillemot and Zimmer 2011; Ahmad *et al.* 2012; Touat *et al.* 2015) (**Figure 1.8**). The extracellular domain is divided into three immunoglobulin (Ig)-like loops: Ig-I, Ig-II and Ig-III (also called D1, D2 and D3).

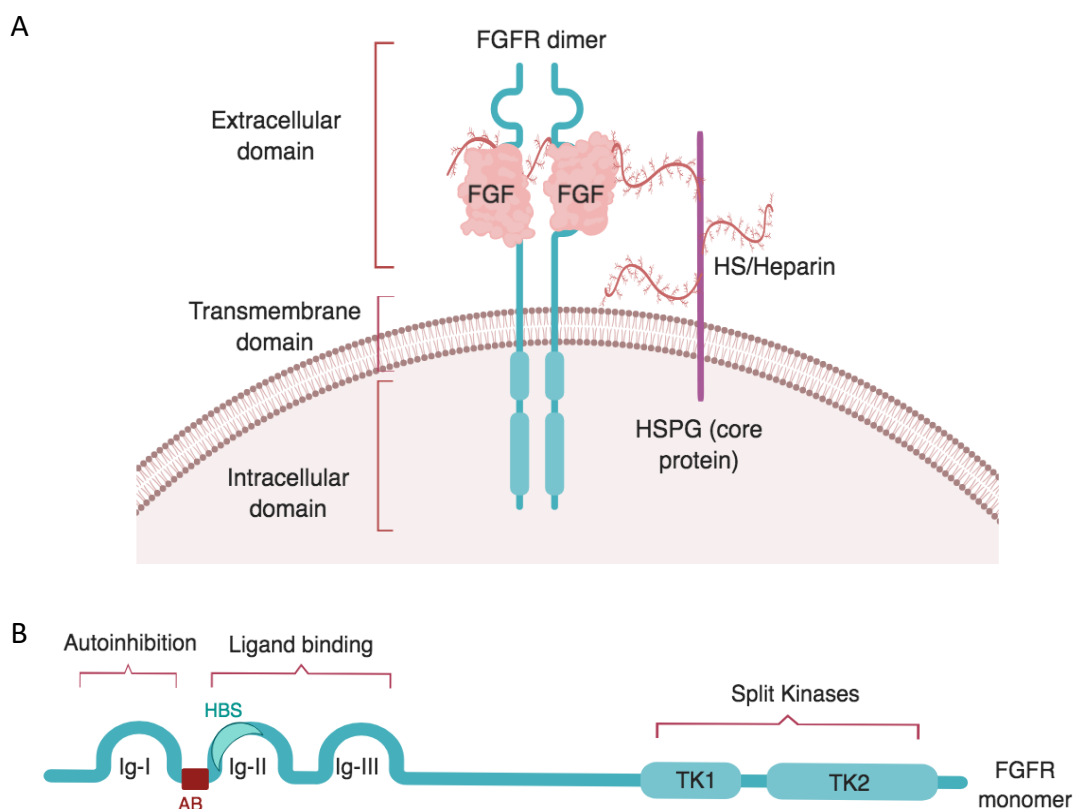


Figure 1.8. FGFR structure. **A)** FGFR possess three domains: a extracellular domain, a single transmembrane domain and a intracellular domain. FGF-FGFR complex is stabilised by a heparin/HS chain of the HSPG. **B)** The extracellular domain of the receptor is composed by three Ig-like domains: Ig-I, Ig-II and Ig-III. Ig-I has autoinhibitory capacity while Ig-II and Ig-III form the ligand binding domain. Ig-II contains the heparin/HS binding site (HBS) and is separated from Ig-I by an acidic box (AB). The cytoplasmatic domain is formed by two tyrosine kinases: tyrosine kinase 1 (TK1) and tyrosine kinase 2 (TK2). Image created with biorender.com.

Ig-I is linked to Ig-II by a 30 amino acid stretch called the acid box, which is rich in serine and acidic residues, and is unique to FGFRs (Mohammadi *et al.* 2005; Tiong *et al.* 2013). Ig-I and the acid box have receptor auto-inhibitory functions and the Ig-II and Ig-III subdomains form the ligand-binding site of the receptor (Wang *et al.* 1995; Beenken and Mohammadi 2009; Dieci *et al.* 2013; Dienstmann *et al.* 2014). Ig-II contains a heparin/HS binding region and an FGF binding activity site. The junction between Ig-II and Ig-III controls heparin and FGF affinity (Rapraeger *et al.* 1991; Yayon *et al.* 1991; Harmer *et al.* 2004; Gong 2014).

Two alternative Ig-III splice isoforms exist in FGFR1-3, but not FGFR4; these are termed Ig-IIIb and Ig-IIIc (Eswarakumar *et al.* 2005; Holzmann *et al.* 2012; Tiong *et al.* 2013; Ohashi *et al.* 2014). Ig-IIIb and Ig-IIIc are generated by exon skipping and are encoded by exons 8 and 9, respectively (**Figure 1.9**). By contrast, exon 7, encoding Ig-IIIa, is present in all splice variants. Post-transcriptional regulation of FGFR isoform expression is controlled by regulatory RNA-binding proteins (RBP) (Dassi 2017). Serine/arginine rich (SR) and heterogeneous nuclear ribonucleoproteins (hnRNP) are two of the most known RBP families (Holzmann *et al.* 2012). RBPs can act as enhancers or silencers of intron and exon splicing. For example, hnRNPs repress exon inclusion in FGFR2 IIIc (Gong 2014). Although RBPs are expressed in all tissues, there are two RBP paralogues that are epithelial cell-type-specific RBPs called epithelial splicing regulatory proteins 1 and 2 (ESRP1 and ESRP2). These two proteins regulate FGFR exon Ig-IIIb expression. In addition, ESRPs are master splice regulators of a set of mRNAs associated with EMT/MET-related splice patterns (Matlin *et al.* 2005). Therefore, a complex series of RNA-protein and protein-protein interactions regulates exon inclusion or exclusion (Holzmann *et al.* 2012).

The expression of FGFR splice variants is tissue-dependent. For example the Ig-IIIb isoform is expressed in epithelial tissues while Ig-IIIc is found in mesenchymal ones (Mohammadi *et al.* 2005; Ahmad *et al.* 2012; Gong 2014; Safa *et al.* 2015). Moreover, their expression changes throughout tissue growth, proliferation and remodelling (Yamaguchi *et al.* 1994).

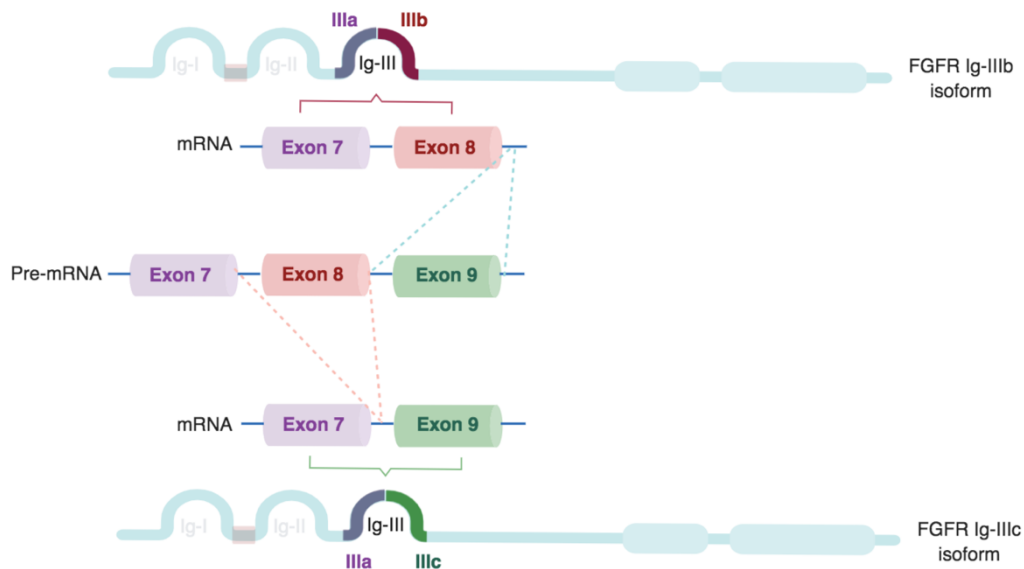


Figure 1.9. Schematic representation of Ig-III splice isoforms (IIIb/IIIc). The Ig-III domain of FGFR1-3 is coded by exons 7-9. Exon 7 codes Ig-IIIa which consists of the N-terminal half of the Ig-III loop. The C-terminal half is form by IIIb or IIIc sequence codified by exon 8 and 9 respectively. Image created with biorender.com.

The FGFR transmembrane domain is crucial for transferring the signal from the extracellular to the intracellular domain, the latter consisting of a juxtamembrane domain, two tyrosine kinase domains and the c-terminal tail (Tiong *et al.* 2013; Gong 2014) (**Figure 1.8**). Although FGFR domains are highly conserved among receptors, the tyrosine kinase domains (TKI: 75-88%; TKII: 80-92%) share the highest homology. The Ig-III is also highly conserved, especially between FGFR1 and FGFR2 (Gong 2014).

Binding of FGF2 to HSPGs causes FGFR dimerization and transphosphorylation of the cytoplasmic tyrosine kinase domain, a process in which the hydroxyl group of the tyrosine receives a γ -phospho group from ATP (Lew *et al.* 2009; Touat *et al.* 2015). As an example, autophosphorylation of FGFR1 tyrosine residues occurs in three steps. Firstly, phosphorylation of Y653 leads to a 50-100 fold increase of the catalytic core activation of the intracellular domain. Secondly, Y583, Y463, Y766 and Y585 sites are consequently phosphorylated and finally, the second tyrosine kinase domain phosphorylation increases the tyrosine kinase activity 10-fold. This sequence of

autophosphorylation follows a specific and controlled order that, if deregulated, can induce malfunction of the pathway (Lew *et al.* 2009).

Different models have been proposed for FGFR dimerization depending on ligand-heparin-receptor complex, specificity between the ligand and the receptor and the heparin length required for the binding (Harmer *et al.* 2004; Mohammadi *et al.* 2005). In the first model, HS increases association between the receptor and the high affinity binding site of the ligand, forming a ternary complex (1:1:1 FGF-HS-FGFR), that then interacts with a second receptor which induces FGFR dimerization through the FGF low affinity binding site (2:1:1 FGFR-HS-FGF). On the other hand, the symmetric model suggests that two individual ternary complexes are formed; the FGFR dimerization will then occur by FGFR-FGFR direct interaction, FGF ligand interaction or by HS-HS link (2:2:2 FGFR-HS-FGF). In this model, HS enhances FGFR dimerization but is not crucial. Finally, according to Harmer *et al.*, in the asymmetric model HS attaches to two FGF-FGFR complexes, binding both FGFs but only one of the receptors (2:1:2 FGFR-HS-FGF) (Harmer *et al.* 2004). Therefore, although different models have been suggested, more research needs to be done to clarify the stoichiometry of FGFR dimerization (Harmer *et al.* 2004; Mohammadi *et al.* 2005; Ori *et al.* 2008).

1.5.4 FGFR signalling pathway

FGF-FGFR stimulates cell signalling pathways related to cell proliferation, survival, cytoskeletal regulation and FGFR degradation (Tiong *et al.* 2013). Cell proliferation is mainly induced by the RAC/JNK, STAT and RAS/MEK/MAPK signalling pathways (Beenken and Mohammadi 2009; Porębska *et al.* 2018). RAC kinases can be activated by the transient phosphorylation of CRK, which simultaneously stimulates RAC phosphorylation through DOCK1 or SOS/RAS (Tiong *et al.* 2013). RAC kinases promote proliferation by activation of JNKs and p38 molecules. On the other hand, the RAS/RAF/MEK/ERK signalling pathway can be activated by FRS2-GRB2-SOS-SHP2 complex assembly or by PKC activation through PLC phosphorylation (Ahmad *et al.* 2012; Dieci *et al.* 2013) (**Figure 1.10**). Cell survival is mainly promoted by phosphorylation of STATs and PI3K/AKT signalling pathway through the FRS2-GRB2-GAB1 complex (Porębska *et al.* 2018). Finally, FGFRs are also implicated in

cytoskeletal regulation as PLC phosphorylation leads to the hydrolysis of PIP₂ into IP₃, inducing calcium release (Dieci *et al.* 2013) (**Figure 1.10**).

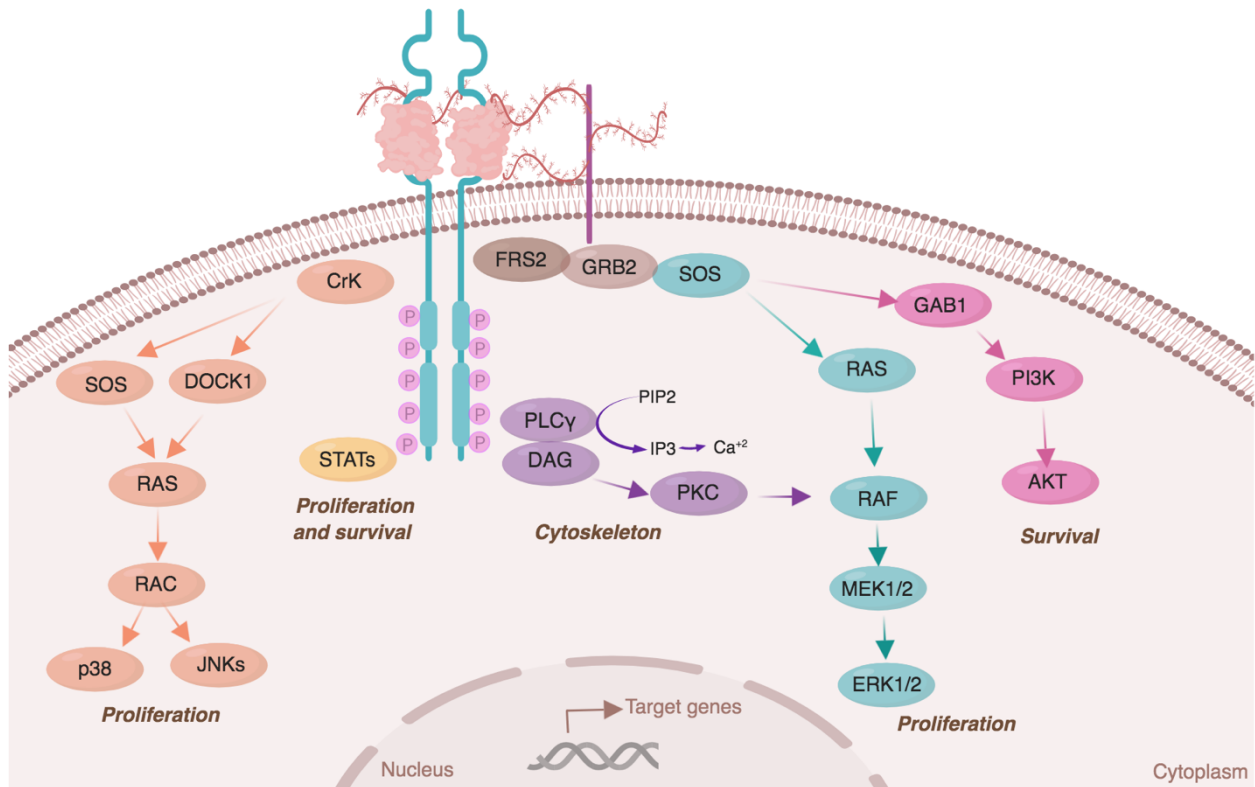


Figure 1.10. FGFR signalling pathway. After ligand-receptor binding, FGFRs dimerise and activate multiple signalling transduction pathways. Each pathway induces the expression of specific target genes related to cell proliferation (STATs, RAS/p38/JNKs and RAS/MAPK/ERK), survival (STATs and PI3K/AKT) and cytoskeleton regulation (PLC/Ca²⁺). Kinases from a specific signalling pathway have the same colour code in this images. Image created with biorender.com.

1.5.5 FGFR signalling pathway regulation

Due to FGF signalling acting upon many biological functions, a regulatory system that controls its timing and balances its activation is required. One of these regulatory systems is FGFR internalization, also referred to as constitutive endocytosis. FGFR synthesis occurs at higher level than its internalization. However, after ligand-binding, FGFR internalization from the plasma membrane accelerates (Opaliński *et al.* 2017). FGFRs mainly utilise clathrin-mediated endocytosis and require SRC-FRS2 complex (Auciello *et al.* 2012). Nonetheless, FGFR3 can also be internalized through clathrin-

independent endocytosis and FGFR1 through a caveolin-mediated system (Haugsten *et al.* 2010; Opaliński *et al.* 2017). The internalization rate depends on receptor type; FGFR1 has the highest internalization rate while FGFR3 has the lowest. Endocytosis of activated FGFRs involves the detachment from the SRC complex (Sandilands *et al.* 2007). FGFRs can then re-translocate to the cytosol, mitochondria, nucleus (to directly regulate gene expression), or to the endosomal compartment for receptor degradation (Opaliński *et al.* 2017); the latter requires the interaction between FRS2-GRB complex and CBL and is also receptor-dependent (Ahmad *et al.* 2012). Indeed, FGFR1 has more ubiquitination sites than FGFR4, which accounts for its higher degradation rates (Tiong *et al.* 2013).

Other regulatory systems of FGFR signalling are the negative regulators SEF, SPRY1/SPRY4 and MKP1/ MKP3. Activation of cell proliferation is counterbalanced by SEF that negatively regulates ERK and AKT activation (Dieci *et al.* 2013). Similarly, SPRY1/SPRY4 molecules strongly reduce proliferation by directly interacting with RAS/RAF kinases or by blocking the FRS2-GRB2-SOS-SHP2 complex. MKP1 and MKP3 also attenuate the FGFR signalling pathway by dephosphorylating MAPK and ERK (Tiong *et al.* 2013) (**Figure 1.11**).

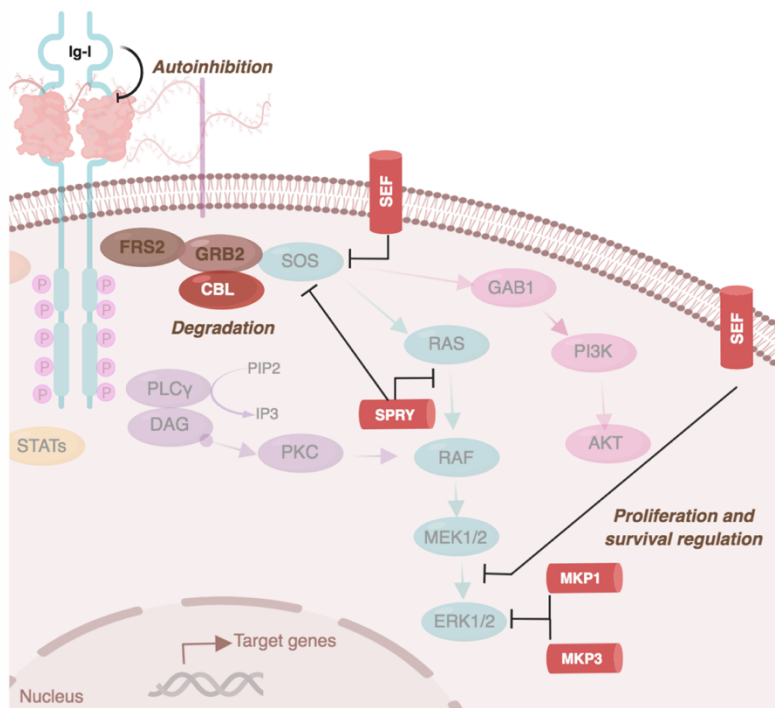


Figure 1.11. FGFR signalling pathway regulation. This pathway is negatively regulated in part by CBL (inducing FGFR degradation after receptor internalization), by SEF, SPRY, MKP1 and MKP3 (which negatively regulate proliferation and survival related pathways). FGFR can regulate its own activation thanks the autoinhibitory function of Ig-I. Image created with biorender.com.

FGFR signalling is also negatively regulated by the autoinhibitory (Ig-I) domain of the receptors (**Figure 1.11**). This is controlled by the electrostatic interactions between the negatively charged acid box with the highly basic heparin binding site in Ig-II (Olsen *et al.* 2004). This complex blocks heparin-FGF binding, thus minimising FGF signalling. Its auto-inhibitory capacity is crucial for the modulation of the pathway as the high amount of HSPGs from the cell surface and the ECM increases the probabilities of FGF-heparin binding and the subsequent activation of the RTK cascade (Mohammadi *et al.* 2005).

Other factors that regulate the FGFR pathway include the ligand affinity for the receptor, as well as the ligand amount and availability. Extracellular FGFs are protected and stored by HSPGs. Heparanases (HPSEs) are directly involved in FGF signalling regulation as they cleave the HS chain, thus releasing FGFs in the vicinity of cells. Depending on the cell type and the growth factor released, HPSEs are therefore involved in cell growth, differentiation, and/or stemness maintenance (Kundu *et al.* 2016). Likewise, sufficient amounts of ligand and heparin/HS proteoglycans are necessary to stabilise FGFR dimerization. The necessary ligand concentration is dependent on the ligand-binding affinity of FGFRs, which depends on the FGFR splice isoforms (Beenken and Mohammadi 2009; Haugsten *et al.* 2010; Holzmann *et al.* 2012). For example, FGF2 activates both FGFR1 IIIb and IIIc isoforms, while it has higher affinity for the isoform IIIc in FGFR2 and FGFR3 (Holzmann *et al.* 2012).

Although these mechanisms are involved in fine-tuning the FGFR signalling pathway, failure in any of them can alter the balance of vital functions of human biology affected by its regulation (Mohammadi *et al.* 2005; Haugsten *et al.* 2010; Ohashi *et al.* 2014).

1.5.6 FGF-FGFR signalling in glioblastoma

1.5.6.1 FGF2 in glioblastoma

Considering the widespread involvement of FGF2 in neural development and adult neurogenesis, its deregulation has been associated with multiple CNS disorders, such as Alzheimer's and Parkinson's diseases and brain tumours. Takahashi *et al.* demonstrated by immunohistochemistry of human tissue sections that FGF2 is highly expressed in high-grade gliomas, compared to low-grade gliomas and the healthy brain (Takahashi *et al.* 1992). In addition, Peles *et al.* reported an increase in the levels

of FGF2 in cerebrospinal fluid of patients with high-grade gliomas compared to low grade gliomas (52 ng/mL and 26 ng/mL, respectively) (Peles *et al.* 2004). Other studies have shown that high expression of cytoplasmic FGF2 carries a poorer prognosis in patients with proneural GBM (Sooman *et al.* 2015). Moreover, its angiogenic properties have linked FGF2 to tumour cells invasion into the healthy parenchyma and glioma necrosis. Necrotic cells can liberate FGF2 to the tumour microenvironment contributing to FGF2 paracrine function (Zagzag *et al.* 1990; Dienstmann *et al.* 2014).

1.5.6.2 FGF2 function in GSC propagation *in vitro*

Apart from its relevance to GBM progression *in vivo*, FGF2 is a crucial factor for the propagation of GSCs *in vitro*. Serum-free medium supplemented with EGF and FGF2 has been broadly used to expand both NSCs and GSCs (Singh *et al.* 2003; Galli *et al.* 2004; Reynolds and Rietze 2005; Kelly *et al.* 2009). GSCs grown in these conditions maintain the expression of NSC markers such as NESTIN, SOX2 and SSEA1 (Lee *et al.* 2006), proliferate at a constant rate and maintain their ability to differentiate (Galli *et al.* 2004; Lee *et al.* 2006). Moreover, these growth factors reduce apoptosis and promote GSCs to enter the S phase of the cell cycle (Kelly *et al.* 2009).

Although EGF and FGF2 induce migration, FGF2 is more relevant for self-renewal capacity, differentiation inhibition and proliferation of GSCs (Auguste *et al.* 2001). Moreover, Podergajs *et al.* showed that FGF2, and not EGF, increased the expression of stemness markers such as CD133 and NESTIN using western blot analyses of patient-derived proneural-GBM cells (Podergajs *et al.* 2013). While these works highlight the importance of exogenous FGF2 for maintaining GSCs, other studies have shown that GSCs cultured without growth factors will still maintain their self-renewal and proliferative capacities (Kelly *et al.* 2009; Takahashi *et al.* 2009). The latter can be explained by the fact that GBM cells can secrete autocrine and paracrine factors that promote tumour growth and angiogenesis, as well as maintaining GSC features (Takahashi *et al.* 1992). Indeed, FGF2 is secreted from glioma cells and endothelial cells to the tumour microenvironment (Baird and Ling 1987; Rogelj *et al.* 1988; Zagzag *et al.* 1990; Vlodavsky *et al.* 2006). This has been proved by Morrison *et al.* as inhibition of endogenous FGF2 in hGBM cell lines by FGF2-specific antisense oligonucleotides decreased cell growth by 80% (Morrison *et al.* 1991). These findings imply that glioma cells are capable of autocrine receptor stimulation, which can lead

to tumour growth and progression (Saiki *et al.* 1999; Yamada *et al.* 1999). Whether this autocrine/paracrine regulation is specific for GSCs is not yet known (Takahashi *et al.* 1992; Hoelzinger *et al.* 2007). These studies suggest that FGF2 and the FGF2-FGFR pathway are prognostic markers of high grade gliomas and crucial factors in GBM cell proliferation (Morrison *et al.* 1990; Loilome *et al.* 2009).

1.5.6.3 *FGFR alterations in carcinogenesis and glioblastoma*

FGFR genomic alterations can occur through *FGFR* overexpression, amplification, mutations, splicing isoforms variations and *FGFR* translocations (Tiong *et al.* 2013; Costa *et al.* 2016). *FGFR* alterations have been found in many different malignancies (lung cancer, bladder cancer, breast cancer etc.), but few *FGFR* aberrations have been detected in GBM (**Table 1.1**) (Lasorella *et al.* 2017). Nonetheless, *FGFR* expression changes in astrocytes can lead to malignant transformation and GBM progression due to activation of mitogenic, migratory and antiapoptotic responses (Morrison *et al.* 1994; Yamada *et al.* 1999; Dienstmann *et al.* 2014).

	Gene amplifications	Point mutations	Chromosomal translocations	FGFR Splice isoforms
<i>FGFR1</i>	Breast, ovarian, bladder and lung cancer	Majority of cancers. Example: Melanoma	Stem cell leukaemia lymphoma (SCLL), GBM	IIIc small cell lung carcinoma I β in breast cancer and GBM
<i>FGFR2</i>	Breast, gastric, lung cancer	Majority of cancers. Example: Endometrial carcinoma	NS	IIIb breast, endometrial, cervical, lung, pancreatic and colorectal cancer IIIc prostate cancers
<i>FGFR3</i>	Bladder cancer	Majority of cancers. Example: bladder cancer	GBM, T-cell lymphoma and bladder	IIIc bladder
<i>FGFR4</i>	Colorectal cancer	Majority of cancers. Example: metastatic nature and rhabdomyosarcoma	NS	NS

Table 1.1. Common *FGFR* genomic aberrations in solid tumours. FGF signalling deregulation is involved in the development of many different human cancers. Four *FGFR* genomic alterations are represented in this table: gene amplification, point mutations, chromosomal translocations and *FGFR* splicing isoforms. Each *FGFR* alteration is linked with the most significant cancers that contain those alterations. The role of the majority of the discovered point mutations in *FGFR* is unknown in cancer. NS (not significant). Adapted from Tiong *et al.* 2013 and Dieci *et al.* 2013.

Different studies have shown an important association between glioma progression and FGF2-FGFR1 expression. FGFR1 mRNA levels are higher in GBM than in the healthy adult brain (Rand *et al.* 2005). FGFR1 is known to induce GBM cell proliferation *in vitro* and its expression is also associated with increased migration of glioma cells and GBM growth, through RAC1/CDC42 and MAPK pathways, respectively (Yamada *et al.* 1999; Fukai *et al.* 2008; Loilome *et al.* 2009; Irschick *et al.* 2013). This is supported by Saiki *et al.* who showed that adenoviral delivery of truncated FGFR1 inhibited GBM growth both *in vitro* and *in vivo* (Saiki *et al.* 1999). Moreover, Gouazé-Andersson *et al.* proved that FGFR1 induced GBM cell radioresistance through PLC- γ , which is also involved in the regulation of hypoxia and apoptosis (Sooman *et al.* 2015; Gouazé-Andersson *et al.* 2016).

Although Rand *et al.* showed no genomic amplification of *FGFR1* among 19 different GBM samples, two point mutations (N546K and R576W) in the tyrosine kinase domain of this receptor have been shown to alter its acidic/basic charge (Rand *et al.* 2005). Consequently, impairment of the specific order by which tyrosine residues are phosphorylated leads to an uncontrolled autophosphorylation of the tyrosine kinase domain and hyperactivation of the pathway (Rand *et al.* 2005; Lew *et al.* 2009). Mutations in similar positions of these tyrosine kinases were found in *FGFR2* and *FGFR3*, however they were not related to GBM (Rand *et al.* 2005). Indeed, less than 0.3% of the discovered mutations in these receptors are related to CNS cancers (cancer.sanger.ac.uk) (Forbes *et al.* 2017). *FGFR2* and *FGFR3* have been reported to be expressed in low levels in GBM (Yamaguchi *et al.* 1994; Parker *et al.* 2014). Moreover, reduced *FGFR2* expression is associated with higher tumour grade and poorer survival in glioma patients (Ohashi *et al.* 2014). Nonetheless, the functional relevance of *FGFR2* signalling in GBM is not yet completely understood.

Although FGFRs do not show frequent mutations or amplifications in GBM, 3% of the aberrations identified have been linked to transforming acidic coiled-coil (*TACC*) fusion genes such as *FGFR1-TACC1* and *FGFR3-TACC3* fusion (Singh *et al.* 2012; Di Stefano *et al.* 2015; Lasorella *et al.* 2017), which was first discovered in GBM (Singh *et al.* 2012; Parker *et al.* 2013). FGFR-TACC fusion proteins have been detected in low- and high-grade gliomas (Di Stefano *et al.* 2015; Lasorella *et al.* 2017). TACC fusion can be produced by different aberrations, although chromosomal translocation

of *FGFR3-TACC3* is the most frequent in GBM (Di Stefano *et al.* 2015). These aberrations are generated by the fusion of a small portion of TACC C-terminus protein joined to the FGFR (Ig-IIIc) N-terminus. This induces ligand-independent activation of the pathway and chromosomal instability (Singh *et al.* 2012). Glioma cells are able to overcome the detrimental effects of these chromosomal alterations owing to their growth advantage (Lasorella *et al.* 2017). Moreover, *FGFR3-TACC3* fusion can be overexpressed in GBM because the 3' UTR of the receptor is lost, blocking the negative regulation of its expression by *mir-99a* (Parker *et al.* 2014).

Previous studies have shown that a switch towards the FGFR IIIc isoform in cancer promotes abnormal regulation of epithelial (Ig-IIIb) and mesenchymal (Ig-IIIc) tissue homeostasis. This switch towards a more mesenchymal phenotype is linked to EMT and to a more invasive and tumorigenic phenotype (Ahmad *et al.* 2012; Ranieri *et al.* 2016). For instance, in pancreatic cancer, *FGFR1* IIIc is expressed in greater levels than *FGFR1* IIIb and the exposure treatment of pancreatic cell lines with FGF1 and FGF2 induces *FGFR1* IIIc, and reduces IIIb expression (Kornmann *et al.* 2002; Chen *et al.* 2008). This supports the notion that splice variants have different affinities for the ligand. *FGFR1* IIIc is also upregulated in astrocytomas (Gong 2014) (**Figure 1.12**). Meanwhile in colorectal cancer *FGFR2* IIIc is upregulated, although Ohasahi *et al.* suggest a tumour suppressor function for both *FGFR2* IIIb and IIIc isoforms in GBM (Ohashi *et al.* 2014). This is supported by Ricol *et al.* who have attributed a tumour suppressor function to *FGFR2* IIIb in bladder cancer (Ricol *et al.* 1999). Thus, more research is needed to better understand the functions of individual FGFR splice variants in different cancers.

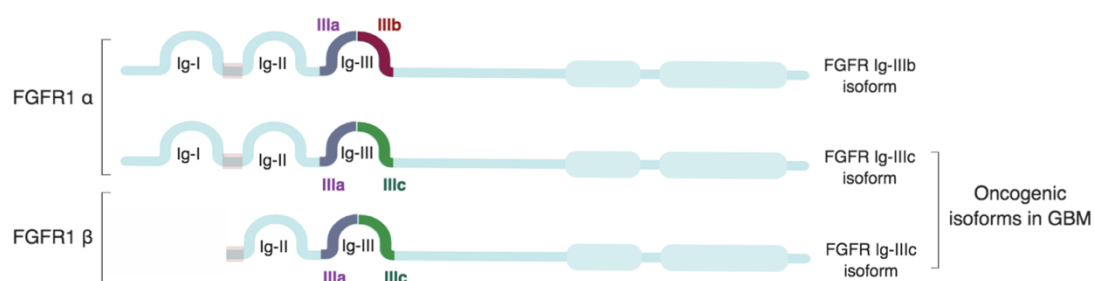


Figure 1.12. FGFR1 splice isoforms in GBM. The splice variant *FGFR1* Ig-IIIc is higher express in astrocytoma. *FGFR1* has another alternative splice variant produced by exclusion of Ig-I domain termed *FGFR1 β* isoform. *FGFR* isoform containing the three *FGFR* domains (extracellular, transmembrane and intracellular) is termed *FGFR α* . Due to the auto-inhibitory function of the Ig-I domain, *FGFR1 β* isoform has considerably higher affinity for FGFs promoting its oncogenic role. Image created with biorender.com.

Although splice variants of FGFR Ig-III are important in cancer, deletions or mutations of the Ig-I domain have also been related to deregulation of the pathway. FGFR containing Ig-I is termed Ig-I α while the deletion of that isoform results in Ig-I β (Jin *et al.* 1999). This mutation has been shown mainly in FGFR1 (**Figure 1.12**). The ratio of alternatively spliced FGFR1 α/β isoforms changes with progression to more aggressive brain cancers. While FGFR1 α is the predominant isoform in low-grade gliomas, high-grade gliomas show a shift towards expression of FGFR1 β (Yamaguchi *et al.* 1994; Jin *et al.* 2000). FGFR1 β increases the receptor-ligand affinity and lacks the auto-inhibitory function of Ig-I domain (Gong 2014). Thus, changes in alternative splicing of the Ig-I may contribute to GBM malignancy by increasing the sensitivity of tumour cells to FGFs present in their environment (Ahmad *et al.* 2012; Ranieri *et al.* 2016).

1.5.6.4 Anti-FGFR therapies in glioblastoma

Oncogenic FGFR signalling promotes malignancy in many cancers. Thus, pharmacological targeting of FGFRs may be therapeutically beneficial. Among the different approaches used for anti-FGFR drug development, small molecules have been the most clinically advanced. These compounds have been classified into two groups: “multitarget TKIs” and “selective or FGFR-specific” drugs (Dieci *et al.* 2013). The first group includes small molecules (e.g. Dovitinib, Nintedanib, Ponatinib, Brivanib) targeting not only FGFRs but also other tyrosine kinase receptors such as VEGFRs and PDGFRs. Although these inhibitors showed some beneficial effects in phase I trials (e.g. modulation of ERK phosphorylation), the toxicity levels related to VEGFR blockage are high. Similarly, FGFR-specific drugs (e.g. AZ4547, BGJ398, LY287445), have also not yielded very promising results as blockage of FGF23 signalling generates patient hyperphosphatemia (Dieci *et al.* 2013). To date, no small-molecule inhibitors targeting individual FGFR subtypes or isoforms exist.

Different selective FGFR drugs have been used to target the FGF-FGFR pathway in GBM. The FGFR inhibitor BGJ398 has been tested in clinical phase II trials (NCT01975701) in malignant glioma patients with FGFR1-TACC1 or FGFR3-TACC3 fusion, and/or activating mutation in FGFR1-3. Although the trial was completed, no results have been published yet.

In addition, an oral pan-FGFR kinase inhibitor, JNJ-42756493, was used to treat FGFR-altered solid tumours in a phase I trial (NCT01703481); 4 out of 23 patients that responded to the treatment had FGFR translocations and 2 of them (recurrent GBM) had FGFR3-TACC3 fusion. This suggests a possible benefit in pharmacological targeting FGFR-TACC fusion proteins in GBM patients (Brennan 2017).

The small molecule Tipifarnib, which is farnesyltransferase inhibitor, has been used in combination with radiotherapy in phase II clinical trials (NCT00209989) to treat newly diagnosed GBM. This therapy aimed to target FGF2 radioresistance through the inhibition of the farnesylated form of RhoB, that mediates hypoxia and radioresistance. A benefit in overall survival of 4.5 months was observed compared to patients treated with standard of care treatment for GBM. Moreover, the authors showed an inverse correlation between FGFR1 expression and benefit in overall survival (Ducassou *et al.* 2013).

In conclusion, despite the advances in drug design of multitarget TKIs and pan-FGF and FGFR-TACC fusion inhibitors, little or partial response has been seen in the median and overall survival of GBM patients. The importance of FGFR signalling for CNS cell survival and apparent intratumoral and intertumoral heterogeneity of FGFR expression has been demonstrated through several studies discussed previously. Therefore, in order to increase the clinical benefit of FGFR therapies in GBM, the development of new inhibitors targeting individual FGFRs and/or their splice variants may prove to be crucial for the treatment of GBM and other cancers.

1.6 Thesis hypothesis and aims

ZEB1, SOX2 and OLIG2 have been described as key stemness-associated transcription factors in GBM (Gangemi *et al.* 2009; Siebzehnruhl *et al.* 2013; Singh *et al.* 2016). They are relevant for GBM progression, invasion and recurrence. Moreover, FGF2, a growth factor highly prevalent in the human brain and widely used to maintain NSCs and GSCs *in vitro*, has been recognized as a crucial oncogenic factor in glioma. Due to the fact that EMT-regulators, such as ZEB1, are known to be induced by trophic factors from the tumour microenvironment (Pollard *et al.* 2009; Haugsten *et al.* 2010) and that ZEB1, SOX2 and OLIG2 expression is co-dependent, we hypothesise that FGF2 may regulate GSC function by activating these stemness-associated transcription factors. This thesis will therefore evaluate the role of FGF2 in GBM tumorigenesis and the mechanism by which FGF2-FGFR may contribute to GSC functions with the following aims:

1. Examine the role of FGF2 in the regulation of ZEB1, SOX2 and OLIG2 and its function in sphere-forming capacity of patient-derived glioblastoma cell lines *in vitro*.
2. Evaluate the expression of FGFR1-3 and their association with GSCs by using knockdown approaches in functional *in vitro* and *in vivo* assays.
3. Investigate the effect of FGFR1 loss on ZEB1, SOX2, and OLIG2 expression, and intracellular signalling pathways downstream of this receptor in hGBM cells.

Chapter 2: Materials and Methods

2.1 Tissue culture

A Safe 2020 Class II Biological Safety Cabinet (Thermo Fisher Scientific) was used for cell culture experiments carried under required sterile techniques. Cells were kept in a Galaxy 170R (Eppendorf) incubator at 37°C, 20% [v/v] O₂ and 5% [v/v] CO₂.

2.1.1 Human cell lines

2.1.1.1 Primary human glioblastoma cells

hGBM Line 0 (L0), Line 1 (L1) and Line 2 (L2) cells, were obtained from Dr Brent Reynolds laboratory at the University of Florida McKnight Brain Institute. These cells were surgically isolated from GBM patient biopsies and authenticated using STR analysis (University of Arizona Genetics Core). They were approved by the Human Tissue Authority (HTA) and have been previously described and used *in vitro* and *in vivo* (Siebzehnrubl *et al.* 2013; Hoang-Minh *et al.* 2018). hGBM cells were grown as floating spheres in Dulbecco's Modified Eagle Medium/Nutrient Mixture F-12 (DMEM/F12) containing GlutaMax and supplemented with 2% bovine serum albumin (BSA; ThermoFisher Scientific), Insulin (Merck), Transferrin-Putrescine-Sodium Selenite (TPN; Merck), progesterone (Merck) and Antibiotic-Antimycotic 100x (Thermo Fisher Scientific) (together, N2) (**Table 2.1**). N2 medium was sterilised with a filter bottle (VWR) prior to being used. Cells were supplement with 20 ng/mL of EGF (Peprotech) and heparin (Merck) twice/week and the formed tumour-spheres were enzymatically disassociated after reaching approximately 150 µm in diameter.

U3019 hGBM cells were characterised and obtained from Uppsala University Human Glioma Cell Culture (HGCC) bio bank (Xie *et al.* 2015). This line was derived from an 86 year-old female tumour biopsy and classified as a proneural subtype of GBM. This cell line was cultured in N2 medium supplemented with 10% [v/v] B-27 Plus Supplement (Thermo Fisher Scientific). Although cells were initially grown in adherent conditions for two passages, they were maintained as floating spheres and supplemented with 20 ng/mL EGF, 20 ng/mL heparin and 10 ng/mL FGF2 (Peprotech). Details of stocks and final concentration of each medium component and feeding solution are specified in **Table 2.1** and **Table 2.2** respectively.

2.1.1.2 Human Embryonic Kidney 293T cell line

HEK 293T cell line was used to produce lentiviral particles. They contained the SV40 T-antigen, needed to replicate vectors carrying the SV40 region (DuBridge *et al.* 1987; Pear *et al.* 1993) and were obtained from Dr Fernando Anjos-Afonso laboratory (European Cancer Stem Cell Research Institute, (ECSCRI), Cardiff University). HEK 293T cells were maintained in Dulbecco's Modified Eagle Medium (DMEM) containing L-glutamine, glucose (Thermo Fisher Scientific) and supplemented with 10% [v/v] heat-inactivated Foetal Bovine Serum (FBS; Seralab) (Kafri *et al.* 1999). FBS heat-inactivation was performed at 56°C during 30 min in an agitating water bath. Cells were passaged every 2-3 days when they reached 70-80% confluency.

2.1.1.3 Cell propagation

hGBM spheres were passaged as previously described (Deleyrolle *et al.* 2011; Siebzehnruhl *et al.* 2013; Hoang-Minh *et al.* 2018). Spheres were collected and centrifuged for 5 min at 400 xg at room temperature (RT) in a Centrifuge 5810R (Eppendorf). Supernatant was removed and cells were enzymatically dissociated for 10 min at 37°C in 500 µL of Accumax (Thermo Fisher Scientific). Cells were washed in 10 mL of (1x) Phosphate Buffer Saline (PBS), centrifuged and cell pellet was thoroughly resuspended 40 times in 200 µL of medium to break up the spheres into single cells. A 200 µL pipette was required for a better dissociation. Cells were plated at a density of 5×10^4 cells/mL in N2 medium. These spheres were serially passaged every 5 days.

HEK 293T cells were grown in adherent conditions. Supernatant was removed and cells were incubated in 5-10 mL of Accumax for 2-5 min at 37°C. The flask was gently tapped to facilitate the detachment of the cells. Cell suspension was collected once the flask was washed with 5-10 mL of (1x) PBS and centrifuged for 5 min at 400 xg at RT. The cell pellet was briefly resuspended and 1:4 dilution was used for cell plating.

PRODUCTS THAT REQUIRE STOCK PREPARATION		
Product	Final concentration	Stock diluted in
Putrescine hydrochloride	16.2 mg/mL	ddH ₂ O
Human Transferrin	100 mg/mL	
Sodium Selenite (Initial stock: 10.5 mg in 10 mL ddH ₂ O)	5.2 µg/mL	
Heparin	2 mg/mL	
Progesterone (Initial stock: 6.3 mg in 10 mL EtOH)	6.3 µg/mL	
Insulin	5 mg/mL	0.1M HCl
EGF	20 µg/mL	DMEM/F12
bFGF2	20 µg/mL	

Table 2.1. Stock concentrations. Required intermediate dilutions for the media additives and feeding solution. Solutions were diluted in double-distilled water (ddH₂O), HCl or medium.

CELL CULTURE MEDIUM		
Product	Volume from stock solution	Final concentration
DMEM/F12	494.5 mL	1:1
Bovine Serum Albumin (BSA)	10 g	2% [w/v]
Antibiotic-Antimycotic 100x	5 mL	1% [v/v]
Putrescine dihydrochloride	500 µL (includes the three products, TPN)	16.2 µg/mL
Human Transferrin		100 µg/mL
Sodium Selenite		5.2 ng/mL
Progesterone	500 µL	6.3 ng/mL
Insulin	500 µL	5 µg/mL
FEEDING SOLUTION		
Product	Volume from stock solution	Final concentration
DMEM/F12	9.4 mL	1:1
EGF	200 µL	0.4 µg/mL
FGF2	200 µL	0.4 µg/mL
Heparin	200 µL	40 µg/mL

Table 2.2. Cell culture medium and feeding solution components. Cell culture medium reagents required from each stock and final concentration in 500 mL of the culture medium. Volume used from EGF, FGF2 and heparin stocks and the final concentration of each reagent in 10 mL of feeding solution. hGBM L0, L1, L2 cells were maintained in FGF2 free conditions. In this case the feeding solution was composed of the same additives excluding FGF2.

2.1.1.4 Differentiation of glioma stem cell progeny

To test differentiation, cells were plated in a density of 5×10^4 cells/mL in growth factor free media supplemented with 10% [v/v] FBS (Singh *et al.* 2003) or 25 ng/mL of BMP4 (Peprotech) (Piccirillo *et al.* 2006; Xi *et al.* 2017). After 48 h of treatment, cells were washed with (1x) PBS and collected to assess stemness factors and FGFRs expression by western blotting.

2.1.2 Cell storage, cryopreservation and freeze-thaw recovery

For cryopreservation, cell pellets were resuspended in fresh medium containing 10% of Dimethyl sulfoxide (DMSO; Merck). A maximum of 1mL solution was quickly transferred to each cryovial, which was previously labelled indicating the date, type, passage and number of frozen cells. Cryovials were then immediately placed in a freezing container (VWR) which was kept at -80°C overnight. After 24 h, the cryovials were transferred into a K Series Cryostorage Freezer System (Worthington Industries) with liquid nitrogen vapor phase for long-term storage. To facilitate cells recovery after thawing, cell pellets were washed twice in (1x) PBS and plated in a 6-well plate. After 24 h the medium was changed to discard the remaining dead cells in the supernatant.

2.1.3 Coating plates with Geltrex

To grow hGBM cells in a monolayer, adherent substrates were required. For cell transduction and transfection, cells were seeded onto plates coated with Geltrex matrix (Thermo Fisher Scientific) using the thin gel method (non-gelling) for human stem cell applications according to manufacturer instructions. Geltrex solution was thawed on ice and diluted in pre-chilled (4°C) medium to a final concentration of 130-150 µg/mL. Sufficient amount of diluted Geltrex was added to cover the entire surface of the well. To promote gelling of the matrix, the plates were incubated for 1h at 37°C. Once the basement membrane matrix was formed, medium was added and cells immediately seeded in specific numbers according to application. Alternatively, the wells were covered with (1x) PBS and the plate was kept at 4°C for up to 2 weeks or at -20°C for longer storage.

2.1.4 Sphere-formation assay

To assess sphere formation capacity, hGBM cells were plated in serum-free medium at low cell density (100 cells per 200 µL). In these conditions only GSCs and progenitor cells will be able to form tumour-spheres (Reynolds and Rietze 2005; Deleyrolle *et al.* 2011). Dissociated hGBM cells were seeded at a concentration of 100 cells/well in a black F-bottom 96-well microplate (Greiner Bio-One). These plates were required to avoid light diffraction when imaging. Cells were cultured in 80 µL/well of medium supplemented with feeding solution and 30 ng/mL of FGF2 when specified. (1x) PBS

was added to the wells at the edges of the plate to avoid medium evaporation. The number of tumour-spheres with a diameter greater than 70 μm were counted using a GelCount analyser (Oxford Optronix) 5 days after seeding. The sphere-forming frequency was calculated by dividing the number of tumour-spheres by the number of plated cells.

2.1.5 Colony Forming Cell (CFC) assay

For clonal expansion analysis, 1×10^3 hGBM single cells were mixed with 400 μL of N2, supplemented with feeding solution, 30 ng/mL of FGF2 (when required) and collagen (Stemcell Technologies) at a 1:3 ratio (collagen/medium) (Bao *et al.* 2006; Louis *et al.* 2008). Collagen-cells mix was slowly pipetted up and down to avoid aggregation of cells within the viscous solution and transferred to a well of a 24-well plate (Greiner Bio-One). (1x) PBS was added to the plate empty spaces to avoid medium evaporation. Cells were cultured at 37°C and supplemented with fresh growth factors twice/week. Colonies greater than 200 μm of diameter were counted using a GelCount analyser two weeks after plating.

2.1.5.1 Limiting dilution CFC assay

Limiting dilution CFC analysis was carried out as described in 2.1.5 with the difference that in this assay three concentrations of cells were plated per well of a 12-well plate (Greiner Bio-One): 2.5×10^3 , 1.5×10^3 or 750 hGBM cells. Number of colonies per well should be proportional to the number of plated cells.

2.1.6 Proliferation rate

To examine proliferative potential, single hGBM cells were seeded in a concentration of 5×10^4 cells/mL and in serum-free medium supplemented with growth factors. Tumour-spheres were disassociated 5 days after plating and the total number of cells was quantified. Fold expansion rate was calculated by dividing the total number of cells between the plated ones.

2.1.7 FGF2 inhibitors

FGF2 inhibitors, NSC-47762, NSC-58057, NSC-65575 and NSC-65576 were obtained from the Developmental Therapeutics Program (DTP), division of Cancer Treatment and Diagnosis, NCI, NIH (USA). These small molecules block the interaction between FGF2 and FGFRs (Pagano *et al.* 2012; Foglieni *et al.* 2016). Compounds were dissolved in DMSO to a stock concentration of 25 mM (**Table 2.3**). The solution was aliquoted after 3-6 h mixing in a shaker at RT and stored at -80°C. For functional assays, cells were treated with four concentrations of each compound: 12.5 μ M, 25 μ M, 50 μ M and 100 μ M. Cells treated with DMSO were used as control cells.

Small Molecule	MW	DMSO (μ L) for 25mM stock
NSC-47762	816	245.2
NSC-58057	926	216
NSC-65575	940	213
NSC-65576	940	213

Table 2.3. FGF2 inhibitor stock concentration. Required DMSO volume for each compound to be diluted to a stock concentration of 25 mM. Cells were treated with 0.49 μ L/mL, 0.9 μ L/mL, 1.9 μ L/mL and 3.9 μ L/mL of the stock solution for a final concentration of 12.5 μ M, 25 μ M, 50 μ M and 100 μ M respectively. The same volumes were used for each concentration DMSO/control.

2.1.8 MTT assay

For cell viability/proliferation assay, 3,000-5000 cells/well, cell line dependent, were plated onto a 96-well plate coated with Geltrex (section 2.1.4) in a volume of 100 μ L/well. The following day, the same volume of medium containing growth factors and/or small molecules, was added to each well. An empty column (without cells) containing 200 μ L/well of medium was used for blank correction. After 4-5 days, 25 μ L/well of Thiazolyl Blue Tetrazolium Bromide (MTT; Merck) stock solution (5mg/mL of MTT in (1x) PBS, used for up to a week when kept in the dark and at 4°C) were added and cells were incubated at 37°C for 3 h. NAD(P)H-dependent cellular oxidoreductase in the mitochondria of live cells, metabolizes MTT to dark blue formazan crystals, which are visible inside treated cells. Medium containing MTT substrate was removed, the reaction was stopped with 100 μ L of DMSO and the solution was pipetted up and down to break up residual crystals of water-insoluble formazan. Colorimetric detection was used to quantify solubilised crystals and was

measured at a wave length of 570 nm in a CLARIOstar (BMG Labtech), with a reference wave length of > 650 nm. Optical density (OD) values were used to calculate the relative cell viability and/or proliferation rate, after normalization to control (Hölsken *et al.* 2006; Siebzehnruhl *et al.* 2013).

2.1.9 ERK1/2 inhibitor

ERK1/2 inhibitor SCH772984 was purchased from Selleckchem and diluted to a stock concentration of 1 mM in DMSO (5 mg into 8.5 mL DMSO as recommended) and stored at -80°C (Kong *et al.* 2017; Soady *et al.* 2017). A second stock solution of 10 µM was prepared. 3×10^5 single cells were plated per well of a 6-well plate without growth factors. The following day, cells were treated with 60 ng/mL of FGF2, 60 ng/mL heparin and 10 nM, 20 nM and 40 nM ERK1/2 inhibitor at different time points (10 min, 30 min and 1 h). Cells were collected and proteins were isolated as described in section 2.8.1.

2.2 Plasmids and DNA preparation

2.2.1 DNA vectors

Plasmids for knockdown of *FGFR1*, *FGFR2*, *FGFR3* and *ZEB1* were purchased from Horizon Discovery (**Table 2.4**). All plasmids were encoded within a GFP-expressing lentiviral vector (pGIPZ backbone) and contained an ampicillin resistance cassette. 100 µg/mL of ampicillin (Merck) was used for selection of clones. Different shRNA were tested for each target gene by western blotting and the most efficient knockdowns were selected to produce lentiviral particles. Short hairpin (sh) FGFRs and shZEB1 plasmid details and sequences can be found in **Figure 2.1** and **Table 2.4**.

Full length FGFR1 Gateway entry clone was a gift from Dominic Esposito (Addgene plasmid #70367). This plasmid had spectinomycin resistance (50 µg/mL). FGFR1 was cloned into an expression vector (pHIV-IRES-mRFP-GW) obtained from Dr Matt Smalley (ECSCRI, Cardiff University), using the Gateway system as explained in section 2.4 (Tornillo *et al.* 2018). Lentiviral particles were generated (section 2.6) with second generation lentiviral packaging plasmid psPAX2 (encoding the *Gag*, *Pol*, *Rev*,

and *Tat* genes) and envelop plasmids pMD2.G (encoding for VSV-G), which were also a gift from Dr Matt Smalley.

Knockdown	Clone ID	Target sequence
FGFR1	V3LHS_634638	TGAACTTCACTGTCTTGCC
	V3LHS_634641	TGTCTTTTTATAGTAGTCG
	V3LHS_634644	CTGTCACCAGGACATTCTCT
FGFR2	V2LHS_262926	ATATTGTTGATATCTCTGG
	V3LHS_363910	CTACCAACTGCTTGAACGT
FGFR3	V2LHS_83489	ATATCTTCACTGGAATCAC
	V2LHS_83493	AGGACCAGACGTCACTCTG
	V3LHS_412937	AACAGTACAGAACGAACCA
ZEB1	V2LHS_226625	TAATTTGTAACGTTATTGC
shControl	RHS4346	-

Table 2.4. FGFRs and ZEB1 Knockdown sequences. Different clones for each human shFGFR were obtained from Horizon Discovery. Clone 1 for each receptor as specified in bold letters (shFGFR1 V3LHS_634638, shFGFR2 V2LHS_262926 and shFGFR3 V2LHS_83489), was the most efficient and was selected for lentiviral production. shZEB1 clones were previously tested and published in Siebzehnrubl *et al.* 2013.

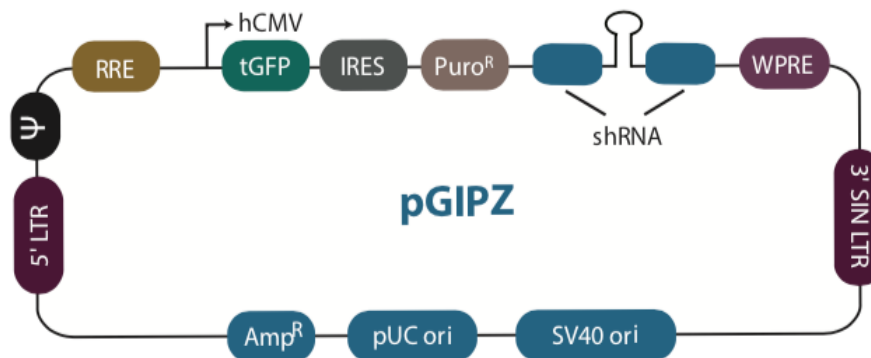


Figure 2.1. pGIPZ shRNA lentiviral vector map. This vector map is a general representation of the shRNA plasmids used (shFGFR1, shFGFR2, shFGFR3, shZEB1). hCMV is the human cytomegalovirus promoter; tGFP is a turbo green fluorescence protein reporter used for visual isolation of cells expressing the vector; PURO, puromycin resistance gene allows transduced cells to be resistant to puromycin antibiotic; PURO and tGFP are expressed in single transcripts due to an internal ribosomal entry site (IRES); shRNA for gene knockdown is a microRNA-adapted shRNA based on miR-30; woodchuck hepatitis posttranscriptional regulatory element (WPRE) enhances plasmid expression in transduced cells and increases virus titer by facilitating mRNA transcript maturation; there are two long termination repeats (LTRs) in the integrated poliovirus that control gene expression: truncated HIV-1 5'LTR that acts as a RNA polymerase II promoter and packaging of viral RNA into virus and 3' self-inactivating LTR (3'SIN LTR). The latter LTR induces transcription termination by polyadenylation signal during viral genome integration preventing viral replication and reduces mutagenesis by limiting the interaction between the transgene and the LTR enhancers; Simian virus 40 (SV40 ori) is essential for transgene maintenance in mammalian cells during viral particles production; pUC ori of replication (pUC ori) is crucial for plasmid replication in *E. coli* promoting high copy plasmid number; Ampicillin resistance gene (*Amp^R*), confers transformed *E. coli* with resistance to ampicillin antibiotic; HIV packaging signal (Ψ) is essential for transfer plasmid packaging; HIV-1 Rev response element (RRE) allows the transport of rev-dependent viral particles from the nucleus to the cytoplasm. Image from Horizon Discovery.

2.2.2 DNA isolation and purification

Plasmids were received as bacteria stabs or glycerol stocks. Bacteria were spread onto pre-warmed (37°C) agar plates containing antibiotics depending on plasmid selection. After 24 h, single bacteria colonies were picked and inoculated into 2 mL of LB broth medium containing the desired antibiotic. The inoculant was incubated for 6-8 h in a shaker at 225 rpm at 37°C, then transferred to a 50 mL volume of the same media and incubated following the same conditions overnight. The next day, the inoculant was centrifuged at 130 xg at 4°C and plasmid DNA isolated using a Qiagen Plasmid Midi Kit (Qiagen) according to manufacturer instructions. The resulting DNA pellet was diluted in 40 µL of Tris-EDTA (TE) Buffer (Qiagen) and quantified on a NanoDrop 2000 spectrophotometer (Thermo Fisher Scientific).

2.3 DNA transformation and ligation

One Shot Top 10 (Thermo Fisher Scientific) or Stbl3 (NEB) competent cells were used for transformation. A vial of competent cells was thawed on ice and used for two transformations/ligations (25 µL per reaction). 1-2 µL containing up to 100 ng of plasmid DNA or ligation reaction were added to the competent cells and the mix carefully flicked before being incubated on ice for 30 min. Cells were heat shocked for 30 sec at 42°C in the water bath and immediately placed on ice to stop the reaction. The solution was mixed with 200 µL of S.O.C medium (Thermo Fisher Scientific) and incubated for 1h at 225 rpm at 37°C in a shaking incubator. 100 µL of the ligation reaction/transformation were spread onto a pre-warmed selecting agar plate and left overnight at 37°C. DNA isolation and purification were performed as previously described in section 2.2.1.

2.4 Gateway cloning system

2.4.1 LR recombinant reaction

Gateway Technology (Thermo Fisher Scientific) was used to clone full-length FGFR1 into a lentiviral expression vector (**Figure 2.2**). A LR recombinant reaction between an entry vector containing FGFR1 and a destination vector with a lentiviral backbone was performed using LR Clonase II enzyme mix (Thermo Fisher Scientific). Negative and positive controls were included along the process as specified in **Table 2.5**. LR

reaction components were briefly vortexed and incubated at 25°C for 1 h. The mix was incubated with 2 μ L of Proteinase K (Thermo Fisher Scientific) at 37°C for 10 min and transformed into One Shot Top 10 competent cells for selection of *attB*-containing expression vector.

Components for LR reaction	Sample	Negative Control	Positive Control
Entry clone (300 ng/reaction)	2 μ L	-	-
Destination vector (300 ng/reaction)	2 μ L	2 μ L	1 μ L
pENTR-gus (50 ng/ μ L)	-	-	1 μ L
5x LR Clonase Reaction Buffer	2 μ L	2 μ L	2 μ L
TE Buffer	2 μ L	5 μ L	3 μ L

Table 2.5. LR recombinant reaction set up. Three different reactions were produced: one containing both destination and entry clones; a negative control containing only the destination vector; and a positive control with the destination vector and a pENTR-gus plasmids provided by Thermo Fisher Scientific. The latter produced an expression clone containing the β -glucuronidase (*gus*). These controls were required to verify expected recombination and expression after LR reaction. After transformation of the LR reaction mixture in *E. coli* strains, many colonies were formed in the reaction containing the gene of interest and the p-ENTR-gus (positive control). However, none or very few colonies were seen in the negative control as it did not contain the entry clone.

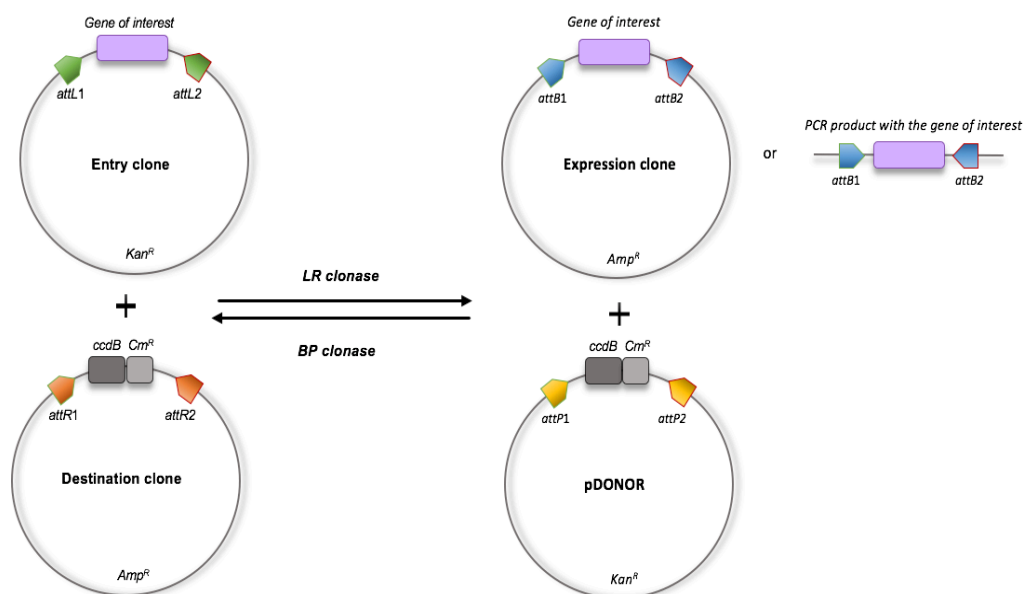


Figure 2.2. Gateway cloning technology. This rapid, efficient and reversible cloning method has been used to transfer DNA fragments into multiple vector systems. It is based on the site-specific recombination properties of bacteriophage λ . These sites are called *att* sites and have been modified to increase the recombination efficiency. LR/BP clonases are recombination enzymes that recognise and cleave *att* sites and ligate the DNA fragments into the new clone. Bacteriophage λ induces recombination through two types of reactions: BP reaction (lysogenic pathway) and LR reactions (lytic pathway). The first reaction recombines DNA flanked by *attB* sites (PCR product or expression vector) with the one from a Donor clone that contains *attP* sites. *attB1* will specifically recombine with *attP1* similarly *attB2* and *attP2*. This reaction is catalysed by BP clonase and it produces an entry clone and an *attR* flanked product. LR reaction is catalysed by a LR clonase enzyme and occurs between an entry clone containing *attL* sites flanking the gene of interest and a destination vector with *attR* sites between a *ccdB* gene. The result of a LR reaction will be an expression vector and clones containing the *ccdB* gene or suicide gene which will be negatively selected. Importantly, each clone has a different resistance gene: entry clones are resistant to Kanamycin and destination vectors to chloramphenicol and ampicillin. Once the gene of interest is recombined, the expression vector will have an ampicillin resistance (Image adapted from Thermo Fisher Scientific gateway cloning technology protocol).

2.4.2 Expression vector verification and amplification

Ampicillin resistant colonies were picked for DNA isolation using a Qiagen Plasmid Mini Kit (Qiagen) according to manufacturer instructions. Restriction enzyme digestion was performed to confirm that the selected clones contained the gene of interest. Restriction enzymes Cla1 and Xho1 were mixed with CutSmart buffer (NEB), water and DNA from the gateway cloned expression vector or the negative control (destination vector alone) (**Table 2.6**). Reagents were incubated at 37°C for 45 min.

Components for FGFR1 enzyme digestion	Expression Clone	Destination vector (- control)
Expression vector (500 ng/reaction)	2.5 μ L	-
Destination vector (500 ng/reaction)	-	3 μ L
Xho1 enzyme	1 μ L	1 μ L
Cla1 enzyme	1 μ L	1 μ L
CutSmart Buffer	4 μ L	4 μ L
ddH ₂ O (to 40ul)	31.5 μ L	31 μ L

Table 2.6. Restriction enzyme digestion. Expression vector refers to the DNA obtained from the colonies picked after the LR reaction. Destination vector is the plasmid in which FGFR1 was transferred. Xho1 and Cla1 enzymes cut the fragment of destination vector DNA contained between the *attR* sites and the *attB* sites as explained in Figure 2.3.

6 μ L of 5x DNA loading buffer blue (BioLine) were added to 25 μ L of the digested DNA and loaded into a 1.6% agarose gel containing 5 μ L of SYBR safe (1:20 dilution; BioLine). DNA was separated by agarose gel electrophoresis for 45 min at 100 V using a Horizontal Electrophoresis System (Bio-Rad) and PowerPac (Bio-Rad) for power supply. DNA bands were compared to a hyperladder 1Kb (BioLine) and visualised with a ChemiDoc MP imaging system (Bio-Rad). Successfully cloned expression vectors (**Figure 2.3** and **Figure 2.4**) were expanded with Stbl3 cells and lentiviral particles were produced (sections 2.3 and 2.6 respectively).

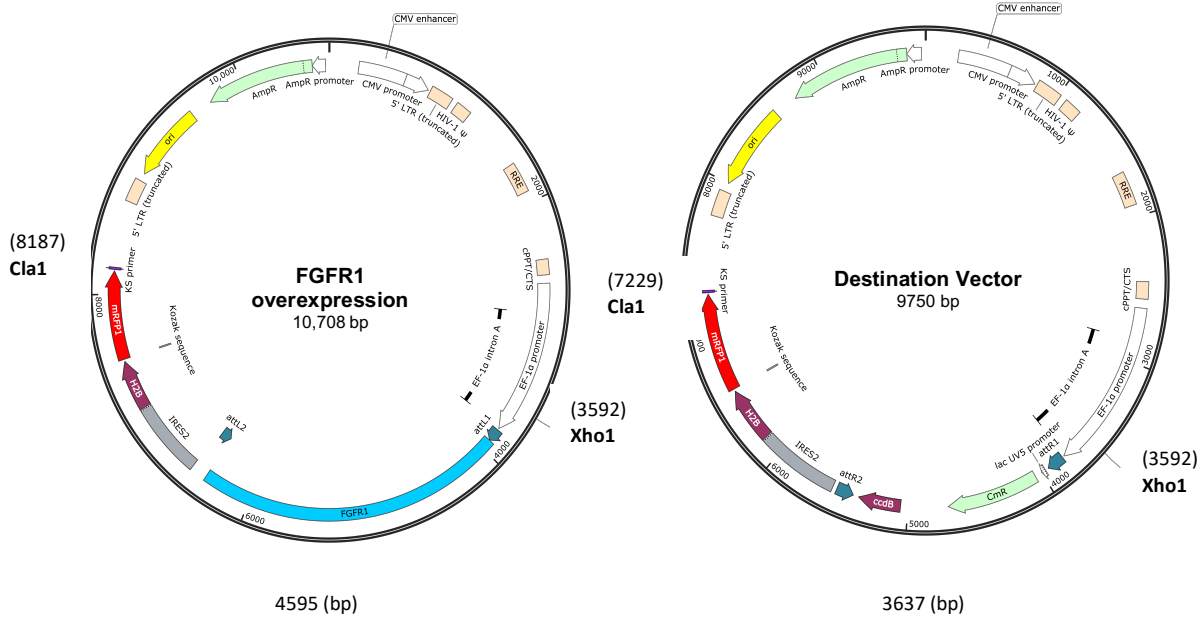


Figure 2.3. Vector maps used for gateway cloning. Maps of the destination vector and final construct (FGFR1 overexpression) were obtained and modified in SnapGene. Location of the enzymes used for DNA digestion, Cla1 and Xho1 and sizes of the clones (FGFR1 overexpression = 10,708 bp and destination vector = 9750 bp) are shown in the map. Vector information: hCMV promoter is used in mammalian expression vector to promote gene expression; central polypurine tract (cPPT)/central termination sequence (CTS) leads to the formation of three-stranded DNA structure, vector integration and transduction efficiency; human elongation factor 1 alpha-encoding (EF-1 α) gene is a promoter that induces high efficiency of gene expression of the cloned gene (the first intron is required for high activity of the promoter); monomeric red fluorescence protein (mRFP) allows for the detection and isolation of cells transduced with FGFR1 overexpression plasmid; chloramphenicol resistance gene (*CmR*) allows *E. coli* to be resistant to this antibiotic. Other vector parts have been explained previously in Figure 1.1.

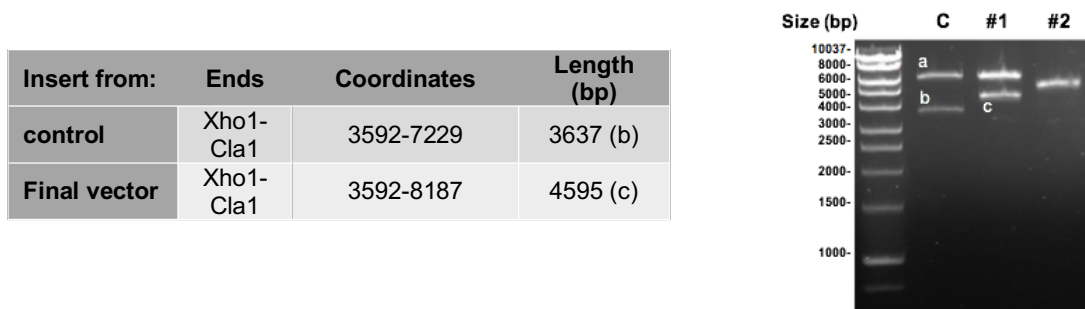


Figure 2.4. Digestion analysis with Xho1 and Cla1 of a FGFR1 expression construct created by LR reaction of an entry clone. (Left) Summary of the location of each enzyme and the size of the products generated after enzyme digestion: (b) 4595 bp from the final vector and (c) 3637 bp from the final product. (Right) Verification of the inserts: a) band of the 6113 bp fragment that contains the plasmid cassette without the region of interest (this fragment will have the same length in all the samples); b) product from the destination vector with the *ccdB* gene; c) product from the final vector containing FGFR1. Therefore samples #1 contains the correct plasmid.

2.5 Transfection

Lipofectamine LTX with Plus reagent (Thermo Fisher Scientific) was used for transiently transfect hGBM cells. 24 h before transfection, 1×10^5 cells/well were seeded in a six-well culture plate coated with Geltrex. 1-2 h before transfection, cells were pre-incubated with 600 μ L of Opti-MEM media (without antibiotics). 1 μ g of plasmid DNA and 2 μ L of Plus reagent, were diluted in 400 μ L of Opti-MEM media in a 1.5 mL collection tube. After 5 min of incubation, 4 μ L of Lipofectamine LTX reagent was added in to the tube. The tube was flick every 10 min and the mix was incubated for 30 min at RT. Solution was added to the cells and 8 h later the transfection medium replaced by complete medium and growth factors according to cell type. Transfected cells were selected with the required antibiotic.

2.6 Production of lentiviral particles

A second-generation lentiviral system was used to produce lentivirus from 2nd and 3rd generation lentiviral transfer plasmids. This system consists of three main components: a plasmid coding for the gene of interest, a packing plasmid (psPAX2) and an envelope plasmid (PMDG2). For the highest production of viral particles, 11.5 μ g of transfer plasmid was mixed with 3.6 μ g and 6 μ g of PMDG2 and PsPax respectively.

2.6.1 Transfection and ultracentrifugation

Lipofectamine 3000 reagent (Thermo Fisher Scientific) was used for production of lentiviral particles. 5×10^6 HEK 293T cells were seeded into a T75 flask (70-80% confluency) one day before transfection. Two different solutions were prepared: A) Lipofectamine 3000 reagent was diluted in Opti-MEM medium (Thermo Fisher Scientific) and vortexed for 2-3 sec and B) lentiviral packaging mix, transfer plasmid and p3000 reagent (Thermo Fisher Scientific) were dissolved in Opti-MEM medium and slowly mixed by pipetting up and down (**Table 2.7**). Solutions A and B were incubated at RT for 5 min before mixing them in a 1:1 ratio. The DNA-lipid complex mix was incubated for 15 min and then carefully added to the HEK 293T cells. After 24 h, the packing medium was replaced for fresh DMEM supplemented with 10% [v/v] FBS. Medium containing lentiviral particles was collected at 48 h and 72 h after

transfection. First and second collections of viral supernatant were combined and filtered through a 0.45 μm pore-size non-viral particle sticking filter and centrifuged for 2:30 h at 4°C and 23,000 rpm (90,000 $\times g$) in an L8-70M Ultracentrifuge, SW32Ti rotor (Beckman) (Kendrick *et al.* 2008; Tornillo *et al.* 2018). Supernatant was discarded and the pelleted viral particles were diluted in 200 μL of medium. Concentrated viral particles were aliquoted and stored at -80°C.

Components	Solution A	Solution B
Opti-MEM	875 μL	1750 μL
Lipofectamine 3000 reagent	35 μL	-
P3000 reagent	-	40 μL
Transfer plasmid: Ex pgipZ shFGFR1 (1.9 $\mu\text{g}/\mu\text{L}$)	-	6 μL
Packing plasmid Ex:PsPax (1.70 $\mu\text{g}/\mu\text{L}$)	-	5.3 μL
Envelop plasmid: Ex:PMDG2 (1.30 $\mu\text{g}/\mu\text{L}$)	-	2.76 μL

Table 2.7. Components required for lentiviral production. Transfer, packing and envelop plasmids concentrations are examples of DNA used to produced shFGFR1 viral particles.

2.6.2 Titration of lentiviral vectors

Infectivity titer of the concentrated virus was required to quantify the amount of virus produced. 5×10^4 HEK 293T cells per well were plated in a Geltrex-coated 12-well plate. Cells were transduced the next day with different dilutions of the neat virus (1:1000, 1:500, 1:100 and 1:50) and replaced with fresh medium (DMEM/10% [v/v] FBS) after 18 h (Regan *et al.* 2012; Tornillo *et al.* 2018). Numbers of positively transduced cells (expressing fluorescent proteins such as eGFP or DsRed) were analysed at day 4 after transduction by flow cytometry. Lentiviral titer (viral particles/mL) was calculated by the number of plated cells (5×10^4) multiplied by the percentage of positively infected cells and divided by the volume (mL) of virus added to the supernatant per well. The number of transduced units (TUs) was multiplied for the Multiplicity of Infection (MOI), in this case MOI=5 (Bayin *et al.* 2014).

$$\text{TUs/mL} = \frac{(5 \times 10^4) \times (\% \text{ of GFP/DsRED cells})}{(\text{mL of virus added})}$$

2.7 Lentiviral transduction of hGBM cells

To knockdown and/or overexpress a gene of interest, hGBM cells were transduced with previously produced lentiviral particles. 24 h before transduction, 1×10^5 cells /well were seeded in a six-well culture plate coated with Geltrex. 1-2 h before transduction, cells were pre-incubated with Opti-MEM media (without antibiotics). 5×10^5 of viral particles (MOI=5) were added and 18 h later the transduction medium replaced by complete medium and growth factors according to cell type. Although transfer plasmids were replication incompetent, a replication test was performed by collecting the medium 48 h after transduction and adding it into cells that were previously seeded in a Geltrex-coated plate. If no transduced cells were observed after 24 h, the produced virus was deemed replication-incompetent (Kendrick *et al.* 2008). Transduced cells were sorted for GFP and/or RFP fluorescence one week after transduction on a BD FACS Aria Fusion (BD Bioscience) to obtain homogeneously fluorescent cell populations (section 2.12.4).

2.8 Protein isolation and preparation of cell lysates

2.8.1 Protein isolation

Suspension hGBM sphere-derived cells were collected, pelleted by centrifugation at 4°C for 5 min at 400 xg and washed with cold (1x) PBS (Thermo Fisher Scientific). Cell pellets ($\sim 1 \times 10^6$ cells) were transferred into a 1.5 mL collection tube and re-suspended in 100 μ L of lysis buffer (250 μ L of (10x) RIPA buffer (Cell Signalling Technology); 25 μ L each of protease inhibitor cocktail (PIC) (Merck), phosphatase inhibitor cocktail 2 (PIC2) (Merck), phosphatase inhibitor cocktail 3 (PIC3) (Merck) and 1.5 mM Phenyl methane sulfonyl fluoride (PMSF) (Merck); 2.25 mL of ddH₂O). Samples were incubated on ice for 30 min (vortexed every 10 min to facilitate cell lysis) and centrifuged at 4°C for 30 min full speed (16,000 xg). Proteins contained in the supernatant were collected, aliquoted, quantified and/or stored at -80°C avoiding more than two freeze and thaw cycles (Siebzehnrubl *et al.* 2009).

2.8.2 Protein quantification

To accurately analyse proteins by Western blotting, the total amount of protein per sample was quantified by Bradford protein assay. 5 μ L each of pre-made protein standard (Bio-Rad)/sample lysate dilution (1:5 and 1:40 in lysis buffer)/blank (lysis buffer alone) were added into different wells of a pre-chilled 96-well plate together with 250 μ L of Quick Start Bradford (1x) Dye Reagent (Bio-Rad) (50:1 Bradford reagent/sample volume ratio) (**Table 2.8**). The mix was incubated at RT for 5 min in the dark. Once the colorimetric reaction was produced, the absorbance of each sample/standard was read at 595 nm using a CLARIOstar microplate reader (BMG Labtech). Absorbance values of protein standards were used to create a standard curve to calculate the final concentration of each sample.

Standard/sample	Volume (μ L)	Bradford Reagent volume(μ L)	Concentration (μ g/mL)
Blank	5	250	0
Standard 1	5	250	125
Standard 2	5	250	250
Standard 3	5	250	500
Standard 4	5	250	750
Standard 5	5	250	1000
Standard 6	5	250	1500
Standard 7	5	250	2000
Sample	5 (of 1:5 and 1:40 dilution)	250	Depending on standard curve

Table 2.8. Standard concentrations used for Bradford assay. 5 μ L of each standard stock and 5 μ L of each diluted sample were dissolved in 250 μ L of Bradford reagent. Each sample and standard were run in duplicates.

2.8.3 Protein separation and transfer to polyvinylidene difluoride (PVDF) membrane

5 to 20 μ g of sample (depending on primary antibody specificity) were mixed with an equal volume of Laemmli (2x) sample buffer (Merck) containing 10% [v/v] 2-mercaptoethanol, 4% [v/v] SDS, 0.004% [v/v] bromophenol blue, 20% [v/v] glycerol and 0.125 M Tris-HCl. Samples were denatured at 95°C for 5 min and kept on ice for 2 min. A Mini-Protean TGX Precast Gels Bis-Tris 10% or 4-15% gradient gel (Bio-Rad) was placed into a loading cassette after carefully removing the comb. The loading cassette was placed into an electrophoresis tank and covered with (1x) Tris-Glycine SDS running buffer (Bio-Rad). 5 μ L of protein ladder was loaded into the first well of

the gel and 10 μ L of the denatured samples to the following wells. The SDS-PAGE gel was run for 30 min at 200 V. Proteins were transferred using the semi-dry transfer method using a Mini Trans-Blot Turbo Transfer System (Bio-Rad). A 0.2 μ m PVDF membrane (Bio-Rad) was activated in methanol (Thermo Fisher Scientific) for 1 min and then placed in trans-blot turbo (1x) transfer buffer (Bio-Rad) to stop the reaction. Two stacks of filter paper were pre-soaked in trans-blot buffer (Bio-Rad). A membrane sandwich was created by placing one of the pre-soaked stacks into the transfer cassette in contact with the positive electrode of the plate, followed by the activated membrane, then the gel and finally the other paper stack contacting the negative electrode. The transfer was run for 7 min at 2.5 A and 20 V.

2.8.4 Protein blotting and visualization

After protein transfer, the PVDF membrane was blocked for 1 h at RT in 5% skimmed dry milk solution or 5% [w/v] BSA (5% milk/BSA powder and 0.1% [v/v] of Tween (Merck) in (1x) Tris-Buffered Saline (TBS) pH 7.4 (Severn Biotech Ltd)) depending on antibody. Blots were probed with primary antibody in blocking solution at 4°C overnight. The membranes were washed three times with 0.1% [v/v] Tween-TBS (TBS-T) for 5 min each, before being incubated for 1 h at RT with the secondary antibody (**Table 2.9**). Membranes were washed again three times with TBS-T and incubated for 5 min in the dark with Clarity Western enhanced chemiluminescence (ECL) substrate (Bio-Rad). ECL allowed protein visualization by chemiluminescence detection of the horseradish peroxidase (HRP) conjugated to the secondary antibody. Excess ECL was removed and the chemiluminescent signal was detected with a ChemiDoc MP Imaging System (Bio-Rad). The obtained results were normalized to GAPDH as housekeeping gene. Image Lab software (Bio-Rad) was used to analyse the results and Image J was used to quantify differences in band intensity between the blotted protein of interest and the housekeeping gene. For phospho-blots, every step described previously was performed at 4°C.

Primary antibodies for western blotting						
Antigen	Host	Clone/Ab ID	Dilution	Protein μ g	Ab diluted in	Supplier
ZEB1	rabbit	HPA 027524	1:2500	2 μ g	2.5% milk	Merck
OLIG2		AB9610	1:500	15 μ g		EMD Millipore
GAPDH		2572289	1:10000	1-20 μ g		EnCor
SOX2		D6D9	1:1000	20 μ g	5% BSA	Cell Signalling Technology
FGFR1		D8E4	1:1000	15 μ g		
FGFR2		D4L2V	1:1000	20 μ g		
FGFR3		C51F2	1:500			
p-ERK1/2 (Thr202/Try204)		4370	1:2000			
Total ERK1/2		9102	1:1000			
p-STAT3 (Tyr705)		D347	1:500			
Total STAT3		D3Z2G	1:500			
p-AKT(Ser473)		9275	1:500			
p-P38 (Thr180/Try182)		9211	1:1000			
Total P38		mouse	L53F8	1:1000		

Secondary antibody for Western Blotting					
Antigen	Host	Dilution	Protein concentration	Ab diluted in	Supplier
Anti-rabbit HRP-linked	-	1:3000	1-20 μ g	5% milk	Cell Signalling Technology
Anti-mouse IgG1 (HRP)	goat	1:3000	1-20 μ g	5% milk	Abcam

Table 2.9. Western Blot antibody list. Description of the dilution of each antibody used for a specific concentration of protein and the required percentage of the required buffer for blocking and/or antibody dilution. All primary antibodies were incubated overnight excluding GAPDH which can also be incubated for 1h at RT. Secondary antibodies were incubated for 1h at RT. p=phospho.

2.9 PathScan Intracellular Signalling Array Kit

PathScan Intracellular Signalling Array Kit (Cell Signalling Technology; reagents described in this section are all from the same company) was used to study changes in phosphorylation or cleavage of 18 well-characterised signalling molecules (**Figure 5.5** in results). Antibodies targeting these molecules were spotted in duplicates onto a glass slide coated with nitrocellulose (Chung *et al.* 2015; Cuyàs *et al.* 2016).

2.9.1 Cell lysates

Cells were washed with ice-cold (1x) PBS, incubated on ice for 20 min with (1x) cell lysis buffer containing 1 nM of PMSF and centrifuged at maximum speed at 4°C. Supernatant was collected and Bradford assay performed as described in section 2.8. Samples were diluted to a final concentration of 1 mg/mL and used immediately before being stored at -80°C.

2.9.2 Assay procedure

Glass slides containing the spotted antibodies and array blocking buffer were brought to RT. The slide and multi-well gasket were affixed and 100 μ L of blocking buffer added to each well without touching the slide surface. Wells were covered with parafilm and the slide/multi-well gasket transferred to a tip box containing a wet paper to avoid evaporation. After 15 min of incubation on an orbital shaker, in the dark and at RT, the solution was gently decanted and 75 μ L of each lysate were added per well. All incubation/washing steps of this protocol were performed on a Stuart Gyrotory rocker, SSL3 (Stuart supplied by Merck) at 70 rpm, unless otherwise specified. Wells were again covered with sealing tape and samples were incubated overnight at 4°C. The following day, the content of the wells were decanted and washed three times with 100 μ L of (1x) array wash buffer (1:20 dilution of (20x) array wash buffer in deionized water) for 5 min at RT. Solution was decanted and samples were incubated in 75 μ L of (1x) detection antibody cocktail (1:10 dilution of (10x) detection antibody cocktail diluted in array diluent buffer) for 1 h at RT and protecting the slide with sealing tape. Once wells were washed four times with 100 μ L of wash buffer for 5 min, 75 μ L of (1x) HRP-linked Streptavidin (1:10 dilution of (10x) HRP-linked Streptavidin in array diluent buffer) were added and incubated for 30 min at RT protecting slide from light and evaporation. Wells were again washed four times with 100 μ L of wash buffer for 5 min.

2.9.3 Bound antibody detection by chemiluminescence

Slide/multi-well gasket was disassembled, placed in a petri dish (Greiner Bio-One) without touching the side of the slide containing the samples and washed with 10 mL of wash buffer for 1 min. Solution was decanted and LumiGLO and peroxide reagents were mixed (0.5 mL of (20x) LumiGLO, 0.5 mL of Peroxide and 9 mL of ddH₂O) immediately before use and added onto the slide ensuring the entire surface was covered with solution. A ChemiDoc MP imaging system was used to develop the slide-based antibody array and images were taken every 30 sec to capture all required exposure times.

2.10 Orthotopic patient-derived glioblastoma xenografts

2.10.1 Mouse strain and husbandry

Animal experiments were approved and authorised by the UK Home Office (project licence 30/3331) under The Animal (Scientific Procedures) Act 1986 (ASPA). Animal procedures were conducted in accordance to institutional guidelines and regulations for animal care and handling. Young female (4-6 weeks old) immune-compromised FOX Chase SCID (CB17/lcr-*Prkdc*^{scid}/lcrIcoCrI) mice (Charles River Laboratories) were used as hosts for xenografts of human tumour cells.

2.10.2 Preparation of cells for implantation

2.10.2.1 Genetically modified hGBM cells

Transduced hGBM spheres (shControl vs knockdown) were dissociated into single cells, strained through a sterile 70 µm mesh EASYstrainer (Greiner Bio-One) and purified by cell sorting. Sorted cells were diluted in N2 to a final concentration of 5×10^4 cells per 5 µL.

2.10.2.2 Sorted cell populations

hGBM cells were stained with the required antibody and sorted as described in section 2.12.5. Sorted cells ('negative' vs 'positive' population) were immediately injected into mice as limiting dilution assay (LDA) implants. For LDA implants, mice were transplanted with 1×10^3 , 1×10^4 or 5×10^4 hGBM cells. Different stem cell frequencies were expected among groups as explained in section 2.13.2 (Siebzehnrubl *et al.* 2013).

2.10.3 Intracranial implantation

Mice underwent induction of general anaesthesia using 3% [v/v] of Isoflurane (Teva) in oxygen for 3-5 min and were then transferred and secured in a stereotaxic frame. General anaesthesia was maintained during the procedure (2% Isoflurane/oxygen). A dab of bland ophthalmic ointment (polyethylene glycol ointment, Lacri-Lube; Allergan) was applied to both eyes. The surgery site was prepared for aseptic surgery with 70% ethanol (VWR) and Videne antiseptic solutions (Escolab) according to Laboratory Animal Science Association (LASA) guidelines. A frame-mounted Micro-Fine U-100

insulin 30G microinjection syringe (BD Bioscience) was lowered into the prepared surgery site and cells injected into the right hemisphere of the brain, in a depth of 3 mm (**Figure 2.5**). Cells were injected at a rate of 0.5 μL per minute and in a volume of 5 μL . After injection of the cells, the micropipette was left in place for an additional 2 min and carefully retracted to avoid back-flow. Mice were placed in a clean, quiet and warm area (37°C) until completely recovered from the surgery and monitored for 24 h.

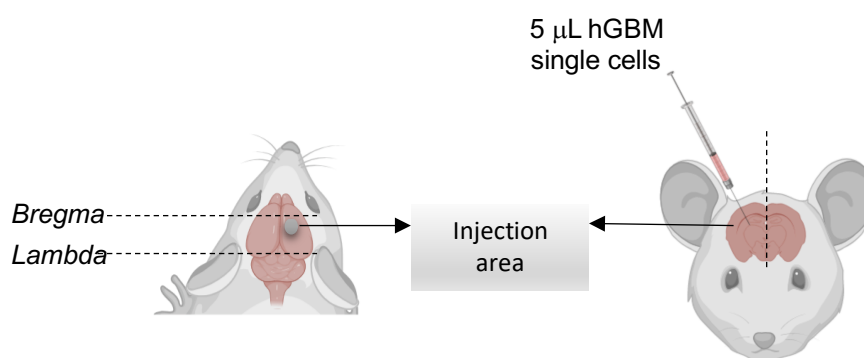


Figure 2.5. Intracranial injection representation. Dorsal view (left) and coronal section (right) of the mouse brain. The injection area is found between bregma point (zero coordinate) and lambda (-4.60mm bregma) approximately at -0.94mm from bregma and in the right hemisphere (Image created with biorender.com).

2.10.4 Tumour growth monitoring

Recipient mice bearing tumours were monitored twice per week during the first 5 weeks after surgery and every other day in the last 2-3 weeks before end point. Mice were monitored and scored for the following criteria (**Table 2.10**): appearance, food and water intake (or gain/loss of weight), natural behaviour, provoked behaviour and movement. Monitoring each individual mouse was possible due to the ear code system shown in **Figure 2.6**. When mice reached the defined end point criteria (**Table 2.10**), they were culled according to schedule 1 using CO_2 overdose. Death was confirmed by toe-pinch response and cessation of breathing.

Health Monitoring Score Chart									
Animal ID		PPL No		PIL No		Protocol 8: Intracranial Injection			
Cage		Sex	Female			Date of surgery:			
Parameter	Observation	Score	Monitoring Date						
Appearance	Normal	0							
	General lack of grooming	1							
	Staring coat, ocular and nasal discharges	2							
	Piloerection, hunched up	3							
Food and water intake	Normal	0							
	5% -15 weight loss	1							
	Over 15% weight loss, but under 20%	2							
	Over 20% weight loss	3							
Natural Behaviour	Normal	0							
	Minor changes e.g. lack of nest	1							
	Less mobile and alert, isolated or restless	2							
	Vocalisation, reduction in grip reflex	3							
Provoked Behaviour	Normal	0							
	Minor depression or exaggerated response	1							
	Moderate change in expected behaviour	2							
	Reacts violently or very weak and pre-comatose	3							
Movement	Normal	0							
	Partial paresis of any limbs	1							
	Paresis of any limbs	2							
	Paralysis or partial paralysis of any limbs	3							
Total score									

Table 2.10. Health monitoring score chart. Each individual mouse was monitored with a Health monitoring Score Chart containing the animal ID (ear notch) and the cage number where the mouse was located. Each monitoring day mouse weight was measured and health parameters scored from 0-3. Action taken was depending on the mouse total score: 0-3=Normal; 4-8=Monitor carefully; and 9-12=Provide relief, observe regularly (seek advice from Named Animal Care & Welfare Officer (NACWO) and or Named Veterinary Surgeon (NVS) if needed). If total score was 12 or greater the mouse was culled by Schedule 1.

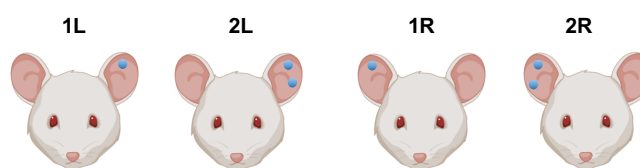


Figure 2.6. Mice ear code per cage. Ear notch was performed the day of the surgery with an ear notch punch of 2 mm. Four different mouse IDs were identified per cage: one notch on the right ear (1R), 2 notches on the right ear (2R), one notch on the left ear (1L) and 2 notches on the left ear (2L) (Image created with biorender.com).

2.10.5 Perfusion fixation and tissue harvesting

Perfusion fixation is a technique performed prior to tissue harvesting that makes use of the vascular system of an animal to deliver fixatives to the tissue of interest. This rapid and uniform fixation method allows tissue preservation before autolysis and degradation of the sample begins (**Figure 2.7**).

Mice were immediately placed on a styrofoam perfusion stage and limbs pinned down to facilitate access to the peritoneal cavity. An incision was made in the skin over the xiphoid process, parallel to the spine and towards the collarbone with a pair of extra fine scissors straight-sharp-blunt 8.5 cm (InterFocus). After removing the skin, the breastbone was lifted with Adson forceps wide grips (InterFocus) and 5-6 lateral cuts were performed through the dermis beneath the rib cage and through the integument and abdominal wall. This procedure revealed the diaphragm which was laterally cut while still holding the breastbone without affecting other organs. This incision was carefully continued towards one side of the rib cage avoiding the contact of the scissors with the lungs or heart. The same procedure was followed on the other side of the rib cage, lifting the sternum away, the ribs were removed by a horizontal cut at the level of the collarbone after carefully cutting the pericardium. Once the pleural cavity was exposed, a 21G butterfly needle (Greiner Bio-One) was inserted into the left ventricle of the mouse heart and to the ascending aorta without reaching the aortic arch. A Westcott Spring Scissors Slightly Curved (Interfocus) was used to make a cut on the animal's right atrium to allow blood and perfusion solutions to drain from the circulatory system. A 20 mL Luer lock IV syringe (Medicina) filled with 20 mL of ice-cold (1x) PBS was attached to the tubing adaptor of the butterfly needle and the solution slowly injected into the mouse vascular system. Once all the blood was

drained and without removing the butterfly needle from the left ventricle, a new syringe filled up with 20 mL of ice-cold solution of 2% [v/v] formalin in (1x) PBS was placed into the tubing adaptor and perfusion fixation was performed. Perfusion quality was confirmed by visual assessment of liver clearance.

Perfusion fixation was followed by mouse decapitation. Iris scissors were used to remove the scalp and expose the skull. Small incisions were performed into the skull bone from the interparietal to the frontal bone without damaging the brain tissue. Once the brain was completely exposed, a spatula was used to release the brain from the skull. The brain was immediately submerged into 4 mL ice-cold 2% formalin in a clean 20 mL scintillation vial (Thermo Fisher Scientific) for overnight post-fixation (Deleyrolle *et al.* 2011; Hoang-Minh *et al.* 2016).

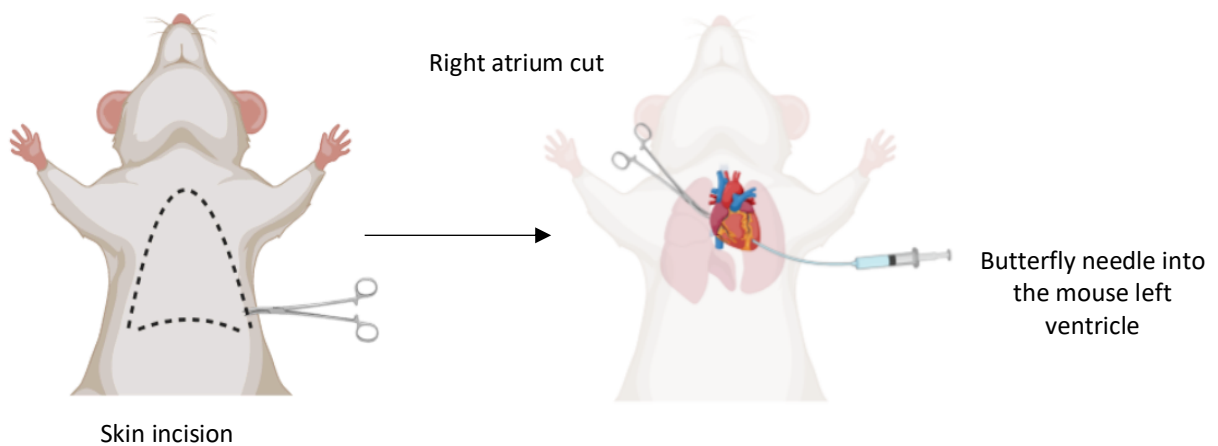


Figure 2.7. Representation of mouse transcatheter perfusion fixation. (left) Area of incision made to exposed first rib cage and then the pleural cavity. (Right) Perfusion fixation through the heart. (Image created with biorender.com).

2.10.6 Cryopreservation

After fixation, brains were kept in 4 mL of (1x) PBS at 4°C to remove the excess fixative. After 24 h brains were submerged in 4 mL of 30% [w/v] sucrose solution (Merck) until they sank to the bottom of the tube (usually within 2 days of incubation at 4°C). This step was required for tissue dehydration. The solution was replaced by 60% [v/v] sucrose diluted 1:1 with Optimal Cutting Temperature (OCT) compound (Thermo Fisher Scientific; final sucrose concentration 30%) and incubated overnight at 4°C. After sucrose/OCT incubation, the tissue was placed on a petri dish, the cerebellum was removed using a sterile scalpel (Swann-Morton) and the brain transferred to a plastic embedding mould (Thermo Fisher Scientific). The brain was orientated with the olfactory bulb facing up to facilitate coronal sectioning. The plastic mould was then filled with OCT and the OCT submerged tissue was frozen in the liquid nitrogen vapour phase. Once the OCT became solid and white in colour (\cong 5 min), the frozen block was stored at -80°C.

2.11 Immunofluorescence of brain sections

2.11.1 Blocking and antibody incubation

30 μ m thick coronal sections were transferred into a 24-well plate (with a maximum of 4 sections per well) using a fine angle paintbrush containing 500 μ L of PBS-T ((1x) PBS, 0.1% Triton X-100; Merck) to wash the tissue, remove the residual cryoprotectant and facilitate tissue permeabilization. The use of the paintbrush and Pasteur pipettes was important to avoid tearing the sections. Each incubation/wash step of this protocol was performed in a 24-well plate on a Rotamax 120 (Heidolph Instruments) at 20 rotations/min and RT unless otherwise specified. To reduce non-specific antibody binding the floating sections were pre-blocked for 1 h in 500 μ L of Fish Skin Gelatin buffer with 0.1% [v/v] Triton X-100 (FBS-T; (1x) PBS, 1% [w/v] BSA, 0.2% [v/v] teleostean gelatin (Merck), 0.1% [v/v] Triton X-100 (Merck), 0.02% [v/v] sodium azide (Merck)). Primary antibodies were diluted in blocking solution as specified in **Table 2.11**. The pre-blocked sections were incubated in 250 μ L of the diluted antibody at 4°C overnight. The sections were then washed 3 times with PBS-T for 10 min each and incubated for 3 h with secondary antibody diluted 1:500 (**Table 2.11**) at RT in the dark to avoid photobleaching. The solution containing secondary

antibody was removed and replaced with nuclear counterstain Hoechst (Merck) diluted in PBS-T for 5 min at RT, followed by 2 additional washes of 10 min in PBS-T.

Primary antibodies for Immunofluorescence				
Antigen	Host	Clone/Ab ID	Dilution	Supplier
FGFR1	mouse	M17D10	1:100	Novous biologicals
FGFR2	rabbit	D4L2V	1:400	Cell Signalling Technology
NESTIN		AB2737583	1:1000	EnCor
GFP	chicken	AB2572314	1:1000	

Secondary antibodies				
Antigen	Host	Fluorochrome	Dilution	Supplier
Anti-chicken	Donkey	Alexa 488	1:500	Thermo Fisher Scientific
Anti-rabbit		Alexa 488		
Anti-mouse		Alexa 594		
Anti-rabbit		Alexa 594		

Table 2.11. List of antibodies used for immunostaining. Antibodies were diluted in FBS-T blocking buffer.

2.11.2 Mounting of immunofluorescence sections

Floating sections were transferred to a glass petri dish filled with PBS-T using a fine angle paintbrush and carefully unrolled and mounted onto clear frosted microscope slides (VWR) submerged in the solution. Each slide was carefully placed in a rack to air-dry for 10 min. ProLong Diamond Antifade mountant (Thermo Fisher Scientific) was thawed at RT and 100 μ L of the mountant pipetted along the centre of the slide. 24 x 60 mm coverslips (Thermo Fisher Scientific) were mounted using forceps, carefully avoiding trapping air bubbles. Slides were vertically propped onto tissue for 10 min to drain the excess of mountant. Mounted slides were stored at 4°C in slide books (2B Scientific) (Siebzehnrubl *et al.* 2013).

2.12 Flow cytometry and cell sorting

2.12.1 Extracellular single cell staining

Single cells suspension was strained with a 70 μ m strainer (Greiner Bio-One), pelleted and washed with cold HBSS (Thermo Fisher Scientific) containing 0.5 mM EDTA (Meck) and 2% BSA. 2.5×10^5 - 5×10^5 cells were incubated for 30-45 min in the dark at 4°C with primary antibody in a volume of 50 μ L per stain. Supernatant was removed by centrifuging the cells for 5 min at 4°C 400 xg and the pellet was incubated with the antibody for 15-20 min in the dark at 4°C. **Table 2.12** describes the list of antibodies,

dilutions, fluorochromes and companies used. Samples were again centrifuged using the same parameters and washed in HBSS/0.5 mM EDTA/DAPI (Merck) to exclude dead cells from the analysis before being transferred into 5 mL polystyrene round bottom tubes (Greiner Bio-One). For all assays, IgG conjugated or unconjugated control was used to detect the background fluorescence of each antibody. Flow cytometry analyses were performed on a 4-laser BD LSR Fortessa™ with FACS Diva software. 10,000-100,000 events were recorded depending on experiment/populations of FGFRs staining. FlowJo 8.7 was used for analysis and gating strategy of each experiment.

2.12.2 Detection of apoptosis by annexin V

Apoptotic cells suffer structural changes in their membrane, exposing phosphatidylserine (PS) residues on the membrane surface. Annexin V in the presence of Ca^{2+} binds to these PSs (Schutte *et al.* 1998; Shounan *et al.* 1998). For quantification of apoptotic/annexin V-positive cells, single cells were plated into Geltrex-coated 12-well plates and treated with DMSO/FGF2 inhibitor as specified in section 2.1.8. 48 h later, the medium was removed and 200 μL of Accumax were added in each well to detach the cells from the substrate. Cells were incubated in annexin V binding buffer (BioLegend) containing annexin V FITC conjugated for 20 min at RT in the dark. Double volume of annexin V binding buffer was added to stop the reaction and samples were analysed by flow cytometry (**Figure 2.8**).

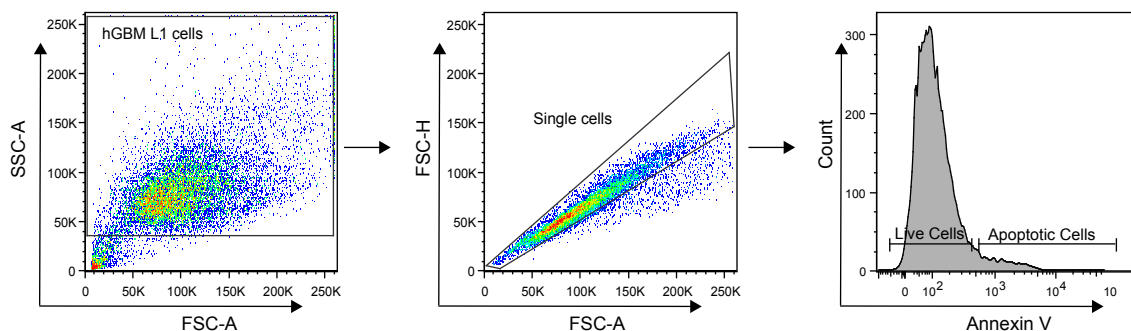


Figure 2.8. Detection of apoptosis using annexin-V. Example of FACS plots showing gate strategy for annexin V staining and histogram representing live cells (annexin V+) and apoptotic cells (annexin V-) populations. 10,000 events in single cell gate were acquired.

2.12.3 Cell Sorting

Sorting experiments were carried out with a FACS Aria™ Fusion using an 85 μm nozzle (BD Bioscience). An un-conjugated control was always included to set up the gating strategy for each experiment.

2.12.4 Purification of transduced cells

After viral transduction (section 2.6), transduced single cells were pelleted, strained and washed with HBSS/0.5 mM EDTA/DAPI before sorting for GFP or/and RFP, depending on the plasmid fluorescence reporter. The gating strategy for FACS purification is shown in **Figure 2.9**. For selection of GFP+ cells, the gate was set in the center of the peak to avoid cells containing multiple viral integration.

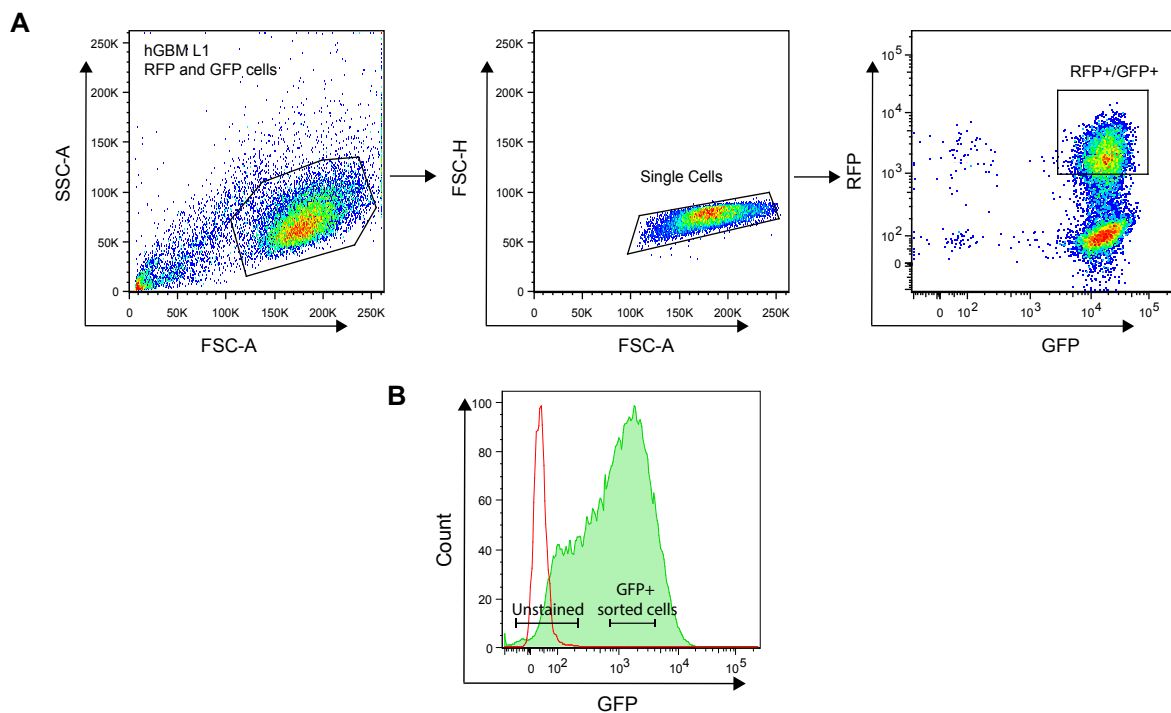


Figure 2.9. Purification of transduced cell populations. **A)** Example of gating strategy to sort hGBM cells transduced with two different constructs; a knockdown lentiviral construct expressing GFP and an overexpression plasmid expression RFP. RFP+/GFP+ cells were isolated to select all positively transduced cells with both plasmids. **B)** Only hGBM cells transduce with lentiviral constructs expressing middle GFP fluorescence were isolated.

2.12.5 FGFR1 + and FGFR1- sorting

1x10⁶ hGBM control cells were stained for FGFR1 (**Table 2.12**) (Dumon *et al.* 2001) and were sorted for FGFR1 high (+) and low (-) expression (gating strategy in **Figure 4.1** of results). Sorted cells were used for CFC and limiting dilution implants (section 2.1.6 and section 2.10.2 respectively).

Primary antibody				
Antigen	Host	Clonality	Dilution	Supplier
FGFR1	mouse	monoclonal	1:50	Thermo Fisher Scientific
FGFR2	rabbit	monoclonal	1:400	Cell Signalling Technology
FGFR3 IgG1 APC-conjugated	mouse	monoclonal	1:50	R&D Systems
Secondary antibody				
Antigen	Host	Fluorochrome	Dilution	Supplier
Anti-mouse	Donkey	Alexa 647	1:400	R&D Systems
Anti-rabbit				
IgG1 Isotype control	mouse	APC	1:50	BD Bioscience

Table 2.12. List of antibodies used for flow cytometry and cell sorting.

2.13 Image acquisition

Immunofluorescence images of brain sections were acquired with a Zeiss Axio Scan Z1 (Zeiss) slide scanner. This microscope acquires images of multiple sections within a slide and/or multiple slides in an automated way. Zen blue software (Zeiss) was used to select the sections to be imaged and adjust the required acquisition settings. For high power and more detail, images were taken in a Zeiss LSM710 confocal microscope (Zeiss) with Zeiss ZEN software (Zeiss).

2.14 Image data analysis

2.14.1 Quantification of KD percentage by immunofluorescence tissue staining

Control and FGFRs knockdown tumours were compared by immunofluorescence of brain sections (section 2.10). Knockdown percentage was obtained by calculating the average of the mean fluorescence intensity (MFI) of at least 5 sections per mouse with ImageJ.

2.14.2 *In vivo* invasion index

To analyse tumour invasion, fluorescence images of whole brain sections were imported to ImageJ and converted to grey-scale. Black and white threshold levels were adjusted to distinguish areas containing tumour (black) from background/parenchyma (white) (**Figure 2.10**). The wand auto-measure tool was used for an unbiased selection of positively stained areas (black) and the perimeter and area of the outlined tumour were measured. To compare invasive characteristics among tumours, the ratio of the squared perimeter distance over the area (P^2/A) was calculated. The result of this formula is termed “invasion index”. A high invasion index equals a more dissociated tumour while a low invasion index indicates a more spherical one (Siebzehnrubl *et al.* 2013). Extracerebral growing parts of the tumour, which can be produced by backflow of cells from the injection site and tumour growth within the ventricles were not included in quantification of invasive tumour areas (**Figure 2.10**).

2.14.3 Tumour-formation frequency analysis of hGBM LDA implants

To analyse tumour formation frequency of LDA implants, brains were kept in (1x) PBS at 4°C after perfusion and overnight fixation. Each brain was placed in a petri dish and hemisected in the coronal plane with a scalpel under visual control on an Olympus SZX7 fluorescence stereomicroscope (Olympus). Tumour-formation was positively identified by GFP expression as the implanted hGBM cells were previously transduced with GFP lentiviral constructs. Only brains bearing tumours within the parenchyma were considered as positive for ‘tumour formation and integration’. Absence of tumour formation was confirmed by inspection of an additional cross-section of the brain after a second coronal cut. Differences in stem cell frequencies between groups were quantified with Extreme Limiting Dilution Analysis (ELDA) software (Hu and Smyth 2009).

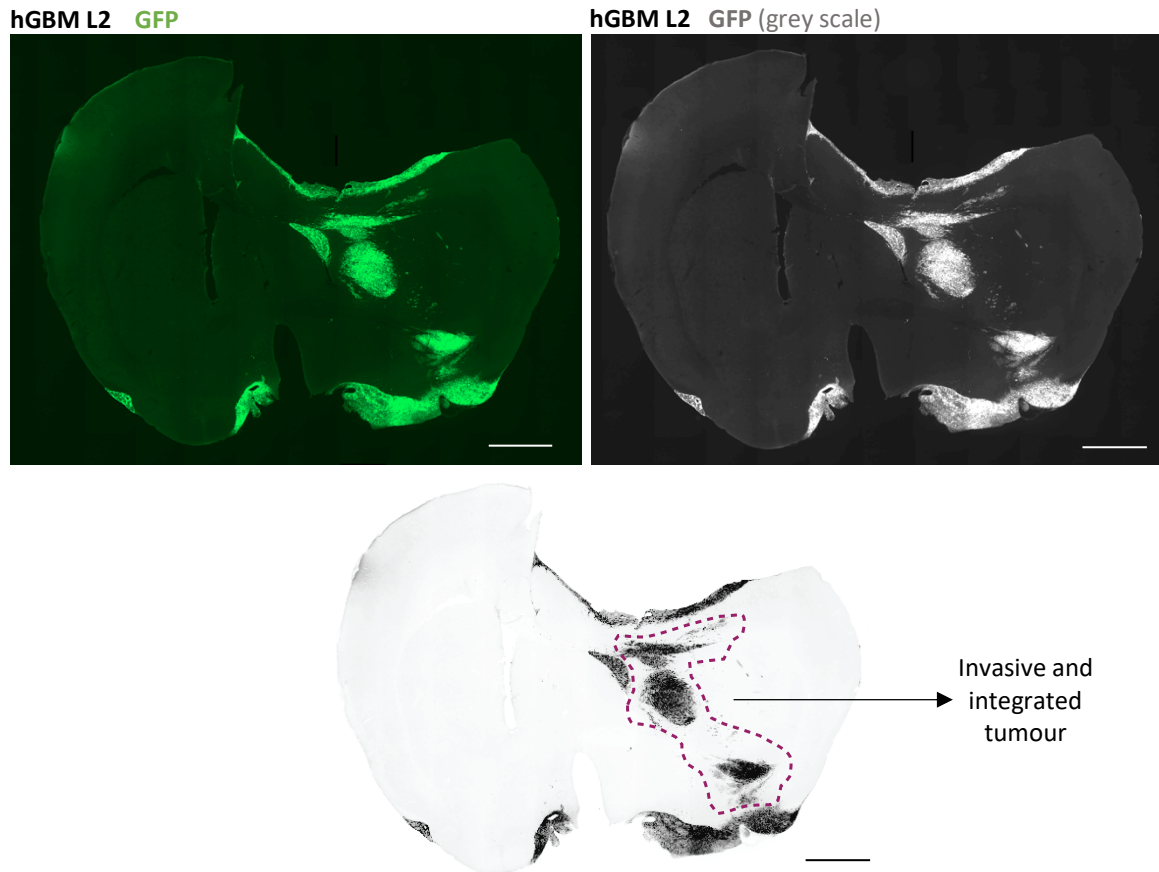


Figure 2.10. Representative image of an invasive tumour . Xenograft of hGBM L2 cells. Tumour cells are represented by GFP staining. To facilitate tumour visualization and invasion quantification, single-colour grey scale images (tumour in white) were inverted (tumour in black). Outline of an invasive tumour (black) is highlighted by a red dashed line. Scale bar 1mm.

2.15 Bioinformatics

The online tool Gliovis (<http://gliovis.bioinfo.cnio.es/>) was used to analysed TCGA, NCI, Gravendeel, Murat and Kamoun mRNA datasets. Further analysis of survival correlations was performed using the Xena platform (<https://xena.ucsc.edu/welcome-to-ucsc-xena/>). Methodology described in Jimenez-Pascual *et al.* 2019.

2.16 Hierarchical cluster analysis

Hierarchical clustering module (Kim *et al.* 2016) from GenePattern (<https://cloud.genepattern.org>) (Reich *et al.* 2006) was used to cluster HGCC cell line expression data (Xie *et al.* 2015) with Pearson correlation as distance measure, using row centering and normalization. Z-Score values from the Glioblastoma Multiforme

(TCGA, Provisional). Tumour Samples with mRNA data (U133 microarray only) (528 samples) data set was downloaded from cBioportal (Cerami *et al.* 2012) and clustered with Pearson correlation as distance measure, using the same GenePattern module as before. Methodology described in Jimenez-Pascual *et al.* 2019.

2.17 Statistical testing

Statistical analyses were performed in GraphPad Prizm 8.1.0 (GraphPad Software, La Jolla, CA). All values reported are mean values \pm standard error of mean (SEM) and statistical tests and number of replicates (n) per experiments are indicated in the text and figure legends. In all analyses, a p-value < 0.05 was deemed significant (*p <0.05 , **p <0.01 , ***p <0.001 , ****p <0.0001). Significant differences among groups were calculated using one-way ANOVA and two-way ANOVA analyses, or unpaired t-test (95% confidence intervals) to compare two groups. Statistical tests are indicated in the figure legends. The Kaplan–Meier method was used to perform survival analyses from day of surgery until death. Animals lost to follow-up were considered censored. Statistical analysis was conducted using the Log-rank (Mantel-Cox) test.

2.18 Products supplier list

Suppliers name and address of the product used in Material and methods are listed in Table 2.13.

Supplier name	Office address
Addgene	LGC Standards Teddington, UK
BD Bioscience	Edmund Halley Road - Oxford Science Park, OX4 4DQ Oxford, UK
Beckman Coulter	Oakley Ct/Kingsmead Business Park/Frederick Pl, High Wycombe HP11 1JU, UK
BioLegend UK Ltd.	Highgate Business Centre, 33 Greenwood Place, London, NW5 1LB, UK
BioLine Reagents Ltd.	Edge Business Centre, Humber Rd, London NW2 6EW, UK
Bio-Rad Laboratories	The Junction, Station Rd, Watford WD17 1ET, UK
BioRender	BioRender, 639 Queen Street West, Toronto, ON, M5V 2B7
BMG Labtech	8 Bell Business Park, Aylesbury HP19 8JR, UK
Cell Signaling Technology	Hamilton House Mabledon Place London, WC1H 9BB UK
Charles River Laboratory	8 Finsbury Circus, Finsbury, London EC2M 7EA, UK
Horizon Discovery	Cambridge Research Park, 8100 Beach Dr, Waterbeach, Cambridge CB25 9TL
Encor Biotechnology	SW 41st Blvd # 40, Gainesville, FL 32608, EE. UU.
Escolab	Winnington Ave, Northwich CW8 4DX
Eppendorf UK Ltd	Endurance House, Vision Park, Histon, Cambridge, CB24 9ZR, UK
GraphPad Software, Inc.	7825 Fay Avenue, Suite 230, La Jolla, CA 92037 USA
Greiner Bio-One GmbH	Unit 5/Brunel Way, Stonehouse GL10 3SX, UK
Heidolph Instruments	Shire hill, Saffron Walden Essex CB11 3AZ, UK
Image J	NIH and the Laboratory for Optical and Computational Instrumentation, USA
InterFocus	Cambridge Rd, Linton, Cambridge CB21 4NN, UK
Leica Microsystems	Davy Avenue Knowlhill, Milton Keynes, MK5 8LB, UK
Medicina Ltd.	Station Rd, Blackrod, Bolton BL6 5BN, UK
Merck Chemicals Ltd	University Pkwy, Chilworth, Southampton SO16 7QD, UK
New England Biolabs (NEB)	Knowl Piece, Wilbury Way, Hitchin, Herts SG4 0TY, UK
Olympus	keymed house, Stock Rd, Southend-on-Sea SS2 5QH, UK
Oxford Optronix Ltd.	East Central, Milton Park, 127 Olympic Ave, Milton, Abingdon OX14 4SA, UK
PeproTech Ltd	PeproTech House, 29 Margravine Road, London, W6 8LL, UK
Qiagen	Fleming Way, Crawley, West Sussex, RH10 9NQ, UK
R&D Systems	McKinley Pl NE, Minneapolis, MN 55413, EE. UU.
Santa Cruz Biotechnology	Inc. Bergheimer Str. 89-2 69115 Heidelberg, Germany
Selleckchem	Karl-Schmid-Str.14, 81829 München, Germany
Seralab International Ltd.	Unit 44, Bolney Grange Business Park, HaywardsHeath, West Sussex RH17 5PB, UK
Severn Biotech Ltd.	Park Lane Industrial Estate, Stourport Rd, Kidderminster DY11 6TJ, UK
STEMCELL Technologies	Cambridge Research Park, Beach Drive, Waterbeach, Cambridge, UK, CB25 9TL, UK
Teva	Ridings Point, Whistler Dr, Castleford WF10 5HX, UK
Thermo Fisher Scientific	Bishop Meadow Road, Loughborough, Leicestershire, LE 1 5RG, UK
VWR International Ltd.	Hunter Blvd, Lutterworth LE17 4XN, UK
Worthington Industries	Princesway CentralTeam Valley Trading Estate Gateshead Tyne & Wear NE11 OUT, UK
ZEISS	Coldhams Lane CB1 3JS Cambridge, UK

Chapter 3: Assessing the role of FGF2 in the regulation of stem-cell associated transcription factors ZEB1, SOX2 and OLIG2

3.1 Introduction

GSCs are multipotent cells with extensive proliferative and self-renewal capacity. They give rise to progenitor cells that can differentiate into mature cancer cells. In contrast to NSCs, GSCs have tumour initiation ability, and are the cause of therapeutic resistance and tumour recurrence in GBM (Hemmati *et al.* 2003; Singh *et al.* 2003; Vanner *et al.* 2014; Hoang-Minh *et al.* 2018). GSC homeostasis is regulated by intrinsic factors such as genetic and epigenetic programs, alongside extrinsic signals from the immune system and environmental elements (Lathia *et al.* 2015). Trophic factors from the tumour microenvironment are essential for GBM development. Specifically, FGF2 is a known oncogenic factor in GBM (Haley and Kim 2014) as it promotes glioma growth (Bian *et al.* 2000), vascularization (Joy *et al.* 1997; Toyoda *et al.* 2013) and GSC self-renewal (Pollard *et al.* 2009). Yet, the exact influence of FGF2 in GSC regulation is still unclear.

Cell intrinsic transcriptional programs have also been linked to GBM progression, especially those driven by the stem-cell associated transcription factors ZEB1, SOX2 and OLIG2. These transcription factors are upregulated in GSCs and are expressed in highly invasive areas of the tumour (Annovazzi *et al.* 2011; Siebzehnrubl *et al.* 2013; Singh *et al.* 2016). Furthermore, they regulate genes related to hypoxic and stress conditions and are related to GBM poor prognosis and tumour recurrence (Hoang-Minh *et al.* 2018). Murine tumour-suppressor-deficient astrocytes transfected with one of these transcriptions did not have tumorigenic capacity (Singh *et al.* 2017). However, astrocytes transfected with the combination of the three, were transformed into GSC-like cells and generated tumours in xenografts models. Those findings and other studies (Siebzehnrubl *et al.* 2013; Singh *et al.* 2016), indicate that ZEB1, SOX2 and OLIG2 form an autonomous transcriptional loop in GBM and can regulate their expression reciprocally (Singh *et al.* 2017).

Cytokines (TNF α and IL6) and growth factors (EGF, TGF β and PDGF) have been identified as molecules from the tumour microenvironment stimulating EMT-related transcription factors like ZEB1 (Joseph *et al.* 2014; Colella *et al.* 2019). However, these studies were only focused on the EMT-process *per se* and the regulation of other EMT-effectors. Therefore, elucidating the upstream drivers that specifically regulate this

triad of stem cell-associated genes (*ZEB1*, *SOX2* and *OLIG2*) in a GSC-related context, is crucial to target GBM progression and recurrence.

3.2 Aims and objectives:

1. To assess whether FGF2 induces the expression of key GSC transcription factors.
2. To study the effect of this growth factor in GSC sphere-formation and clonogenic capacity by pharmacological inhibition of its function.
3. To characterise the correlation between FGFRs, *ZEB1*, *SOX2* and *OLIG2* in GBM.
4. To compare the expression profiles of these genes in GSCs and differentiated populations of tumour cells.

3.3 Results

3.3.1 FGF2 induces expression of stem cell-associated transcription factors

Although FGF2 has been reported to be highly expressed in GBM and to have a crucial function in tumour growth, its role in stemness regulation has not been demonstrated. We therefore sought to define how FGF2 acts on GSCs by firstly analysing the correlation between FGF2 and the GSC-associated transcription factors ZEB1, SOX2 and OLIG2 (Singh *et al.* 2017). TCGA gene expression analysis demonstrates that each of these transcription factors correlates with *FGF2* (**Figure 3.1A**). To validate this data, we performed Western blot analysis of primary patient-derived GBM cells that have been cultured in EGF only and have been treated with different concentrations of FGF2 for 48h (**Figure 3.1B**, left). Our results indicate that 30 ng/mL of FGF2 induces the highest expression of ZEB1. Selecting this concentration as the standard amount of FGF2 to activate GSC-associated transcription factors, our results show that this growth factor also increases the expression of SOX2 and OLIG2 (**Figure 3.1B**, right).

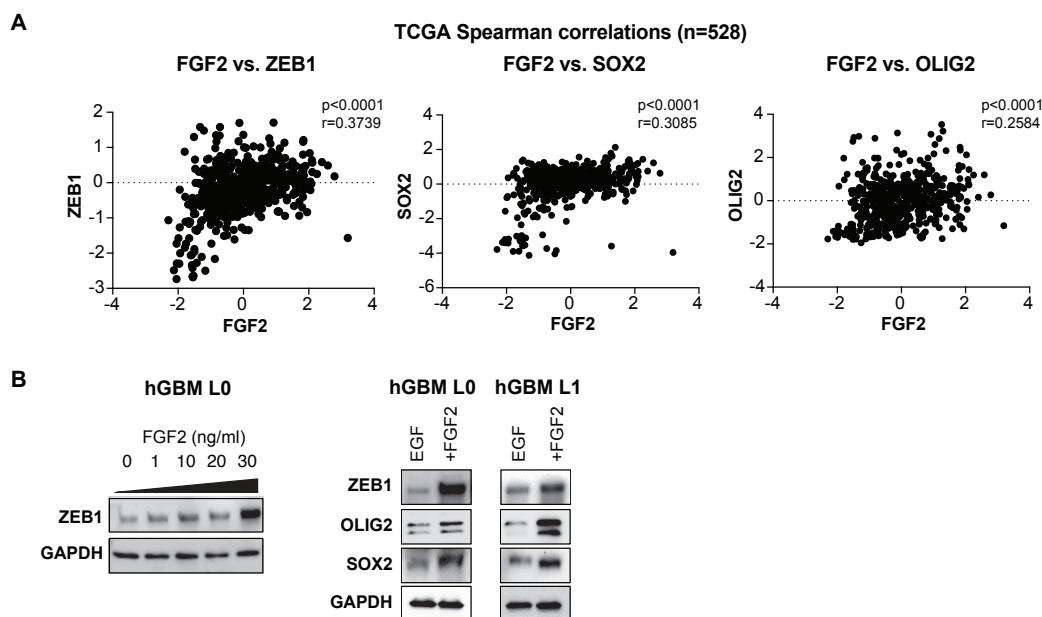


Figure 3.1. FGF2 is associated to stemness in GBM. **A**) Spearman correlation *FGF2* and *ZEB1* (left), *SOX2* (middle) and *OLIG2* (right) using the GBM (TCGA) tumour samples with mRNA data (U133 microarray only) dataset (n=528 samples), based on expression z-scores. Data shows a significant positive correlation for FGF2 and each transcription factor ($p < 0.0001$). Bioinformatic analysis performed by Dr. Karl Holmberg Olausson (Uppsala University). **B**) Treatment of primary patient-derived GBM cells with FGF2 after 48h increases ZEB1 expression in a dose-dependent manner (hGBM L0 n=3). Treatment of hGBM L0 and L1 with 30 ng/mL of FGF2 also increased the expression of SOX2 and OLIG2 (hGBM L0 n=5, hGBM L1 n=3). The expression of ZEB, SOX2 and OLIG2 was assessed after 48h as this time point was used by other studies to analyse expression of stemness markers after FGF2 treatment (Podergajs *et al.* 2013).

3.3.2 FGF2 induces sphere-formation capacity

The combination of EGF and FGF2 has been broadly used to maintain the stemness characteristics of NSCs and GSCs in culture (Singh *et al.* 2003; Galli *et al.* 2004; Reynolds and Rietze 2005; Kelly *et al.* 2009). To verify that FGF2 is capable of inducing sphere-formation *in vitro*, we used patient-derived hGBM cells that have been cultured in two different conditions: EGF only (hGBM L2/L1/L0) or EGF+FGF2 (hGBM U3019) (**Figure 3.2**). Treatment with FGF2 increases sphere-formation capacity in hGBM L2, hGBM L0 and hGBM L1 cells (**Figure 3.2A**). By the contrary, withdrawal of FGF2 in U3019 cultures abolishes the formation of spheres (**Figure 3.2B**). As 30 ng/mL of FGF2 was the most efficient concentration in inducing sphere-forming frequency of GSCs and promoting the expression of ZEB1, SOX2 and OLIG2 (**Figure 3.1B**), we chose this as standard concentration *in vitro*, unless otherwise specified. This is in-line with previous studies, which used 20-30 ng/mL of FGF2 for *in vitro* assays (Bajetto *et al.* 2013; Podergajs *et al.* 2013).

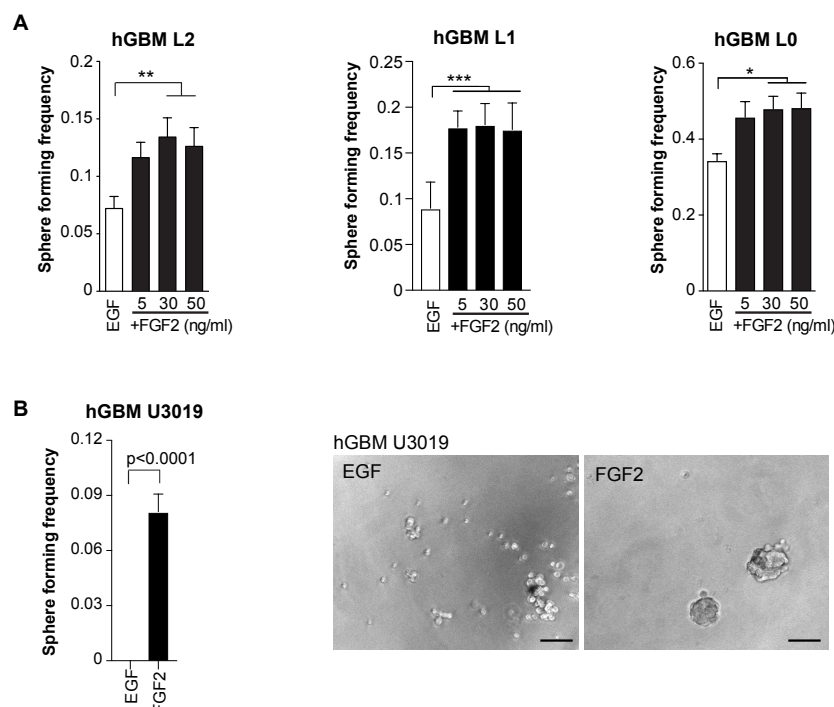


Figure 3.2. FGF2 induces sphere-formation capacity of GSCs. A) FGF2 treatment results in an increase in sphere-forming frequency of GSCs in a dose-dependent manner (5 ng/mL, 30 ng/mL and 50 ng/mL of FGF2) relative to control, EGF only treated cells (hGBM L2 n=14, L1=14, L0 n=10, one-way ANOVA, Dunnett's multiple comparison test). **B)** Sphere-formation capacity is abolished when FGF2 is withdrawn (hGBM U3019 n=4, two-tailed t-test) (left). Representative images of sphere-formation in hGBM U3019 in EGF only and EGF+FGF2 conditions (right). "n" indicates the number of independent experiments (biological replicates). Data are mean \pm SEM. Scale bar 1 μ m.

To further assess the function of FGF2 in stemness, we screened for FGF2 antagonists, NSC47762, NSC58057, NSC65575 and NSC65576 for their ability to block sphere-formation (**Figure 3.3A**). These small molecules block FGF2 activity by directly inhibiting FGF2/HSPG binding and by allosterically affecting FGF2/FGFR interaction (Pagano *et al.* 2012; Foglieni *et al.* 2016). Our results identify 2-Naphthalenesulfonic acid (NSC65575) as a potential FGF2 antagonist in GBM, as this compound reduced sphere- and colony-formation of patient-derived GBM cells in a dose-dependent manner (**Figure 3.3B** and **Figure 3.3C**).

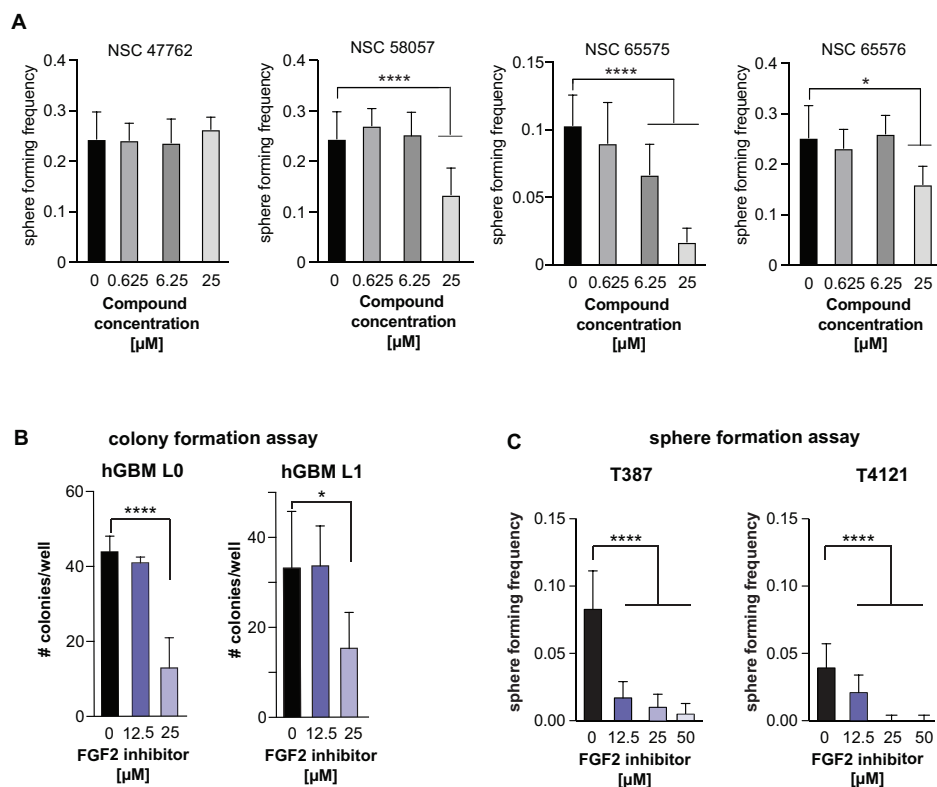


Figure 3.3. Pharmacological inhibition of FGF2 reduces sphere/colony-formation capacity *in vitro*. **A)** Sphere-forming assay using four compounds (NSC47762, NSC58057, NSC65575, NSC65576) that have been shown to block binding of FGF2 to its receptors (hGBM L0 n=3, one-way ANOVA, Dunnett's multiple comparison test). Bar graphs show sphere-forming frequency 5 days after plating, relative to vehicle control (DMSO), represented by "0 compound concentration". NSC 65575 was the most effective compound in this assay. **B)** This was tested in subsequent colony-forming assays (hGBM L0 and L1 n=5, one-way ANOVA, Dunnett's multiple comparison test) and **(C)** was validated independently in the laboratory of our collaborator Prof Justin D. Lathia (Lerner Research Institute, Cleveland) (hGBM T387 and hGBM T4121 n=5, one-way ANOVA, Dunnett's multiple comparison test). "n" indicates the number of independent experiments (biological replicates). Data are mean \pm SEM.

As previously describe, sphere and colony forming assays consist on different approaches to measure the same hallmark which in this case is the capacity of the cells to self-renew. While the sphere-forming assay can overestimate the number of *in vitro* stem cells, the colony-forming assay is more robust as the cells are embedded in a

semi-solid collagen matrix ensuring that a colony is derived from a single cell and not from cell aggregates (see section 2.1.5 and 1.3.6.2 for more details). Using a variety of approaches to assess stemness strongly validate our data and generates significant results to implicate FGF2 in GSC regulation.

To exclude the possibility that the observed reduction in sphere-forming frequency is due to toxicity of the compound, cell viability and cell apoptotic assays were performed (**Figure 3.4**). MTT assay demonstrates NSC65575 does not reduce cell viability at any concentration tested in previous assays (**Figure 3.4A**). Indeed there is a tendency to increase cell proliferation under these conditions which will be discussed in section 3.4. Furthermore, flow cytometry analysis of annexin-V staining shows no increase in cell apoptosis after treatment with 50 μ M NSC65575 (**Figure 3.4B**).

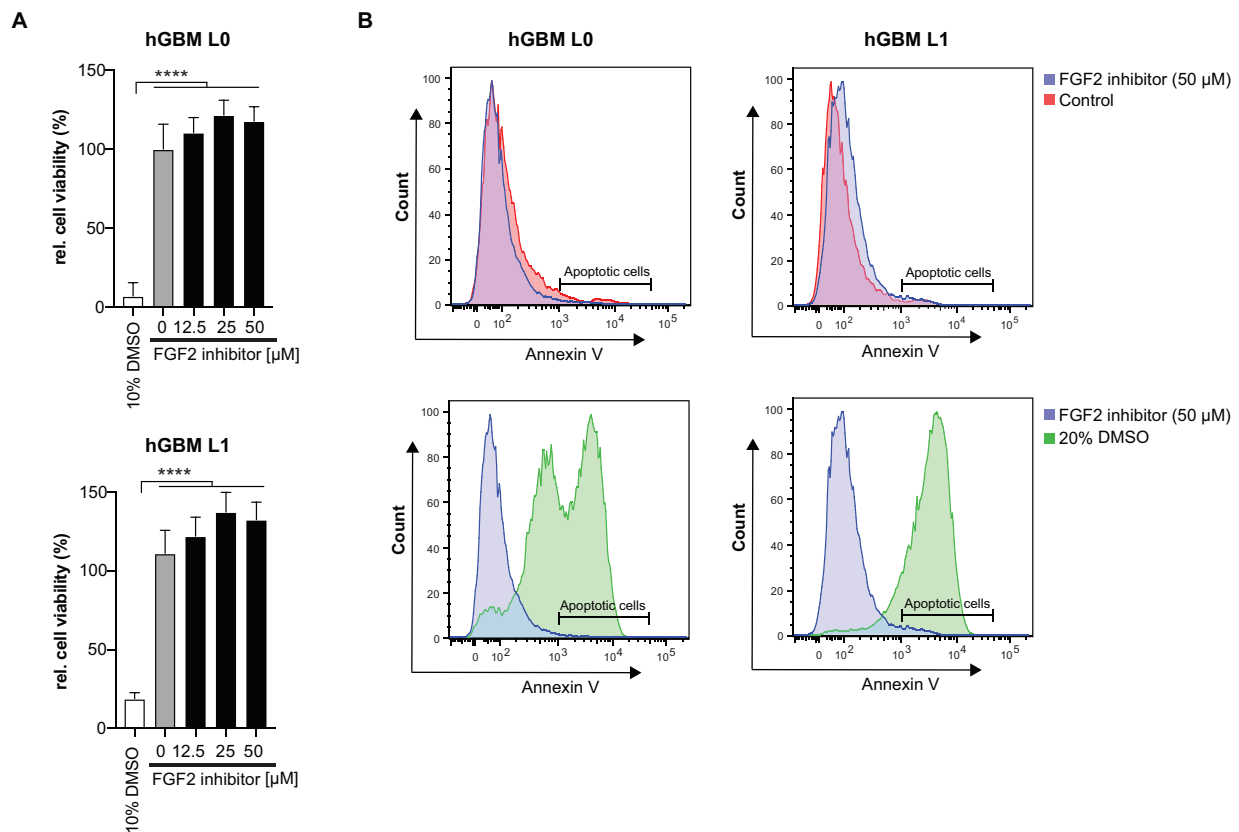


Figure 3.4. FGF2 inhibitor is not toxic to patient-derived hGBM cells. A) MTT cell viability assay of hGBM cells treated with NSC65575 in 3 different concentrations. “0 FGF2 inhibitor concentration” represents the control (DMSO at same concentration than 50 μ M of the compound). Bar graphs show cell viability relative to 10% DMSO treatment at 5 days. This concentration of DMSO is used as cell viability control, due to its high cell toxicity. FGF2 inhibitor did not affect cell viability (hGBM L0 n=7, hGBM L1 n=5, one-way ANOVA, Dunnett’s multiple comparison test). **B)** Representative FACS plots showing annexin-V staining of hGBM cells after 48 h treatment with 50 μ M NSC65575. Upper plots show no difference in apoptosis between inhibitor and control (DMSO at same concentration). Lower plots show a shift to the right in the X axis (higher annexin-V staining) of the population treated with 20% of DMSO due to its high toxicity, compared to cells treated with the compound (hGBM L0 n=3, hGBM L1 n=3). “n” indicates the number of independent experiments (biological replicates). Data are mean \pm SEM.

3.3.3 Association of FGFRs with stem cell transcription factors using TCGA data analysis

In order to determine whether any FGF2 receptor (FGFR1-4) may show a correlation with stemness-associated transcription factors, we performed hierarchical cluster analysis of TCGA data (Jimenez-Pascual *et al.* 2019). This bioinformatic approach revealed the existence of three different clusters using *FGF2*, *FGFR1-4*, *ZEB1*, *SOX2* and *OLIG2* expression as determinant. These clusters are represented by cluster 1, cluster 2 and cluster 3 in **Figure 3.5A**. The smallest cluster and the one with the lowest expression of all examined genes, was cluster 2. On the other hand, a correlation between *FGF2*, *FGFR1-3* and stem cell transcription factors was observed in cluster 1 which was formed by approximately 30% of the samples. Finally, cluster 3 comprises most of the analysed specimens (>50%) and only shows high expression of *ZEB1* and *SOX2*. Interestingly, the overall expression of FGFRs is low throughout the three clusters.

Due to the TCGA data used could be affected by the presence of other cells (non-tumour cells) in the patient samples analysed, we further validate our results using the HGCC dataset. The latter provides information about GBM molecular subtypes (classical, mesenchymal, proneural and neural) (Verhaak *et al.* 2010) and is derived from GBM patient cell lines that are propagated in stem cell conditions (Xie *et al.* 2015). This dataset also revealed the existence of three main clusters (**Figure 3.5B**). Despite cluster 2 and cluster 3 are represented by different molecular signatures, cluster 1 is mainly enriched for mesenchymal subclass. Interestingly, this cluster showed a high correlation with *FGFR1* (**Figure 3.5B**). The latter was corroborated using Gliovis data portal (Bowman *et al.* 2017). Similarly, expression of *FGFR1* was higher in mesenchymal and classical subtypes compared to proneural GBM (**Figure 3.5C**). Therefore, these results outline an association of FGF2 and stemness-related transcription factors in an important fraction of GBM specimens and a possible link between FGFRs and different molecular signatures.

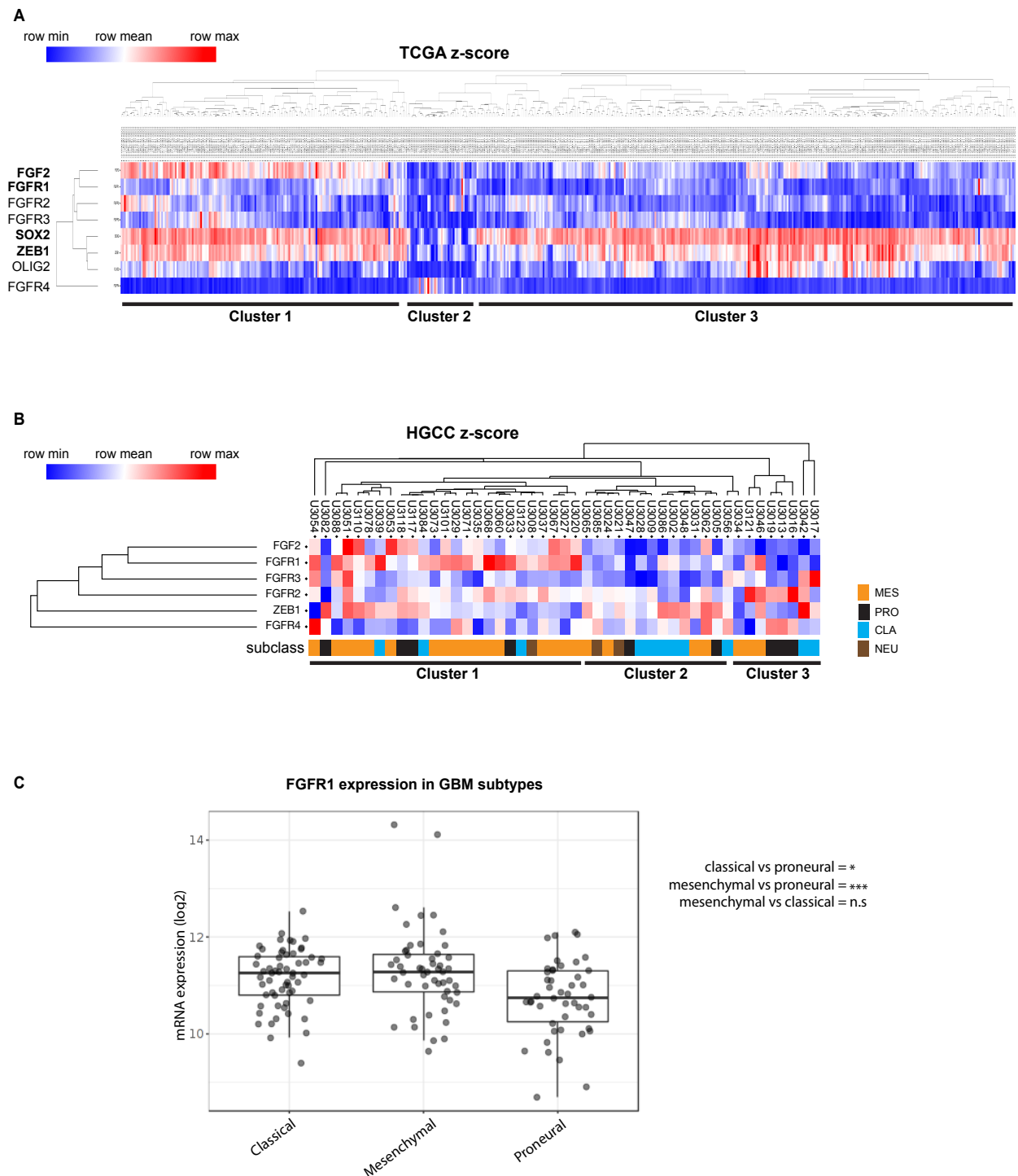


Figure 3.5. Hierarchical clustering of TCGA data. A) Supervised hierarchical clustering of TCGA data (n=528) using *FGF2*, *FGFR1-4*, *ZEB1*, *SOX2* and *OLIG2* reveals three separate clusters. **B)** These clusters could be validated in the HGCC dataset (www.hgcc.se). Bioinformatic analysis performed by Dr Karl Holmberg Olausson (Uppsala University). **C)** Overview of *FGFR1* expression in TCGA GBM datasets (RNA-seq platform) using Gliovis data portal (Bowman *et al.* 2017). The difference between classical/mesenchymal vs proneural subtype is significant (Tukey's test).

3.3.4 Expression analysis of FGFRs in patient-derived GBM cells

We performed western blot analysis to determine the protein levels of FGFR1-4 in the patient-derived cells used in this study (**Figure 3.6A**). hGBM L0, L1 and L2 express FGFR1-3 while FGFR4 is absent compared to a positive control (HEPG2 cells). HEPG2 is an immortalised cell line derived from patients with hepatocellular carcinoma (Knowles *et al.* 1980), reported to have high expression of FGFR4 (www.proteinatlas.org). TCGA cluster analysis (**Figure 3.5**) supports these results, thus we did not further investigate the function of FGFR4 in GBM. Consequently, we used flow cytometry to quantify FGFR1-3 expression on GBM cells (**Figure 3.6B**). We found FGFR2 was expressed in a large fraction of cells (30-50%). Expression of FGFR3 varies among samples, ranging from 20% of cells in hGBM L0 and L1 to less than 10% in L2, which is in-line with western blot data (**Figure 3.6A**). By contrast, FGFR1 was expressed in a small subset of each cell line (1-5%). Importantly, FGFR1 and FGFR2 expression profiles were consistent between hGBM cells maintained in EGF (hGBM L0, L1 and L2) or in EGF+FGF2 (hGBM U3019), indicating that these conditions did not affect FGFR expression.

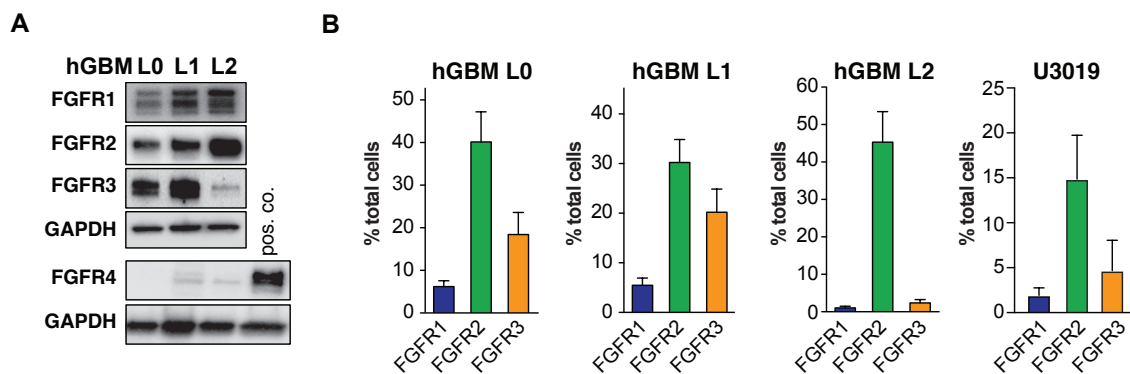


Figure 3.6. FGFR expression and populations in patient-derived hGBM cells. **A)** FGFR expression in hGBM L0, L1 and L2 by western blot. FGFR4 expression is compared to HEPG2 cells as a positive control. FGFR1-3, but not FGFR4, are expressed in the three cell lines. **B)** Flow cytometry quantification of FGFR1-3 expression in patient-derived hGBM lines (n=3 independent experiments/sample; FACS analysis was performed by Anja Kordowski, MSc student from our group).

3.3.5 FGFR1 expression decreases in differentiated hGBM cells

We have assessed the expression of FGFRs and stem cell transcription factors (ZEB1, SOX2 and OLIG2) under culture conditions conducive to GSC maintenance (sphere cultures in defined medium supplemented with growth factors). We next determined the expression of these genes in differentiated GBM cells (**Figure 3.7A**). GSCs have been shown to differentiate upon removal of growth factors, adhesion to Matrigel and addition of 10% serum *in vitro* (Singh *et al.* 2003; Gangemi *et al.* 2009). As Matrigel contains high amounts of FGF2, we use Geltrex as the growth factor-depleted adhesion substrate. Under these conditions, GSCs lose their self-renewal, multipotency and tumorigenic capacity. We found that FGFR1 expression is enriched in GSC cultures, whereas its levels decrease under differentiation conditions (**Figure 3.7B**). The expression of ZEB1, SOX2 and OLIG2 followed the same pattern while FGFR2 and FGFR3 increased (**Figure 3.7B**). Since serum contains an undefined mixture of growth factors and cytokines, we repeated the experiment in medium supplemented with BMP4, a cytokine that elicits a pro-differentiation effect on GSCs (Piccirillo *et al.* 2006). The same expression patterns were observed under BMP4 or serum treatment. In addition, a clear change towards epithelial-like phenotypes was seen in differentiated cells plated on Geltrex (**Figure 3.7C**). Under non-adherent conditions, serum treated cells did not form spheres, instead, they grew in a monolayer whose morphology resembled fibroblast-like cells, consistent with observations from previous studies (Lee *et al.* 2006). Cells under BMP4 treatment formed spheres, but of smaller diameter than those under stemness conditions. These findings may indicate an important role of FGFR1 in maintaining the undifferentiated state of GSCs, as FGFR1 expression patterns are associated with GSCs and stem cell transcription factors. Nonetheless, this will be reviewed in future chapters.

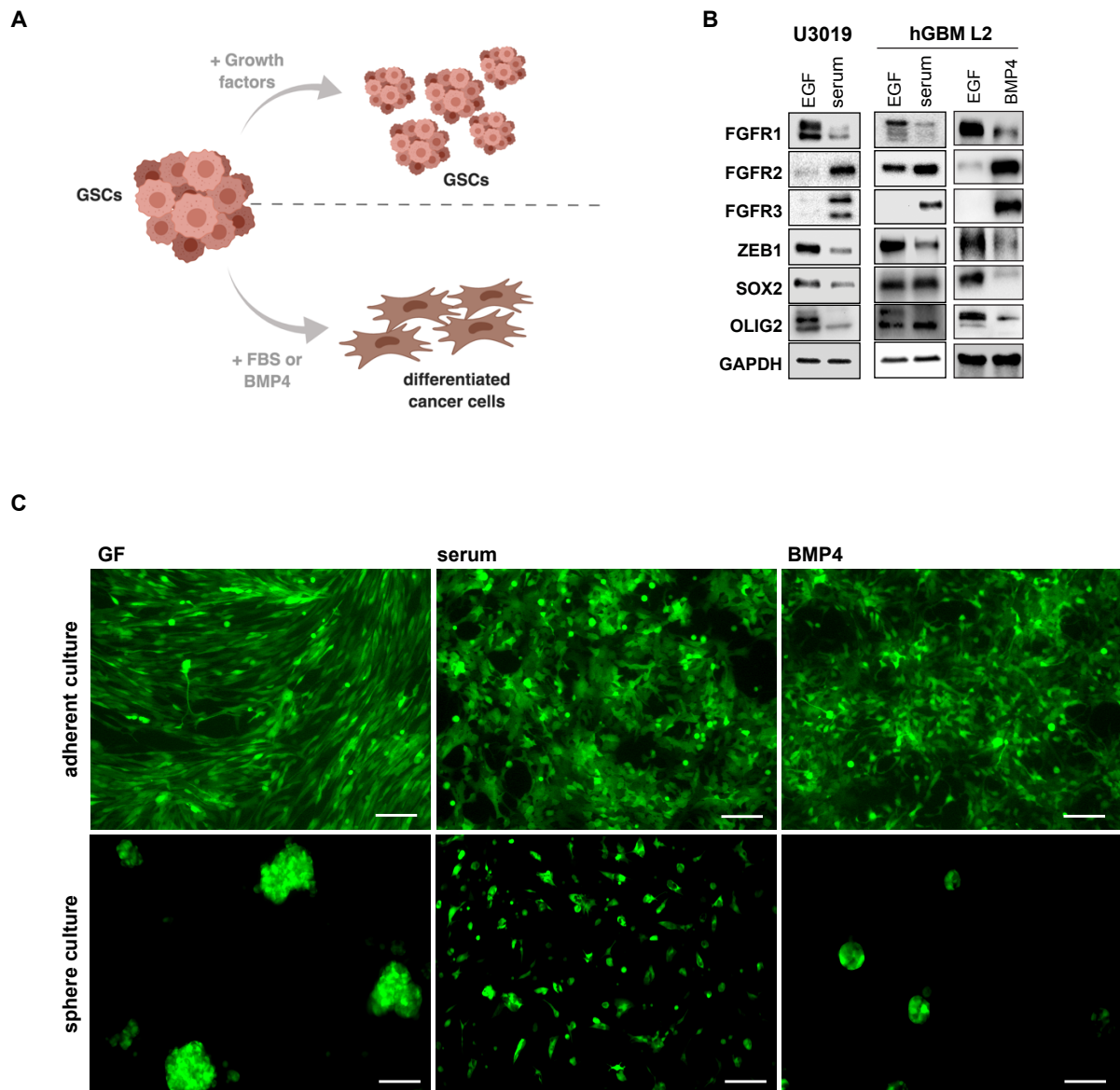


Figure 3.7. Differentiation of GSCs. **A)** Schematic representation of GSC characteristics maintained under growth factor conditions or the induction of GSCs differentiation under serum or BMP4 treatment (Image created with BioRender.com). **B)** Expression of FGFR1-3, ZEB1, SOX2 and OLIG2 after 4 days of treatment with 10% serum or 25 ng/mL BMP4 relative to EGF treated cells. **C)** Cell morphology was assessed in hGBM L2 cells transduced with a GFP-expression vector and plated in adherent conditions on Geltrex substrate or in suspension. Only cells treated with growth factors (GF) maintained their proliferative capacity and formed spheres of approximately 70 μm in diameters. Scale bar = 100 μm .

3.4 Discussion

In this study, we investigate the function of FGF2 as an inducer of stem cell-associated transcription factors. We also explore its role in promoting self-renewal capacity *in vitro* by pharmacologically blocking its activity with a small molecule inhibitor, NSC65575. Finally, we examine the correlation among FGF2, FGFRs and the aforementioned transcription factors using TCGA data analysis of GBM patient samples.

Our results identify FGF2 as an important mitogen for the maintenance of GSCs. This has been suggested by others before as EGF and FGF2 are growth factors broadly used to maintain NSC and GSC cultures (Reynolds and Weiss 1992; Haley and Kim 2014). However, the underlying molecular mechanism by which FGF2 regulates stemness in GSCs is not completely understood. Our results indicate that FGF2 promotes the expression of ZEB1, SOX2 and OLIG2. These transcription factors are known to mediate GSC maintenance and therapy resistance in GBM patients (Siebzehnrubl *et al.* 2013; Singh *et al.* 2017). Consistent with our data, other studies have demonstrated that FGF2 induces ZEB1 expression in corneal endothelium (Lee *et al.* 2018) and in ovarian cancer (Lau *et al.* 2013). Importantly, we demonstrated significant correlation of FGF2 with these transcription factors using TCGA data analysis of GBM samples, which supports the association of FGF2 with stemness phenotypes.

FGF2 has been reported to be crucial for GSC self-renewal capacity *in vitro* (Pollard *et al.* 2009; Haley and Kim 2014). In support of this, we observed a dose-dependent increase in sphere-forming frequency of hGBM cells after FGF2 treatment. Bajetto *et al.* demonstrated that FGF2 was more relevant for extensive growth of GSCs in culture than EGF (Bajetto *et al.* 2013). The authors showed that only a minor subpopulation of patient-derived GBM cells were responsive to EGF, while the growth of the largest population was induced by FGF2. In addition, FGF2 treated cells formed spheres in limiting dilution sphere-formation assays while EGF treated did not. These findings partly support our results that showed GSC self-renewal increased with FGF2. However, spheres were also present under EGF only treatment, though smaller in size and at a reduced frequency.

Importantly, our data also showed a decrease in GSC clonogenicity when FGF2 function was pharmacologically inhibited. The FGF2 inhibitors used were previously tested in endothelial cells, aiming to mimic the function of thrombospondin, a protein that blocks angiogenesis by interfering with the FGF-FGFR complex (Pagano *et al.* 2012; Foglieni *et al.* 2016). The authors described a reduction in endothelial cell proliferation and vessel sprouting from aortic rings embedded in Matrigel in the presence of 30 ng/mL of FGF2 and 25-100 μ M of NSC65575 (Foglieni *et al.* 2016). As this compound blocked FGF/HSPG/FGFR interaction and showed no off-target effects on other tyrosine kinase receptors, we attempted to assess the efficiency of this small molecule inhibitor in GSCs. Our results indicate that 12.5 μ M of NSC65575 was sufficient to inhibit sphere- and colony-forming frequency of GSCs. Chemically the FGF2 inhibitors used in this study differ in the presence or the absence of methyl groups which constitute aromatic extensions that modulate dramatically the efficiency in small-molecule drugs (Barreiro *et al.* 2011). This effect is called the “magic methyl effect” and in this case it generates an hydrophobic pocket that docks into FGF2 stabilizing the ligand-compound binding and improving the affinity and potency of the inhibitor in more than 100-fold (Schönherr and Cernak 2013; Foglieni *et al.* 2016). As an example, compound NSC47762 lacks this aromatic extension (Foglieni *et al.* 2016) and shows not effect in sphere-forming capacity (**Figure 3.3A**). In contrast, NSC65575 contains two methyl groups and its inhibitory effect is significant. This may explain the difference between the compounds elucidating a response and those that did not in GSC self-renewal capacity.

Foglieni *et al.* showed no toxicity of NSC65575 compound in endothelial cultures (Foglieni *et al.* 2016). This finding is in-line with our apoptotic data. Conversely, **Figure 3.4A** shows an increase in cell viability after FGF2 inhibitor treatment. The latter could be associated with a biphasic dose-response caused by a phenomenon called “hormesis”. This phenomenon is common in pharmacology and characterised by the stimulation of tumour cell proliferation at low doses followed by its inhibition at high doses (Calabrese 2008). Thus, in order to eliminate the duality in function of this drug, a dose-response curve measuring cell-viability *in vitro* and BrdU *in vivo* experiments of GBM xenografts under NSC65575 treatment will determine the correct/suitable dosage of this drug.

The levels of FGF2 are higher in GBM than in normal brain and correlate with poorer prognosis and high-grade gliomas (Auguste *et al.* 2001; Peles *et al.* 2004). We showed that FGF2 was highly expressed in 30% of the hGBM patient samples analysed by TCGA. Similarly FGFR1 was reported to be high in GBM (Morrison *et al.* 1994; Rand *et al.* 2005; Kowalski-Chauvel *et al.* 2019). By contrast, FGFR2 and FGFR3 were downregulated (Yamaguchi *et al.* 1994; Parker *et al.* 2014). Although analysis of the TCGA GBM dataset using GlioVis (Bowman *et al.* 2017) supported these studies, we found overall low expression of the four receptors in our TCGA cluster analysis. In addition, the HGCC gene expression data validated a correlation between *FGFR1* expression and the mesenchymal and classical subtype of GBM samples enriched in *ZEB1* and *SOX2* expression. In support of this, TCGA GBM data analysed using GlioVis also showed a significant increase of *FGFR1* in mesenchymal and classical subtypes compared to proneural GBM. In contrast, FACS analysis of hGBM cells used in this study showed FGFR2 to be the highest FGFR expressed while FGFR1 the lowest. FGFR4 was not expressed in any of the cell lines used which was supported by our TCGA cluster analysis. Variations in FGFR expression depending on hGBM cell lines have been previously reported (Loilome *et al.* 2009; Gouazé-Andersson *et al.* 2016), and can be explained by the high inter- and intratumoral heterogeneity characteristic of GBM (Verhaak *et al.* 2010; Capper *et al.* 2018).

Finally, we attempted to describe the expression of these receptors and key stem cell transcription factors in differentiated tumour cells. In other studies, a loss of NSC- and GSC-related markers such as NESTIN and SOX2 was observed in differentiated cancer cells (Gangemi *et al.* 2009; Garros-Regulez *et al.* 2016). These findings are consistent with our results that showed a decrease in SOX2 expression when GSCs were cultured in differentiation medium. In addition, we also reported a downregulation of ZEB1 and OLIG2 which indicates that these three factors are co-expressed in stem-cell like populations. These results are in-line with a previous study that reported a cross-regulation interdependence between the three transcription factors in GBM (Singh *et al.* 2017). Importantly, our results suggest that only FGFR1 is associated with an undifferentiated state of cancer cells indicating that this receptor is functionally relevant for the maintenance of GSCs, contrary to FGFR2 and FGFR3 that are upregulated in mature cancer cells/non-GSCs. In support of this, Wang *et al.* used TCGA and CGGA data analysis of patient samples and found a correlation between

FGFR3 expression and differentiated cellular functions which was associated with less malignant processes in GBM (Wang *et al.* 2016).

Taken together these findings identify FGF2 as an important upstream regulator of the stem-cell associated transcription factors ZEB1, SOX2 and OLIG2, which outlines a direct effect of FGF2 in GSC maintenance (**Figure 3.8**). Since our results demonstrated that *FGFR1* is the only receptor downregulated in differentiated GBM cells and this receptor has been associated with GBM tumour progression (Yamada *et al.* 1999; Fukai *et al.* 2008; Loilome *et al.* 2009; Irschick *et al.* 2013), we hypothesized that FGF2 may regulate GSCs through *FGFR1*. However, *in vitro* functional data and *in vivo* experiments would be required to test this hypothesis.

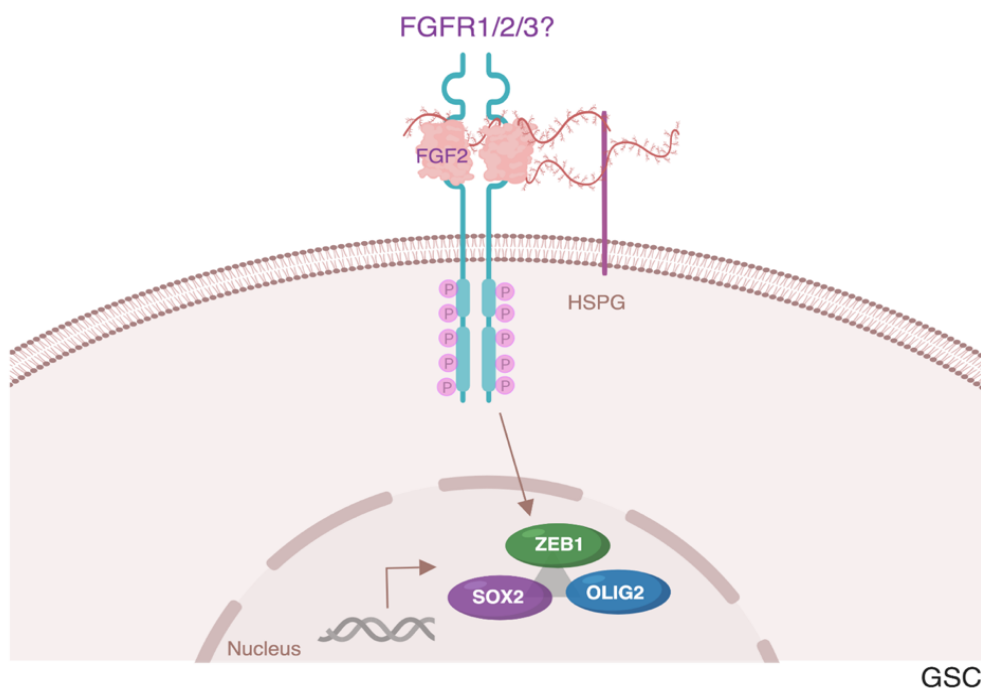


Figure 3.8: Diagram depicting the role of FGF2 in GSCs. FGF2 binding to FGFRs activates signalling transduction pathways that induce the expression of ZEB1, SOX2 and OLIG2 transcription factors involved in stemness maintenance. We will explore in the next sections how FGF2 promotes this function and which FGFR or FGFRs are involved in GSC regulation (Image created with biorender.com).

Chapter 4: Investigating the role of FGFR1-3 in GSC regulation

4.1 Introduction

FGF2-FGFR binding promotes the activation of cell proliferation, survival, tissue repair and other crucial cellular processes (Eswarakumar *et al.* 2005; Guillemot and Zimmer 2011; Irschick *et al.* 2013). These receptors are type I transmembrane proteins (Jennings 1989) and part of the receptor tyrosine kinase family. They consist of an extracellular, transmembrane and intracellular domain (Harmer *et al.* 2004; Haugsten *et al.* 2010; Ahmad *et al.* 2012; Touat *et al.* 2015). The extracellular domain is relevant for the ligand-receptor binding, which is stabilised by HSPGs, proteoglycans present on the cell surface and in the ECM (Roghani *et al.* 1994; Haugsten *et al.* 2010). FGF2-mediated functions are translated from the transmembrane region to the intracellular domain, which leads to the activation of a variety of signalling cascades upon ligand-receptor binding and FGFR dimerization.

The FGF2-FGFR pathway has been described as a prognostic marker of high-grade gliomas. Moreover, the activation of these receptors is associated with GBM outgrowth (Morrison *et al.* 1990; Loilome *et al.* 2009). *FGFR* genomic alterations (e.g. amplifications, mutations and translocations) are rare compared to other tyrosine kinases receptors relevant for GBM, such as *EGFR* and *PDGFR α* (Verhaak *et al.* 2010; Lasorella *et al.* 2017). *FGFR* alterations and functions have been broadly studied in other cancers like bladder (Rhijn *et al.* 2002), gastric (Dutt *et al.* 2008), breast (Chin *et al.* 2006) and prostate (Murphy *et al.* 2010). However, the exact function of each receptor in GBM is incompletely understood. FGFR1 has been linked to GBM proliferation (Yamada *et al.* 1999; Loilome *et al.* 2009) and radioresistance (Sooman *et al.* 2015; Gouazé-Andersson *et al.* 2016). FGFR3 function in GBM is most frequently associated with chromosomal translocations, known as the *FGFR3-TACC* fusion (Di Stefano *et al.* 2015), while *FGFR2* downregulation is described as a marker of poor prognosis (Ohashi *et al.* 2014).

Over the last decade, studies of FGF2 and its receptors in GBM have mainly focused on their growth-mediating capacities; however, less is known about the role of these receptors in GSC regulation. Recently, two studies have outlined a possible link between FGFR1 and stemness regulation (Gouazé-Andersson *et al.* 2018; Kowalski-Chauvel *et al.* 2019). Both papers lack *in vitro* rescue experiments and *in vivo* models

relevant for studying stemness in GBM, as will be discussed later on. As we previously showed an association between FGF2 and GSCs and because, to our knowledge, there are no studies that clearly defined the molecular mechanism of how FGFRs regulate stemness in GBM, we next sought to investigate the role of each FGFR in GSC maintenance.

4.2 Aims and objectives:

1. To determine the function of FGFR1-3 in hGBM cells employing shRNA-mediated knockdown *in vitro*.
2. To analyse the effects of *FGFR1-3* loss in GBM progression and invasion by transplanting FGFR1-3 knockdown cells into immunocompromised mice.
3. To assess the association of *FGFR1-3* with GBM patient outcome using TCGA data.

4.3 Results

4.3.1 *FGFR1* knockdown impairs hGBM cell proliferation and clonogenic capacity

To investigate the biological impact of these receptors in GBM, we transiently transfected patient-derived GBM cells with shRNA-mediated knockdown constructs against human *FGFR1-3* (see Table 2.4). Control and knockdown lentiviral constructs were encoded within a GFP-expressing lentiviral vector containing an ampicillin resistance cassette (see section 2.2 for more details). The efficiency of each FGFR knockdown was compared to control cells and validated by western blot analysis in hGBM L0 cells (**Figure 4.1A**). All shRNAs satisfactorily attenuated FGFR expression, and construct #1 of each receptor was selected for production of lentiviral particles and downstream experiments. GFP positive cells were FACS-purified and knockdown specificity verified by western blot in hGBM L2 and hGBM U3019 cells (**Figure 4.1B**). *FGFR1* knockdown increased the expression of *FGFR2* and decreased the levels of *FGFR3* in hGBM U3019 while *shFGFR2* and *shFGFR3* did not have effects on the other receptors. This may either be an off-target effect of the shRNA used, or it could indicate a co-regulation between FGFRs in GBM which will be discussed in section 4.4. We further corroborated knockdown efficiency by flow cytometry analysis (**Figure 4.1C**).

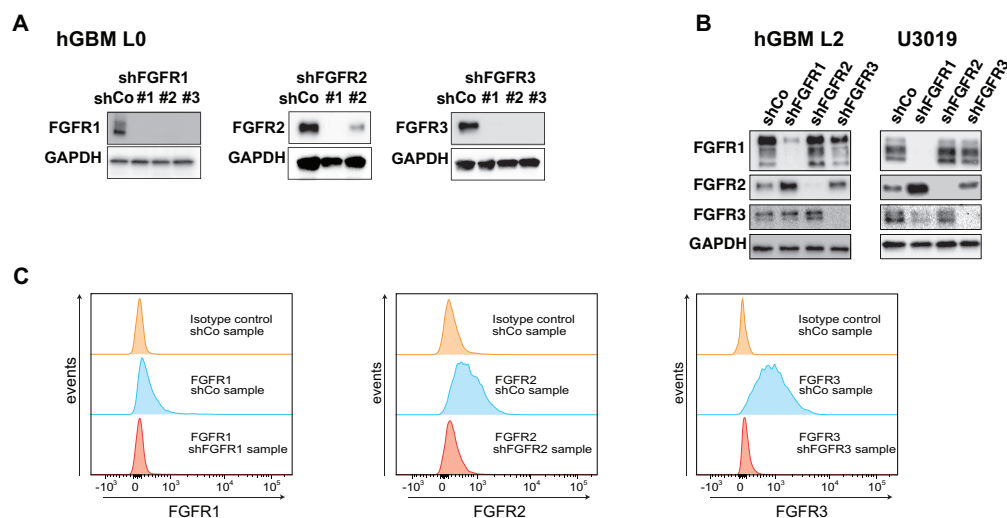


Figure 4.1. Knockdown validation of human short hairpin constructs against *FGFR1*, *FGFR2* and *FGFR3* (shFGFR1-3). **A**) Patient-derived GBM cells were transfected with plasmids encoding for shRNA against human *FGFR1-3* (or control). Three different constructs (represented by #1, #2 and #3) were used for shFGFR1 and shFGFR3 and two for shFGFR2. FGFR knockdowns were measured by western blot analysis. In all cases construct #1 was selected. **B**) hGBM cells transduced with shFGFR1-3 clone #1 lentiviral particles. Western blot demonstrates specificity of FGFR knockdown constructs. **C**) *FGFR1-3* knockdowns clone #1 were verified by extracellular FACS (FACS analysis was performed by Anja Kordowski, MSc student from our group). Shown are histograms for staining intensity (x-axis) versus event counts (y-axis) for isotype control, *FGFR1-3* stained samples, and *FGFR1-3* knockdown samples (hGBM L0, n=3). "n" indicates the number of independent experiments (biological replicates).

To functionally test the relation between these receptors and GSCs, we performed sphere-formation assays of shFGFR1-3 hGBM cells. *FGFR1* loss consistently reduced sphere-forming capacity in all hGBM cells (**Figure 4.2A**), while shFGFR2 had no effect. However, *FGFR3* function was cell line specific (**Figure 4.2A**). Due to FGF2 being more relevant for sphere-formation than EGF as we and others have shown (Bajetto *et al.* 2013), we attempted to examine sphere-forming frequency of shFGFR1-3 in hGBM cells after FGF2 treatment. FGF2 stimulation rescued sphere-forming capacity after knockdown of *FGFR2* or *FGFR3*, but not *FGFR1* (**Figure 4.2B**). These results are consistent among the three cell lines and indicate that *FGFR1* is essential to mediate the effect of FGF2 on hGBM cell self-renewal.

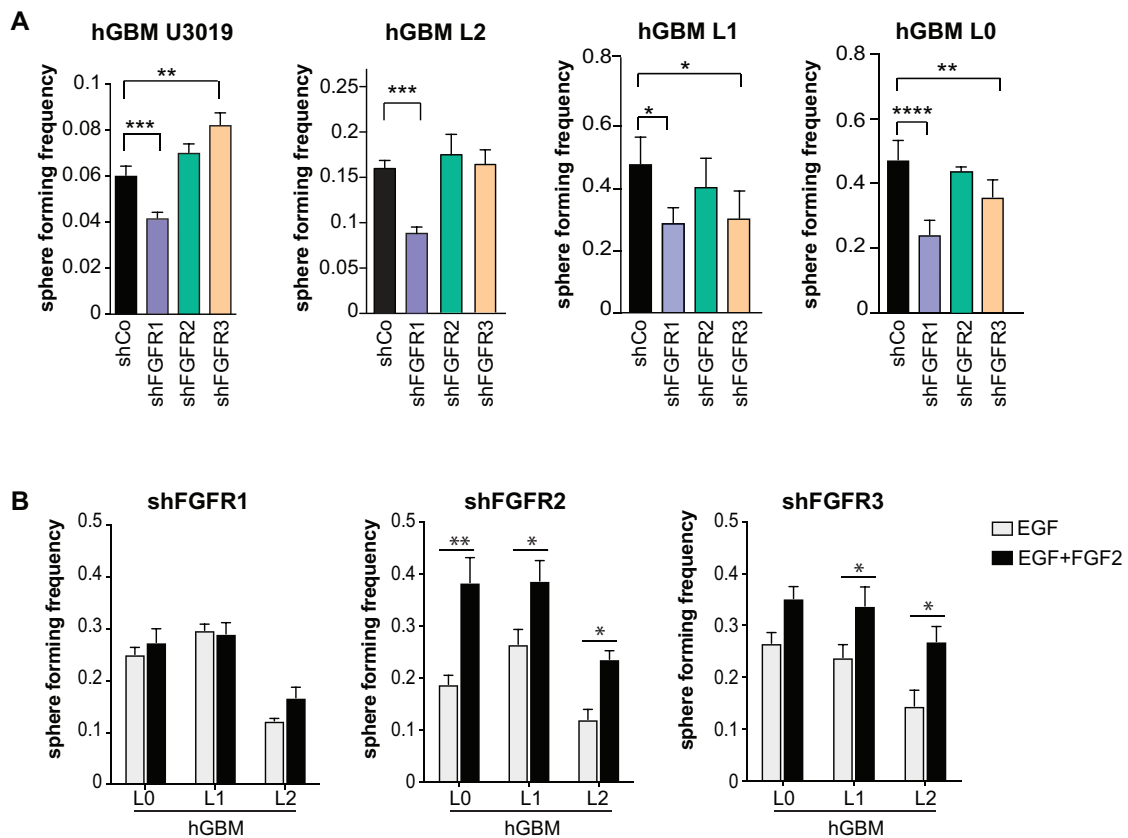


Figure 4.2. *FGFR1* knockdown reduces sphere-forming capacity. **A)** shCo and shFGFR1-3 hGBM cells were treated with EGF+FGF2. Knockdown of *FGFR1*, but not *FGFR2* results in decreased sphere-forming frequency compared to control cells. By the contrary, the effect of shFGFR3 varies among cell lines (hGBM L2 n=6, U3019 n=9, hGBM L1 n=6, hGBM L0 n=5, one-way ANOVA, Dunnett's multiple comparison test). **B)** Sphere-forming assays with EGF or EGF+FGF2 reveal that knockdown of *FGFR1* consistently blocks self-renewal in three patient-derived GBM cell lines. On the other hand, loss of *FGFR2* and *FGFR3* increased self-renewal in response to FGF2 stimulation (hGBM L0 n=6, hGBM L1 n=6, hGBM L2 n=6, two-way ANOVA, Sidak's multiple comparisons test). Number of spheres were quantified 5 days (hGBM L0-L2) and 7 days (hGBM U3019) after plating. "n" indicates the number of independent experiments (biological replicates). Data are mean \pm SEM.

To exclude possible off-target effects of the shFGFR1 construct used (shFGFR1#1), we assessed sphere-forming capacity of hGBM cells transduced with three aforementioned shFGFR1 plasmids. In support of previous results, shFGFR1 clones #1, #2, #3 reduced the number of spheres formed, although clone #1 was the most efficient (**Figure 4.3A**). These results were also confirmed by colony-forming assay (**Figure 4.3B** and **Figure 4.3C**). Colonies with a 200-600 μm diameter were quantified 2 weeks after plating. Finally, the reduction in spheres and colonies after *FGFR1* loss was also accompanied by a decrease in proliferation (**Figure 4.3D**). Taken together, these results identify *FGFR1* as a key receptor for transducing FGF2 signal to GSC maintenance and proliferation *in vitro*.

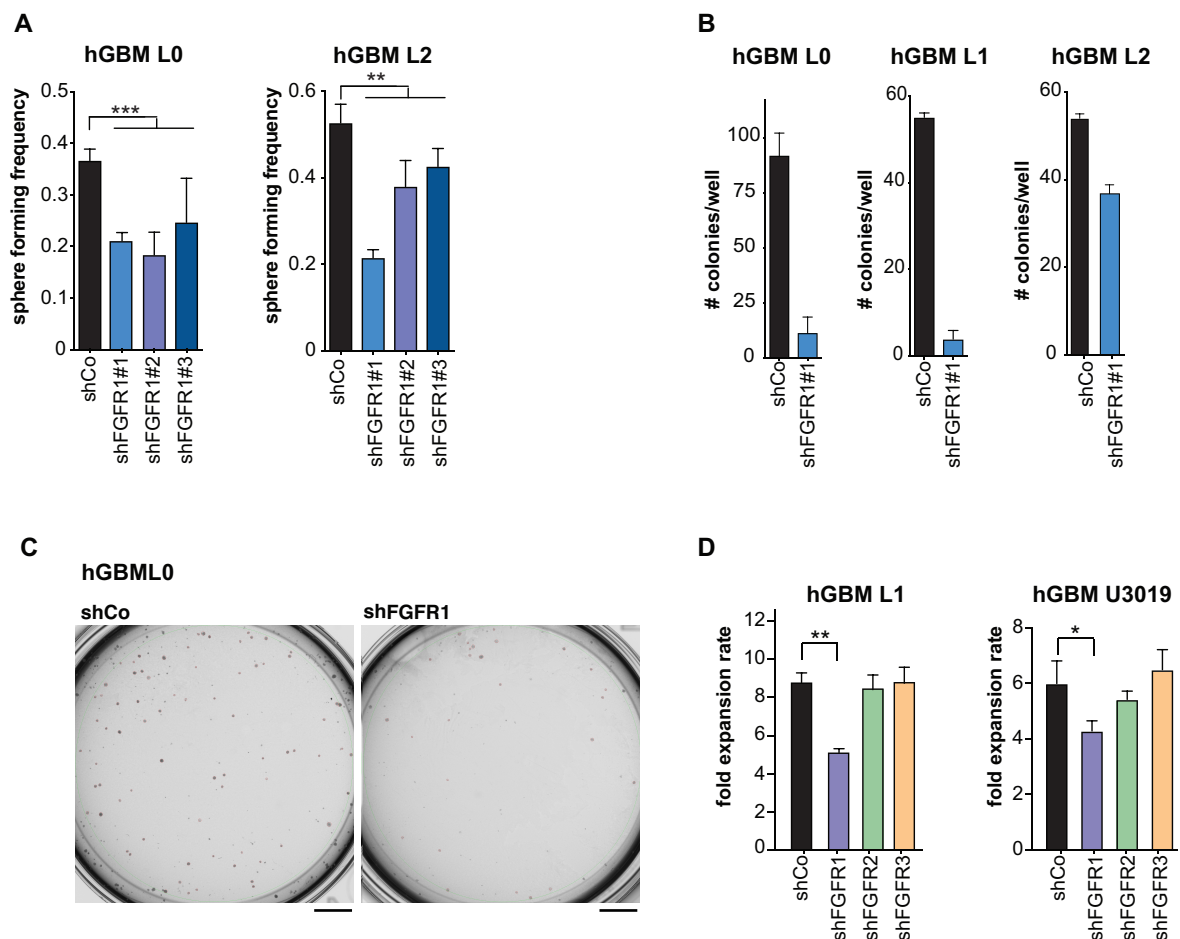


Figure 4.3. *FGFR1* knockdown decreases clonogenic capacity and proliferation. A) Bar graphs show a decrease in sphere-forming frequency of hGBM cells transduced with shFGFR1 clone #1, #2, #3. Cells were treated with EGF+FGF2 and number of spheres quantified 5 days after plating (hGBM L0 n=7, hGBM L2 n=4, one-way ANOVA, Dunnett's multiple comparison test). **B)** shFGFR1#1 was selected for subsequent CFC assay. Colonies were fed with growth factors twice a week and number of colonies quantified after 14 days (hGBM L0, L1, L2 n=2). Despite this assay shows a reduction in colony formation, at least one more biological replicate will be needed to assess statistical significance. **C)** Representative image of shCo vs shFGFR1 colonies. Scale bar = 5 mm. **D)** Fold expansion rate significantly decreased after *FGFR1* loss in hGBM L1 and hGBM U3019 cells (hGBM L1 n=8, hGBM U3019 n=7, one-way ANOVA, Dunnett's multiple comparison test). "n" indicates the number of independent experiments (biological replicates). Data are mean \pm SEM.

4.3.2 Functional rescue of shFGFR1 by targeted expression of this receptor

In view of the fact that *FGFR1* knockdown decreases sphere-formation in all hGBM cell lines tested, we next investigated whether this effect can be rescued by *FGFR1* overexpression. We first produced FGFR1-overexpressing constructs by cloning full-length FGFR1 into a lentiviral expression vector using gateway technology (section 2.4). This construct contained a RFP reporter (while shFGFR1/shCo cells express GFP), enabling FACS purification of shFGFR1/shCo cells transduced with FGFR1 overexpression lentiviral particles (thus, GFP+/RFP+ cells) (**Figure 4.4A**). Western blot analysis for FGFR1 expression showed that the cloned overexpression plasmid successfully rescued FGFR1 expression protein levels in shFGFR1 cells (**Figure 4.4B**). In addition, full-length FGFR1 expression increased sphere-forming frequency in control cells and rescued the number of spheres in FGFR1 knockdown cells to control levels (**Figure 4.4C**).

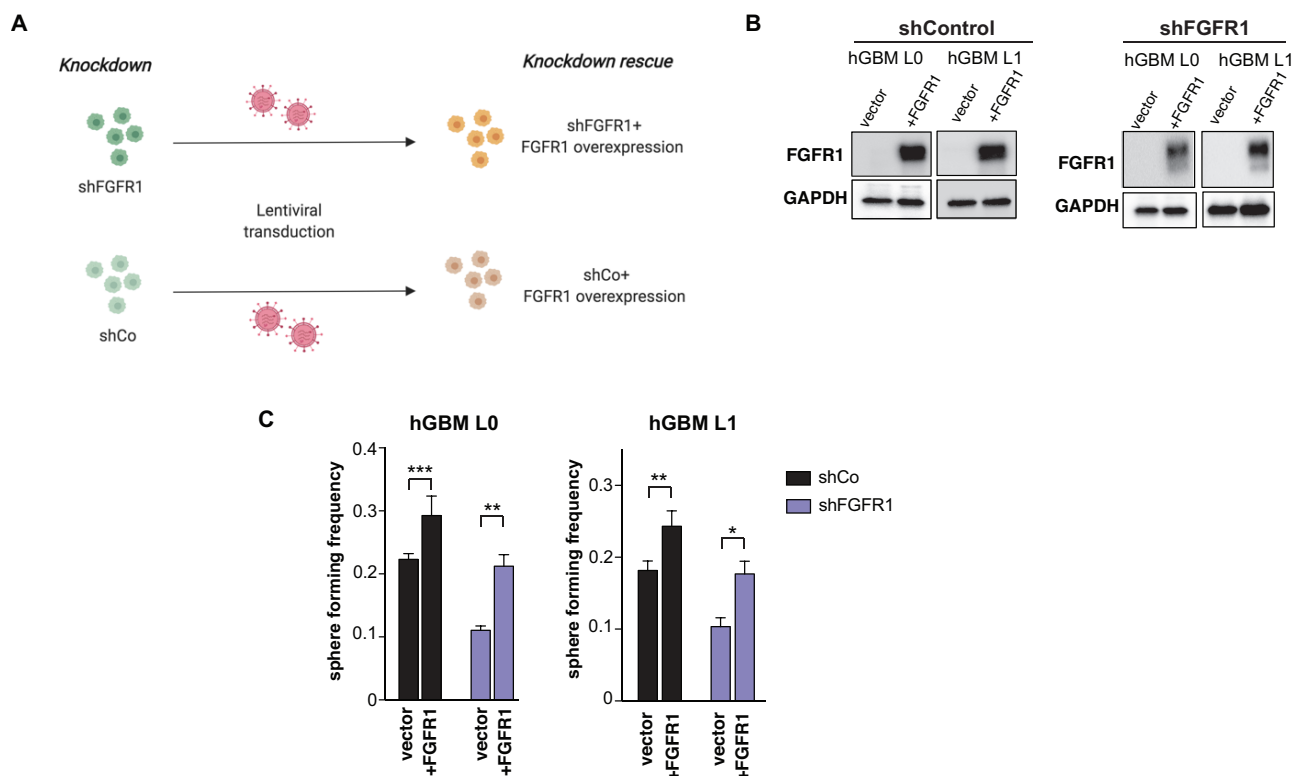


Figure 4.4. *FGFR1* overexpression increases sphere-formation in control and *FGFR1* knockdown cells. **A**) Schematic of experimental procedure. shFGFR1 and shCo cells were transduced with FGFR1 overexpression lentiviral particles. Cells positive for both reporters GFP and RFP were sorted by FACS (Image created with biorender.com). **B**) Western blot analysis shows an increase in FGFR1 expression upon FGFR1 overexpression in shCo and shFGFR1 hGBM L0 and hGBM L1 cells. **C**) *FGFR1* significantly increases sphere-formation in both shCo (black bars) and shFGFR1 cells (blue bars). Number of spheres were quantified 5 days after plating (hGBM L0 n=9, hGBM L1 n=9, two-way ANOVA, Sidak's multiple comparisons test). "n" indicates the number of independent experiments (biological replicates). Data are mean \pm SEM.

4.3.3 Endogenous *FGFR1* promotes clonogenic capacity

To further substantiate the pivotal role of *FGFR1* in GSCs, we investigated the ability of *FGFR1*-expressing cells to form colonies. hGBM L0 cells were stained for *FGFR1* and sorted by FACS into *FGFR1*⁺ and *FGFR1*⁻ cells (**Figure 4.5A** and **Figure 4.5B**). The histogram in **Figure 4.5B** shows positive *FGFR1* staining in hGBM L0 cells compared to an isotype control. Immediately after sorting, cells were plated in serial dilutions in collagen matrix to test for colony-formation. Limiting dilution assay shows *FGFR1*⁺ cells have greater colony-forming potential than the *FGFR1*⁻ population (**Figure 4.5C** and **Figure 4.5D**).

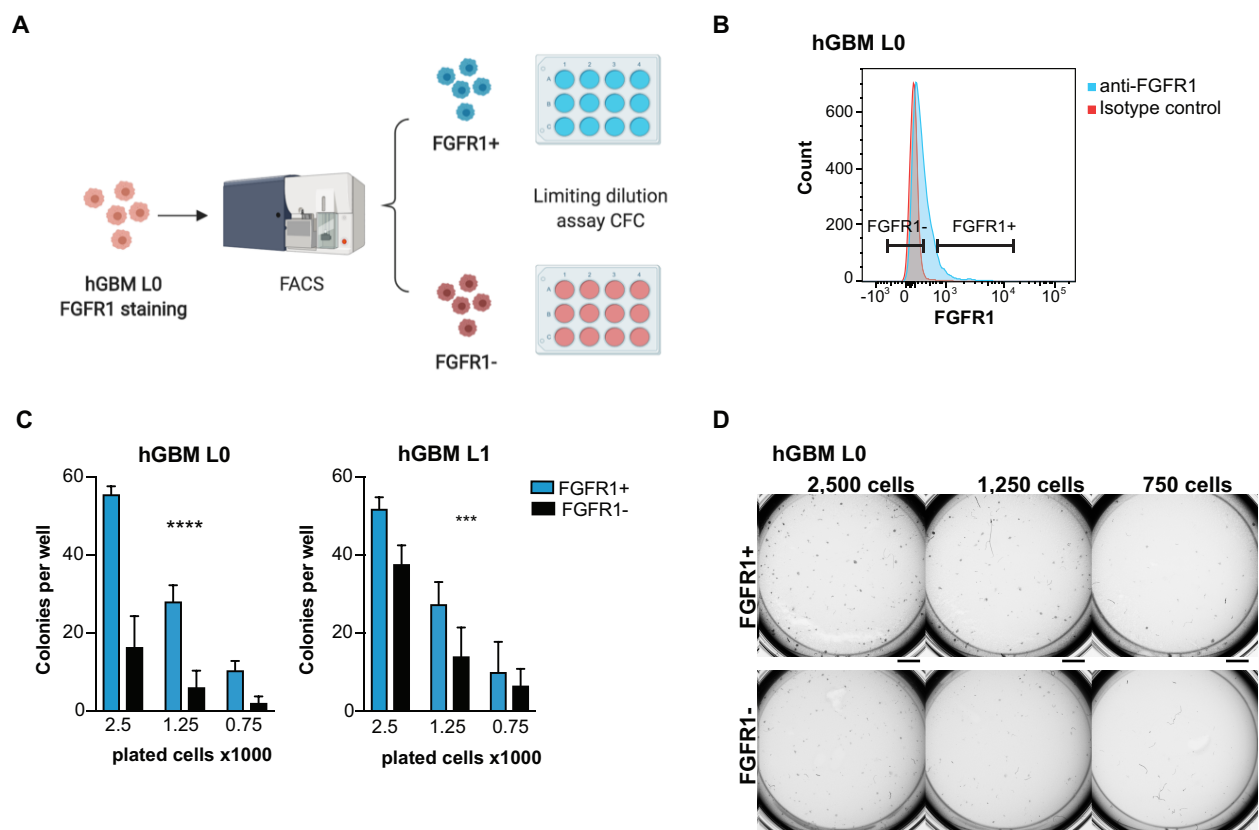


Figure 4.5. *FGFR1*⁺ cells induce colony-formation. **A)** Schematic representation of the experimental procedure. hGBM L0 stained with *FGFR1* antibody are isolated by FACS, into *FGFR1*⁺ and *FGFR1*⁻ cells and immediately plated for CFC assay (Image created with biorender.com). **B)** Histogram representing the gating strategy to sort *FGFR1*⁺, *FGFR1*⁻ and the isotype control. **C)** *FGFR1*⁺/⁻ were plated in collagen matrix in three different concentrations: 2,500/1,250 and 750 cells per well. Cells were fed twice a week with growth factors and the number of colonies per well quantified 14 days after plating. *FGFR1*⁺ have greater clonogenicity (hGBM L0 n=7, two-way ANOVA, Sidak's multiple comparisons test). Data are mean \pm SEM. **D)** Representative image of hGBM L0 CFC in both populations and in the three different plating densities. Scale bar = 2 mm. "n" indicates the number of independent experiments (biological replicates).

4.3.4 *FGFR1* knockdown increases survival of tumour-bearing mice

To our knowledge, currently there are no studies that specifically describe and compare the tumorigenic function of *FGFR1-3* *in vivo*. Therefore, to assess the biological impact of these receptors in tumour progression and survival, we used GBM xenograft mouse models. Primary patient-derived GBM cells were transduced with *FGFR1-3* knockdown (or shControl) lentiviral particles. GFP positive cells were purified and intracranially implanted into immune-compromised Fox-Chase SCID mice. Mice reaching the defined endpoint criteria were culled (see section 2.10 for more details), and tissue harvested for histological analysis. Percent survival of mice bearing tumours derived from sh*FGFR1-3* hGBM cells was examined, and mouse brain tissue sections analysed by immunofluorescence staining (**Figure 4.6A**).

We initially compared survival time of mice transplanted with hGBM L0, L1 and L2 cells. Our results identified hGBM L1 as the most aggressive cell line as mice bearing hGBM L1 tumours died 30 - 35 days post transplantation (**Figure 4.6B**). Mice implanted with hGBM L2 cells had the longest survival ranging from 50 - 70 days (**Figure 4.6B**). These cell lines were previously used in xenograft models by Siebzehnruhl *et al.* who demonstrated that hGBM L2 was an invasive cell line (Siebzehnruhl *et al.* 2013). As we aimed to investigate invasion index of sh*FGFR1-3* tumours, we selected the most invasive hGBM cell line, hGBM L2, for our xenograft models.

Mean fluorescence intensity (MFI) was quantified in sh*FGFR1*/shControl tumour sections to assess *FGFR1* knockdown efficiency. *FGFR1* MFI was 61% lower in patient-derived GBM sh*FGFR1* cells than in the control (**Figure 4.6C** and **Figure 4.6D**). Our results demonstrate a significant increase in survival of mice implanted with sh*FGFR1*#1 and sh*FGFR1*#2 hGBM cells compared to control mice (**Figure 4.6E**). Mice implanted with sh*FGFR1*#1 hGBM survived longer than those implanted with sh*FGFR1*#2, which is consistent with our previous sphere and colony-forming data where we already demonstrated a higher knockdown efficiency of this clone. In line with these results, hGBM L0 sh*FGFR1*#1 also showed a significant improvement in survival compared to controls (**Figure 4.6F**). Together, these data identify *FGFR1* as a crucial receptor regulating tumour progression.

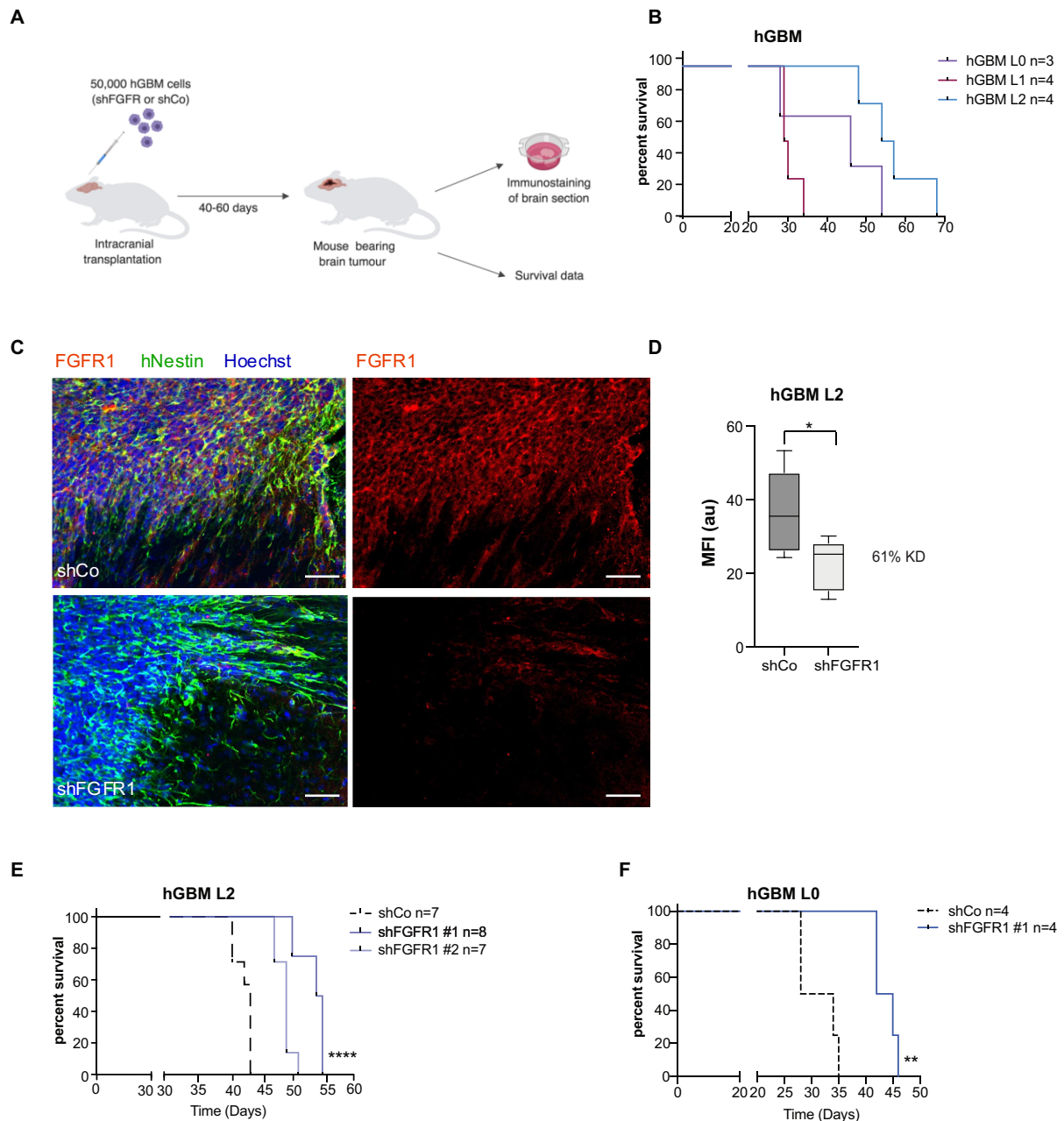


Figure 4.6. *FGFR1* knockdown increases survival of tumour-bearing mice. **A)** Schematic representation of intracranial transplantation of hGBM cells transduced with shFGFR1-3 (or shCo) constructs. 50,000 cells were transplanted in a volume of 5 μ L per mouse. Mice started showing neurological symptoms 40-60 days after transplantation depending on cell line. Brain tissue sections were analysed by immunostaining and survival was examined by Kaplan-Meier analysis (Image created with biorender.com). **B)** Kaplan-Meier curves of mice bearing tumours derived from hGBM L0 (n=3, median survival 46 days), hGBM L1 (n=4, median survival 29.5 days) and hGBM L2 (n=4, median survival 55.5 days) were compared. **C)** Immunofluorescence shows *FGFR1* is absent in *FGFR1* knockdown tumours (lower panels) compared to control sections (upper panels). **D)** Knockdown of *FGFR1* (61%) was quantified by measuring the MFI of shCo and shFGFR1 stained sections (n=3, unpaired t-test). Scale bar = 100 μ m (Immunofluorescence analysis performed by Nawal Alshahrany, MSc Student from the lab). **E)** Orthotopic implantation of shFGFR1#1-hGBM L2 (n=7, median survival=54.5 days) and shFGFR1#2-hGBM L2 (n=8, median survival 49 days) cells increased survival time of tumour-bearing mice compared to controls (n=7, median survival 43 days). **F)** Orthotopic implantation of shFGFR1#1-hGBM L0 (n=4, median survival 43.5 days) also showed significant survival benefits compared to controls (n=4, median survival 31 days). “n” indicates the number of independent experiments (biological replicates). Statistical analysis for survival data: Long-rank test.

On the other hand, immunofluorescence of shFGFR2 hGBM L2 tumour sections, showed a *FGFR2* knockdown efficiency of 55% (**Figure 4.7A** and **Figure 4.7B**). An evaluation of *FGFR3* staining in shFGFR3 tumour sections was not possible as we did not have a suitable anti-*FGFR3* antibody for immunostaining analysis. Our results indicate that *FGFR2* knockdown increased median survival time in mice (**Figure 4.6C**). No survival benefit was seen after *FGFR3* knockdown compared to the control group (**Figure 4.7D**). Finally, to verify that the transplantation technique was successful, we transplanted shZEB1 hGBM cells. In line with the data from Siebzehnruhl *et al.*, our results showed a significant increase in survival after *ZEB1* loss (**Figure 4.7E**) (Siebzehnruhl *et al.* 2013).

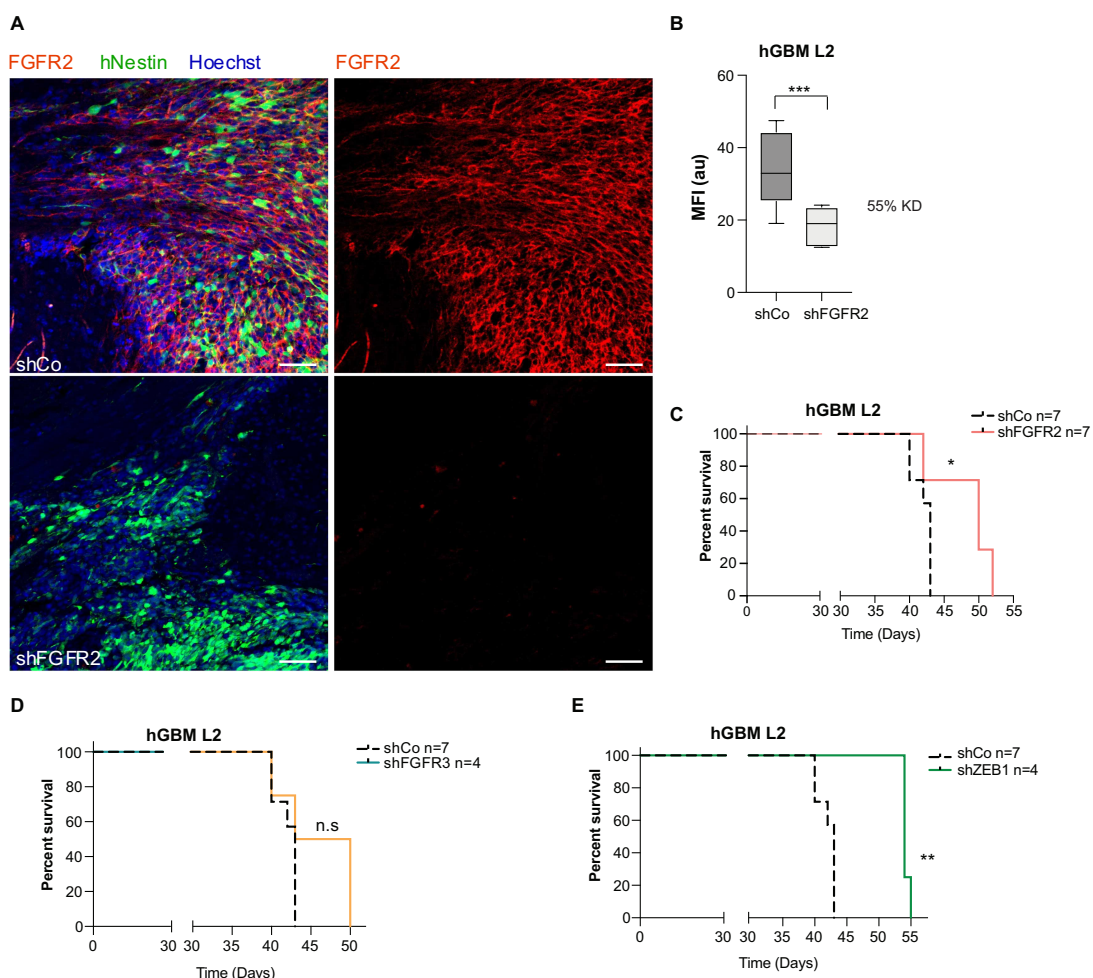


Figure 4.7. *FGFR2* and *FGFR3* knockdown effects on survival of tumour-bearing mice. A) Immunofluorescence shows *FGFR2* is absent in *FGFR2* knockdown tumours (lower panels) compared to control sections (upper panels). Scale bar 100 μ m (Immunofluorescence analysis performed by Nawal Alshahrany MSc Student from the lab). **B)** Knockdown of *FGFR2* (55%) was quantified by measuring the MFI of shCo and shFGFR2 sections (n=3, unpaired t-test). **C)** Orthotopic implantation of shFGFR2-hGBM L2 cells increased survival of tumour-bearing mice (n=7, median survival 50 days, shCo n=7, median survival 43 days), while **D)** shFGFR3-hGBM L2 cells transplantation had no effect on mice survival (n=4, median survival 46.5 days). **E)** Significant results were also obtained from shZEB1 transplantations (n=4, median survival 54 days). “n” indicates the number of independent experiments (biological replicates). Statistical analysis for survival data: Long-rank test.

4.3.5 Limiting dilution orthotopic xenografts indicate FGFR1 is enriched in GSCs

Our previous *in vivo* results identified FGFR1 as a marker of tumour progression and survival in GBM. To investigate whether this receptor is also functionally associated with GSC self-renewal and tumour-formation capacity, we performed *in vivo* limiting dilution cell transplantation assays (LDA) using shFGFR1 hGBM cells. LDA is an experimental technique used to determine the proportion of GSCs, or GSC frequency, in the total population of cancer cells (Richichi *et al.* 2016). To calculate GSC frequency, different cell numbers are implanted into immunocompromised mice, expecting a correlation between the number of implanted cells and the number of mice bearing tumours (Al-Hajj *et al.* 2003). One of the first studies using this approach in brain cancer xenografts was Singh *et al.* (Singh *et al.* 2004). Subsequent studies have used LDA to identify GSCs *in vivo* (Deleyrolle *et al.* 2011; Siebzehnrubl *et al.* 2013; Richichi *et al.* 2016).

We performed orthotopic implantations of FGFR1 knockdown and control cells in three different groups of mice: a first group implanted with 50,000 cells, a second one with 10,000 cells and the last one with 1,000 cells (**Figure 4.8A**). hGBM L0 cells were selected for this experiment because this cell line shows greater expression of FGFR1 compared to hGBM L1 and hGBM L2 (FACS plots **Figure 3.6**). Numbers of mice bearing tumours were quantified, and stem cell frequency was analysed by extreme limiting dilution analysis (ELDA) (Hu and Smyth 2009) (**Figure 4.8A**). Our results demonstrate an approximate 6-fold decrease in GSC frequency after *FGFR1* knockdown. To complement this data, we also used limiting dilution orthotopic xenografts to determine the stem cell frequency of FGFR1+ and FGFR1- cell populations. hGBM L0 cells were stained for FGFR1, FACS-purified and immediately transplanted into mice as described in **Figure 4.8C**. ELDA of tumour-formation demonstrated an approximate 5-fold enrichment of GSCs in FGFR1+ cells (**Figure 4.8D**). Together, these data strongly support that FGFR1 induces GSC self-renewal and tumour initiation capacity.

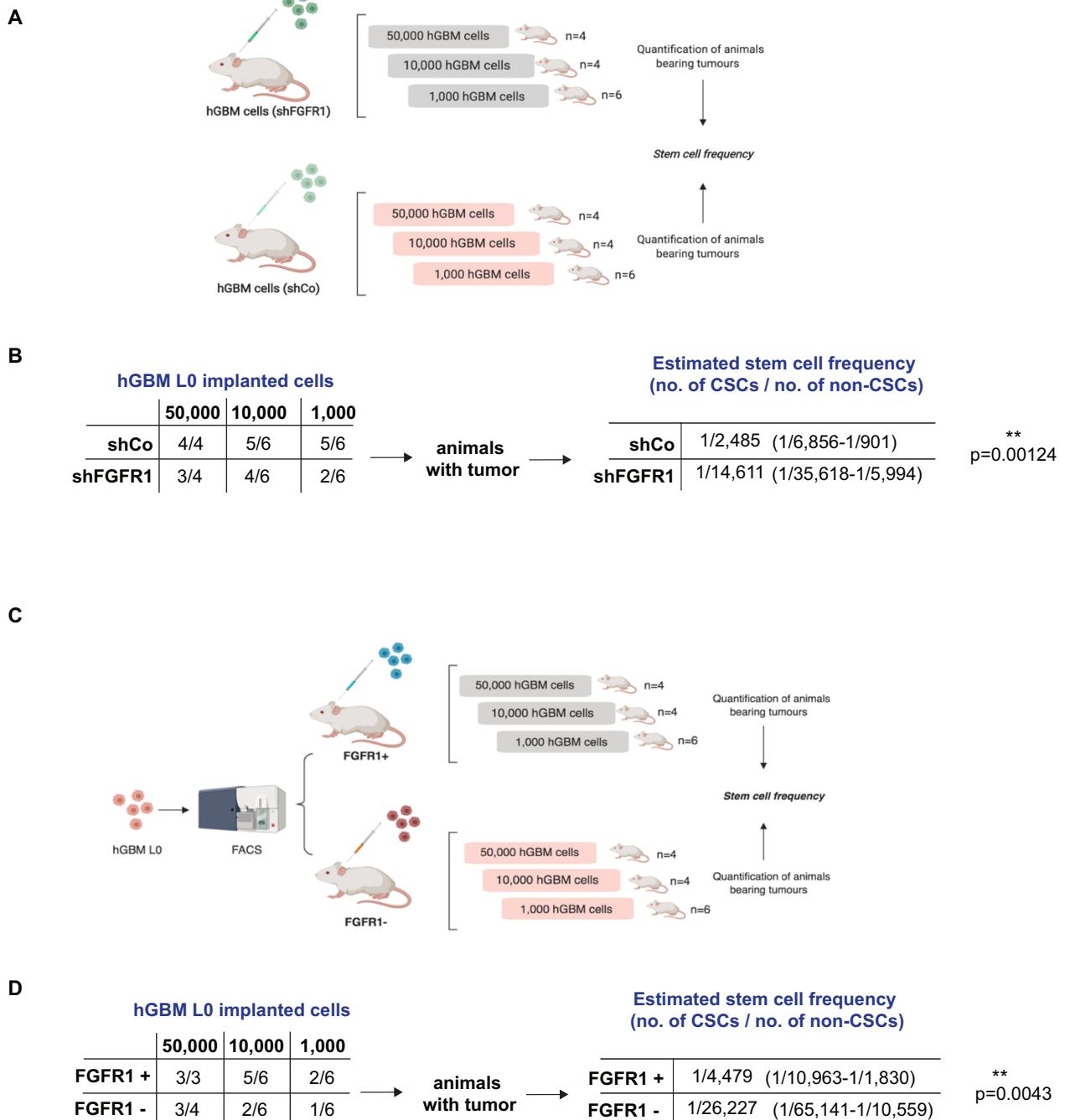


Figure 4.8. Limiting dilution orthotopic xenografts. A) Schematic representation of LDA xenografts of shFGFR1 (green cells) and shCo (light green cells) hGBM L0 cells. Immunocompromised mice were implanted with three different concentrations of shFGFR1 (or shCo) cells: 50,000/10,000/1,000 cells (n=4, n=6 and n=6 respectively). Cells were intracranially implanted in a volume of 5 μ L. Number of mice bearing tumours was quantified. Estimated stem cell frequency (number of GSCs per number of non-GSCs) and lower and upper stem cell frequency confidence intervals (in brackets) are indicated in B) and D) right panel. **B)** GSC frequency was significantly higher in shCo (~ 1 GSC per 2,485 cancer cells) compared to shFGFR1 (~ 1 GSC per 14,611 cancer cells). **C)** Schematic representation of LDA xenografts of hGBM L0 cells sorted for FGFR1+ (blue cells) and FGFR1- (red cells). **D)** GSC frequency of FGFR1+ cells (~ 1 GSC per 4,479 cancer cells) was significantly higher than in the FGFR1- population (~ 1 GSC per 26,227 cancer cells). Stem cell frequency was calculated using ELDA. Chi square test was used to assess the differences in stem cell frequencies between groups. “n” indicates the number of independent experiments (biological replicates). A) and C) were created with biorender.com.

4.3.6 *FGFR1* expression correlates with poor patient outcome in GBM

We next used Kaplan-Meier analysis of the TCGA Glioblastoma Multiforme (provisional) dataset to further investigate which FGFR may be most relevant for patient outcome. This analysis confirmed that high expression of *FGFR1* is associated with poor outcome (**Figure 4.9A**), while for *FGFR2* the relationship was inverse with augmented *FGFR2* expression correlating to a better prognosis (**Figure 4.9B**). No significant correlation was apparent for *FGFR3* and patient survival (**Figure 4.9C**). Although we excluded *FGFR4* from our analysis, we assessed its impact in patient outcome. In line with *FGFR3* data, *FGFR4* had no significant effect (**Figure 4.9D**). These findings support our *in vivo* data, where mice implanted with *FGFR1* knockdown cells showed longer survival than the controls and further highlight the crucial role of this receptor in patient outcome.

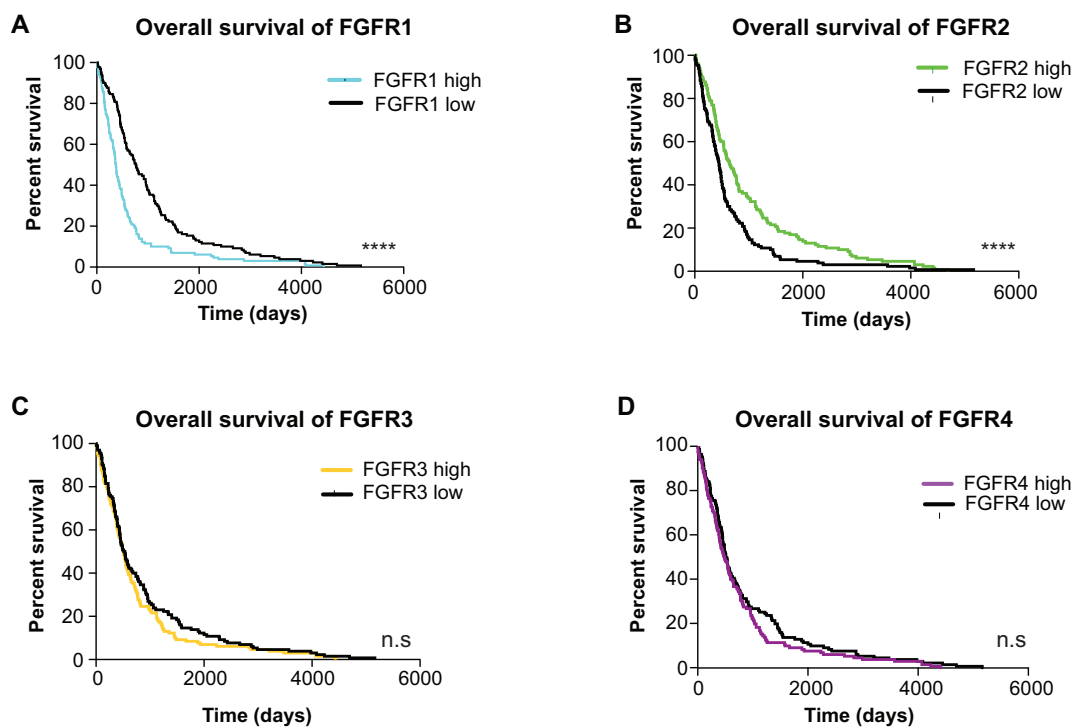


Figure 4.9. Correlation of *FGFR* expression with patient survival. Kaplan-Meier analysis of TCGA GBM data (n=260), stratified for above-median (high) or below-median (low) gene expression shows a significantly poorer survival in **A**) *FGFR1* high tumours, but **B**) increased survival of *FGFR2* high tumours. **C**) *FGFR3* and **D**) *FGFR4* expression has no effect on survival. Median survival per group in days: *FGFR1* high=375; *FGFR1* low=771 d; *FGFR2* high=648 d; *FGFR2* low=448 d; *FGFR3* high=506 d; *FGFR3* low=535 d; *FGFR4* high=492 d; *FGFR4* low=532 d. Statistical analysis: Log Rank Test. Bioinformatic analysis performed by Dr Daniel J. Silver (Cleveland Clinic). “n” indicates the number of independent experiments (biological replicates).

4.3.7 *FGFR1* knockdown reduces invasion in GBM xenografts

Factors regulating cell adhesion molecules, ECM and cytoskeletal remodelling are crucial for glioma invasion (Brabletz and Brabletz 2010). ZEB1 is one of the key determinants regulating invasion and it is highly expressed in the invasion front of the tumour (Siebzehnruhl *et al.* 2013). In addition, SOX2 and OLIG2 are also important factors associated with GSC migration (DeCarvalho *et al.* 2010; Singh *et al.* 2016). As we have previously showed that FGF2 promotes the expression of ZEB1, SOX2 and OLIG2 and regulates stemness through FGFR1, we hypothesised that FGFR1 may also be associated with invasive phenotypes in GBM. Immunostaining of shFGFR1, shFGFR2, shFGFR3 and control tumours was performed to assess tumour morphology and invasion. To facilitate tumour visualization and invasion quantification, grayscale fluorescence images were inverted into black (tumour mass) on white. **Figure 4.10A** shows representative images of mouse brain sections containing FGFR1-3 knockdown tumours compared to control. A clear tumour mass integrated in the brain parenchyma was appreciated in shFGFR2, shFGFR3 and control tumours. However, shFGFR1 hGBM cells only formed small tumours in the vicinities of the ventricular area and close to the implantation site. To compare invasive characteristics among tumours, the ratio of the squared perimeter distance over the area (P^2/A) per section was calculated. This formula produces a dimensionless number ('Invasion Index') that has been previously used to quantify GBM invasion and dispersal in xenografts (Siebzehnruhl *et al.* 2013; Hoang-Minh *et al.* 2018). Only tumours growing within the brain parenchyma were quantified as "invasive and integrated tumour" areas as described in section 2.14. **Figure 4.10B** shows individual values for each of the sections stained per brain. Our data demonstrated that FGFR1 knockdown significantly reduced GBM invasion compared to shFGFR2, shFGFR3 and control xenografts (**Figure 4.10C**). Taken together these finding suggests that FGFR1 may confer GSCs with invasive characteristics.

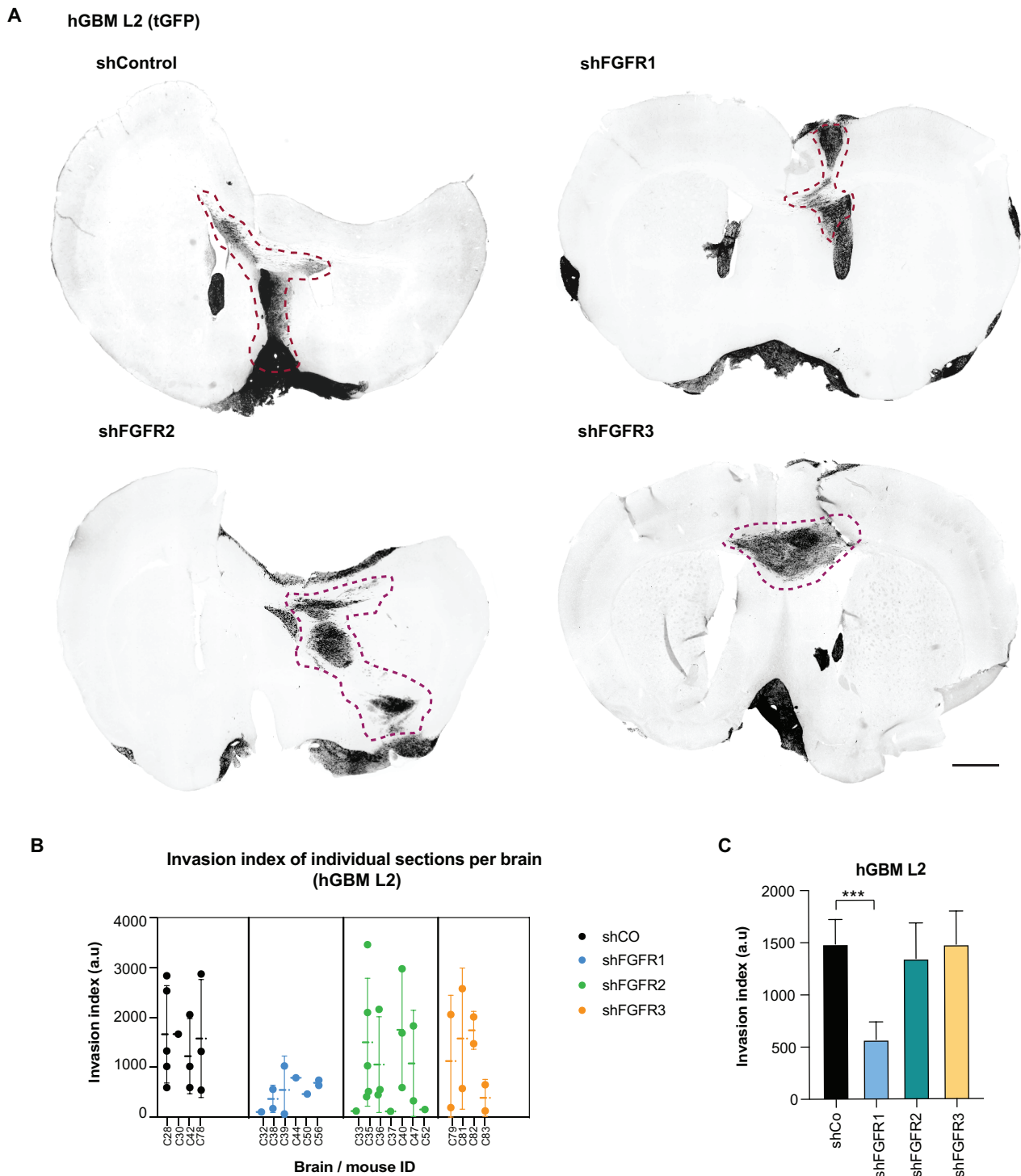


Figure 4.10. *FGFR1* knockdown reduces tumour invasion. A) Representative images of shFGFR1 (upper-right), shFGFR2 (lower-left), shFGFR3 (lower-right), shControl (upper-left) tumours stained with GFP to boost the fluorescence signal of the GFP-expressing implanted cancer cells. Fluorescence images were inverted to single-colour black on white. Outline of a tumour mass (black) highlighted by dashed red lines. Representative scale bar 1mm applies to all images. **B)** Graph showing individual invasion indices of all stained sections (y axis) per group (x axis represents the brain/mouse ID): shCo (black), shFGFR1 (blue), shFGFR2 (green), shFGFR3 (orange). Dots correspond to individual stained sections per brain. Only invasive sections per brain were analysed. Solid line represents confidence interval and mean. **C)** Average invasion index across all quantified sections demonstrates that only *FGFR1* knockdown significantly reduces invasion. shCo n=4, shFGFR1 n=6, shFGFR2 n=7, shFGFR3 n=5. Statistical analysis: Data are mean \pm SEM, one-way ANOVA, Dunnett's multiple comparisons test. "n" indicates the number of independent experiments (biological replicates).

4.4 Discussion

In this chapter, we perform a comprehensive analysis of the biological impact of *FGFR1*, *FGFR2* and *FGFR3* knockdowns in GBM. We examine the sphere-forming and clonogenicity capacity of these cells *in vitro* and their invasive, tumour-formation and tumour progression characteristics *in vivo*. We also study these features in *FGFR1+* and *FGFR1-* sorted cells and use TCGA dataset analysis to examine the association of each FGFR with patient survival.

The FGF2-FGFR pathway is involved in the activation of mitogenic, anti-apoptotic and invasive cell responses crucial for GBM progression (Yamada *et al.* 1999; Dienstmann *et al.* 2014). However, less is known about the specific mechanisms involved in FGF2-FGFR-mediated GSC regulation. Our data demonstrate that *FGFR2* knockdown does not affect GSC sphere-forming capacity, while the effect of *FGFR3* loss is cell line dependent. The latter could be the result of heterogeneous expression of *FGFR3*, differences in *FGFR3* splicing variants and/or possible mutations of this receptor among cell lines which would be interesting to investigate further. Importantly, *FGFR1* knockdown reduced sphere-forming capacity in every hGBM cell line tested. This data was corroborated by a recent study from Kowalski-Chauvel *et al.* who showed that both $\alpha 6$ integrin and *FGFR1* knockdown reduced sphere numbers in two primary patient-derived GBM lines (Kowalski-Chauvel *et al.* 2019). Nonetheless, this study lacks a combination of experimental approaches such as; colony forming assay, rescue experiments and *in vivo* models required to validate its results. We therefore showed that *FGFR1* knockdown not only decreases sphere-forming capacity, but also colony-forming features of hGBM cells. In addition, to further substantiate the pivotal role of *FGFR1* in GSC regulation we rescued this phenotype by overexpressing *FGFR1*. Finally, we demonstrated that FGF2 treatment induced sphere-forming capacity of sh*FGFR2* and sh*FGFR3* but not sh*FGFR1* hGBM cells, which corroborated FGF2-FGFR1-mediated sphere-formation response.

On the other hand, inhibition of FGFR signalling has been linked to an anti-proliferative function in cancer (Brooks *et al.* 2012). In GBM, *FGFR1* expression was associated with an increase in cell proliferation (Stachowiak *et al.* 1997; Loilome *et al.* 2009; Kowalski-Chauvel *et al.* 2019), but whether other FGFRs also contributed to this

function was not directly tested by these studies. Our results identified FGFR1 as a potential translator of FGF2 cues in hGBM cell proliferation, while FGFR2 and FGFR3 did not have a significant impact. Ohashi *et al.* suggested a link between tumours with higher expression of FGFR2 and significantly less proliferation as identified by Ki-67 staining (Ohashi *et al.* 2014). Nevertheless, a direct link with FGFR2 signalling was not clearly described. Another study analysing glioma TCGA data identified a negative correlation between *FGFR3* expression and genes associated with mitosis and cell cycle (Wang *et al.* 2016). Therefore, further work (e.g. BrdU *in vivo* experiments) needs to be performed to understand the role of FGFR2 and FGFR3 in GBM growth and proliferation.

In addition, FGFR1 signalling has been associated with higher glioma grade, malignancy and radioresistance (Yamaguchi *et al.* 1994; Gouazé-Andersson *et al.* 2016). Using GBM xenografts from FGFR1 knockdown hGBM cells, we demonstrated that loss of *FGFR1* reduces tumour growth and increases mice survival. Furthermore, our results from Kaplan-Meier analysis of the TCGA GBM data indicate that *FGFR1* is related with poorer patient survival. These findings are consistent with previous studies that identified *FGFR1* as a prognostic factor for overall survival and progression duration in GBM patients (Ducassou *et al.* 2013). On the other hand, an inverse correlation between *FGFR2* expression and glioma grade has been described (Ohashi *et al.* 2014). Renu *et al.* demonstrated *FGFR2* was depleted in at least a third of the GBM samples in the TCGA dataset which also coincided with *PTEN* deletion (Renu *et al.* 2015). These deletions are associated with loss of Chr. 10q which is described as unfavourable prognosis factor (Daido *et al.* 2004). Similarly, our TCGA data analysis demonstrated a link between high levels of *FGFR2* and improved patient survival. By the contrary, our FGFR2 knockdown xenografts resulted in increased survival compared to control mice. Therefore, further work is required to understand the role of FGFR2 signalling in GBM tumorigenesis. In contrast, we showed no change in the survival of immunocompromised mice transplanted with FGFR3 knockdown. This is in line with our analysis of TCGA GBM data, which demonstrated that *FGFR3* had no impact on overall survival in glioma patients.

Functionally, FGFR1 expression in malignant glioma has been associated with increased migration of cancer cells (Fukai *et al.* 2008; Gouazé-Andersson *et al.* 2018).

In addition, we demonstrated that *FGFR1* loss also results in reduced tumour invasion *in vivo*. Despite *FGFR2* promoting migration and invasion in other cancers (Nomura *et al.* 2008; Stehbens *et al.* 2018; Kim *et al.* 2019), to our knowledge no studies ascribe this function to *FGFR2* in GBM as yet. Our results demonstrate that *FGFR2* signalling is not associated with GBM invasion *in vivo*. On the other hand, a recent study investigating gene expression using single-cell RNA-Seq in GBM patient samples found that *FGFR3* levels were five-fold higher in infiltrative GBM cells compared to the tumour core (Darmanis *et al.* 2017). While this may suggest an association of *FGFR3* with tumour invasion, it is not known if this receptor functionally promotes this function in GBM. Complementary to our *FGFR2* data, our results showed no effect in invasion of *FGFR3* knockdown tumours. Nonetheless, it remains to be tested whether this lack of effect is cell line specific.

As the findings described in this section outline a crucial role of *FGFR1* in GBM progression and since to our knowledge no current studies investigate cell surface expression of *FGFR1* as possible GSC marker, we further examined whether this receptor could be used to enrich GSCs. We employed limiting dilution assays of *FGFR1+* and *FGFR1-* sorted cell populations *in vitro* and *in vivo*. Our results demonstrated *FGFR1+* cells showed higher colony-forming capacity *in vitro* and increased tumour-formation capacity *in vivo* compared to cells negative for *FGFR1*. These findings are consistent with an enrichment of GSCs in *FGFR1+* cells, which is confirmed by the higher stem cell frequency in this population analysed by ELDA software.

On the other hand, our western blot data analysis indicates that *FGFR1* knockdown increased *FGFR2* levels which suggests that *FGFR1* may promote the growth of more aggressive tumours by inhibiting *FGFR2* expression. Crosstalk between different tyrosine kinase receptors has been described in GBM and other cancers (Huang *et al.* 2007; Ware *et al.* 2013; Tiash and Chowdhury 2015). Nonetheless, to our knowledge crosstalk between *FGFR* subtypes has not been identified in gliomas. To assess whether *FGFR1* actually regulates *FGFR2*, overexpression and rescue experiments will be needed. As an example, a reduction in *FGFR2* levels in *FGFR1* overexpressing cells and in sh*FGFR1* cells transduced with *FGFR1* expression constructs would be expected. Moreover analysis of the cell surface *FGFR* expression patterns in *FGFR1-*

3 sorted populations and FGFR1-3 knockdown cells by flow cytometry would help to understand the complex interaction between FGFRs in GBM.

In conclusion, we performed a comprehensive analysis of the functions of FGFR1-3 in GBM and outlined FGFR1 as important regulator of tumour progression, proliferation, invasion and tumour-formation in GBM (**Figure 4.11**). Whether this receptor is associated with key GSC/stemness-related transcription factors will be tested in the next chapter.

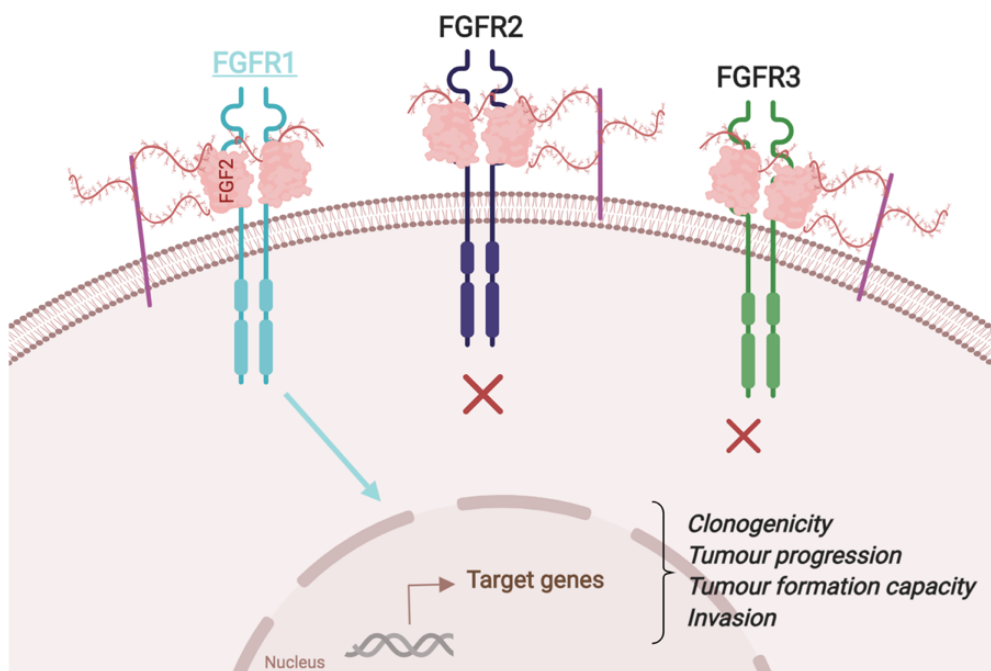


Figure 4.11. Diagram depicting the role of FGFR1-3 in GSCs. FGFR1 promotes the activation (represented by a blue arrow) of downstream targets and genes associated with stemness, invasion, tumour progression and formation. FGFR2 and FGFR3 are not involved (represented by red crosses) in the regulation of these cell responses. Image created with biorender.com

Chapter 5: FGF2 signals through FGFR1 and ERK1/2 to regulate stemness-associated transcription factors

5.1 Introduction

Extracellular stimuli are received at the cell surface, and transduced into specific cellular responses through the activation of an extensive network of signalling pathways (Lake *et al.* 2016). Tyrosine kinase receptors act as mediators and translators of these cues by the phosphorylation of their cytoplasmatic tyrosine kinase domain. For this to happen, the hydroxyl group of the tyrosine residues receives a γ -phospho group from ATP, which triggers subsequent phosphorylation events on downstream targets (Lew *et al.* 2009; Touat *et al.* 2015). Among the tyrosine receptor kinase family, FGFRs orchestrate the activation of multi-protein complexes associated with cell proliferation, survival, cytoskeletal regulation and receptor degradation (Tiong *et al.* 2013). FGFR-mediated cell survival is mainly promoted by the activation of PI3K/AKT and STATs signalling (Porębska *et al.* 2018), while RAC/JNK/p38 and RAS/MEK/MAPK signalling pathways are relevant for cell proliferation (Beenken and Mohammadi 2009; Porębska *et al.* 2018).

Tyrosine kinase receptor aberrations lead to the constitutive activation of these pathways resulting in abnormal cellular responses associated with tumorigenesis (Soni *et al.* 2005). The RAS signal-regulated kinases, ERK1/2 and PI3K/AKT, are two of the main hyperactivated pathways in GBM (Holland *et al.* 2000; Hannen *et al.* 2017). Holland *et al.* demonstrated that constitutive activation of Ras/Akt (using lentiviral vectors encoding for the mutant form of K-Ras, RCAS-*Kras*) induced malignant transformation of neural progenitors into high-grade gliomas (Holland *et al.* 2000). On the other hand, the ERK1/2-dependent RAF/MEK pathway, is associated with mesenchymal subtypes in GBM (Brennan *et al.* 2013), with its inhibition being linked to differentiation of GSCs and a decrease in MGMT expression (Yang *et al.* 2008; Soeda *et al.* 2009; Sato *et al.* 2011). Importantly, dual inhibition of ERK1/2 and PI3K/AKT reduces sphere-formation *in vitro* and tumour-formation *in vivo* (Sunayama *et al.* 2010).

STAT3 is also associated with maintenance of GSCs (Chang *et al.* 2017), as its knockout reduces clonogenicity capacity (Xie *et al.* 2019). Furthermore, STAT3 is a marker of poor prognosis in GBM as it promotes invasion, anti-apoptosis and GBM progression (Gong *et al.* 2015; Chang *et al.* 2017). The role of p38 in GSC regulation

is more controversial. Some studies describe p38 as a tumour suppressor (Frey *et al.* 2006; Han and Sun 2007), while others associate p38 inhibition with a decrease of GSC proliferation and a regulation of their transient amplifying state (Soeda *et al.* 2017).

Due to these signalling pathways being crucial for GSC maintenance, along with our previous demonstration that FGFR1 is the only FGFR associated with stemness in GBM, we sought to assess how FGFR1 regulates stemness-associated transcription factors and identify the downstream signalling pathway(s) involved in FGFR1-mediated GSC control.

5.2 Aims and objectives:

1. To investigate whether FGFR1 regulates ZEB1, SOX2 and OLIG2 expression in hGBM cells.
2. To examine which intracellular signalling pathways are activated after FGF2 treatment
3. To study FGFR1-mediated signalling pathways by performing phospho-western blot analysis in FGFR1 knockdown cells.

5.3 Results

5.3.1 FGFR1 regulates stem cell transcription factors in GBM.

Previous chapters demonstrated that FGF2-FGFR1 regulates GSCs and that FGF2 induces the expression of ZEB1, SOX2 and OLIG2. We next investigated whether expression of this triad of stemness-associated transcription factors is mediated by FGFR1. Western blot analysis of FGFR1 knockdown cell lysates shows a decrease in the protein levels of ZEB1, SOX2 and OLIG2 compared to control cells (**Figure 5.1A** and **Figure 5.1C**). We further demonstrated that hGBM cells transduced with a full-length FGFR1 overexpression construct exhibit increased levels of these transcription factors compared to cells transduced with an empty vector (**Figure 5.1B** and **Figure 5.1C**).

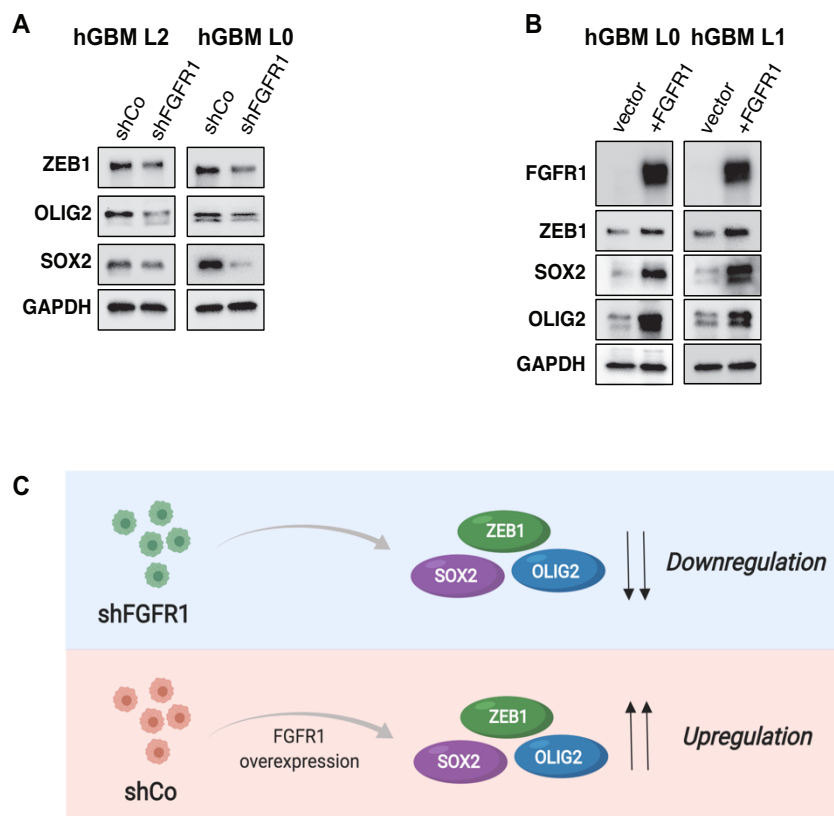


Figure 5.1. FGFR1 knockdown decreases ZEB1,SOX2 and OLIG2 expression while the inverse effect is seen after FGFR1 overexpression. A) Knockdown FGFR1 hGBM L2 and hGBM L0 cells were treated with 30 ng/mL FGF2 (+EGF/heparin) for 48 h. Cell lysates of these cells were subjected to immunoblot analysis with ZEB1, SOX2 and OLIG2 antibodies. GAPDH was used as loading control. **B)** hGBM L0 and hGBM L1 cells were transduced with full-length FGFR1 expression or control lentiviral particles and subsequently treated with 30 ng/mL FGF2 (+EGF/Heparin) for 48h. Cell lysates of these cells were subjected to immunoblot analysis with the indicated antibodies from A) including FGFR1. **C)** Schematic representation of the conclusion from A) and B) (Image created with biorender.com).

To verify that ZEB1, SOX2 and OLIG2 are downstream targets of *FGFR1*, we performed rescue experiments with *FGFR1* knockdown and ZEB1 knockdown hGBM cells. Considering that Singh *et al.* demonstrated a cross-regulation interdependency between these transcription factors in GSCs (Singh *et al.* 2017), we selected ZEB1 knockdown for our rescue experiments hypothesising that shSOX2 and shOLIG2 would have similar effects. We find that *FGFR1* overexpression rescues ZEB1, SOX2 and OLIG2 protein levels in *FGFR1* knockdown cells (**Figure 5.2A**). Importantly, *FGFR1* overexpression is not sufficient to fully rescue the expression of these transcription factors in cells carrying a ZEB1 knockdown (**Figure 5.2A**). In view of the fact that ZEB1, SOX2 and OLIG2 are associated with self-renewal and stemness we also performed sphere-forming assay experiments. Similarly, our data indicates an increase in sphere-forming capacity in control cells transduced with *FGFR1* overexpression, while this phenotype could not be rescued after ZEB1 loss (**Figure 5.2B** and **Figure 5.2C**). This indicates that ZEB1 is downstream of *FGFR1*.

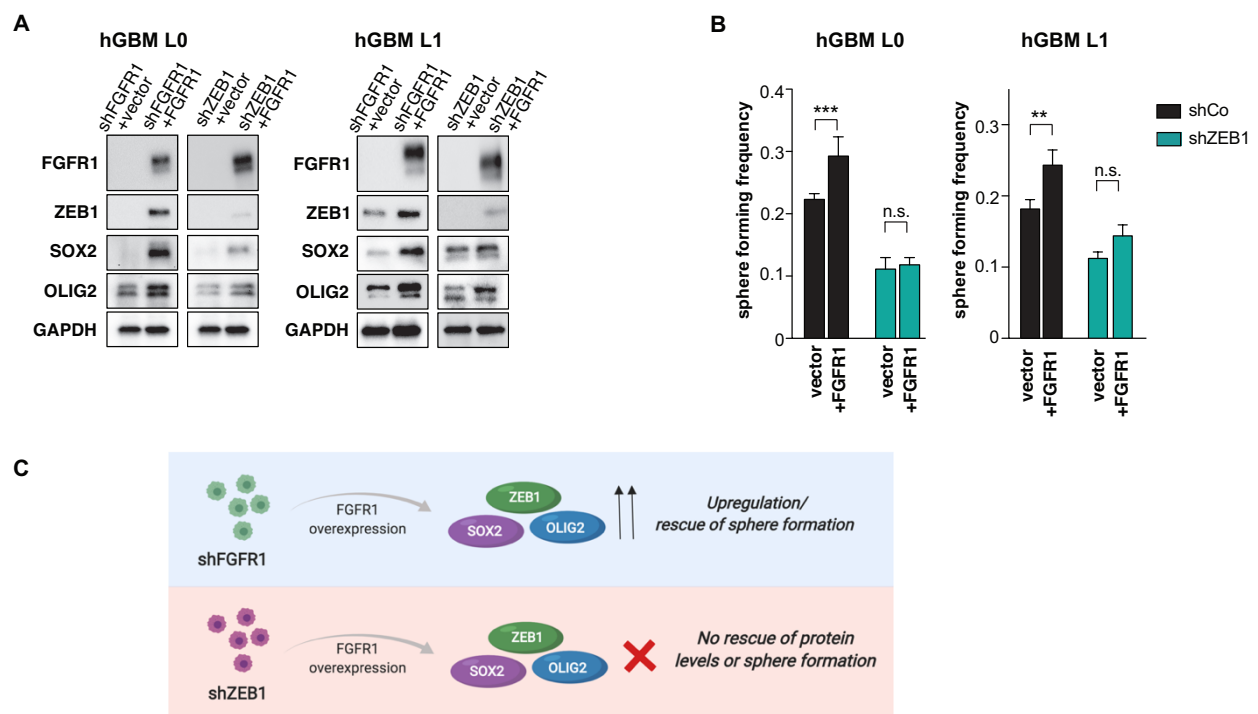


Figure 5.2. ZEB1, SOX2 and OLIG2 expression in *FGFR1* knockdown cells is rescued after *FGFR1* overexpression. A) shFGFR1 and shZEB1 hGBM L0 and hGBM L1 cells were transduced with an empty vector (control) or and *FGFR1* overexpression construct. Cell lysates were subjected to immunoblot analysis with the indicated antibodies. GAPDH was used as loading control. The expression of these transcription factor is rescued after *FGFR1* expression in shFGFR1 cells but not after ZEB1 loss. **B)** control (black bars) and shZEB1 (green bars) hGBM L0 and hGBM L1 cells were transduced with an empty vector (control) or and *FGFR1* overexpression construct. Sphere-formation could not be rescued in ZEB1 knockdown cells. Number of spheres was quantified 5 days after plating (hGBM L0 n=9, hGBM L1 n=9, two-way ANOVA). Data are mean \pm SEM. **C)** Schematic representation of conclusions from A) and B) (Image created with biorender.com).

Finally, we investigated the expression of these transcription factors in FGFR1⁺ and FGFR1⁻ cell populations. Our results indicate that FGFR1⁺ cells show greater enrichment for ZEB1, SOX2 and OLIG2 at the protein level compared to the FGFR1⁻ population (**Figure 5.3A** and **Figure 5.3B**). Together, this data strongly supports that ZEB1, SOX2 and OLIG2 are downstream targets of FGF2/FGFR1 signalling.

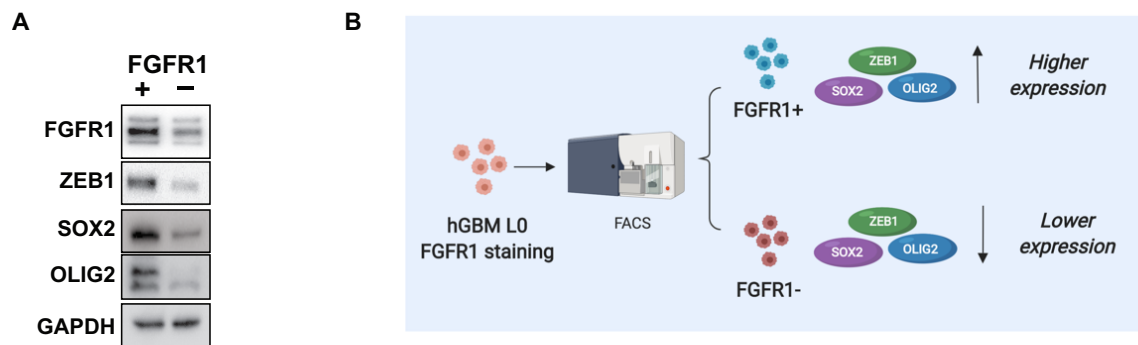


Figure 5.3. FGFR1 is endogenously associated with a stem cell population. A) Extracellular FGFR1 staining was performed in hGBM L0 cells. FGFR1⁺ and FGFR1⁻ cells were lysed immediately after cell sorting and lysates were subjected to immunoblot analysis with the indicated antibodies. GAPDH was used as loading control. FGFR1⁺ cells express higher levels of FGFR1, ZEB1, SOX2 and OLIG2. **B)** Schematic representation of experimental procedure and results (Image created with biorender.com).

5.3.2 ERK1/2, STAT3 and p38 phosphorylation increases after FGF2 stimulation

We next sought to investigate which intracellular signalling pathways are activated through the FGF2-FGFR1 axis in hGBM cells. In order to simultaneously analyse different pathways, we use a PathScan Intracellular Signalling Array. This kit allows for the detection of 18 well-characterised signalling molecules that are phosphorylated or cleaved by a wide range of extracellular signals (e.g. growth factors, cytokines, hormones). The PathScan is a slide-based antibody array and follows the same principle as a dot blot assay (**Figure 5.4A**). Each slide contains 8 different squares coated with nitrocellulose where 18 phospho-antibodies are spotted in duplicates. **Figure 5.4A**, shows a graph with the 18 signalling pathways targeted in this array, with numbers indicating the position of each targeted molecule on the slide. Number 1 and 2 represent positive and negative controls, respectively.

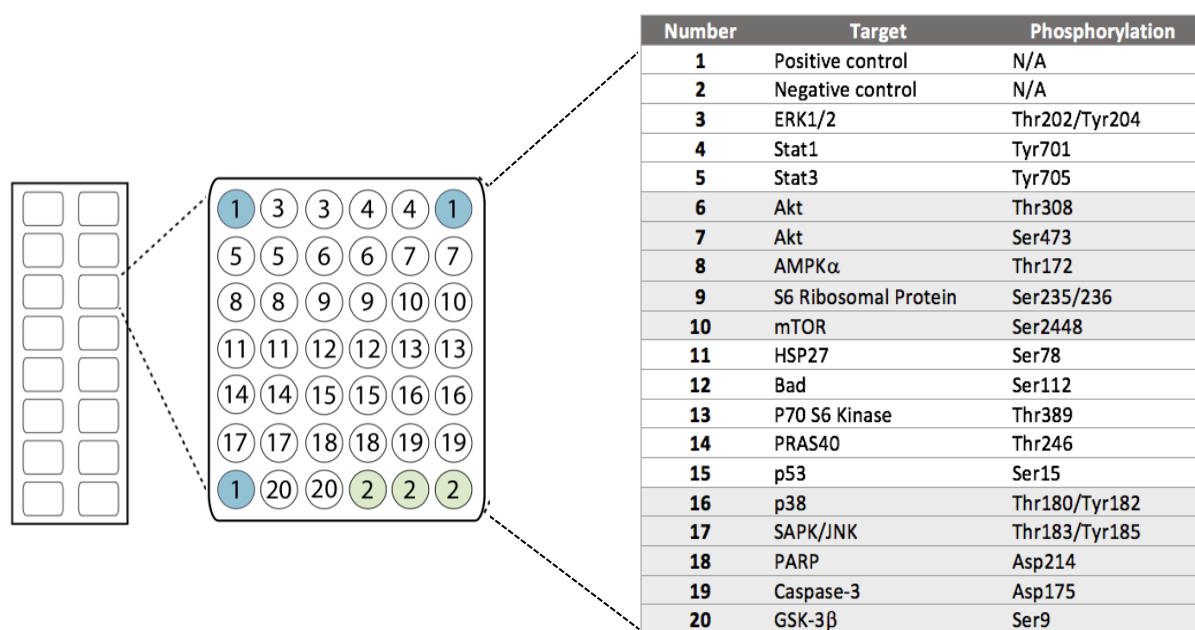


Figure 5.4. PathScan intracellular signalling-array map. Target map of the PathScan intracellular signalling array kit (chemiluminescent readout). Representation of a pad-slide (left). Targets 1 and 2 represent positive and negative controls respectively, and targets 3-20 correspond to 18 signalling molecules detected when phosphorylated (targets 1-17 and 20) or cleaved (targets 18 and 19). Phosphorylation/cleaved sites on each targeted molecule are provided in the table. Image from Cell Signalling Technology protocols.

hGBM L0 cells were deprived of growth factors that could promote the activation of intracellular signalling cascades for 48h. Cells were treated with 60 ng/mL of FGF2 and heparin for 10 min (**Figure 5.5A**, right panel), and untreated cells were used as control (**Figure 5.5A**, left panel). Proteins were isolated and immediately used for the array without going through freeze and thaw cycles. To visually examine phosphorylation/cleavage of targeted molecules it is necessary to compare **Figure 5.5A** with **Figure 5.4** as the latter represents the target map. To accurately identify differences in phosphorylation among targets we quantified the dot/target intensity of treated and untreated cells using Image J (**Figure 5.5B**). STAT3, ERK1/2, p38 and HSP27 showed the highest increase in phosphorylation levels (**Figure 5.5B**). These results are only an estimate as the signalling-array was performed once and therefore all targets would need to be validated. Nonetheless, as the three pathways with the highest phosphorylation levels after FGF2 treatment were also the most relevant kinases for GBM progression, we chose to further examine STAT3, ERK1/2 and p38 phosphorylation by western blot analysis. Despite HSP27 was also upregulated

(Figure 5.5B), it was excluded from follow up experiments as this kinase is mainly involved in the regulation of cell stress and apoptosis (Belkacemi and Hebb 2014), and its link with stemness markers has not been demonstrated in GBM.

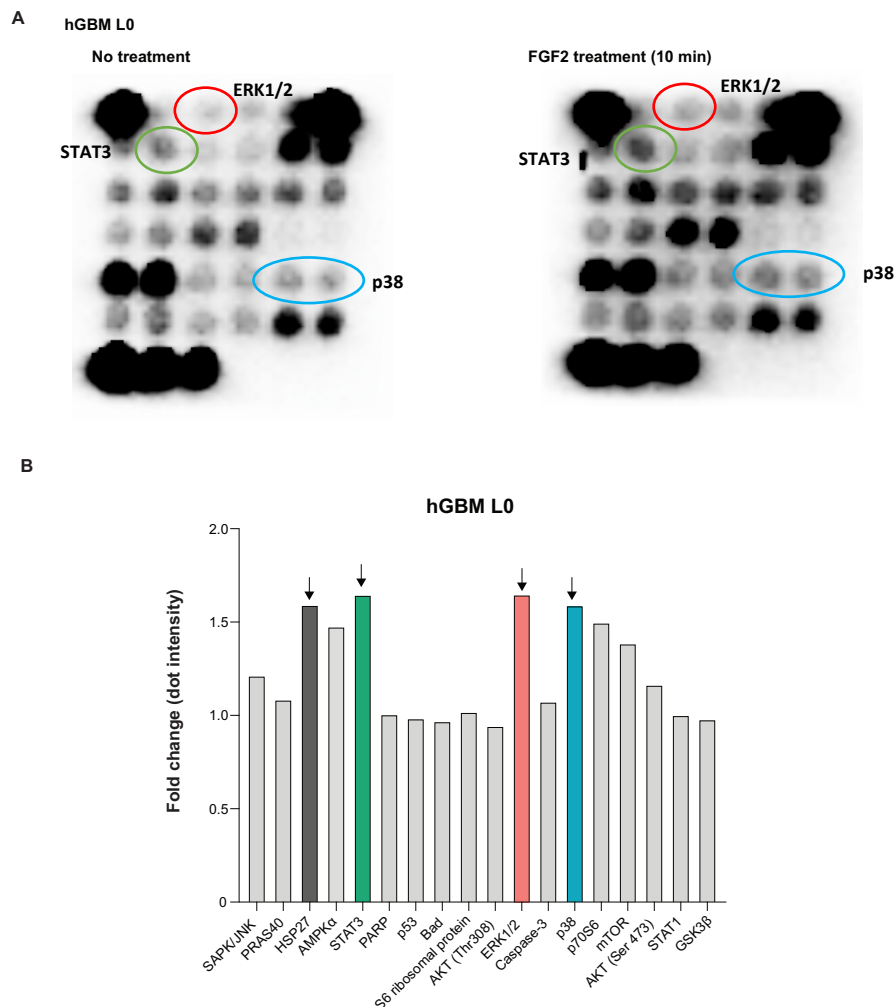


Figure 5.5. Intracellular signalling array of hGBM L0 cells. A) Pad-slide shows activation of different signalling pathways in hGBM L0 treated with 60 ng/mL of FGF2 and heparin (right panel), compared to untreated cells (left panel). ERK1/2 (red circle), STAT3 (green circle) and p38 (blue circle) were selected for follow up experiments. **B)** Quantification of pad-slide dot intensities (kinases phosphorylation levels) using Image J. Bar graphs represent fold-change between untreated and treated cells (n=1). Arrows indicate the targets with highest phosphorylation levels after FGF2 treatment: HSP27 (dark grey bar), STAT3 (green bar), ERK1/2 (red bar) and p38 (blue bar).

5.3.3 FGFR1 regulates ERK1/2 phosphorylation

In order to validate the targets selected from the PathScan array, we performed western blot analysis of p-STAT3, p-ERK1/2, and p-p38. Despite AKT not being highlighted in the PathScan (Figure 5.5), we arbitrarily chose to further examine it as it has a major function in GBM. We used antibodies that specifically identify the

phosphorylation sites described in **Figure 5.4**: STAT3 Tyr705, ERK1/2 Thr202/Tyr204 and p38 Thr180/Tyr182, AKT Ser473. Moreover, antibodies targeting total STAT3, total ERK1/2 and total p38 corroborated that changes in phosphorylation were not associated with a change in total protein levels. FGFR1 knockdown and control cells were treated with 60 ng/mL of FGF2 and heparin for 10 min, 30 min or 60 min (**Figure 5.6A**). Our data clearly shows an increase in ERK1/2 phosphorylation after FGF2 treatment. Phosphorylation of p38 also increased, but not as strongly as p-ERK1/2. Importantly, FGFR1 knockdown decreased ERK1/2 phosphorylation, whereas STAT3 phosphorylation increased. No changes were observed in p38 or AKT phosphorylation (**Figure 5.6B**). We further validated the decrease of p-ERK1/2 in shFGFR1 hGBM L0 cells (**Figure 5.6C**). Taken together, these results indicate ERK1/2 is crucial for translation of FGF2-FGFR1 signals in hGBM cells.

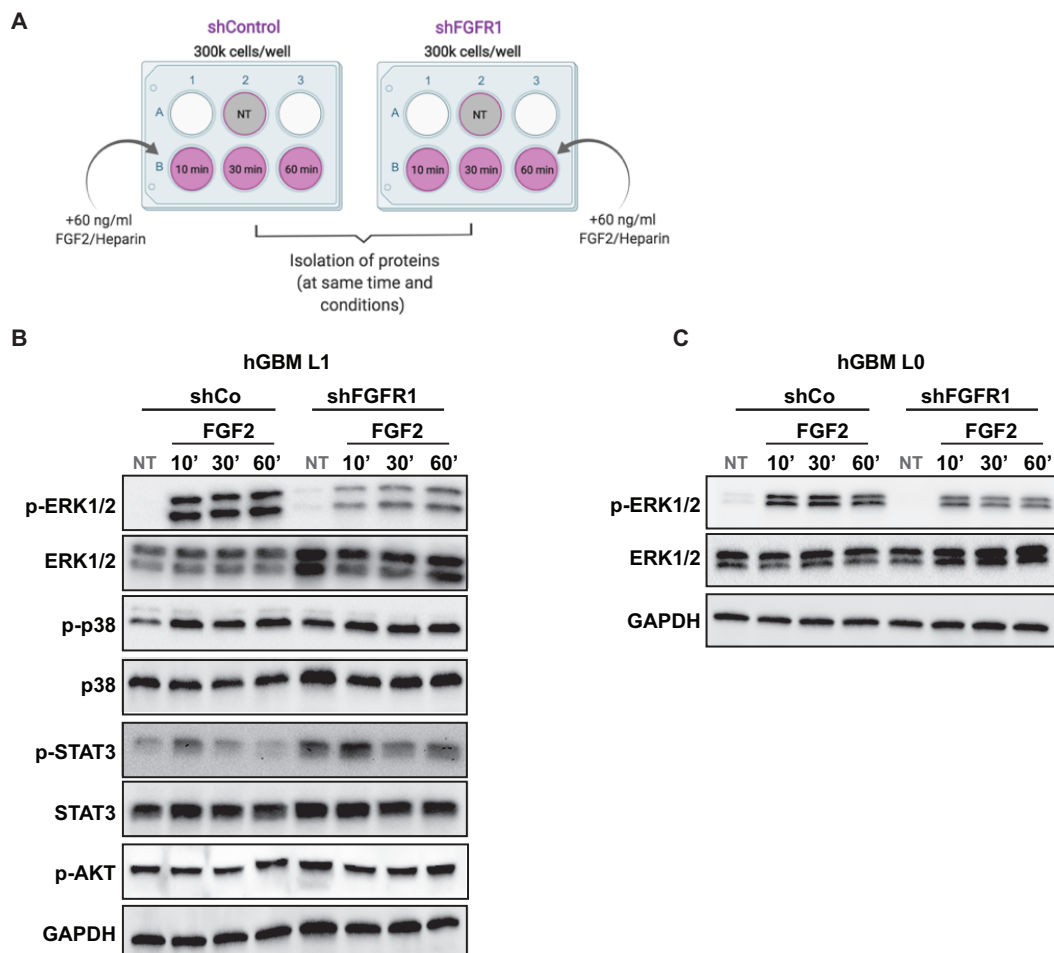


Figure 5.6. FGFR1 knockdown decreases ERK1/2 phosphorylation. **A)** Experiment schematics. 3×10^5 shCo and shFGFR1 cells were plated and treated with 60 ng/mL of FGF2 and heparin for 10 min, 30 min and 60 min. Proteins were isolated at the same time and conditions to avoid differences between shCo and shFGFR1 phosphorylation patterns (Image created with biorender.com). **B)** Western blot analysis of p-ERK1/2, total ERK1/2, p-p38, total p38, p-STAT3, total STAT3 and p-AKT compared to GAPDH. Knockdown of FGFR1 in hGBM L1 decreases p-ERK1/2 and increases STAT3. **C)** FGFR1 knockdown also decreases p-ERK1/2 in hGBM L0 cells. NT= non-treated, p=phosphorylated.

5.3.4 ZEB1 is regulated by ERK1/2 signalling

As FGFR1 regulates ERK1/2 phosphorylation and ZEB1, SOX2 and OLIG2 expression, we next examined whether ERK1/2 is an intermediary to these stemness-related transcription factors. To test this, we pharmacologically blocked ERK1/2 signalling using a specific inhibitor (SCH772984). This compound inhibits the intrinsic kinase activity of ERK as well as the phosphorylation of ERK by MEK (Morris *et al.* 2013). We first optimised the concentration of SCH772984 required to attenuate ERK1/2 signalling (**Figure 5.7A**). DMSO treatment was used as control, and DMSO/SCH772984 were added simultaneously with 60 ng/mL of FGF2 and heparin. Our results demonstrate that 10 nM of SCH772984 are sufficient to block ERK1/2 signalling. Secondly, a treatment time course indicates that ERK1/2 function is blocked within 10 min (**Figure 5.7B**). Finally, blocking of ERK1/2 signalling for 30 min with 10 nM of SCH772984 results in a clear decrease in ZEB1 expression (**Figure 5.7C**). Taken together, these findings demonstrate FGF2-FGFR1 regulates ZEB1 expression through ERK1/2 signalling, outlining a molecular mechanism by which FGFR1 regulates GSCs.

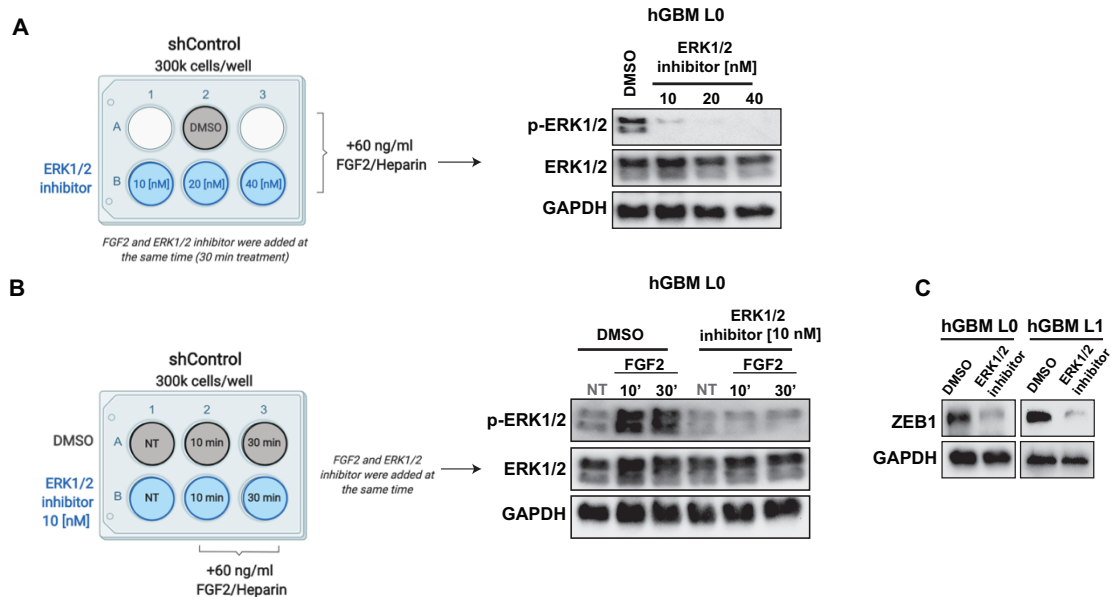


Figure 5.7. ERK1/2 inhibitor, SCH772984, reduces ZEB1 expression. A) Optimization of ERK1/2 inhibitor concentration. 3×10^5 hGBM L0 cells were treated with DMSO (control) or ERK1/2 inhibitor in three concentrations: 10 nM, 20 nM and 40 nM. 60 ng/mL of FGF2 and heparin were added simultaneously with the inhibitor or DMSO. 10 nM are sufficient to block ERK1/2 phosphorylation. **B)** 3×10^5 cells were treated with DMSO or inhibitor (10 nM) and 60 ng/mL of FGF2 for 10 min or 30 min. **C)** Western blot showing 10 nM of ERK1/2 inhibitor for 30 min reduces ZEB1 expression in hGBM L0 and hGBM L1 cells. NT= non-treated cells and p=phosphorylated. A) and B) (left) were created with biorender.com.

5.4 Discussion

In this study, we investigate the function of FGF2-FGFR1 axis as regulator of key stemness-associated transcription factors. We assess the expression of ZEB1, SOX2 and OLIG2 through rescue experiments and in FGFR1^{+/-} sorted populations. We analyse an array of intracellular signalling pathways to examine the molecular mechanism involved in FGFR1-mediated GSC regulation. Finally, we pharmacologically inhibit MAPK signalling by using SCH772984 ERK1/2 inhibitor.

We previously described a decrease in FGFR1, ZEB1, SOX2 and OLIG2 expression in differentiated cancer cells and a correlation between FGF2 and these transcription factors. We now demonstrated that FGFR1 knockdown decreases expression of ZEB1, SOX2 and OLIG2 in hGBM cells. These results are supported by two recent studies that showed FGFR1 loss decreased EMT-related transcription factors (Gouazé-Andersson *et al.* 2018) and OLIG2 (Kowalski-Chauvel *et al.* 2019) in GSCs. While both studies assumed a link of FGFR1 with stemness markers, they lack rescue experiments to validate this hypothesis. Our results not only demonstrated these transcription factors are downregulated in FGFR1 knockdown cells, but also that their expression could be rescued when these cells are transduced with full-length FGFR1 expression vectors. We further validated this mechanism by showing FGFR1⁺ cells are enriched in this triad of transcription factors compared to the FGFR1⁻ population. As ZEB1, SOX2 and OLIG2 seem to be co-dependent in GBM (Singh *et al.* 2017), we selected ZEB1 for follow-up rescue experiments. Our data indicate that FGFR1 overexpression cannot rescue ZEB1, SOX2, OLIG2 expression and sphere-forming capacity in ZEB1 knockdown cells, which validates that these transcription factors are downstream of FGF2-FGFR1. Similarly, studies in lung cancer cell lines have shown that SOX2 knockdown was not rescued by FGFR1 overexpression (Wang *et al.* 2018). In addition, Kowalski-Chauvel *et al.* showed ZEB1 can regulate FGFR1 (Kowalski-Chauvel *et al.* 2019). Taken together, these findings indicate that not only FGFR1 is an upstream regulator of ZEB1, SOX2 and OLIG2 as we have shown, but also outlines the existence of a feedback-loop between ZEB1 and FGFR1.

These transcription factors can be regulated by a variety of intracellular signals activated by a wide range of extracellular stimuli. In GBM, the most frequently dysregulated kinase pathways are MEK/ERK and PI3K/AKT/mTOR, whose

hyperactivation has been associated with tumorigenesis and GSC maintenance (Sunayama *et al.* 2010; Hannen *et al.* 2017). While these signalling cascades have been extensively studied, we chose an unbiased approach, utilising a phospho-kinase array to examine FGF2 signalling in hGBM cells. Our results indicate p38, STAT3 and ERK1/2 are highly responsive to FGF2 treatment. In support of these findings, Tomlinson *et al.* also found p38, ERK1/2 and STAT3/5/6 to be activated in human urothelial cancer after 30 min of FGF2 stimulation (Tomlinson *et al.* 2012). These proteins are downstream effectors of the STAT and MAPK families of signalling cascades and are relevant for GBM progression. STAT3 has been shown to activate cell proliferation, anti-apoptosis, GSC maintenance and invasion (Chang *et al.* 2017). P38 regulates proliferation and GSC quiescence (Soeda *et al.* 2017). On the other hand, ERK1/2 is hyperactivated in GBM and is associated with poor prognosis (Sunayama *et al.* 2010). Validation of the phosphorylated proteins identified in the phospho-kinase array showed that FGF2 induced ERK1/2 and p38 activation, but not STAT3. Wu *et al.* have demonstrated that FGF2 can induce STAT3 activation through JAK and PI3K/AKT pathways in hGBM cells (Wu *et al.* 2014). However, our western blot data shows AKT is not activated by FGF2. Furthermore, we found FGFR1 knockdown results in a decrease of p-ERK1/2, while no effect was seen on p38 phosphorylation. This suggests p38 may be phosphorylated through other FGFR, such as FGFR2, since both p38 and FGFR2 have been described as tumour suppressors in GBM (Frey *et al.* 2006; Han and Sun 2007; Ohashi *et al.* 2014). Interestingly, STAT3 phosphorylation increased in FGFR1 knockdown cells. ERK1/2 inhibition can promote the activation of other signalling pathways such as STAT3 and AKT in GBM (Sunayama *et al.* 2010; Xie *et al.* 2019). This may explain the increased of STAT3 in shFGFR1 cells. Nonetheless, to prove this hypothesis in the cell lines used, an analysis of STAT3 phosphorylation upon ERK1/2 inhibition with either shRNA or small molecule inhibitors would be required. Sunayama *et al.* showed that simultaneous inhibition of AKT and ERK1/2 resulted in longer survival in GBM xenografts, suggesting a cross-inhibitory function between both kinases in GBM (Sunayama *et al.* 2010). Nonetheless, we found AKT was not affected by FGFR1 loss. These findings indicate that FGFR1 regulates ERK1/2 independently of AKT in these hGBM cells. In line with our results, Tomlinson *et al.* also described an axis between FGF2-FGFR1 and ERK1/2 activation in bladder cancer cell lines (Tomlinson *et al.* 2012). Of interest, Kowalski-Chauvel *et al.* showed that ERK1/2 can also regulate

FGFR1 expression in GBM (Kowalski-Chauvel *et al.* 2019). A similar effect was previously described by Zakrzewska *et al.* who identified ERK1/2 as a negatively regulator of FGF-FGFR1 signalling in human bone osteosarcoma epithelial cells (Zakrzewska *et al.* 2013).

Considering that ERK1/2 hyperactivation plays a crucial role in GBM, ERK1/2 inhibitors have been broadly studied in preclinical experiments. We used a small-molecule ERK1/2 inhibitor to examine the effect of a functional loss of ERK signalling on the expression of stemness-associated transcription factors. SCH772984 was identified as a high-affinity inhibitor of ERK1/2 (Morris *et al.* 2013) and has been shown to successfully block FGF2-FGFR-mediated mammalian organoids branching *in vitro* (Soady *et al.* 2017). Our results demonstrated SCH772984 efficiently inhibited ERK1/2 phosphorylation and ablated the effect of FGF2 on expression of the stem cell-associated transcription factor, ZEB1. Using another ERK1/2 inhibitor, UO126, Chang *et al.* showed that loss of ERK1/2 reduced FGF2-mediated NESTIN expression in C6 glioma cells (Chang *et al.* 2013). These cells were cultured in FBS and subsequently deprived from it 24 h prior inhibitor/FGF2 treatment. As FBS contains an undefined number of cytokines and growth factors, FGF2/ERK1/2/NESTIN axis cannot be completely attributed to FGF2 signalling in this case (Chang *et al.* 2013). However, Sunayama *et al.* demonstrated that ERK1/2 inhibition not only reduced NESTIN, but also MSI1, BMI and SOX2 protein levels in hGBM cells, using the same inhibitor in serum-free, defined medium (Sunayama *et al.* 2010). This data is in line with our results and further corroborates the link between ERK1/2 and key stemness markers in GBM.

Development of ERK1/2 inhibitors is important for the treatment of cancer, as targeting this kinase directly suppresses the MAPK pathway. Conversely, blocking other molecules from the same family upstream of ERK has less efficiency and can promote tumour resistance (Hannen *et al.* 2017). Of interest, the ERK1/2 inhibitor used in our *in vitro* experiments (SCH772984) has been reported as one of the most promising ERK inhibitors as it blocks ERK1/2 in melanoma cells resistant to BRAF and MEK inhibitors (Morris *et al.* 2013). Furthermore, its clinical-grade analogue MK-8353/SCH900353 has been tested in a phase I clinical trial of melanoma patients (NCT01358331) where three out of fifteen patients with BRAF^{V600}-mutated

melanomas, exhibited response to treatment (Moschos *et al.* 2018). Although SCH772984 is not specific for GBM treatment, this compound can cross the blood-brain barrier in *in vivo* models of ischemia-induced brain infarction (Chen *et al.* 2017). Currently, patient response to treatments targeting single molecules of MAPK family in GBM has been low, highlighting the need of combinatorial therapies. The upregulation of tyrosine kinase receptors is one of the main problems related to this therapy resistance (Sunayama *et al.* 2010). Of interest, Machado *et al.* showed that combination of FGFR1 knockdown and MEK inhibitor (Trametinib), reduced tumour growth and tumour progression in KRAS-mutant lung cancer models (Machado *et al.* 2016). FGFR1 has been associated with radioresistance in GBM and we have demonstrated its link to GSC regulation. As inhibition of ERK1/2 may promote the upregulation of this receptor, a combination of FGFR1 and ERK1/2 inhibitors could be a potential therapy for treating GBM.

In conclusion, in this chapter we have confirmed ZEB1, SOX2 and OLIG2 are regulated by FGFR1 and that ERK1/2 is a downstream intermediary to FGF2-FGFR1 mediating expression of the stemness transcription factor ZEB1 in GBM (**Figure 5.8**)

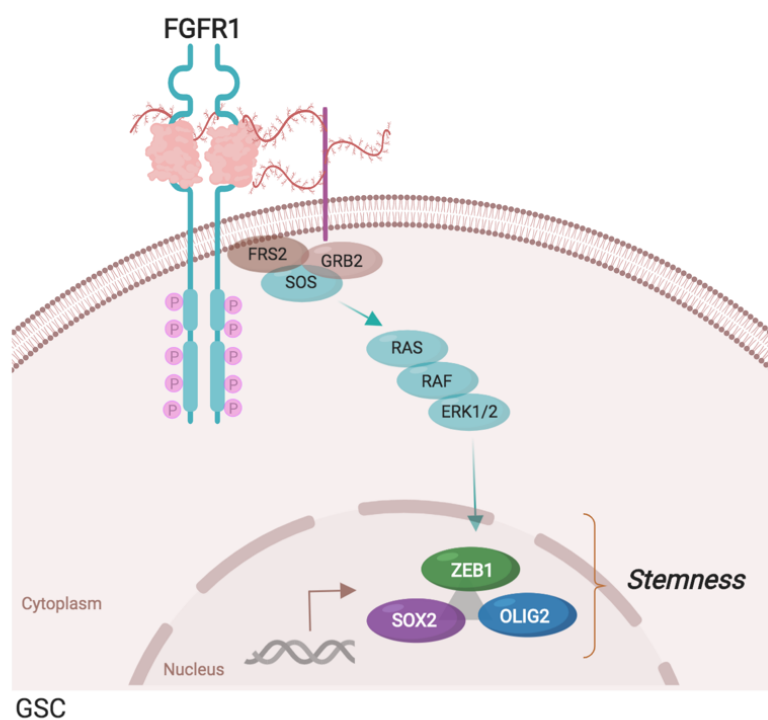


Figure 5.8. FGF2-FGFR1 axis regulates ZEB1 through ERK1/2 signalling cascade. FGFR1 regulates ZEB1, SOX2, OLIG and specifically activates ZEB1 through ERK1/2. Due to the co-dependence of these transcription factors, we hypothesise that FGFR1 may be also regulating SOX2 and OLIG2 through this signalling pathway (Image created with biorender.com).

Chapter 6: Conclusions

In this thesis, we have studied the role of FGF2-FGFR signalling in GSC regulation. This has been assessed using different genetic and pharmacological approaches to modify the levels of FGFR1-3 and inhibit the interaction between FGF2 and these receptors. We have demonstrated a crucial role for FGFR1 in tumour-formation in xenograft models and in the regulation of key stem cell transcription factors associated with GSC invasion, progression and tumour recurrence. This work outlines a point of fragility in current anti-FGFR therapies and highlights the importance of the development of FGFR-specific drugs which may constitute a translational therapeutic strategy to treat GBM.

6.1 FGF2 is associated with stemness-related transcription factors

Chapter 3 of this thesis assessed the effects of FGF2 treatment on patient derived GBM cells. Despite the broadly studied function of FGF2 in GSC self-renewal *in vitro* (Haley and Kim 2014), hGBM progression (Bian *et al.* 2000) and vascularization (Toyoda *et al.* 2013), less was known about its direct role regulating GSCs. The data presented here suggest that FGF2 has an important part in inducing clonogenicity and expression of key stemness, invasion and therapy resistance regulators (ZEB1, SOX2 and OLIG2) in GBM (Siebzehnrubl *et al.* 2013; Singh *et al.* 2017). Whether this also happens in NSCs remains to be tested. On the other hand, FGF2 can be secreted to the tumour microenvironment from different cells such as microglia, astrocytes and blood vessels. To assess if these cells release the same proportion of FGF2 in normal and in malignant conditions ELISA analysis of conditioned medium from these cell populations and co-staining of FGF2 and astrocytic, microglia or endothelial markers would be required.

6.2 FGFR2 and FGFR3 do not regulate GSCs

Reduction in *FGFR2* has been linked with higher glioma grade (Ohashi *et al.* 2014). In addition, we and others have demonstrated a correlation between the expression of this receptor and better prognosis in TCGA data analysis of GBM patient samples (Ohashi *et al.* 2014). However, our results of cell-surface FGFR expression patterns indicated FGFR2 was the most prevalent FGFR in hGBM cells. Furthermore, *in vivo* implantation of FGFR2 knockdown hGBM cells showed an increase in survival of tumour-bearing mice. In support of our data, Miraux *et al.* showed a decreased in

tumour growth *in vivo* after inhibition of FGFR2 signalling (Miraux *et al.* 2004). On the other hand, FGFR2 did not affect hGBM cell clonogenicity or proliferation *in vitro*. These data, together with the fact that FGFR2 expression increased in differentiated cancer cells, suggest that FGFR2 is not associated with GSC regulation. Consequently, additional analysis assessing stemness and proliferation of FGFR2+ and FGFR2- populations *in vitro* and tumorigenicity *in vivo* performing limiting dilution transplants, would clarify the function of this receptor in GBM.

Similarly, our data suggest that FGFR3 signalling is not associated with stemness in hGBM cells. FGFR3 expression profiles and clonogenic capacity in FGFR3 knockdown cells were cell line dependent. Moreover, *FGFR3* loss had no significant effect on survival of shFGFR3 xenografts compared to controls. *FGFR3* has an oncogenic function when fused with TACC coiled-coil domain in GBM (Singh *et al.* 2012). Therefore, it would be interesting to examine whether the hGBM cell lines used in this study contained FGFR3-TACC fusion and to assess if this may affect the tumour-formation capacity of these cell lines *in vivo*. Finally, as this study has focused particularly on the effects of FGF2 in GSC regulation, further work could assess whether other FGFs are involved in the activation of stem cell transcription factors through FGFR2 and FGFR3 signalling pathways.

6.3 FGF2-FGFR1-ERK1/2 signalling as therapeutic target in GBM

FGF2-FGFR1 has been associated with GBM growth and radioresistance (Saiki *et al.* 1999; Gouazé-Andersson *et al.* 2016). However, the relation between this receptor and GSC maintenance remained incompletely understood. Chapter 4 describes for first time, to our knowledge, a detailed assessment of *FGFR1* knockdown in hGBM cells *in vitro* and *in vivo*, demonstrates that *FGFR1* is functionally relevant for self-renewal capacity and tumour-formation in GBM and identifies FGFR1 as a potential cell surface marker of GSCs. These results outline a new way of isolating GSCs and offer a potential novel therapy to treat GBM. As we demonstrated that blocking FGFR1 expression increased the survival of mice bearing tumours and described FGFR1 as a key regulator of tumorigenicity in GBM, pharmacological targeting of this receptor in combination with standard of care therapy may help increasing patient survival. Despite the development of small molecules (e.g. PD173074, BGJ398, AZ4547) that show selectivity of FGFRs over other RTKs (see **section 4.2**), currently there are no

specific drugs with selectivity for individual FGFRs (Dieci *et al.* 2013). As our results indicate divergent functions of FGFR1-3 in GBM, the development of FGFR subtype-specific inhibitors may be crucial for treating this disease, while at the same time reducing unwanted effects on other systems. In addition, small molecules that specifically block the binding of FGF2 with FGFR1 may be also beneficial as we showed FGF2 function was translated through FGFR1 in a GSC context. Finally, the latter would benefit from a significant increase in the number of patients that are currently being recruited for clinical trials on drugs targeting FGFRs.

On the other hand, chapter 5 further investigated the molecular mechanism by which FGF2 pathway controls stemness and revealed that this growth factor activates FGFR1 on the GSC cell surface, which in turn induces expression of stem cell-associated transcription factors through the ERK1/2 signalling cascade (**Figure 6.1**). Therefore, ERK1/2 could be also targeted with current ERK1/2 inhibitors that can cross the blood-brain barrier, such as the one used in this study, SCH772984 (Chen *et al.* 2017). In conclusion, a combination of FGFR1-specific and ERK1/2 small molecule inhibitors may provide new targeted approaches to block the FGF2-FGFR1 axis in GSCs which may contribute to delay tumour recurrence and increase patient survival.

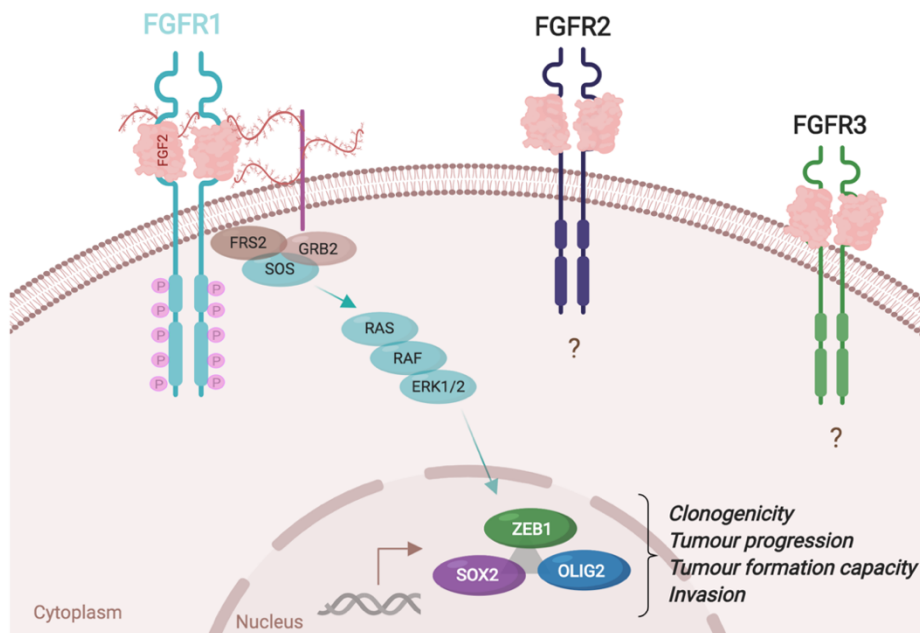


Figure 6.1. Diagram depicting the FGF2-FGFR1-ZEB1 signalling pathway described in this thesis. This image is an extension of Figures 3.8, Figure 4.11 and Figure 5.8. FGF2-FGFR1 regulates ZEB1, SOX2 and OLIG2 and mediates GSC self-renewal and maintenance. Despite FGFR2 and FGFR3 do not seem to be associated with a GSC population, additional work is needed to clarify their function in GBM. Image created with biorender.com.

6.4 FGFR1 controls the release of FGF2 through ADAMDEC1

Although this thesis has mainly focused on investigating the role of FGF2-FGFR signalling, we have also examined a mechanism by which GSCs release FGF2 from the tumour microenvironment (Jimenez-Pascual *et al.* 2019) in collaboration with Prof Justin D. Lathia (Lerner Research Institute, Cleveland).

As described in chapter 1 (**section 1.4**), molecules from the ECM act as a reservoir of FGF2 and other trophic factors (Eswarakumar *et al.* 2005; Ahmad *et al.* 2012; Touat *et al.* 2015). However, matrix metalloproteinases induce the release of these growth factors by promoting ECM degradation and enabling tumour invasion and intravasation of cancer cells (Le *et al.* 2003). In addition, members of the A Disintegrin and Metalloproteinase (ADAM) family of zinc-dependent proteinases, have been described as relevant for tumour invasion, recurrence and GSC regulation (Dong *et al.* 2015; Sarkar *et al.* 2015). Data from our collaborators showed that within this family of metalloproteinases, ADAMDEC1 was the most prevalent in GBM. GBM TCGA data analysis demonstrated a correlation between ADAMDEC1, glioma grade, and patient survival. Moreover, immunohistochemistry on patient specimens indicated that this protease was highly expressed in hGBM cells. Experimentally, its loss of function led to a reduction of sphere formation, proliferation, SOX2 expression and increased survival of tumour-bearing mice compared to controls. This data outlined a key role for ADAMDEC1 on the regulation of GSCs. Interestingly, ELISA analysis of GSC (CD133+) and non-tumour stem cells (CD133-) treated with ADAMDEC1 for 48 h, showed that only GSC cultures released FGF2 in the media. These results together with western blot analysis of phospho-FGFR1 demonstrated ADAMDEC1 regulated FGFR signalling.

Furthermore, we showed that FGFR1 loss of function decreased ADAMDEC1 expression, while full-length FGFR1 expression led to the inverse effect. As we found that FGFR1 regulates key stemness-associated transcription factors through ERK1/2 signalling, we next investigated whether this kinase was involved in the described pathway. Our western blot data not only demonstrated that ERK1/2 inhibition decreased ADAMDEC1, but also that ZEB1 was directly associated with the regulation of this metalloproteinase. In conclusion, we found that ADAMDEC1 promotes FGF2-FGFR1-mediated GSC self-renewal and maintenance by activating ZEB1, which at

the same time controls the activation of ADAMDEC1, revealing a positive feed-back loop that contributes to GSC maintenance in GBM.

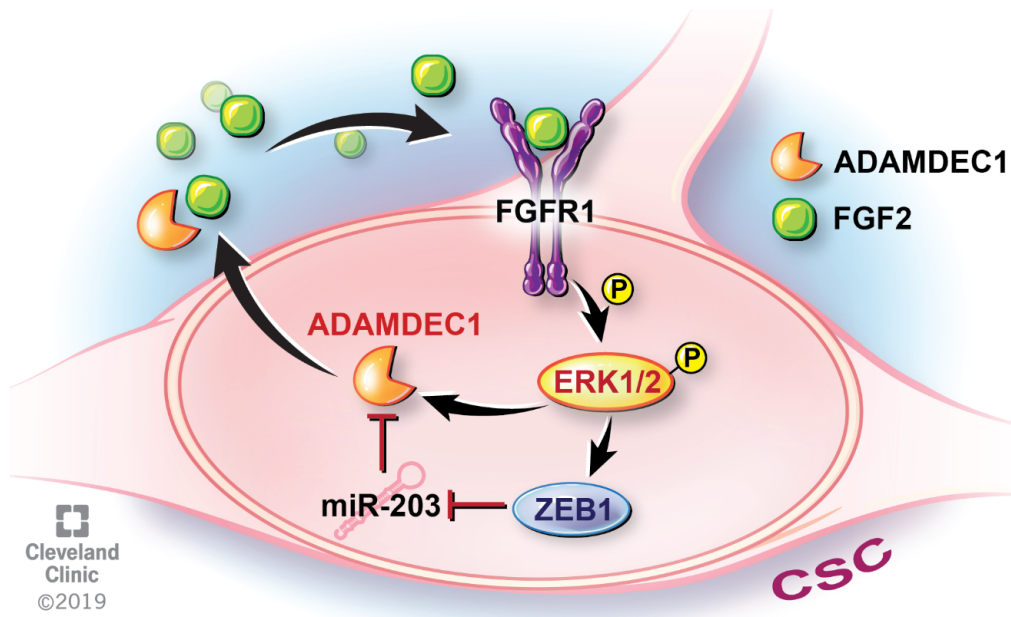


Figure 6.2. Diagram depicting the ADAMDEC1-FGFR1-ZEB1 feedback loop. In GSC, ADAMDEC1 releases FGF2 to the tumour microenvironment, which binds to FGFR1 and mediates the activation of the stem cell associated transcription factor ZEB1 through ERK1/2 signalling. Simultaneously, ZEB1 regulates ADAMDEC1 expression, completing a positive feedback loop that contributed to GSC self-renewal and maintenance. Image from Jimenez-Pascual *et al.* 2019 .

6.5 Future directions

FACS analysis of FGFR1-3 expression in chapter 3 demonstrated the existence of different populations of hGBM cells based on their FGFR profiles. Considering that these receptors seem to have divergent roles in GBM, FGFR expression may be used to isolate GSCs from non-tumour cells. Our data already revealed the importance of FGFR1 as a potential marker of GSCs. Nonetheless, the function of cell-surface FGFR2 and FGFR3 is not yet understood. Therefore, isolation of hGBM cell populations based on FGFR surface expression, and the subsequent assessment of their functional characteristics would be required. In addition, examining whether these populations co-express different FGFRs may contribute to the understanding of whether the development of monotherapies targeting individual receptors is needed. This could be assessed by flow cytometric analysis of hGBM cells co-stained for FGFRs, by immunofluorescence of these receptors in GBM patient samples, or by analysing cell-surface FGFRs upon FGFR1-3 knockdown. Finally, identifying

downstream targets of FGFR-specific populations, particularly for FGFR2 and FGFR3, would assess the link of cell-surface FGFRs with gene expression signatures involved in GBM progression. In conclusion, this work would be relevant to understand whether other FGFRs could be used to isolate cell populations based on their stemness capacity and add additional markers for identifying GSCs.

On the other hand, chapter 1 described the importance of FGFR splice variants in cancer (Beenken and Mohammadi 2009). The switch from FGFR-IIIb towards FGFR-IIIc is associated with tumour invasion and progression. Importantly, FGFR1 IIIc is upregulated in astrocytomas while, FGFR2 IIIb and IIIc seem to be downregulated in GBM (Gong 2014; Ohashi *et al.* 2014). In addition, FGF2 has different affinities for these splice variants depending on the FGFR subtype (Holzmann *et al.* 2012). Therefore, analysing which FGFR isoform is involved in the regulation of key GSC/stemness-related transcription factors and assessing their predominance in FGFR1-3 cell sorted populations by RNA-seq analysis, would address the relevance of these splice variants for GSC maintenance and GBM progression and recurrence.

References

- Acanda De La Rocha, A.M., López-Bertoni, H., Guruceaga, E., González-Huarriz, M., Martínez-Vélez, N., Xipell, E., Fueyo, J., et al.** (2016). Analysis of SOX2-regulated transcriptome in glioma stem cells. *PLoS ONE* **11**(9):1–20.
- Adair, J.E., Johnston, S.K., Mrugala, M.M., Beard, B.C., Guyman, L.A, Baldock, A.L, Bridge, C.A, et al.** (2014). Gene therapy enhances chemotherapy tolerance and efficacy in glioblastoma patients. *Journal of Clinical Investigation* **124**(9):4082–4092.
- Adams, J.M and Strasser, A.** (2008). Is tumor growth sustained by rare cancer stem cells or dominant clones? *Cancer Research* **68**(11):4018–4021.
- Ahmad, I., Iwata, T. and Leung, H.Y** (2012). Mechanisms of FGFR-mediated carcinogenesis. *Biochimica et Biophysica Acta - Molecular Cell Research* **1823**(4):850–860.
- Ahmed, A.U, Auffinger, B. and Lesniak, M.S** (2013). Understanding glioma stem cells: Rationale, clinical relevance and therapeutic strategies. *Expert Review of Neurotherapeutics* **13**(5):545–555.
- Al-Hajj, M., Wicha, M.S., Benito-Hernandez, A., Morrison, S.J. and Clarke, M.F.** (2003). Prospective identification of tumorigenic breast cancer cells. *Proceedings of the National Academy of Sciences of the United States of America* **100**(7):3983–8.
- Alcantara-Llaguno, S.R., Sun, D., Pedraza, A., Vera, E., Wang, Z., Burns, D.K. and Parada, L.F** (2019). Cell-of-origin susceptibility to glioblastoma formation declines with neural lineage restriction. *Nature Neuroscience* **22**(4):545–555.
- Alcantara-Llaguno, S.R, Wang, Z., Sun, D., Chen, J., Xu, J., Kim, E., Hatanpaa, K.J, et al.** (2015). Adult Lineage-Restricted CNS Progenitors Specify Distinct Glioblastoma Subtypes. *Cancer Cell* **28**(4):429–440.
- Aldape, K., Brindle, K.M., Chesler, L., Chopra, R., Gajjar, A., Gilbert, M.R, Gottardo, N., et al.** (2019). Challenges to curing primary brain tumours. *Nature Reviews Clinical Oncology*:1–12.
- Allen, N. and Barres, B.** (2009). Neuroscience: Glia - more than just brain glue. *Nature* **457**(7230):675–677.
- Alonso, M.M., Diez-Valle, R., Manterola, L., Rubio, A., Liu, D., Cortes-Santiago, N., Urquiza, L., et al.** (2011). Genetic and epigenetic modifications of Sox2 contribute to the invasive phenotype of malignant gliomas. *PLoS ONE* **6**(10):1–11.
- Altman, J. and Das, G.O** (1965). Autoradiographic and histological evidence of postnatal hippocampal neurogenesis in rats. *Journal of Comparative Neurology* **124**(3):319–335.
- Annovazzi, L., Mellai, M., Caldera, V., Valente, G. and Schiffer, D.** (2011). SOX2 expression and amplification in gliomas and glioma cell lines. *Cancer Genomics and Proteomics* **8**(3):139–147.
- Araque, A. and Navarrete, M.** (2010). Glial cells in neuronal network function. *Philosophical Transactions of the Royal Society B: Biological Sciences* **365**(1551):2375–2381.
- Atif, F., Patel, N.R., Yousuf, S. and Stein, D.G** (2015). The synergistic effect of combination

progesterone and temozolomide on human glioblastoma cells. *PLoS ONE* **10**(6):1–11.

Auciello, G., Cunningham, D.L., Tatar, T., Heath, J. and Rappoport, J.Z (2012). Regulation of fibroblast growth factor receptor signalling and trafficking by Src and Eps8. *Journal of Cell Science* **126**(2):613–624.

Auguste, P., Gursel, D.B., Lemiere, S., Reimers, D., Cuevas, P., Carceller, F., Di Santo, J.P., et al. (2001). Inhibition of fibroblast growth factor/fibroblast growth factor receptor activity in glioma cells impedes tumor growth by both angiogenesis-dependent and -independent mechanisms. *Cancer Research* **61**(4):1717–1726.

Avilion, A.A, Nicolis, S.K, Pevny, L.H., Perez, L., Vivian, N. and Lovell-Badge, R. (2003). Multipotent cell lineages in early mouse development depend on SOX2 function. *Genes and Development* **17**(1):126–140.

Bachoo, R.M, Maher, E.A, Ligon, K.L, Sharpless, N.E, Chan, S.S, You, M.J., Tang, Y., et al. (2002). Epidermal growth factor receptor and Ink4a/Arf: governing terminal differentiation and transformation stem cell to astrocyte axis. *Cancer Cell* **1**(3):269–77.

Bai, C.B, Auerbach, W., Lee, J.S., Stephen, D. and Joyner, A.L (2002). Gli2, but not Gli1, is required for initial Shh signaling and ectopic activation of the Shh pathway. *Development* **129**(20):4753–61.

Baird, A. and Ling, N. (1987). Fibroblast growth factors are present in the extracellular matrix produced by endothelial cells in vitro: Implications for a role of heparinase-like enzymes in the neovascular response. *Biochemical and Biophysical Research Communications* **142**(2):428–35.

Bajetto, A., Porcile, C., Pattarozzi, A., Scotti, L., Aceto, A., Daga, A., Barbieri, F., et al. (2013). Differential role of EGF and bFGF in human GBM-TIC proliferation: Relationship to EGFR-tyrosine kinase inhibitor sensitivity. *Journal of Biological Regulators and Homeostatic Agents* **27**(1):143–54.

Balss, J., Meyer, J., Mueller, W., Korshunov, A., Hartmann, C. and von Deimling, A. (2008). Analysis of the IDH1 codon 132 mutation in brain tumors. *Acta Neuropathologica* **116**(6):597–602.

Bao, S., Wu, Q., McLendon, R.E., Hao, Y., Shi, Q., Hjelmeland, A.B., Dewhirst, M.W., et al. (2006). Glioma stem cells promote radioresistance by preferential activation of the DNA damage response. *Nature* **444**(7120):756–760.

Barazzuol, L., Jena, R., Burnet, N.G., Meira, L.B., Jeynes, J.C., Kirkby, K.J. and Kirkby, N.F. (2013). Evaluation of poly (ADP-ribose) polymerase inhibitor ABT-888 combined with radiotherapy and temozolomide in glioblastoma. *Radiation Oncology* **8**(1):1–11.

Barreiro, E.J, Kummerle, A.E and Fraga, C.A (2011). The methylation effect in medicinal chemistry. *Chemical Reviews* **111**:5215–5246.

Baumann, N. and Pham-Dinh, D. (2001). Biology of Oligodendrocyte and Myelin in the Mammalian Central Nervous System. *Physiological Reviews* **81**(2):871–927.

Bayin, N.S., Modrek, A.S., Dietrich, A., Lebowitz, J., Abel, T., Song, H.R., Schober, M., et al. (2014). Selective lentiviral gene delivery to CD133-expressing human glioblastoma stem cells. *PLoS ONE* **9**(12):1–22.

- Beenken, A. and Mohammadi, M.** (2009). The FGF family: biology, pathophysiology and therapy. *Nature reviews. Drug discovery* **8**(3):235–53.
- Belkacemi, L. and Hebb, M.O.** (2014). HSP27 knockdown produces synergistic induction of apoptosis by HSP90 and kinase inhibitors in glioblastoma multiforme. *Anticancer Research* **34**(9):4915–27.
- Van Den Bent, M.J., Smits, M., Kros, J.M. and Chang, S.M.** (2017). Diffuse infiltrating oligodendroglioma and astrocytoma. *Journal of Clinical Oncology* **35**(21):2395–2409.
- Bian, X.W., Du, L.L., Shi, J.Q., Cheng, Y.S. and Liu, F.X.** (2000). Correlation of bFGF, FGFR-1 and VEGF expression with vascularity and malignancy of human astrocytomas. *Analytical and Quantitative Cytology and Histology* **22**(3):267–74.
- Bondy, M.L., Scheurer, M.E., Malmer, B., Barnholtz-Sloan, J.S., Davis, F.G., Il'yasova, D., Kruchko, C., et al.** (2008). Brain tumor epidemiology: Consensus from the Brain Tumor Epidemiology Consortium. *Cancer* **113**(7):1953–1968.
- Bonnet, D. and Dick, J.E.** (1997). Human acute myeloid leukemia is organized as a hierarchy that originates from a primitive hematopoietic cell. *Nature Medicine* **3**(7):730–737.
- Bowman, R.L., Wang, Q., Carro, A., Verhaak, R.G and Squatrito, M.** (2017). GliOVis data portal for visualization and analysis of brain tumor expression datasets. *Neuro-Oncology* **19**(1):139–141.
- Brabletz, S. and Brabletz, T.** (2010). The ZEB/miR-200 feedback loop--a motor of cellular plasticity in development and cancer? *EMBO reports* **11**(9):670–677.
- Brabletz, T., Kalluri, R., Nieto, M.A. and Weinberg, R.A.** (2018). EMT in cancer. *Nature Reviews Cancer* **18**(2):128–134.
- Brat, D.J., Castellano-Sanchez, A.A., Hunter, S.B., Pecot, M., Cohen, C., Hammond, E.H., Devi, S.N., et al.** (2004). Pseudopalisades in glioblastoma are hypoxic, express extracellular matrix proteases, and are formed by an actively migrating cell population. *Cancer research* **64**(3):920–7.
- Brennan, C.** (2017). FGFR-TACC approaches the first turn in the race for targetable GBM mutations. *Neuro-Oncology* **19**(4):461–462.
- Brennan, C.W., Verhaak, R.G., McKenna, A., Campos, B., Nounshmehr, H., Salama, S.R., Zheng, S., et al.** (2013). The somatic genomic landscape of glioblastoma. *Cell* **155**(2):462–77.
- Brooks, A.N., Kilgour, E. and Smith, P.D.** (2012). Molecular pathways: Fibroblast growth factor signaling: A new therapeutic opportunity in cancer. *Clinical Cancer Research* **18**(7):1855–1862.
- Burk, U., Schubert, J., Wellner, U., Schmalhofer, O., Vincan, E., Spaderna, S. and Brabletz, T.** (2008). A reciprocal repression between ZEB1 and members of the miR-200 family promotes EMT and invasion in cancer cells. *EMBO reports* **9**(6):582–9.
- Calabrese, C., Poppleton, H., Kocak, M., Hogg, T.L., Fuller, C., Hamner, B., Oh, E.Y., et al.** (2007). A perivascular niche for brain tumor stem cells. *Cancer Cell* **11**(1):69–82.
- Calabrese, E.J.** (2008). Hormesis and medicine. *British Journal of Clinical Pharmacology* **66**(5):594–617.

- Cameron, H.A., Woolley, C.S., McEwen, B.S. and Gould, E.** (1993). Differentiation of newly born neurons and glia in the dentate gyrus of the adult rat. *Neuroscience* **56**(2):337–44.
- Canoll, P. and Goldman, J.E.** (2008). The interface between glial progenitors and gliomas. *Acta Neuropathologica* **116**(5):465–77.
- Capper, D., Jones, D.T.W, Sill, M., et al** (2018). DNA methylation-based classification of central nervous system tumours. *Revista Ecuatoriana de Neurologia* **26**(3):283–288.
- Ceccarelli, M., Barthel, F.P., Malta, T.M., Sabedot, T.S., Salama, S.R., Murray, B.A., Morozova, O., et al.** (2016). Molecular Profiling Reveals Biologically Discrete Subsets and Pathways of Progression in Diffuse Glioma. *Cell* **164**(3):550–563.
- Cerami, E., Gao, J., Dogrusoz, U., Gross, B.E., Sumer, S.O., Aksoy, B.A., Jacobsen, A., et al.** (2012). The cBio cancer genomics portal: an open platform for exploring multidimensional cancer genomics data. *Cancer discovery* **2**(5):401–4.
- Chakravarti, A., Erkinen, M.G., Nestler, U., Stupp, R., Mehta, M., Aldape, K., Gilbert, M.R., et al.** (2006). Temozolomide-mediated radiation enhancement in glioblastoma: A report on underlying mechanisms. *Clinical Cancer Research* **12**(15):4738–4746.
- Chambers, I., Colby, D., Robertson, M., Nichols, J., Lee, S., Tweedie, S. and Smith, A.** (2003). Functional expression cloning of Nanog, a pluripotency sustaining factor in embryonic stem cells. *Cell* **113**(5):643–55.
- Chang, K.W., Huang, Y.L., Wong, Z.R., Su, P.H., Huang, B.M., Ju, T.K. and Yang, H.Y.** (2013). Fibroblast growth factor-2 up-regulates the expression of nestin through the Ras-Raf-ERK-Sp1 signaling axis in C6 glioma cells. *Biochemical and Biophysical Research Communications* **434**(4):854–860.
- Chang, N., Ahn, S.H., Kong, D.S., Lee, H.W. and Nam, D.H.** (2017). The role of STAT3 in glioblastoma progression through dual influences on tumor cells and the immune microenvironment. *Molecular and Cellular Endocrinology* **451**:53–65.
- Chen, G., Wang, J., Liu, Z. and Kornmann, M.** (2008). Exon III splicing of fibroblast growth factor receptor 1 is modulated by growth factors and cyclin D1. *Pancreas* **37**(2):159–164.
- Chen, J., Li, Y., Yu, T.S., McKay, R.M., Burns, D.K., Kernie, S.G. and Parada, L.F.** (2012). A restricted cell population propagates glioblastoma growth after chemotherapy. *Nature* **488**(7412):522–526.
- Chen, W., Feng, J. and Tong, W.** (2017). Phosphorylation of astrocytic connexin43 by ERK1/2 impairs blood-brain barrier in acute cerebral ischemia. *Cell and Bioscience* **7**(43):1–9.
- Cheng, T., Roth, B., Choi, W., Black, P.C., Dinney, C. and McConkey, D.J.** (2013). Fibroblast Growth Factor Receptors-1 and -3 Play Distinct Roles in the Regulation of Bladder Cancer Growth and Metastasis: Implications for Therapeutic Targeting. *PLoS ONE* **8**(2):1–12.
- Chin, K., DeVries, S., Fridlyand, J., Spellman, P.T., Roydasgupta, R., Kuo, W.L., Lapuk, A., et al.** (2006). Genomic and transcriptional aberrations linked to breast cancer pathophysiology. *Cancer Cell*

10(6):529–41.

Chung, S., Dwabe, S., Elshimali, Y., Sukhija, H., Aroh, C. and Vadgama, J. V. (2015). Identification of novel biomarkers for metastatic colorectal cancer using angiogenesis-antibody array and intracellular signaling array. *PLoS ONE* **10**(8):1–14.

Codrici, E., Enciu, A-M., Popescu, I-D., Mihai, S. and Tanase, C. (2016). Glioma Stem Cells and Their Microenvironments: Providers of Challenging Therapeutic Targets. *Stem Cells International* **2016**(18):1–20.

Cohen, A.L., Holmen, S.L and Colman, H. (2013). IDH1 and IDH2 Mutations in Gliomas. *The New England Journal of Medicine* **13**(5):345.

Cohnheim, J. (1867). Ueber entzündung und eiterung. *Path Anat Physiol Klin Med* **40**:1–79.

Colella, B., Faienza, F. and Di Bartolomeo, S. (2019). EMT Regulation by Autophagy: A New Perspective in Glioblastoma Biology. *Cancers* **11**(3):1–21.

Costa, R., Carneiro, B.A., Taxter, T., Tavora, F.A., Kalyan, A., Pai, S.A., Chae, Y.K., et al. (2016). *FGFR3-TACC3* fusion in solid tumors: mini review. *Oncotarget* **7**(34):55924–55938.

Cuyàs, E., Fernández-Arroyo, S., Alarcón, T., Lupu, R., Joven, J. and Menendez, J.A. (2016). Germline BRCA1 mutation reprograms breast epithelial cell metabolism towards mitochondrial-dependent biosynthesis: evidence for metformin-based “starvation” strategies in BRCA1 carriers. *Oncotarget* **7**(33):52974–52992.

Dacey, M.L. and Wallace, R.B. (1974). Postnatal neurogenesis in the feline cerebellum: A structural functional investigation. *Acta Neurobiologiae Experimentalis* **34**(2):253–263.

Dai, C., Celestino, J.C., Okada, Y., Louis, D.N., Fuller, G.N. and Holland, E.C. (2001). PDGF autocrine stimulation dedifferentiates cultured astrocytes and induces oligodendrogliomas from and oligoastrocytomas neural progenitors and astrocytes in vivo. *Genes and Development* **15**(15):1913–1925.

Daido, S., Takao, S., Tamiya, T., Ono, Y., Terada, K., Ito, S., Ouchida, M., et al. (2004). Loss of heterozygosity on chromosome 10q associated with malignancy and prognosis in astrocytic tumors, and discovery of novel loss regions. *Oncology Reports* **12**(4):789–95.

Dang, L., White, D.W., Gross, S., Bennett, B.D., Bittinger, M.A., Driggers, E.M., Fantin, V.R., et al. (2009). Cancer-associated IDH1 mutations produce 2-hydroxyglutarate. *Nature* **462**(7274):739–744.

Darmanis, S., Sloan, S.A., Croote, D., Mignardi, M., Chernikova, S., Samghababi, P., Zhang, Y., et al. (2017). Single-Cell RNA-Seq Analysis of Infiltrating Neoplastic Cells at the Migrating Front of Human Glioblastoma. *Cell Reports* **21**(5):1399–1410.

Dassi, E. (2017). Handshakes and Fights: The Regulatory Interplay of RNA-Binding Proteins. *Frontiers in Molecular Biosciences* **4**(67):1–7.

DeAngelis, L.M (2001). Brain Tumors. *The New England Journal of Medicine* **344**(2):114–123.

DeCarvalho, A.C., Nelson, K., Lemke, N., Lehman, N.L., Arbab, A.S., Kalkanis, S. and Mikkelsen,

- T. (2010). Gliosarcoma stem cells undergo glial and mesenchymal differentiation in vivo. *Stem Cells* **28**(2):181–190.
- Dehay, C., Savatier, P., Cortay, V. and Kennedy, H. (2001). Cell-cycle kinetics of neocortical precursors are influenced by embryonic thalamic axons. *The Journal of neuroscience*. **21**(1):201–14.
- Deleyrolle, L.P., Ericksson, G., Morrison, B.J., Lopez, A., Burrage, K., Burrage, P., Vescovi, A., et al. (2011). Determination of somatic and cancer stem cell self-renewing symmetric division rate using sphere assays. *PLoS ONE* **6**(1):1–11.
- Deleyrolle, L.P., Rietze, R.L. and Reynolds, B.A. (2008). The neurosphere assay, a method under scrutiny. *Acta Neuropsychiatrica* **20**(1):2–8.
- Detillieux, K.A., Sheikh, F., Kardami, E. and Cattini, P.A. (2003). Biological activities of fibroblast growth factor-2 in the adult myocardium. *Cardiovascular Research* **57**(1):8–19.
- Dieci, M.V., Arnedos, M., Andre, F. and Soria, J.C. (2013). Fibroblast growth factor receptor inhibitors as a cancer treatment: from a biologic rationale to medical perspectives. *Cancer Discovery* **3**(3):264–279.
- Dienstmann, R., Rodon, J., Prat, A., Perez-Garcia, J., Adamo, B., Felip, E., Cortes, J., et al. (2014). Genomic aberrations in the FGFR pathway: Opportunities for targeted therapies in solid tumors. *Annals of Oncology* **25**(3):552–563.
- Doetsch, F. (2003). The glial identity of neural stem cells. *Nature Neuroscience* **6**(11):1127–1134.
- Doetsch, F., Caille, I., Lim, D.A., Garcia-Verdugo, J.M. and Alvarez-Buylla, A. (1999). Subventricular zone astrocytes are neural stem cells in the adult mammalian brain. *Cell* **97**(6):703–716.
- Doetsch, F., Petreanu, L., Caille, I., Garcia-Verdugo, J.M. and Alvarez-Buylla, A. (2002). EGF converts transit-amplifying neurogenic precursors in the adult brain into multipotent stem cells. *Neuron* **36**(6):1021–1034.
- Dong, F., Eibach, M., Bartsch, J.W., Dolga, A.M., Schlomann, U., Conrad, C., Schieber, S., et al. (2015). The metalloprotease-disintegrin ADAM8 contributes to temozolomide chemoresistance and enhanced invasiveness of human glioblastoma cells. *Neuro-Oncology* **17**(11):1474–1485.
- DuBridge, R.B., Tang, P., Hsia, H.C., Leong, P.M., Miller, J.H. and Calos, M.P. (1987). Analysis of mutation in human cells by using an Epstein-Barr virus shuttle system. *Molecular and Cellular Biology* **7**(1):379–387.
- Ducassou, A., Uro-Coste, E., Verrelle, P., Filleron, T., Benouaich-Amiel, A., Lubrano, V., Sol, J.C., et al. (2013). $\alpha\beta 3$ Integrin and Fibroblast growth factor receptor 1 (FGFR1): Prognostic factors in a phase I-II clinical trial associating continuous administration of Tipifarnib with radiotherapy for patients with newly diagnosed glioblastoma. *European Journal of Cancer* **49**(9):2161–2169.
- Dumon, K.R., Ishii, H., Vecchione, A., Trapasso, F., Baldassarre, G., Chakrani, F., Druck, T., et al. (2001). Fragile histidine triad expression delays tumor development and induces apoptosis in human pancreatic cancer. *Cancer Research* **61**(12):4827–36.

- Dutt, A., Salvesen, H.B., Chen, T.H., Ramos, A.H., Onofrio, R.C., Hatton, C., Nicoletti, R., et al.** (2008). Drug-sensitive FGFR2 mutations in endometrial carcinoma. *Proceedings of the National Academy of Sciences* **105**(25):8713–7.
- Edwards, L.A., Woolard, K., Son, M.J., Li, A., Lee, J., Ene, C., Mantey, S.A., et al.** (2011). Effect of brain- and tumor-derived connective tissue growth factor on glioma invasion. *Journal of the National Cancer Institute* **103**(15):1162–1178.
- Eswarakumar, V.P., Lax, I. and Schlessinger, J.** (2005). Cellular signaling by fibroblast growth factor receptors. *Cytokine and Growth Factor Reviews* **16**(2):139–149.
- Fidoamore, A., Cristiano, L., Antonosante, A., D'Angelo, M., Di Giacomo, E., Astarita, C., Giordano, A., et al.** (2016). Glioblastoma Stem Cells Microenvironment: The Paracrine Roles of the Niche in Drug and Radioresistance. *Stem Cells International* **2016**(18):1–17.
- Foglieni, C., Pagano, K., Lessi, M., Bugatti, A., Moroni, E., Pinessi, D., Resovi, A., et al.** (2016). Integrating computational and chemical biology tools in the discovery of antiangiogenic small molecule ligands of FGF2 derived from endogenous inhibitors. *Scientific Reports* **6**(23432):1–13.
- Forbes, S.A., Beare, D., Boutselakis, H., Bamford, S., Bindal, N., Tate, J., Cole, C.G., et al.** (2017). COSMIC: Somatic cancer genetics at high-resolution. *Nucleic Acids Research* **45**(D1):D777–D783.
- Frey, M.R., Dise, R.S., Edelblum, K.L. and Polk, D.B.** (2006). p38 kinase regulates epidermal growth factor receptor downregulation and cellular migration. *EMBO Journal* **25**(24):5683–92.
- Frezza, C., Tennant, D.A. and Gottlieb, E.** (2010). IDH1 Mutations in Gliomas: When an Enzyme Loses Its Grip. *Cancer Cell* **17**(1):7–9.
- Friedmann-Morvinski, D., Bushong, E.A., Ke, E., Soda, Y., Marumoto, T., Singer, O., Ellisman, M.H., et al.** (2012). Dedifferentiation of neurons and astrocytes by oncogenes can induce gliomas in mice. *Science* **338**(6110):1080–1084.
- Frinchi, M., Bonomo, A., Trovato-Salinaro, A., Condorelli, D.F., Fuxe, K., Spampinato, M.G. and Mudò, G.** (2008). Fibroblast growth factor-2 and its receptor expression in proliferating precursor cells of the subventricular zone in the adult rat brain. *Neuroscience Letters* **447**(1):20–25.
- Fukai, J., Yokote, H., Yamanaka, R., Arao, T., Nishio, K. and Itakura, T.** (2008). EphA4 promotes cell proliferation and migration through a novel EphA4-FGFR1 signaling pathway in the human glioma U251 cell line. *Molecular Cancer Therapeutics* **7**(9):2768–2778.
- Galli, R., Binda, E., Orfanelli, U., Cipelletti, B., Gritti, A., De Vitis, S., Fiocco, R., et al.** (2004). Isolation and characterization of tumorigenic, stem-like neural precursors from human glioblastoma. *Cancer Research*. **64**(19):7011–7021.
- Gangemi, R.M., Griffero, F., Marubbi, D., Perera, M., Capra, M.C., Malatesta, P., Ravetti, G.L., et al.** (2009). SOX2 silencing in glioblastoma tumor-initiating cells causes stop of proliferation and loss of tumorigenicity. *Stem Cells* **27**(1):40–48.
- Garros-Regulez, L., Aldaz, P., Arrizabalaga, O., Moncho-Amor, V., Carrasco-Garcia, E., Manterola, L., Moreno-Cugnon, L., et al.** (2016). mTOR inhibition decreases SOX2-SOX9 mediated

glioma stem cell activity and temozolomide resistance. *Expert Opinion on Therapeutic Targets* **20**(4):393–405.

Glick, R.P., Lichtor, T., Lin, H., Tarlock, K. and Cohen, E.P. (2006). Immunogene therapy as a treatment for malignant brain tumors in young mice. *Journal of Neurosurgery: Pediatrics* **105**(1):65–70.

Globus, J.H. and Kuhlenbeck, H. (1944). The subependymal cell plate (matrix) and its relationship to brain tumors of the ependymal type. *Journal of Neuropathology and Experimental Neurology* **3**(1):1–35.

Goldberg, JS. and Hirschi, KK. (2009). Diverse roles of the vasculature within the neural stem cell niche. *Regenerative Medicine* **4**(6):879–897.

Gong, A.H., Wei, P., Zhang, S., Yao, J., Yuan, Y., Zhou, A.D., Lang, F.F., et al. (2015). FoxM1 drives a feed-forward STAT3-activation signaling loop that promotes the self-renewal and tumorigenicity of glioblastoma stem-like cells. *Cancer Research* **75**(11):2337–2348.

Gong, S.G. (2014). Isoforms of Receptors of Fibroblast Growth Factors. *Journal of Cellular Physiology* **229**(12):1887–1895.

Goodenberger, M.L. and Jenkins, R.B. (2012). Genetics of adult glioma. *Cancer Genetics* **205**(12):613–621.

Goossens, S., Vandamme, N., Van Vlierberghe, P. and Berx, G. (2017). EMT transcription factors in cancer development re-evaluated: Beyond EMT and MET. *Biochimica et Biophysica Acta - Reviews on Cancer* **1868**(2):584–591.

Gouazé-Andersson, V., Delmas, C., Taurand, M., Martinez-Gala, J., Evrard, S., Mazoyer, S., Toulas, C., et al. (2016). FGFR1 induces glioblastoma radioresistance through the PLCg/Hif1a pathway. *Cancer Research* **76**(10):3036–3044.

Gouazé-Andersson, V., Ghérardi, M.J., Lemarié, A., Gilhodes, J., Lubrano, V., Arnauduc, F., Moyal, E.C.J., et al. (2018). FGFR1/FOXM1 pathway: a key regulator of glioblastoma stem cells radioresistance and a prognosis biomarker. *Oncotarget* **9**(60):31637–31649.

Greaves, M. and Maley, C.C. (2012). Clonal evolution in cancer. *Nature* **481**(7381):306–13.

Griguer, C.E., Oliva, C.R., Gobin, E., Marcorelles, P., Benos, D.J., Lancaster, J.R. and Gillespie, G.Y. (2008). CD133 is a marker of bioenergetic stress in human glioma. *PLoS ONE* **3**(11):1–11.

Gritti, A., Parati, E.A., Cova, L., Frolichsthal, P., Galli, R., Wanke, E., Faravelli, L., et al. (1996). Multipotential stem cells from the adult mouse brain proliferate and self-renew in response to basic fibroblast growth factor. *The Journal of neuroscience* **16**(3):1091–1100.

Guillemot, F. and Zimmer, C. (2011). From cradle to grave: The multiple roles of fibroblast growth factors in neural development. *Neuron* **71**(4):574–588.

Haas, T.L., Sciuto, M.R., Brunetto, L., Valvo, C., Signore, M., Fiori, M.E., di Martino, S., et al. (2017). Integrin $\alpha 7$ Is a Functional Marker and Potential Therapeutic Target in Glioblastoma. *Cell Stem Cell* **21**(1):35–50.

- Haley, E.M. and Kim, Y.** (2014). The role of basic fibroblast growth factor in glioblastoma multiforme and glioblastoma stem cells and in their in vitro culture. *Cancer Letters* **346**(1):1–5.
- Han, J. and Sun, P.** (2007). The pathways to tumor suppression via route p38. *Trends in Biochemical Sciences* **32**(8):364–71.
- Hanahan, D. and Weinberg, R.A.** (2000). The hallmarks of cancer. *Cell* **100**(1):57–70.
- Hannen, R., Hauswald, M. and Bartsch, J.W.** (2017). A rationale for targeting extracellular regulated kinases ERK1 and ERK2 in glioblastoma. *Journal of Neuropathology and Experimental Neurology* **76**(10):838–847.
- Harmer, N.J., Ilag, L.L., Mulloy, B., Pellegrini, L., Robinson, C.V. and Blundell, T.L.** (2004). Towards a resolution of the stoichiometry of the fibroblast growth factor (FGF)-FGF receptor-heparin complex. *Journal of Molecular Biology* **339**(4):821–834.
- Hart, M.G., Garside, R., Rogers, G., Stein, K. and Grant, R.** (2013). Temozolomide for high grade glioma. *Cochrane Database of Systematic Reviews* **30**(4):1–60.
- Haugsten, E.M., Wiedlocha, A., Olsnes, S. and Wesche, J.** (2010). Roles of Fibroblast Growth Factor Receptors in Carcinogenesis. *Molecular Cancer Research* **8**(11):1439–1452.
- Heddleston, J.M., Li, Z., McLendon, Z.E., Hjelmeland, A.B. and Rich, J.N.** (2009). The hypoxic microenvironment maintains glioblastoma stem cells and promotes reprogramming towards a cancer stem cell phenotype. *Cell Cycle* **8**(20):3274–84.
- Hemmati, H.D., Nakano, I., Lazareff, J.A., Masterman-Smith, M., Geschwind, D.H., Bronner-Fraser, M. and Kornblum, H.I.** (2003). Cancerous stem cells can arise from pediatric brain tumors. *Proceedings of the National Academy of Sciences* **100**(25):15178–83.
- Hoang-Minh, L.B., Deleyrolle, L.P., Siebzehnrubl, D., Ugartemendia, G., Futch, H., Griffith, B., Breunig, J.J., et al.** (2016). Disruption of KIF3A in patient-derived glioblastoma cells: effects on ciliogenesis, hedgehog sensitivity, and tumorigenesis. *Oncotarget* **7**(6):7029–43.
- Hoang-Minh, L.B., Siebzehnrubl, F.A., Yang, C., Suzuki-Hatano, S., Dajac, K., Loche, T., Andrews, N., et al.** (2018). Infiltrative and drug-resistant slow-cycling cells support metabolic heterogeneity in glioblastoma. *The EMBO Journal* **37**(23).
- Hoelzinger, D.B., Demuth, T. and Berens, M.E.** (2007). Autocrine factors that sustain glioma invasion and paracrine biology in the brain microenvironment. *Journal of the National Cancer Institute* **99**(21):1583–1593.
- Holland, E.C., Celestino, J., Dai, C., Schaefer, L., Sawaya, R.E. and Fuller, G.N.** (2000). Combined activation of Ras and Akt in neural progenitors induces glioblastoma formation in mice. *Nature Genetics* **25**(1):55–7.
- Hölsken, A., Eyüpoglu, I.Y., Lueders, M., Tränkle, C., Dieckmann, D., Buslei, R., Hahnen, E., et al.** (2006). Ex vivo therapy of malignant melanomas transplanted into organotypic brain slice cultures using inhibitors of histone deacetylases. *Acta neuropathologica* **112**(2):205–15.

- Holzmann, K., Grunt, T., Heinzle, C., Sampl, S., Steinhoff, H., Reichmann, N., Kleiter, M., et al.** (2012). Alternative splicing of fibroblast growth factor receptor IgIII loops in cancer. *Journal of Nucleic Acids* **2012**(950508):1–12.
- Hu, Y. and Smyth, G.K.** (2009). ELDA: Extreme limiting dilution analysis for comparing depleted and enriched populations in stem cell and other assays. *Journal of Immunological Methods* **347**(1–2):70–8.
- Huang, P.H., Cavenee, W.K., Furnari, F.B. and White, F.M.** (2007). Uncovering therapeutic targets for glioblastoma: A systems biology approach. *Cell Cycle* **6**(22):2750–2754.
- Huszthy, P.C., Daphu, I., Niclou, S.P., Stieber, D., Nigro, J.M., Sakariassen, P.O., Miletic, H., et al.** (2012). In vivo models of primary brain tumors: Pitfalls and perspectives. *Neuro-Oncology* **14**(8):979–93.
- Ignatova, T.N., Kukekov, V.G., Laywell, E.D., Suslov, O.N., Vrionis, F.D. and Steindler, D.A.** (2002). Human cortical glial tumors contain neural stem-like cells expressing astroglial and neuronal markers in vitro. *Glia* **39**(3):193–206.
- Ikushima, H., Todo, T., Ino, Y., Takahashi, M., Miyazawa, K. and Miyazono, K.** (2009). Autocrine TGF- β Signaling Maintains Tumorigenicity of Glioma-Initiating Cells through Sry-Related HMG-Box Factors. *Cell Stem Cell* **5**(5):504–14.
- Irschick, R., Trost, T., Karp, G., Hausott, B., Auer, M., Claus, P. and Klimaschewski, L.** (2013). Sorting of the FGF receptor 1 in a human glioma cell line. *Histochemistry and Cell Biology* **139**(1):135–148.
- Itoh, N. and Ornitz, D.M.** (2011). Fibroblast growth factors: From molecular evolution to roles in development, metabolism and disease. *Journal of Biochemistry* **149**(2):121–130.
- Jäkel, S. and Dimou, L.** (2017). Glial Cells and Their Function in the Adult Brain: A Journey through the History of Their Ablation. *Frontiers in Cellular Neuroscience* **11**(24):1–17.
- Jennings, M.** (1989). Topography of membrane proteins. *Annual Review of Biochemistry* **58**:999–1027.
- Jeon, H.M., Sohn, Y.W., Oh, S.Y., Kim, S.H., Beck, S., Kim, S. and Kim, H.** (2011). ID4 imparts chemoresistance and cancer stemness to glioma cells by derepressing miR-9*-mediated suppression of SOX2. *Cancer Research* **71**(9):3410–21.
- Jiapaer, S., Furuta, T., Tanaka, S., Kitabayashi, T. and Nakada, M.** (2018). Potential Strategies Overcoming the Temozolomide Resistance for Glioblastoma. *Neurologia medico-chirurgica* **58**(10):405–421.
- Jimenez-Pascual, A., Hale, J.S., Kordowski, A., Pugh, J., Silver, D.J., Bayik, D., Roversi, G., et al.** (2019). ADAMDEC1 maintains a growth factor signaling loop in cancer stem cells. *Cancer Discovery*.
- Jin, W., Bi, W., Huang, E.S.C. and Cote, G.J.** (1999). Glioblastoma cell-specific expression of fibroblast growth factor receptor-1 β requires an intronic repressor of RNA splicing. *Cancer Research* **59**(2):316–319.
- Jin, W., McCutcheon, I.E., Fuller, G.N., Huang, E.S.C. and Cote, G.J.** (2000). Fibroblast growth factor

receptor-1 α -exon exclusion and polypyrimidine tract-binding protein in glioblastoma multiforme tumors. *Cancer Research* **60**(5):1221–1224.

Johannessen, T.A., Mukherjee, J., Viswanath, P., Ohba, S., Ronen, S.M., Bjerkvig, R. and Pieper, R.O. (2016). Rapid Conversion of Mutant IDH1 from Driver to Passenger in a Model of Human Gliomagenesis. *Molecular Cancer Research* **14**(10):976–983.

Joo, K.M., Kim, S.Y., Jin, X., Song, S.Y., Kong, D.S., Lee, J.I., Jeon, J.W., et al. (2008). Clinical and biological implications of CD133-positive and CD133-negative cells in glioblastomas. *Laboratory Investigation* **88**(8):808–15.

Joseph, J. V., Conroy, S., Tomar, T., Eggens-Meijer, E., Bhat, K., Copray, S., Walenkamp, A.M.E., et al. (2014). TGF- β is an inducer of ZEB1-dependent mesenchymal transdifferentiation in glioblastoma that is associated with tumor invasion. *Cell Death and Disease* **5**(10):1443–14.

Joy, A., Moffett, J., Neary, K., Mordechai, E., Stachowiak, E.K., Coons, S., Rankin-Shapiro, J., et al. (1997). Nuclear accumulation of FGF-2 is associated with proliferation of human astrocytes and glioma cells. *Oncogene* **14**(2):171–183.

Kafri, T., van Praag, H., Ouyang, L., Gage, F.H. and Verma, I.M. (1999). A packaging cell line for lentivirus vectors. *Journal of virology* **73**(1):576–84.

Kahlert, U.D., Suwala, A.K., Raabe, E.H., Siebzehnruhl, F.A., Suarez, M.J., Orr, B.A., Bar, E.E., et al. (2015). ZEB1 Promotes Invasion in Human Fetal Neural Stem Cells and Hypoxic Glioma Neurospheres. *Brain Pathology* **25**(6):724–732.

Kalluri, R. and Weinberg, R.A. (2009). Review series The basics of epithelial-mesenchymal transition. *Journal of Clinical Investigation* **119**(6):1420–1428.

Kaplan, M.S. and Hinds, J.W. (1977). Neurogenesis in the adult rat: Electron microscopic analysis of light radioautographs. *Science* **197**(4308):1092–4.

Kelly, J.J., Stechishin, O., Chojnacki, A., Lun, X., Sun, B., Senger, D.L., Forsyth, P., et al. (2009). Proliferation of human glioblastoma stem cells occurs independently of exogenous mitogens. *Stem Cells* **27**(8):1722–1733.

Kendrick, H., Regan, J.L., Magnay, F.A., Grigoriadis, A., Mitsopoulos, C., Zvelebil, M. and Smalley, M.J. (2008). Transcriptome analysis of mammary epithelial subpopulations identifies novel determinants of lineage commitment and cell fate. *BioMed Central Genomics* **9**(591):1–28.

Kettenmann, H. and Verkhratsky, A. (2013). Glial Cells. *Neuroscience in the 21st Century: From Basic to Clinical* **15**:475–506.

Kim, D., Kim, J., Hur, J.K., Been, K.W., Yoon, S.H. and Kim, J.S. (2016). Genome-wide analysis reveals specificities of Cpf1 endonucleases in human cells. *Nature Biotechnology* **34**(8):863–868.

Kim, H.S., Kim, J.H., Jang, H.J., Han, B. and Zang, D.Y. (2019). Pathological and prognostic impacts of FGFR2 overexpression in gastric cancer: A meta-analysis. *Journal of Cancer* **10**(1):20–27.

Kleihues, P., Burger, P.C. and Scheithauer, B.W. (1993). Histological Typing of Tumours of the

Central Nervous System. *World Health Organization* **21**:1–9.

Knowles, B.B., Howe, C.C. and Aden, D.P. (1980). Human hepatocellular carcinoma cell lines secrete the major plasma proteins and hepatitis B surface antigen. *Science* **209**(4455):497–9.

Kong, X., Kuilman, T., Shahrabi, A., Boshuizen, J., Kemper, K., Song, J.Y., Niessen, H.W.M., et al. (2017). Cancer drug addiction is relayed by an ERK2-dependent phenotype switch. *Nature* **550**(7675):270–274.

Kornmann, M., Ishiwata, T., Matsuda, K., Lopez, M.E., Fukahi, K., Asano, G., Beger, H.G., et al. (2002). IIIc isoform of fibroblast growth factor receptor 1 is overexpressed in human pancreatic cancer and enhances tumorigenicity of hamster ductal cells. *Gastroenterology* **123**(1):301–313.

Kosty, J., Lu, F., Kupp, R., Mehta, S. and Lu, Q.R. (2017). Harnessing OLIG2 function in tumorigenicity and plasticity to target malignant gliomas. *Cell Cycle* **16**(18):1654–1660.

Kowalski-Chauvel, A., Gouaze-Andersson, V., Baricault, L., Martin, E., Delmas, C., Toulas, C., Cohen-Jonathan-Moyal, E., et al. (2019). Alpha6-integrin regulates FGFR1 expression through the ZEB1/YAP1 transcription complex in glioblastoma stem cells resulting in enhanced proliferation and stemness. *Cancers* **11**(3):1–15.

Kowalski-Chauvel, A., Modesto, A., Gouaze-andersson, V., Baricault, L., Gilhodes, J., Delmas, C., Lemarie, A., et al. (2018). Alpha-6 integrin promotes radioresistance of glioblastoma by modulating DNA damage response and the transcription factor Zeb1. *Cell Death and Disease* **9**(872):1–12.

Kundu, S., Xiong, A., Spyrou, A., Wicher, G., Marinescu, V.D., Edqvist, P., Zhang, L., et al. (2016). Heparanase Promotes Glioma Progression and Is Inversely Correlated with Patient Survival. *Molecular Cancer Research* **14**(12):1243–1253.

Lake, D., Corrêa, S.A. and Müller, J. (2016). Negative feedback regulation of the ERK1/2 MAPK pathway. *Cellular and Molecular Life Sciences* **73**(23):4397–4413.

Lamouille, S., Xu, J. and Derynck, R. (2014). Molecular mechanisms of epithelial-mesenchymal transition. *Nature Reviews Molecular Cell Biology* **15**(3):178–96.

Laremore, T.N., Zhang, F., Dordick, J.S., Liu, J. and Linhardt, R.J. (2009). Recent progress and applications in glycosaminoglycan and heparin research. *Current Opinion in Chemical Biology* **13**(5–6):633–640.

Larson, E.W., Peterson, H.E, Lamoreaux, W.T., Mackay, A.R., Fairbanks, R.K., Call, J.A., et al. (2014). Clinical outcomes following salvage gamma knife radiosurgery for recurrent glioblastoma. *World Journal of Clinical Oncology* **5**(2):142–48.

Lasorella, A., Sanson, M. and Lavarone, A. (2017). FGFR-TACC gene fusions in human glioma. *Neuro-Oncology* **19**(4):475–483.

Lathia, J.D., Hitomi, M., Gallagher, J., Gadani, S.D., Adkins, J., Vasanji, A., Liu, L., et al. (2011). Distribution of CD133 reveals glioma stem cells self-renew through symmetric and asymmetric cell divisions. *Cell Death and Disease* **2**(9):1–12.

- Lathia, J.D., Mack, S.C., Mulkearns-Hubert, E.E., Valentim, C.L. and Rich, J.N.** (2015). Cancer stem cells in glioblastoma. *Genes and Development* **29**(12):1203–1217.
- Lathia, J.D., Gallagher, J., Heddleston, J.M., Wang, J., Eyler, C.E., MacSwords, J., Wu, Q., et al.** (2010). Integrin Alpha 6 regulates glioblastoma stem cells. *Cell Stem Cell* **6**(5):421–32.
- Lathia, J.D. and Liu, H.** (2017). Overview of Cancer Stem Cells and Stemness for Community Oncologists. *Targeted Oncology* **12**(4):387–399.
- Lau, M.T., So, W.K. and Leung, P.C.K.** (2013). Fibroblast Growth Factor 2 Induces E-Cadherin Down-Regulation via PI3K/Akt/mTOR and MAPK/ERK Signaling in Ovarian Cancer Cells. *PLoS ONE* **8**(3):1–11.
- Le, D.M., Besson, A., Fogg, D.K., Choi, K., Waisman, D.M., Goodyer, C.G., Rewcastle, B., et al.** (2003). Exploitation of astrocytes by glioma cells to facilitate invasiveness: a mechanism involving matrix metalloproteinase-2 and the urokinase-type plasminogen activator-plasmin cascade. *The Journal of neuroscience : the official journal of the Society for Neuroscience* **15**(23):4034–43.
- Lee, J.G., Jung, E. and Heur, M.** (2018). Fibroblast growth factor 2 induces proliferation and fibrosis via SNAI1-mediated activation of CDK2 and ZEB1 in corneal endothelium. *Journal of Biological Chemistry* **293**(10):3758–3769.
- Lee, J., Kotliarova, S., Kotliarov, Y., Li, A., Su, Q., Donin, N.M., Pastorino, S., et al.** (2006). Tumor stem cells derived from glioblastomas cultured in bFGF and EGF more closely mirror the phenotype and genotype of primary tumors than do serum-cultured cell lines. *Cancer Cell* **9**(5):391–403.
- Lee, J.H., Lee, J.E., Kahng, J.Y., Kim, S.H., Park, J.S., Yoon, S.J., Um, J.Y., et al.** (2018). Human glioblastoma arises from subventricular zone cells with low-level driver mutations. *Nature* **560**(7717):243–247.
- Lee, P.L., Johnson, D.E., Cousens, L.S., Fried, V.A. and Williams, L.T.** (1989). Purification and complementary DNA cloning of a receptor for basic fibroblast growth factor. *Science* **245**(4913):57–60.
- Leelatian, N. and Ibrrie, R.A.** (2016). Head of the Class: OLIG2 and Glioblastoma Phenotype. *Cancer Cell* **29**(5):613–615.
- Lehmann, W., Mossmann, D., Kleemann, J., Mock, K., Meisinger, C., Brummer, T., Herr, R., et al.** (2016). ZEB1 turns into a transcriptional activator by interacting with YAP1 in aggressive cancer types. *Nature communications* **7**(10498).
- Lew, E.D., Furdul, C.M., Anderson, K.S. and Schlessinger, J.** (2009). The precise sequence of FGF receptor autophosphorylation is kinetically driven and is disrupted by oncogenic mutations. *Science Signaling* **2**(58):1–11.
- Li, L., Liu, F. and Ross, A.H.** (2003). PTEN regulation of neural development and CNS stem cells. *Journal of Cellular Biochemistry* **88**(1):24–8.
- Li, Z., Bao, S., Wu, Q., Wang, H., Eyler, C., Sathornsumetee, S., Shi, Q., et al.** (2009). Hypoxia-Inducible Factors Regulate Tumorigenic Capacity of Glioma Stem Cells. *Cancer Cell* **15**(6):501–513.

- Liberzon, A., Birger, C., Thorvaldsdóttir, H., Ghandi, M., Mesirov, J.P. and Tamayo, P.** (2015). The Molecular Signatures Database Hallmark Gene Set Collection. *Cell Systems* **1**(6):417–425.
- Ligon, K.L., Huillard, E., Mehta, S., Kesari, S., Liu, H., Alberta, J.A., Bachoo, R.M., et al.** (2007). Olig2-Regulated Lineage-Restricted Pathway Controls Replication Competence in Neural Stem Cells and Malignant Glioma. *Neuron* **53**(4):503–517.
- Lima, F.R., Kahn, S.A., Soletti, R.C., Biasoli, D., Alves, T., da Fonseca, A.C., Garcia, C., et al.** (2012). Glioblastoma: Therapeutic challenges, what lies ahead. *Biochimica et Biophysica Acta - Reviews on Cancer* **1826**(2):338–349.
- Liu, Y., El-Naggar, S., Darling, D.S, Higashi, Y. and Dean, D.C.** (2008). Zeb1 links epithelial-mesenchymal transition and cellular senescence. *Development* **135**(3):579–588.
- Loilome, W., Joshi, A.D., ap Rhys, C.M, Piccirillo, S., Vescovi, A.L., Gallia, G.L. and Riggins, G.J.** (2009). Glioblastoma cell growth is suppressed by disruption of fibroblast growth factor pathway signaling. *Journal of Neuro-Oncology* **94**(3):359–366.
- Lois, C. and Alvarez-Buylla, A.** (1994). Long-distance neuronal migration in the adult mammalian brain. *Science* **264**(5162):1145–8.
- Losman, J.A. and Kaelin, W.G.** (2013). What a difference a hydroxyl makes: Mutant IDH, (R)-2-hydroxyglutarate, and cancer. *Genes and Development* **27**(8):836–852.
- Louis, D.N., Perry, A., Reifenberger, G., von Deimling, A., Figarella-Branger, D., Cavenee, W.K, Ohgaki, H., et al.** (2016). The 2016 World Health Organization Classification of Tumors of the Central Nervous System: a summary. *Acta Neuropathologica* **131**(3):803–820.
- Louis, D.N., Ohgaki, H., Wiestler, O.D., Cavenee, W.K., Burger, P.C., Jouvet, A., Scheithauer, B.W., et al.** (2007). The 2007 WHO classification of tumours of the central nervous system. *Acta Neuropathologica* **114**(2):97–109.
- Louis, S.A., Rietze, R.L., Deleyrolle, L., Wagey, R.E., Thomas, T.E., Eaves, A.C. and Reynolds, B.A.** (2008). Enumeration of neural stem and progenitor cells in the neural colony-forming cell assay. *Stem Cells* **26**(4):988–996.
- Lu, F., Chen, Y., Zhao, C., Wang, H., He, D., Xu, L., Wang, J., et al.** (2016). Olig2-Dependent Reciprocal Shift in PDGF and EGF Receptor Signaling Regulates Tumor Phenotype and Mitotic Growth in Malignant Glioma. *Cancer Cell* **29**(5):669–683.
- Luo, L., Guo, K., Fan, W., Lu, Y., Chen, L., Wang, Y., Shao, Y., et al.** (2017). Niche astrocytes promote the survival, proliferation and neuronal differentiation of co-transplanted neural stem cells following ischemic stroke in rats. *Experimental and Therapeutic Medicine* **13**(2):645–650.
- Luskin, M.B.** (1993). Restricted proliferation and migration of postnatally generated neurons derived from the forebrain subventricular zone. *Neuron* **11**(1):173–89.
- Ma, D.K., Bonaguidi, M.A., Ming, G.L. and Song, H.** (2009). Adult neural stem cells in the mammalian central nervous system. *Cell Research* **19**(6):672–82.

- Ma, Y.H., Mentlein, R., Knerlich, F., Kruse, M.L., Mehdorn, H.M. and Held-Feindt, J.** (2008). Expression of stem cell markers in human astrocytomas of different WHO grades. *Journal of Neuro-Oncology* **86**(1):31–45.
- Maher, E.A., Furnari, F.B., Bachoo, R.M., Rowitch, D.H., Louis, D.N., Cavenee, W.K. and DePinho, R.A.** (2001). Malignant glioma: Genetics and biology of a grave matter. *Genes and Development* **15**(11):1311–33.
- Mamun, M. A, Mannoor, K., Cao, J., Qadri, F. and Song, X.** (2018). SOX2 in cancer stemness: tumor malignancy and therapeutic potentials. *Journal of Molecular Cell Biology*:1–14.
- Manchado, E., Weissmueller, S., Morris, J.P., Chen, C.C., Wullenkord, R., Lujambio, A., De Stanchina, E., et al.** (2016). A combinatorial strategy for treating KRAS-mutant lung cancer. *Nature* **534**(7609):647–51.
- Mansouri, S., Nejad, R., Karabork, M., Ekinci, C., Solaroglu, I., Aldape, K.D. and Zadeh, G.** (2016). Sox2: regulation of expression and contribution to brain tumors. *CNS oncology* **5**(3):159–173.
- Marqués-Torrejón, M.Á., Porlan, E., Banito, A., Gómez-Ibarlucea, E., Lopez-Contreras, A.J., Fernández-Capetillo, Ó., Vidal, A., et al.** (2013). Cyclin-dependent kinase inhibitor p21 controls adult neural stem cell expansion by regulating Sox2 gene expression. *Cell Stem Cell* **12**(1):88–100.
- Marshall, G., Reynolds, B.A. and Laywell, E.D.** (2007). Using the Neurosphere Assay to Quantify Neural Stem Cells In Vivo. *Current Pharmaceutical Biotechnology* **8**(3):141–145.
- Matlin, A.J., Clark, F. and Smith, C.W.** (2005). Understanding alternative splicing: Towards a cellular code. *Nature Reviews Molecular Cell Biology* **6**(5):386–398.
- McLendon, R., Friedman, A., Bigner, D., Van Meir, E.G., Brat, D.J., Mastrogianakis, G.M., Olson, J.J., et al.** (2008). Comprehensive genomic characterization defines human glioblastoma genes and core pathways. *Nature* **455**:1061–1068.
- Mehta, S., Huillard, E., Kesari, S., Maire, C.L., Golebiowski, D., Harrington, E.P., Alberta, J.A., et al.** (2011). The Central Nervous System-Restricted Transcription Factor Olig2 Opposes p53 Responses to Genotoxic Damage in Neural Progenitors and Malignant Glioma. *Cancer Cell* **19**(3):359–71.
- Meijer, D.H., Kane, M.F., Mehta, S., Liu, H., Harrington, E., Taylor, C.M., Stiles, C.D., et al.** (2012). Separated at birth? the functional and molecular divergence of OLIG1 and OLIG2. *Nature Reviews Neuroscience* **13**(12):819–31.
- Van Meir, E.G. Van, Hadjipanayis, C.G., Norden, A.D., Shu, H., Wen, P.Y. and Olson, J.J.** (2010). Exciting New Advances in Neuro-Oncology: The Avenue to a Cure for Malignant Glioma. *A Cancer Journal for Clinicians* **60**(3):166–193.
- Mich, J.K., Signer, R.A., Nakada, D., Pineda, A., Burgess, R.J., Vue, T.Y., Johnson, J.E., et al.** (2014). Prospective identification of functionally distinct stem cells and neurosphere-initiating cells in adult mouse forebrain. *eLife* **3**(02669):1–27.
- Miroux, S., Lemièrre, S., Pineau, R., Pluderi, M., Canioni, P., Franconi, J.M., Thiaudière, E., et al.** (2004). Inhibition of FGF receptor activity in glioma implanted into the mouse brain using the tetracyclin-

regulated expression system. *Angiogenesis* **7**(2):105–113.

Modrek, A.S., Golub, D., Khan, T. et al. (2017). Low-grade astrocytoma mutations in IDH1, P53, and ATRX cooperate to Block differentiation of human neural stem cells via repression of SOX2. *Cell Reports* **21**(5):1267–1280.

Mogi, M., Harada, M., Kondo, T., Riederer, P. and Nagatsu, T. (1996). Interleukin-2 but not basic fibroblast growth factor is elevated in parkinsonian brain. *Journal of Neural Transmission* **103**(8–9):1077–1081.

Mohammadi, M., Olsen, S.K. and Ibrahimi, O.A. (2005). Structural basis for fibroblast growth factor receptor activation. *Cytokine and Growth Factor Reviews* **16**(2):107–137.

Molina, E.S., Pillat, M.M., Moura-Neto, V., Lah, T.T. and Ulrich, H. (2014). Glioblastoma stem-like cells: approaches for isolation and characterization. *Journal of Cancer Stem Cell Research* **2**(e7007):1–19.

Morris, E.J., Jha, S., Restaino, C.R., Dayananth, P., Zhu, H., Cooper, A., Carr, D., et al. (2013). Discovery of a novel ERK inhibitor with activity in models of acquired resistance to BRAF and MEK inhibitors. *Cancer Discovery* **3**(7):742–750.

Morrison, R.S, Yamaguchi, F., Bruner, J.M., Tang, M., McKeegan, W. and Berger, M.S. (1994). Fibroblast growth factor receptor gene expression and immunoreactivity are elevated in human glioblastoma multiforme. *Cancer Research* **54**(10):2794–2799.

Morrison, R.S, Yamaguchi, F., Saya, H., Bruner, J.M., Yahanda, A.M., Donehower, L.A. and Berger, M. (1994). Basic fibroblast growth factor and fibroblast growth factor receptor I are implicated in the growth of human astrocytomas. *Journal of Neuro-Oncology* **18**(3):207–216.

Morrison, R.S., Gross, J.L., Herblin, W.F., Reilly, T.M., Lasala, P.A., Alterman, R.L., Moskal, J.R., et al. (1990). Basic fibroblast growth factor-like activity and receptors are expressed in a human glioma cell line. *Cancer Research* **50**(8):2524–2529.

Morrison, R.S., Sharma, A., de Vellis, J. and Bradshaw, R.A. (1986). Basic fibroblast growth factor supports the survival of cerebral cortical neurons in primary culture. *Neurobiology* **83**(19):7537–7541.

Morshead, C.M., Garcia, A.D., Sofroniew, M. V. and Van Der Kooy, D. (2003). The ablation of glial fibrillary acidic protein-positive cells from the adult central nervous system results in the loss of forebrain neural stem cells but not retinal stem cells. *European Journal of Neuroscience* **18**(1):76–84.

Moschos, S.J., Sullivan, R.J., Hwu, W.J., Ramanathan, R.K., Adjei, A.A., Fong, P.C., Shapira-Frommer, R., et al. (2018). Development of MK-8353, an orally administered ERK1/2 inhibitor, in patients with advanced solid tumors. *Journal of Clinical Investigation* **3**(4):1–18.

Murphy, T., Darby, S., Mathers, M.E. and Gnanapragasam, V.J. (2010). Evidence for distinct alterations in the FGF axis in prostate cancer progression to an aggressive clinical phenotype. *Journal of Pathology* **220**(4):452–60.

Myers, J.M., Martins, G.G., Ostrowski, J. and Stachowiak, M.K. (2003). Nuclear trafficking of FGFR1: A role for the transmembrane domain. *Journal of Cellular Biochemistry* **88**(6):1273–1291.

- Nieto, M.A., Huang, R.Y., Jackson, R.A. and Thiery, J.P.** (2016). Emt: 2016. *Cell* **166**(1):21–45.
- Niwa, H., Miyazaki, J. and Smith, A.G.** (2000). Quantitative expression of OCT3 / 4 defines differentiation , dedifferentiation or self-renewal of ES cells . *Nat Genet* **24**(4):2–6.
- Nomura, S., Yoshitomi, H., Takano, S., Shida, T., Kobayashi, S., Ohtsuka, M., Kimura, F., et al.** (2008). FGF10/FGFR2 signal induces cell migration and invasion in pancreatic cancer. *British Journal of Cancer* **99**(2):305–313.
- Noushmehr, H., Weisenberger, D.J., Diefes, K., Phillips, H.S., Pujara, K., Berman, B.P., Pan, F., et al.** (2010). Identification of a CpG Island Methylator Phenotype that Defines a Distinct Subgroup of Glioma. *Cancer Cell* **17**(5):510–522.
- Nowell, P.C.** (1976). The clonal evolution of tumor cell populations. *Science* **94**(4260):23–8.
- Ohashi, R., Matsuda, Y., Ishiwata, T. and Naito, Z.** (2014). Downregulation of fibroblast growth factor receptor 2 and its isoforms correlates with a high proliferation rate and poor prognosis in high-grade glioma. *Oncology Reports* **32**(3):1163–1169.
- Ohgaki, H. and Kleihues, P.** (2007). Genetic Pathways to Primary and Secondary Glioblastoma. *The American Journal of Pathology* **170**(5):1445–1453.
- Ohgaki, H. and Kleihues, P.** (2011). Genetic profile of astrocytic and oligodendroglial gliomas. *Brain Tumor Pathology* **28**(3): 177–183.
- Ohgaki, H. and Kleihues, P.** (2013). The Definition of Primary and Secondary Glioblastoma. *Clinical Cancer Research* **19**(4):764–773.
- Ohka, F., Natsume, A. and Wakabayashi, T.** (2012). Current trends in targeted therapies for glioblastoma multiforme. *Neurology Research International* **2012**(2):1–13.
- Olar, A. and Aldape, K.D.** (2014). Using the Molecular Classification of Glioblastoma to Inform Personalized Treatment Adriana. *Journal Pathology* **232**(2):165–177.
- Oliver, T.G., Graseder, L.L., Carroll, A.L., Kaiser, C., Gillingham, C.L., Lin, S.M., Wickramasinghe, R., et al.** (2003). Transcriptional profiling of the Sonic hedgehog response: A critical role for N-myc in proliferation of neuronal precursors. *Proceedings of the National Academy of Sciences* **100**(12):7331–6.
- Olsen, S.K., Ibrahimi, O.A., Raucci, A., Zhang, F., Eliseenkova, A. V, Yayon, A., Basilico, C., et al.** (2004). Insights into the molecular basis for fibroblast growth factor receptor autoinhibition and ligand-binding promiscuity. *Proceedings of the National Academy of Sciences* **101**(4):935–940.
- Omar, A.I. and Mason, W.P.** (2009). Temozolomide: The evidence for its therapeutic efficacy in malignant astrocytomas. *Core Evidence* **4**:93–11.
- Opaliński, Ł., Sokołowska-Wędzina, A., Szczepara, M., Zakrzewska, M. and Otlewski, J.** (2017). Antibody-induced dimerization of FGFR1 promotes receptor endocytosis independently of its kinase activity. *Scientific Reports* **7**(1):1–12.
- Ori, A., Wilkinson, M.C. and Fernig, D.G.** (2008). The heparanome and regulation of cell function:

structures, functions and challenges. *Frontiers in Bioscience* **13**:4309–4338.

Osuka, S. and Van Meir, E.G. (2017). Overcoming therapeutic resistance in glioblastoma: The way forward. *Journal of Clinical Investigation* **127**(2):415–426.

Otani, R., Uzuka, T. and Ueki, K. (2017). Classification of adult diffuse gliomas by molecular markers—a short review with historical footnote. *Japanese Journal of Clinical Oncology* **47**(1):02–06.

Ozawa, T., Riester, M., Cheng, Y.K., Huse, J.T., Squatrito, M., Helmy, K., Charles, N., et al. (2014). Most human non-GCIMP glioblastoma subtypes evolve from a common proneural-like precursor glioma. *Cancer Cell* **26**(2):288–300.

Pagano, K., Torella, R., Foglieni, C., Bugatti, A., Tomaselli, S., Zetta, L., Presta, M., et al. (2012). Direct and allosteric inhibition of the FGF2/HSPGs/FGFR1 ternary complex formation by an antiangiogenic, thrombospondin-1-mimic small molecule. *PLoS ONE* **7**(5):1–11.

Paolillo, M., Boselli, C. and Schinelli, S. (2018). Glioblastoma under Siege: An Overview of Current Therapeutic Strategies Mayra. *Brain Sciences* **8**(1):1–13.

Parker, B.C., Annala, M.J, Cogdell, D.E, Granberg, K.J, S.Y., Ji, P., Gumin, J., Z, H., Hu, L., et al. (2013). The tumorigenic FGFR3-TACC3 gene fusion escapes miR-99a regulation in glioblastoma. *Journal of Clinical Investigation* **123**(2):1–9.

Parker, B.C., Engels, M., Annala, M. and Zhang, W. (2014). Emergence of FGFR family gene fusions as therapeutic targets in a wide spectrum of solid tumours. *The Journal of Pathology* **232**(1):4–15.

Parpura, V., Heneka, M.T., Montana, V., Oliet, S.H.R., Schousboe, A., Haydon, P.G., Stout, R.F., et al. (2012). Glial cells in (patho)physiology. *Journal of Neurochemistry* **121**(1):4–27.

Pastrana, E., Cheng, L.C. and Doetsch, F. (2009). Simultaneous prospective purification of adult subventricular zone neural stem cells and their progeny. *Proceedings of the National Academy of Sciences* **106**(15):6387–92.

Pastrana, E., Silva-Vargas, V. and Doetsch, F. (2011). Eyes wide open: A critical review of sphere-formation as an assay for stem cells. *Cell Stem Cell* **8**(5):486–98.

Patel, A.P., Tirosh, I., Trombetta, J.J., Shalek, A.K., Gillespie, S.M., Wakimoto, H., Cahill, D.P., et al. (2014). Single-cell RNA-seq highlights intratumoral heterogeneity in primary glioblastoma. *Science* **344**(6190):1396–401.

Paw, I., Carpenter, R.C., Watabe, K., Debinski, W. and Lo, H.W. (2015). Mechanisms regulating glioma invasion. *Cancer Letters* **362**(1):1–7.

Pear, W.S., Nolan, G.P., Scott, M.L. and Baltimore, D. (1993). Production of high-titer helper-free retroviruses by transient transfection. *Proceedings of the National Academy of Sciences* **90**(18):8392–6.

Peiffer, J. and Kleihues, P. (1999). Hans-Joachim Scherer (1906-1945), Pioneer in Glioma Research. *Brain Pathology* **9**(2):241–245.

Peles, E., Lidar, Z., Simon, A.J., Grossman, R., Nass, D. and Ram, Z. (2004). Angiogenic factors in

the cerebrospinal fluid of patients with astrocytic brain tumors. *Neurosurgery* **55**(3):562–567.

Peng, C., Li, N., Ng, Y.K., Zhang, J., Meier, F., Theis, F.J., Merkerschlager, M., et al. (2012). A Unilateral Negative Feedback Loop Between miR-200 microRNAs and Sox2/E2F3 Controls Neural Progenitor Cell-Cycle Exit and Differentiation. *Journal of Neuroscience* **32**(38):13292–13308.

Pettmann, B., Weibel, M., Sensenbrenner, M. and Labourdette, G. (1985). Purification of two astroglial growth factors from bovine brain. *FEBS Letters* **189**(1):102–8.

Phillips, H.S., Kharbanda, S., Chen, R., Forrest, W.F., Soriano, R.H., Wu, T.D., Misra, A., et al. (2006). Molecular subclasses of high-grade glioma predict prognosis, delineate a pattern of disease progression, and resemble stages in neurogenesis. *Cancer Cell* **9**(3):157–173.

Phuphanich, S., Wheeler, C.J., Rudnick, J.D., Mazer, M., Wang, H., Nuño, M.A., Richardson, J.E., et al. (2013). Phase I trial of a multi-epitope-pulsed dendritic cell vaccine for patients with newly diagnosed glioblastoma. *Cancer Immunology, Immunotherapy* **62**(1):125–35.

Piccirillo, S.G., Reynolds, B.A., Zanetti, N., Lamorte, G., Binda, E., Broggi, G., Brem, H., et al. (2006). Bone morphogenetic proteins inhibit the tumorigenic potential of human brain tumour-initiating cells. *Nature* **444**(7120):761–765.

Pisapia, D.J. (2017). The Updated World Health Organization Glioma Classification. *Archives of Pathology & Laboratory Medicine* **141**:1633–1644.

Podergajs, N., Brekka, N., Radlwimmer, B., Herold-Mende, C., Talasila, K.M., Tiemann, K., Rajcevic, U., et al. (2013). Expansive growth of two glioblastoma stem-like cell lines is mediated by bFGF and not by EGF. *Radiology and Oncology* **47**(4):330–337.

Pollard, S.M., Yoshikawa, K., Clarke, I.D., Danovi, D., Stricker, S., Russell, R., Bayani, J., et al. (2009). Glioma Stem Cell Lines Expanded in Adherent Culture Have Tumor-Specific Phenotypes and Are Suitable for Chemical and Genetic Screens. *Cell Stem Cell* **4**(6):568–580.

Porębska, N., Latko, M., Kucińska, M., Zakrzewska, M., Otlewski, J. and Opaliński, Ł. (2018). Targeting Cellular Trafficking of Fibroblast Growth Factor Receptors as a Strategy for Selective Cancer Treatment. *Journal of Clinical Medicine* **8**(1):1–28.

Postigo, A.A. (2003). Opposing functions of ZEB proteins in the regulation of the TGF β /BMP signaling pathway. *EMBO Journal* **22**(10):2443–2452.

Qian, X., Davis, A.A., Goderie, S.K. and Temple, S. (1997). FGF2 concentration regulates the generation of neurons and glia from multipotent cortical stem cells. *Neuron* **18**(1):81–93.

Quinn, J.A., Desjardins, A., Weingart, J., Brem, H., Dolan, M.E., Delaney, S.M., Vredenburgh, J., et al. (2005). Phase I trial of temozolomide plus O6-benzylguanine for patients with recurrent or progressive malignant glioma. *Journal of Clinical Oncology* **23**(28):7178–7187.

Quinn, J.A., Jiang, S.X., Reardon, D.A., Desjardins, A., Vredenburgh, J.J., Rich, J.N., Gururangan, S., et al. (2009). Phase II Trial of Temozolomide Plus O6-Benzylguanine in Adults with Recurrent, Temozolomide-Resistant Malignant Glioma. *Journal of Clinical Oncology* **27**(8):1262–1267.

- Raballo, R., Rhee, J., Lyn-Cook, R., Leckman, J.F., Schwartz, M.L. and Vaccarino, F.M.** (2000). Basic fibroblast growth factor (Fgf2) is necessary for cell proliferation and neurogenesis in the developing cerebral cortex. *The Journal of neuroscience* **20**(13):5012–23.
- Rahman, M., Deleyrolle, L., Vedam-Mai, V., Azari, H., Abd-El-Barr, M. and Reynolds, B.A.** (2011). The cancer stem cell hypothesis: Failures and pitfalls. *Neurosurgery* **68**(2):531–545.
- Ramon y Cajal, S.** (1928). *Degeneration and Regeneration of the Nervous System*. Oxford, England: Clarendon Press.
- Ramón y Cajal, S.** (1913). Contribución al conocimiento de la neuroglía del cerebro humano. *Trabajo de laboratorio de investigación en Biología. Universidad de Madrid*.
- Rand, V., Huang, J., Stockwell, T., Ferriera, S., Buzko, O., Levy, S., Busam, D., et al.** (2005). Sequence survey of receptor tyrosine kinases reveals mutations in glioblastomas. *Proceedings of the National Academy of Sciences* **102**(40):14344–14349.
- Ranieri, D., Rosato, B., Nanni, M., Magenta, A., Belleudi, F. and Torrisi, M.R.** (2016). Expression of the FGFR2 mesenchymal splicing variant in epithelial cells drives epithelial-mesenchymal transition. *Oncotarget* **7**(5):5440–5460.
- Rapraeger, A.C., Krufka, A. and Olwin, B.B.** (1991). Requirement of heparan sulfate for bFGF-mediated fibroblast growth and myoblast differentiation. *Science* **252**(5013):1705–8.
- Regan, J.L., Kendrick, H., Magnay, F.A., Vafaizadeh, V., Groner, B. and Smalley, M.J.** (2012). C-Kit is required for growth and survival of the cells of origin of Brca1-mutation-associated breast cancer. *Oncogene* **31**(7):869–883.
- Reich, M., Liefeld, T., Gould, J., Lerner, J., Tamayo, P. and Mesirov, J.P.** (2006). GenePattern 2.0. *Nature Genetics* **38**(5):500–501.
- Renu, D., Aggarwal, P., Cherukuri, S. and Pramila, T.** (2015). Molecular Subtypes in Glioblastoma Multiforme: Integrated Analysis Using Agilent GeneSpring and Mass Profiler Professional Multi-Omics Software. *Agilent Technologies*:1–12.
- Reynolds, B.A. and Rietze, R.L.** (2005). Neural stem cells and neurospheres—re-evaluating the relationship. *Nature Methods* **2**(5):333–336.
- Reynolds, B.A. and Weiss, S.** (1992). Generation of neurons and astrocytes from isolated cells of the adult mammalian central nervous system. *Science* **255**(5052):1707–10.
- Rheinbay, E., Suvà, M.L., Gillespie, S.M., Wakimoto, H., Patel, A.P., Shahid, M., Oksuz, O., et al.** (2013). An Aberrant Transcription Factor Network Essential for Wnt Signaling and Stem Cell Maintenance in Glioblastoma. *Cell Reports* **3**(5):1567–1579.
- Rhijn, B.W., Tilborg, A.A., Lurkin, I., Bonaventure, J., de Vries, A., Thiery, J.P., van der Kwast, T.H., et al.** (2002). Novel fibroblast growth factor receptor 3 (FGFR3) mutations in bladder cancer previously identified in non-lethal skeletal disorders. *European Journal of Human Genetics* **10**(12):819–24.

- Ricci-Vitiani, L., Pallini, R., Biffoni, M., Todaro, M., Invernici, G., Cenci, T., Maira, G., et al.** (2010). Tumour vascularization via endothelial differentiation of glioblastoma stem-like cells. *Nature* **468**(7325):824–8.
- Richichi, C., Osti, D., Del Bene, M., Fornasari, L., Patanè, M., Pollo, B., DiMeco, F., et al.** (2016). Tumor-initiating cell frequency is relevant for glioblastoma aggressiveness. *Oncotarget* **7**(44):71491–71503.
- Ricol, D., Cappellen, D., El Marjou, A., Gil-Diez-De-Medina, S., Girault, J.M., Yoshida, T., Ferry, G., et al.** (1999). Tumour suppressive properties of fibroblast growth factor receptor 2-IIIb in human bladder cancer. *Oncogene* **18**(51):7234–7243.
- Del Rio-Hortega, P.** (1921). El tercer elemento de los centros nerviosos: Histogénesis y evolución normal; Éxodo y distribución regional de la microglía. *Memorias de la Real Sociedad Española de Historia Natural, 1921* **16**(1):1–54.
- Del Rio Hortega, P.** (1928). Tercera aportación al conocimiento morfológico e interpretación funcional de la oligodendroglía. *Memorias de la Real Sociedad Española de Historia Natural* **40**:163–118.
- Rogelj, S., Weinberg, R.A., Fanning, P. and Klagsbrun, M.** (1988). Basic fibroblast growth factor fused to a signal peptide transforms cells. *Nature* **331**(6152):173–175.
- Roghani, M., Mansukhani, A., Dell’Era, P., Bellosta, P., Basilico, C., Rifkin, D.B. and Moscatelli, D.** (1994). Heparin increases the affinity of basic fibroblast growth factor for its receptor but is not required for binding. *Journal of Biological Chemistry* **269**(6):3976–84.
- Safa, A.R., Saadatzadeh, M.R., Cohen-Gadol, A.A., Pollok, K.E. and Bijangi-Vishehsaraei, K.** (2015). Glioblastoma stem cells (GSCs) epigenetic plasticity and interconversion between differentiated non-GSCs and GSCs. *Genes and Diseases* **2**(2):152–163.
- Sager, O., Dincoglan, F., Demiral, S., Uysal, B., Gamsiz, H., Dirican, B. and Beyzadeoglu, M.** (2018). A concise review of immunotherapy for glioblastoma. *Neuroimmunol Neuroinflammation* **5**(25):1–11.
- Saiki, M., Mima, T., Takahashi, J.C., Tani, S., Yukawa, H., Ueno, H., Mikawa, T., et al.** (1999). Adenovirus-mediated gene transfer of a truncated form of fibroblast growth factor receptor inhibits growth of glioma cells both in vitro and in vivo. *Journal of Neuro-Oncology* **44**(3):195–203.
- Sampson, J.H., Heimberger, A.B., Archer, G.E., Aldape, K.D., Friedman, A.H., Friedman, H.S., Gilbert, M.R., et al.** (2010). Immunologic escape after prolonged progression-free survival with epidermal growth factor receptor variant III peptide vaccination in patients with newly diagnosed glioblastoma. *Journal of Clinical Oncology* **28**(30):4722–9.
- Sanai, N., Alvarez-Buylla, A. and Berger, M.S.** (2005). Neural Stem Cells and the Origin of Gliomas. *New England Journal of Medicine* **353**(8):811–22.
- Sánchez-Tilló, E., Siles, L., de Barrios, O., Cuatrecasas, M., Vaquero, E.C., Castells, A. and Postigo, A.** (2011). Expanding roles of ZEB factors in tumorigenesis and tumor progression. *American journal of cancer research* **1**(7):897–912.

- Sandilands, E., Akbarzadeh, S., Vecchione, A., McEwan, D.G., Frame, M.C. and Heath, J.K.** (2007). Src kinase modulates the activation, transport and signalling dynamics of fibroblast growth factor receptors. *EMBO Reports* **8**(12):1162–1169.
- Sarkar, S., Zemp, F.J., Senger, D., Robbins, S.M. and Yong, V.W.** (2015). ADAM-9 is a novel mediator of tenascin-C-stimulated invasiveness of brain tumor-initiating cells. *Neuro-Oncology* **17**(8):1095–105.
- Sarrazin, S., Lamanna, W.C. and Esko, J.D.** (1965). Heparan Sulfate Proteoglycans Stephane. *Neoplasma* **12**(5):549–556.
- Sato, A., Sunayama, J., Matsuda, K.I., Seino, S., Suzuki, K., Watanabe, E., Tachibana, K., et al.** (2011). MEK-ERK signaling dictates DNA-repair gene MGMT expression and temozolomide resistance of stem-like glioblastoma cells via the MDM2-p53 axis. *Stem Cells* **29**(11):1942–51.
- Sayal, K.K., Higgins, G.S. and Hammond, E.M.** (2016). Uncovering the influence of the FGFR1 pathway on glioblastoma radiosensitivity. *Annals of Translational Medicine* **4**(24):2–5.
- Schiffer, D., Annovazzi, L., Casalone, C., Corona, C. and Mellai, M.** (2018). Glioblastoma: Microenvironment and niche concept. *Cancers* **11**(1):1–17.
- Schönherr, H. and Cernak, T.** (2013). Profound methyl effects in drug discovery and a call for new C-H methylation reactions. *Angewandte Chemie - International Edition* **52**:12256–12267.
- Schutte, B., Nuydens, R., Geerts, H. and Ramaekers, F.** (1998). Annexin V binding assay as a tool to measure apoptosis in differentiated neuronal cells. *Journal of neuroscience methods* **86**(1):63–9.
- Schwartzbaum, J.A., Fisher, J.L., Aldape, K.D. and Wrensch, M.** (2006). Epidemiology and molecular pathology of glioma. *Nature Clinical Practice Neurology* **2**(9):494–503.
- Seidel, S., Garvalov, B.K., Wirta, V., Von Stechow, L., Schänzer, A., Meletis, K., Wolter, M., et al.** (2010). A hypoxic niche regulates glioblastoma stem cells through hypoxia inducible factor 2 α . *Brain* **133**(4):983–995.
- Shackleton, M., Quintana, E., Fearon, E.R. and Morrison, S.J.** (2009). Heterogeneity in Cancer: Cancer Stem Cells versus Clonal Evolution. *Cell* **138**(5):822–829.
- Shouan, Y., Feng, X. and O’Connell, P.J.** (1998). Apoptosis detection by annexin V binding: a novel method for the quantitation of cell-mediated cytotoxicity. *Journal of immunological methods* **217**(1-2):61–70.
- Siebzehrubl, F.A., Reynolds, B.A., Vescovi, A., Steindler, D.A. and Deleyrolle, L.P.** (2011). The Origins of Glioma: E Pluribus Unum? **59**(8):1135–11.
- Siebzehrubl, F.A., Silver, D.J., Tugertimur, B., Deleyrolle, L.P., Siebzehrubl, D., Sarkisian, M.R., Devers, K.G., et al.** (2013). The ZEB1 pathway links glioblastoma initiation, invasion and chemoresistance. *EMBO Molecular Medicine* **5**(8):1196–1212.
- Siebzehrubl, F.A., Jeske, I., Muller, D., Buslei, R., Coras, R., Hahnen, E., Huttner, H.B., et al.** (2009). Spontaneous in vitro transformation of adult neural precursors into stem-like cancer cells. *Brain*

Pathology **19**(3):399–408.

Silber, J.R., Bobola, M.S., Ghatan, S., Blank, A., Kolstoe, D.D. and Berger, M.S. (1998). 06-Methylguanine-DNA Methyltransferase Activity in Adult Gliomas: Relation to Patient and Tumor Characteristics. *Cancer Research* **58**(5):1068–1073.

Silver, D.J. and Lathia, J.D. (2018). Revealing the glioma cancer stem cell interactome, one niche at a time. *Journal of Pathology* **244**(3):260–264.

Singh, D., Chan, J.M., Zoppoli, P., Niola, F., Sullivan, R., Castano, A., Liu, E.M., et al. (2012). Transforming fusions of FGFR and TACC genes in human glioblastoma. *Science* **337**(6099):1231–1235.

Singh, D.K., Kollipara, R.K., Vemireddy, V., Yang, X.L., Sun, Y., Regmi, N., Klingler, S., et al. (2017). Oncogenes Activate an Autonomous Transcriptional Regulatory Circuit That Drives Glioblastoma. *Cell Reports* **18**(4):961–976.

Singh, S.K., Clarke, I.D., Terasaki, M., Bonn V.E., Hawkins, C., Squire, J. and Dirks, P.B. (2003). Identification of a Cancer Stem Cell in Human Brain Tumors. *Proceedings of the National Academy of Sciences* **432**(25):5821–5828.

Singh, S.K., Fiorelli, R., Kupp, R., Rajan, S., Szeto, E., Lo Cascio, C., Maire, C.L., et al. (2016). Post-translational Modifications of OLIG2 Regulate Glioma Invasion through the TGF- β Pathway. *Cell Reports* **16**(4):950–966.

Singh, S.K., Hawkins, C., Clarke, I.D., Squire, J.A., Bayani, J., Hide, T., Henkelman, R.M., et al. (2004). Identification of human brain tumour initiating cells. *Nature* **432**(7015):396–401.

Soady, K.J., Tornillo, G., Kendrick, H., Meniel, V., Olijnyk-Dallis, D., Morris, J.S., Stein, T., et al. (2017). The receptor protein tyrosine phosphatase PTPRB negatively regulates FGF2-dependent branching morphogenesis. *Development* **144**(20):3777–3788.

Soeda, A., Lathia, J., Williams, B.J., Wu, Q., Gallagher, J., Androutsellis-Theotokis, A., Giles, A.J., et al. (2017). The p38 signaling pathway mediates quiescence of glioma stem cells by regulating epidermal growth factor receptor trafficking. *Oncotarget* **8**(20):33316–33328.

Soeda, A., Park, M., Lee, D., Mintz, A., Androutsellis-Theotokis, A., McKay, R.D., Engh, J., et al. (2009). Hypoxia promotes expansion of the CD133-positive glioma stem cells through activation of HIF-1 α . *Oncogene* **28**(45):3949–59.

Song, W.S., Yang, Y.P., Huang, C.S., Lu, K.H., Liu, W.H., Wu, W.W., Lee, Y.Y., et al. (2016). Sox2, a stemness gene, regulates tumor-initiating and drug-resistant properties in CD133-positive glioblastoma stem cells. *Journal of the Chinese Medical Association* **79**(10):538–545.

Soni, D., King, J.A., Kaye, A.H. and Hovens, C.M. (2005). Genetics of glioblastoma multiforme: mitogenic signaling and cell cycle pathways converge. *Journal of Clinical Neuroscience* **12**(1):1–5.

Sooman, L., Freyhult, E., Jaiswal, A., Navani, S., Edqvist, P.H., Pontén, F., Tchougounova, E., et al. (2015). FGF2 as a potential prognostic biomarker for proneural glioma patients. *Acta Oncologica* **54**(3):385–394.

- Sottoriva, A., Spiteri, I., Piccirillo, S.G., Touloumis, A., Collins, V.P., Marioni, J.C., Curtis, C., et al.** (2013). Intratumor heterogeneity in human glioblastoma reflects cancer evolutionary dynamics. *Proceedings of the National Academy of Sciences* **110**(10):4009–4014.
- Stachowiak, E.K., Maher, P.A., Tucholski, J., Mordechai, E., Joy, A., Moffett, J., Coons, S., et al.** (1997). Nuclear accumulation of fibroblast growth factor receptors in human glial cells - Association with cell proliferation. *Oncogene* **14**(18):2201–2211.
- Di Stefano, A.L., Fucci, A., Frattini, V., Labussiere, M., Mokhtari, K., Zoppoli, P., Marie, Y., et al.** (2015). Detection, characterization, and inhibition of FGFR-TACC fusions in IDH wild-type glioma. *Clinical Cancer Research* **21**(14):3307–3317.
- Stehbens, S.J., Ju, R.J., Adams, M.N., Perry, S.R., Haass, N.K., Bryant, D.M. and Pollock, P.M.** (2018). FGFR2-activating mutations disrupt cell polarity to potentiate migration and invasion in endometrial cancer cell models. *Journal of Cell Science* **131**(15):1–16.
- Steinberg, F., Zhuang, L., Beyeler, M., Kälin, R.E., Mullis, P.E., Brändli, A.W. and Trueb, B.** (2010). The FGFR1 receptor is shed from cell membranes, binds Fibroblast Growth Factors (FGFs), and antagonizes FGF signaling in *Xenopus* embryos. *Journal of Biological Chemistry* **285**(3):2193–2202.
- Stupp, R., Hegi, M.E., Mason, W.P., et al.** (2009). Effects of radiotherapy with concomitant and adjuvant temozolomide versus radiotherapy alone on survival in glioblastoma in a randomised phase III study: 5-year analysis of the EORTC-NCIC trial. *Lancet Oncology* **10**(5):459–466.
- Stupp, R., Mason, W., Van de Bent, M., et al.** (2005). Radiotherapy plus concomitant and adjuvant temozolomide for glioblastoma. *The New England Journal of Medicine* **325**(10):987–996.
- Stupp, R., Taillibert, S., Kanner, A.A., Kesari, S., Steinberg, D.M., Toms, S.A., Taylor, L.P., et al.** (2015). Maintenance therapy with tumor-Treating fields plus temozolomide vs temozolomide alone for glioblastoma a randomized clinical trial. *Journal of the American Medical Association* **314**(23):2535–2543.
- Sturm, D., Witt, H., Hovestadt, V., Khuong-Quang, D.A., Jones, D.T.W., Konermann, C., Pfaff, E., et al.** (2012). Hotspot mutations in H3F3A and IDH1 define distinct epigenetic and biological subgroups of glioblastoma. *Cancer Cell* **22**(4):425–437.
- Subramanian, A., Tamayo, P., Mootha, V.K., Mukherjee, S., Ebert, B.L., Gillette, M.A., Paulovich, A., et al.** (2005). Gene set enrichment analysis: a knowledge-based approach for interpreting genome-wide expression profiles. *Proceedings of the National Academy of Sciences* **102**(43):15545–15550.
- Sunayama, J., Matsuda, K.I., Sato, A., Tachibana, K., Suzuki, K., Narita, Y., Shibui, S., et al.** (2010). Crosstalk between the PI3K/mTOR and MEK/ERK pathways involved in the maintenance of self-renewal and tumorigenicity of glioblastoma stem-like cells. *Stem Cells* **28**(11):1930–1939.
- Sundar, S.J., Hsieh, J.K., Manjila, S., Lathia, J.D. and Sloan, A.** (2014). The role of cancer stem cells in glioblastoma. *Neurosurgical Focus* **37**(6):1–9.
- Sutter, R., Yadirgi, G. and Marino, S.** (2007). Neural stem cells, tumour stem cells and brain tumours: dangerous relationships? *Biochimica et Biophysica Acta* **1776**(2):125–137.

- Suvà, M.L., Rheinbay, E., Gillespie, S.M., Patel, A.P., Wakimoto, H., Rabkin, S.D., Riggi, N., et al.** (2014). Reconstructing and reprogramming the tumor-propagating potential of glioblastoma stem-like cells. *Cell* **157**(3):580–94.
- Takahashi, J.A., Fukumoto, M., Igarashi, K., Oda, Y., Kikuchi, H. and Hatanaka, M.** (1992). Correlation of basic fibroblast growth factor expression levels with the degree of malignancy and vascularity in human gliomas. *J Neurosurg* **76**(5):792–8.
- Takahashi, K. and Yamanaka, S.** (2006). Induction of pluripotent stem cells from mouse embryonic and adult fibroblast cultures by defined factors. *Cell* **126**(4):663–76.
- Takahashi, N., Yamamoto, E., Ino, K., Miyoshi, E., Nagasaka, T., Kajiyama, H., Shibata, K., et al.** (2009). High expression of N-acetylglucosaminyltransferase V in mucinous tumors of the ovary. *Oncology Reports* **22**(5):1072–32.
- The Cancer Genome Atlas Network** (2008). Comprehensive genomic characterization defines human glioblastoma genes and core pathways. *Nature* **455**(7216):1061–1068.
- Thiery, J.P., Acloque, H., Huang, R.Y.J. and Nieto, M.A.** (2009). Epithelial-Mesenchymal Transitions in Development and Disease. *Cell* **139**(5):871–890.
- Thomson, S., Petti, F., Mercado, P., Bean, J., Monaghan, M., Seymour, S.L., Argast, G.M., et al.** (2011). A systems view of epithelial – mesenchymal transition signaling states. *Clinical and Experimental Metastasis* **28**(2):137–155.
- Tiash, S. and Chowdhury, E.H.** (2015). Growth factor receptors: promising drug targets in cancer. *Journal of Cancer Metastasis and Treatment* **1**(3):190–200.
- Tiong, K.H., Mah, L.Y. and Leong, C.O.** (2013). Functional roles of fibroblast growth factor receptors (FGFRs) signaling in human cancers. *Apoptosis* **18**(12):1447–1468.
- Toedt, G., Barbus, S., Wolter, M., Felsberg, J., Tews, B., Blond, F., Sabel, M.C., et al.** (2011). Molecular signatures classify astrocytic gliomas by IDH1 mutation status. *International Journal of Cancer* **128**(5):1095–1103.
- Tomlinson, D.C., Baxter, E.W., Loadman, P.M., Hull, M.A. and Knowles, M.A.** (2012). FGFR1-induced Epithelial to mesenchymal transition through MAPK/PLC γ /COX-2-mediated mechanisms. *PLoS ONE* **7**(6).
- Tomlinson, D.C. and Knowles, M.A.** (2010). Altered splicing of FGFR1 is associated with high tumor grade and stage and leads to increased sensitivity to FGF1 in bladder cancer. *The American journal of pathology* **177**(5):2379–86.
- Tornillo, G., Knowlson, C., Kendrick, H., Cooke, J., Mirza, H., Aurrekoetxea-Rodríguez, I., Vivanco, M. d. M., et al.** (2018). Dual Mechanisms of LYN Kinase Dysregulation Drive Aggressive Behavior in Breast Cancer Cells. *Cell Reports* **25**(13):3674–3692.
- Touat, M., Ileana, E., Postel-Vinay, S., André, F. and Soria, J.C.** (2015). Targeting FGFR signaling in cancer. *Clinical Cancer Research* **21**(12):2684–2694.

- Toyoda, K., Tanaka, K., Nakagawa, S., Thuy, D.H., Ujifuku, K., Kamada, K., Hayashi, K., et al.** (2013). Initial contact of glioblastoma cells with existing normal brain endothelial cells strengthen the barrier function via fibroblast growth factor 2 secretion: A new in vitro blood-brain barrier model. *Cellular and Molecular Neurobiology* **33**(4):489–501.
- Trowell, O.A, Chir, B. and Willmer, E.N.** (1939). Studies on the Growth of Tissues in Vitro. *Journal of Experimental Biology* **16**(10):60–70.
- Tsigelny, I.F., Kouznetsova, V.L., Lian, N. and Kesari, S.** (2016). Molecular mechanisms of OLIG2 transcription factor in brain cancer. *Oncotarget* **7**(33):53074–101.
- Turner, C.A., Watson, S.J. and Akil, H.** (2012). The Fibroblast Growth Factor Family: Neuromodulation of Affective Behavior. *Neuron* **76**(1):160–174.
- Ulasov, I. V., Nandi, S., Dey, M., Sonabend, A.M. and Lesniak, M.S.** (2011). Inhibition of Sonic Hedgehog and Notch Pathways Enhances Sensitivity of CD133+ Glioma Stem Cells to Temozolomide Therapy. *Molecular Medicine* **17**(1–2):103–112.
- Valent, P., Bonnet, D., De Maria, R., Lapidot, T., Copland, M., Melo, J. V, Chomienne, C., et al.** (2012). Terminology : the Devil Is in the Details. *Nature Publishing Group* **12**(11):767–775.
- Vandewalle, C., Van Roy, F. and Berx, G.** (2009). The role of the ZEB family of transcription factors in development and disease. *Cellular and Molecular Life Sciences* **66**(5):773–787.
- Vanner, R.J., Remke, M., Gallo, M., Selvadurai, H.J., Coutinho, F., Lee, L., Kushida, M., et al.** (2014). Quiescent Sox2 + Cells Drive Hierarchical Growth and Relapse in Sonic Hedgehog Subgroup Medulloblastoma. *Cancer Cell* **26**(1):33–47.
- Vasile, F., Dossi, E. and Rouach, N.** (2017). Human astrocytes: structure and functions in the healthy brain. *Brain Structure and Function* **222**(5):2017–2029.
- Verhaak, R.G., Hoadley, K.A., Purdom, E., Wang, V., Qi, Y., Wilkerson, M.D., Miller, C.R., et al.** (2010). Integrated Genomic Analysis Identifies Clinically Relevant Subtypes of Glioblastoma Characterized by Abnormalities in PDGFRA, IDH1, EGFR, and NF1. *Cancer Cell* **17**(1):98–110.
- Vescovi, A.L., Galli, R. and Reynolds, B.A.** (2006). Brain tumour stem cells. *Nature reviews. Cancer* **6**(6):425–36.
- Vigneswaran, K., Neill, S. and Hadjipanayis, C.G.** (2015). Beyond the World Health Organization grading of infiltrating gliomas: advances in the molecular genetics of glioma classification. *Annals of translational medicine* **3**(7):95.
- Vlodavsky, I., Folkman, J., Sullivan, R., Fridman, R., Ishai-Michaeli, R., Sasse, J. and Klagsbrun, M.** (2006). Endothelial cell-derived basic fibroblast growth factor: synthesis and deposition into subendothelial extracellular matrix. *Proceedings of the National Academy of Sciences* **84**(8):2292–2296.
- Wagner, J.P., Black, I.B. and DiCicco-Bloom, E.** (1999). Stimulation of neonatal and adult brain neurogenesis by subcutaneous injection of basic fibroblast growth factor. *The Journal of neuroscience* **19**(14):6006–16.

- Wake, H., Moorhouse, A.J. and Nabekura, J.** (2012). Functions of microglia in the central nervous system-beyond the immune response. *Neuron Glia Biology* **7**(1):47–53.
- Wang, F., Kan, M., Yan, G., Xu, J. and McKeegan, W.L.** (1995). Alternately spliced NH2-terminal immunoglobulin-like loop I in the ectodomain of the fibroblast growth factor (FGF) receptor 1 lowers affinity for both heparin and FGF-1. *Journal of Biological Chemistry* **270**(17):10231–10235.
- Wang, J., Sakariassen, P., Tsinkalovsky, O., Immervoll, H., Bøe, S.O., Svendsen, A., Prestegarden, L., et al.** (2008). CD133 negative glioma cells form tumors in nude rats and give rise to CD133 positive cells. *International Journal of Cancer* **122**(4):761–768.
- Wang, K., Ji, W., Yu, Y., Li, Z., Niu, X., Xia, W. and Lu, S.** (2018). FGFR1-ERK1/2-SOX2 axis promotes cell proliferation, epithelial–mesenchymal transition, and metastasis in FGFR1-amplified lung cancer. *Oncogene* **37**(39):5340–5354.
- Wang, R., Chadalavada, K., Wilshire, J., Kowalik, U., Hovinga, K.E., Geber, A., Fligelman, B., et al.** (2010). Glioblastoma stem-like cells give rise to tumour endothelium. *Nature* **468**(7325):829–33.
- Wang, Z., Zhang, C., Sun, L., Liang, J., Liu, X., Li, G., Yao, K., et al.** (2016). FGFR3, as a receptor tyrosine kinase, is associated with differentiated biological functions and improved survival of glioma patients. *Oncotarget* **7**(51):84587–84593.
- Ware, K.E., Hinz, T.K., Kleczko, E., Singleton, K.R., Marek, L.A., Helfrich, B.A., Cummings, C.T., et al.** (2013). A mechanism of resistance to gefitinib mediated by cellular reprogramming and the acquisition of an FGF2-FGFR1 autocrine growth loop. *Oncogenesis* **2**(3):39–9.
- Watanabe, T., Nobusawa, S., Kleihues, P. and Ohgaki, H.** (2009). IDH1 mutations are early events in the development of astrocytomas and oligodendrogliomas. *American Journal of Pathology* **174**(4):1149–1153.
- Weiss, S., Dunne, C., Hewson, J., Wohl, C., Wheatley, M., Peterson, A.C. and Reynolds, B.A.** (1996). Multipotent CNS stem cells are present in the adult mammalian spinal cord and ventricular neuroaxis. *The Journal of neuroscience* **16**(23):7599–609.
- Weller, M., Butowski, N., Tran, D.D., Recht, L.D., Lim, M., Hirte, H., Ashby, L., et al.** (2017). Rindopemut with temozolomide for patients with newly diagnosed, EGFRvIII-expressing glioblastoma (ACT IV): a randomised, double-blind, international phase 3 trial. *The Lancet Oncology* **18**(10):1373–1385.
- Weller, M., Wick, W., Aldape, K., Brada, M., Berger, M., Pfister, S.M., et al.** (2015). Glioma. *Nature Reviews Disease Primers* **1**(15017):1–18.
- Wellner, U., Schubert, J., Burk, U.C., Schmalhofer, O., Zhu, F., Sonntag, A., Waldvogel, B., et al.** (2009). The EMT-activator ZEB1 promotes tumorigenicity by repressing stemness-inhibiting microRNAs. *Nature cell biology* **11**(12):1487–1495.
- Werner, S., Unsicker, K. and von Bohlen und Halbach, O.** (2011). Fibroblast growth factor-2 deficiency causes defects in adult hippocampal neurogenesis, which are not rescued by exogenous fibroblast growth factor-2. *Journal of Neuroscience Research* **89**(10):1605–1617.

- Wick, W., Gorlia, T., Bendszus, M., Taphoorn, M., Sahm, F., Harting, I., et al.** (2017). Lomustine and Bevacizumab in Progressive Glioblastoma. *The New England Journal of Medicine* **377**:1954–63.
- Woodbury, M.E. and Ikezu, T.** (2014). Fibroblast growth factor-2 signaling in neurogenesis and neurodegeneration. *Journal of Neuroimmune Pharmacology* **9**(2):92–101.
- Wu, J., Feng, X., Zhang, B., Li, J., Xu, X., Liu, J., Wang, X., et al.** (2014). Blocking the bFGF/STAT3 interaction through specific signaling pathways induces apoptosis in glioblastoma cells. *Journal of Neuro-Oncology* **120**(1):33–41.
- Xi, G., Best, B., Mania-Farnell, B., James, C.D. and Tomita, T.** (2017). Therapeutic Potential for Bone Morphogenetic Protein 4 in Human Malignant Glioma. *Neoplasia* **19**(4):261–270.
- Xie, B., Zhang, L., Hu, W., Fan, M., Jiang, N., Duan, Y., Jing, D., et al.** (2019). Dual blockage of STAT3 and ERK1/2 eliminates radioresistant GBM cells. *Redox Biology* **24**(101189):1–13.
- Xie, Q., Wu, Q., Horbinski, C.M., Flavahan, W.A., Yang, K., Zhou, W., Dombrowski, S.M., et al.** (2015). Mitochondrial control by DRP1 in brain tumor initiating cells. *Nature Neuroscience* **18**(4):501–510.
- Xie, Y., Bergström, T., Jiang, Y., Johansson, P., Marinescu, V.D., Lindberg, N., Segerman, A., et al.** (2015). The Human Glioblastoma Cell Culture Resource: Validated Cell Models Representing All Molecular Subtypes. *EBioMedicine* **2**(10):1351–1363.
- Yamada, S.M., Yamaguchi, F., Brown, R., Berger, M.S. and Morrison, R.S.** (1999). Suppression of glioblastoma cell growth following antisense oligonucleotide-mediated inhibition of fibroblast growth factor receptor expression. *Glia* **28**(1):66–76.
- Yamaguchi, F., Saya, H., Bruner, J.M. and Morrison, R.S.** (1994). Differential expression of two fibroblast growth factor-receptor genes is associated with malignant progression in human astrocytomas. *Proceedings of the National Academy of Sciences* **91**(2):484–8.
- Yang, J.Y., Zong, C.S., Xia, W., Yamaguchi, H., Ding, Q., Xie, X., Lang, J.Y., et al.** (2008). ERK promotes tumorigenesis by inhibiting FOXO3a via MDM2-mediated degradation. *Nature Cell Biology* **10**(2):138–148.
- Yayon, A., Klagsbrun, M., Esko, J.D., Leder, P. and Ornitz, D.M.** (1991). Cell surface, heparin-like molecules are required for binding of basic fibroblast growth factor to its high affinity receptor. *Cell* **64**(4):841–848.
- Zagzag, D., Miller, D., Sato, Y., Rifkin, D. and Burstein, D.** (1990). Immunohistochemical localization of basic fibroblast growth factor in bovine ovarian follicles. *Molecular and Cellular Endocrinology* **50**:1393–7398.
- Zakrzewska, M., Haugsten, E.M., Nadratowska-Wesolowska, B., Oppelt, A., Hausott, B., Jin, Y., Otlewski, J., et al.** (2013). ERK-mediated phosphorylation of fibroblast growth factor receptor 1 on Ser 777 inhibits signaling. *Science Signaling* **6**(262):1–16.
- Zhang, X., Wang, B. and Li, J.P.** (2014). Implications of heparan sulfate and heparanase in neuroinflammation. *Matrix Biology* **35**:174–81.

Zheng, W., Nowakowski, R.S. and Vaccarino, F.M. (2004). Fibroblast growth factor 2 is required for maintaining the neural stem cell pool in the mouse brain subventricular zone. *Developmental Neuroscience* **26**(2–4):181–196.

Zhu, P. and Zhu, J.J. (2017). Tumor treating fields: a novel and effective therapy for glioblastoma: mechanism, efficacy, safety and future perspectives. *Chinese Clinical Oncology* **6**(4):1–15.

Zhu, T.S., Costello, M.A., Talsma, C.E., Flack, C.G., Crowley, J.G., Hamm, L.L., He, X., et al. (2011). Endothelial cells create a stem cell niche in glioblastoma by providing NOTCH ligands that nurture self-renewal of cancer stem-like cells. *Cancer Research* **6**(4):1–15.

Zhu, Y., Guignard, F., Zhao, D., Liu, L., Burns, D.K., Mason, R.P., Messing, A., et al. (2005). Early inactivation of p53 tumor suppressor gene cooperating with NF1 loss induces malignant astrocytoma. *Cancer Cell* **8**(2):119–130.